Andras Kemeny
Stéphane Espié
Frédéric Mérienne
Editors

NEW DEVELOPMENTS IN DRIVING SIMULATION DESIGN AND EXPERIMENTS

Driving Simulation Conference Europe 2014 Proceedings

Arts et Métiers ParisTech, Paris, France

September 4-5, 2014

Actes

Stéphane Espié
Andras Kemeny
Frédéric Mérienne
Editors

New Developments in Driving Simulation Design and Experiments

Driving Simulation Conference
Europe 2014 Proceedings

Arts et Métiers ParisTech
Paris, France

September 4-5, 2014

Direction

Andras Kemeny andras.kemeny@renault.com
Renault, Technical Center for Simulation
1 Avenue du Golf, 78288 Guyancourt
Arts et Metiers ParisTech
2 rue Thomas Dumorey, 71100 Chalon-sur-Saône

Organisation Committee

Stéphane Espié, Ifsttar
Andras Kemeny, Renault, Arts et Metiers ParisTech
Frédéric Mérienne, Arts et Metiers ParisTech

Scientific Committee

Jost Bernasch, The Virtual Vehicle (Austria)
Alain Berthoz, CNRS-Collège de France (France)
Erwin R. Boer, ECI (United States)
Heinrich H. Bülthoff, Max Planck Institute for Biological Cybernetics (Germany)
Viola Cavallo, IFSTTAR (France)
Mehmet Dagdelen, Renault (France)
Stéphane Espié, IFSTTAR (France)
Peter Goeldl, BMW Group R&T (Germany)
Jeff Greenberg, Ford Motor Co. (United States)
Franck Mars, Irccyn (France)
Stéphane Masfrand, PSA (France)
Frédéric Mérienne, Arts et Métiers ParisTech (France)
Lena Nilsson, VTI (Sweden)
Paolo Pretto, Max Planck Institute for Biological Cybernetics (Germany)
Hans-Peter Schöner, Daimler AG (Germany)
Anca Stratulat, PSA (France)
Eberhard Zeeb, Daimler AG (Germany)

PREFACE

The DSC Europe conference held this year again for the 3rd time at the Arts et Métiers ParisTech on September 4th and 5th 2014, is a gathering event between two communities: scientific researchers interested in driver's behavior and perception and developers of technologies for the rendering of the behavior and environment of vehicles.

These proceedings contain the full paper versions of the oral presentation given at the conference and short summaries of the posters presented at the conference. Papers are listed in the same order as at the conference, according the different session: Perception and Human Factors, Simulation Architecture and Design, including a new sub-session - Connected Simulation, Motion Rendering, Simulation Design and Architecture and Product Solutions and Posters.

Authors of the best papers were asked to submit an extended version to the SCS journal, Special Issue in Driving Simulation. In addition an electronic version of the conference papers are available on line on the DSC Europe website, two years after the conference, thus in September 2016 the electronic versions of the papers presented in September 2014.

These DSC Europe 2014 proceedings bring again a panorama of recent developments in simulation rendering techniques and virtual prototyping applications as well as of perception and human factors studies in the field of driving simulation.

The DSC Europe Organization Committee

PROGRAMME

Introduction

- **Virtual reality and Driving Simulation at the benefit of automotive engineering**
  Olivier Colmard, Andras Kemeny

Perception and Human Factors

- **Are we there yet? An objective mechanism to support the assessment of driving simulator utility**
  Erwin R. Boer, A. Hamish Jamson, Sunjoo K. Advani, Anthony J. Horrobin
- **Real vs virtual driving or how to improve the realism of a dynamic driving simulator**
  Anca Stratulat, Emmanuelle Diaz, Philippe Vars, Stephane Masfrand, Laurent Leblond, Guillaume Gruel, Marcelo Martins Meira, Florian Savona, Christophe Bourdin
- **Presence studied in a driving simulator**
  Christophe Deniaud, Vincent Honnet, Benoît Jeanne, Daniel Mestre
- **Validating On-the-limit properties of a driving simulator**
  M. Hjort, S. Kharrazi, O. Eriksson, M Hjälmdahl, J. Andersson Hultgren
- **Colour-Difference Assessment for Driving Headlight Simulation**
  Quentin Vidal, Sylvain Michelin, Baptiste Laborie, Andras Kemeny
- **Variable Roll-Rate Perception in Driving Simulation**
  Paolo Pretto, Alessandro Nesti, Suzanne Nooij, Martin Losert, Heinrich H. Bülthoff
- **Simulation sickness comparison between a limited field of view virtual reality head mounted display (Oculus) and a medium range field of view static ecological driving simulator (Eco2)**
  Baris Aykent, Zhao Yang, Frédéric Merienne, Andras Kemeny
- **How much visual attention does braking require? A study of the effect of memory of the scene on driver's braking behavior**
  Mehdi Saffarian, John W. Senders
- **Roll tilt thresholds for 8 DOF driving simulators**
  Zhou Fang, Florent Colombet, Jean-Christophe Collinet, Andras Kemeny
- **The influence of lateral tilt/translation, roll and yaw scale factors on driving performances on an advanced dynamic simulator**
  Florian Savona, Anca Stratulat, Emmanuelle Diaz, Vincent Honnet, Gilles Houze, Philippe Vars, Stéphane Masfrand, Vincent Roussarie, Christophe Bourdin
- **Coping with complex driving scenarios: Exploratory Scenario Design**
  Julian Schindler, Tobias Hesse
- **Effects of haptic versus visual modalities when combined with sound in forward collision warnings**
  Mikael Ljung Aust
- **Driver Distraction among Commercial Vehicle Operators: A Study Using a Driving Simulator to Enhance Control**
  Ronald W. Tarr, Eric Paul Totten

Motion Rendering

- **An Algorithm for False Cue Reduction and Prepositioning**
  IG Salisbury, DJN Limebeer
- **The Effect of Motion Cueing on Simulator Comfort, Perceived Realism, and Driver Performance during Low Speed Turning**
  Gary Bertollini, Yi Glaser, Joseph Szczerba, Ron Wagner
- **An MPC approach to the design of motion cueing algorithms for a high performance 9 DOFs driving simulator**
  Mattia Bruschetta, Fabio Maran, Alessandro Beghi, Diego Minen
- **Review and prospects of Renault's MPC based motion cueing algorithm for driving simulator**
  Zhou Fang, Andras Kemeny
- **Subjective Evaluation of Different Motion Cueing Algorithms Implemented on ATMOS Driving Simulator**
  Imad Al Qaisi, Daniel Zimmermann, Andreas Kohlstedt, Sandra Gausemeier, Ansgar Trächtler

Simulation Design and Architecture

- **Real vs. simulated surrounding traffic – Does it matter?**
  Dominik Muehlbacher, Lena Rittger, Christian Maag
- **A Networked Multi-Drivers Simulation Platform for Interactive Driving Behavior Study**
  Jing Xu, Yingzi Lin
- **Scalable and Detail-Preserving Ground Surface Reconstruction from Mobile Laser Systems for Driving Simulators Engines**
  Daniela Craciun, Jean-Emmanuel Deschaud, François Goulette
- **Steerable Video: Generating Video-Based Environments for Driving Simulation**
  Michael Brogan, Charles Markham, Sean Commins, Catherine Deegan
- ***Development and Validation of a Safety Architecture of a Wheeled Mobile Driving Simulator***
  Alexander Betz, Paul Wagner, Torben Albrecht , Hermann Winner
- **Comfort analyses of the Hydractive suspension using a driving simulator**
  S. Barale, P. Vars, J. Guillet, M. Alirand, J. Lagnier, P. Toulemont

Product Solution and Posters

- **Design and Performance of the VTI Sim IV**
  Jonas Jansson, Jesper Sandin, Bruno Augusto, Martin Fischer, Björn Blissing, Laban Källgren
- **Modular and scalable driving simulator hardware and software for the development of future driver assistance and automation systems**
  Martin Fischer, Andreas Richter, Julian Schindler, Jens Plättner, Gerald Temme, Johann Kelsch, Dirk Assmann, Frank Köster
- **OpenDriving: An Open Source Driving Simulation Software**
  Zhitao Xiong
- **SleepNoise - a simulator based study of the effects of noise on driver sleepiness**
  Eva Lahti, Anders Genell, Anna Anund
- **Small-scale traffic demonstrator with driving simulator**
  Oleksandr Goloborodko, Georg-Peter Ostermeyer

- **Combined motion of a hexapod with a XY-table system for lateral movements**
  Jürgen Pitz, Minh-Tri Nguyen, Gerd Baumann, Hans-Christian Reuss
- **Effect of simulated rumble strips in static driving simulator – Pre-study**
  Plouzeau Jérémy, Paillot Damien, Aykent Baris, Mérienne Frédéric
- **Robot based Driving and Operation Simulation with a spherical fixed Screen**
  Eduardo Pena Vina, Andrey Gizatullin, Manuel Schiewe, Michael Kleer, Klaus Dreßler
- **Nissan's New High Performance Driving Simulator for Vehicle Dynamics Performance & Man-Machine Interface Studies**
  Yoshiki Yasuno, Eiichi Kitahara, Takashi Takeuchi, Masashi Tsushima, Haruki Saitou, Masayuki Imamura, Erina Ueno
- **HDR simulation of intelligent LED road studs**
  Nguyen-Thong Dang, Fabrice Vienne, Roland Brémond

INTRODUCTION

Olivier Colmard[1], Andras Kemeny[2]

(1): VP, PLM, CAE and Digital Mock-Up, Renault, Test and Service Engineering, DEA-T
olivier.colmard@renault.com

(2): Director, LIV, Renault-Arts et Métiers ParisTech. Head of VR and Immersive Simulation, Renault, Test and Services Engineering, DEA-TD. Chairman of the DSC Europe 2014

Driving simulation with automotive applications has started in the 70-s and is still in development. Daimler has built a new scale 1 driving simulator just a couple of years ago, and at DSC Europe 2012 we could learn about the characteristics of this high performance installation. The Renault-Nissan Alliance, which have had already more than a half dozen simulators in use, has seen the advent of new simulation technology combining traditional driving simulation and virtual reality technologies, used for autonomous vehicle and vehicle augmented reality applications at Renault. It will see in the coming years one of the world most advanced driving simulator installed at Nissan, Japan, for advanced vehicle dynamics and man-machine interface studies. Finally the Alliance is also using for vehicles developed in common by Daimler and Renault Daimler's high performance driving simulator, showing also the new trend of shared use of advanced simulation technology.

Driving simulation is now appearing also in virtual reality installations, such as head-mounted display systems and CAVE-s. Nevertheless, in these installations, all the well-known problems when using static driving simulators are newly experienced, including simulation sickness, due mainly to visuo-vestibular conflict and unacceptable transport delays. On the other hand, the very high resolutions 4K and better display systems are providing near eye resolution and high image quality image rendering, authorizing new applications, such vehicle styling, architecture and perceived quality.

Another new application domain is connected vehicle simulation and DSC Europe 2014 may experience some renewed discussions for a better use of these applications. As the world is continuously connected today and entering the vehicle there should not be any disruption, on the contrary, new services should appear, simulation platforms for connected vehicles should become a standard in the automotive industry.

Renault continuously supports since a number of years the Driving Simulation Conferences, since 1995. This shows the strong commitment the Renault Nissan Alliance puts in these techniques and methods with the corresponding user processes. At Renault the digital expertise sector includes more than 1200 people dedicated to digital engineering design. This domain is coupled more and more with immersive simulation technics, including driving simulation and virtual reality. The birth of the LIV – Laboratory of Immersive Simulation, a research laboratory between Renault and Arts et Métiers ParisTech in 2011 is a good example of this commitment.

We are very much pleased to host this new edition of the Driving Simulation Conference Europe 2014 at Arts et Métiers ParisTech this year and wish a rich exchange with the authors and participants during the conference.

Perception and Human Factors

Are We There Yet? An Objective Mechanism to Support the Assessment of Driving Simulator Utility

Erwin R. Boer[2], A. Hamish Jamson[1], Sunjoo K. Advani[3], Anthony J. Horrobin[1]

(1) Institute for Transport Studies, University of Leeds, UK.
a.h.jamson@its.leeds.ac.uk
a.j.horrobin@its.leeds.ac.uk

(2) Entropy Control Inc., San Diego, USA.
ErwinBoer@EntropyControl.com

(3) International Development of Technology, Breda, NL.
s.advani@idt-engineering.com

Abstract – Virtual prototyping using driving simulators offers a highly cost effective alternative to test track evaluations. A pressing question asked by car manufacturers is what level of simulator fidelity is needed for evaluating a particular vehicle, vehicle sub-system, driver control interface, or driver infotainment system. This paper adopts a driver modelling perspective to addresses this question and defines a process based on a simulator utility-triplet to establish whether a simulator yields absolute behavioural fidelity for a particular driving task. The adopted driver model is a cybernetic cascade model that includes perception of multi-modal cues that drivers use to assess vehicle state relative to the environmental constraints. These multi-modal cues in the simulator are perceived through the particular simulator's rendering transfer function that may cause driver adaptations to yield the desired performance level. By exploring the degree to which model coefficients differ from those observed in reality across a number of basis-tasks, an objective assessment is established to objectively compare and contrast different prototype evaluation environments.

Key words: Cybernetic Driver Model, Simulator behavioural Fidelity, Driver Performance Assessment, Cue Rendering, Virtual Prototyping.

1. Introduction

Research driving simulators are commonly used to facilitate scientific evaluations of driver behaviour. Whilst designers of such simulators strive to reproduce high quality visual, vestibular, proprioceptive and auditory cues within their facilities, both financial and technological constraints limit a simulator's capability to fully recreate a real driving environment. When established [e.g. Bel1], demonstration of a driving simulator's relative behavioural validity [Bla1] justifies its use in driver behavioural studies [Kap1].

A much less frequent use of driving simulation is in the support of vehicle design. Such virtual prototyping has the advantage of reducing the need to develop expensive physical vehicle prototypes, but carries with it the unenviable burden of guaranteeing the simulator's absolute behavioural fidelity. However, with a task-based approach, this burden becomes realistic. The nature of vehicle design is that a number of specific driving manoeuvres define typical objective evaluations of a vehicle's performance, ride, handling and stability characteristics. In effect, this allows a corresponding task-based assessment of simulator fidelity, not unlike the competency-based approach of the International Civil Aviation Organisation's (ICAO, 2010) published recommendation (ICAO 9625) to National Aviation Authorities to regulate member state's use of Flight Simulation Training Devices (FSTD).

In order to tie the technical requirements of a FSTD more closely to the level of pilot training or skills assessment required, ICAO 9625 provides a mapping between a FSTD's characteristics and the associated training that may be performed with devices having such features. This certification is made against a list of tasks dictated by the procedural and methodical nature of commercial pilot training and skills evaluation. By defining the tasks required of the pilot, the demands required of the simulator itself are more easily identified. With this task classification central, it becomes possible to define acceptable simulator

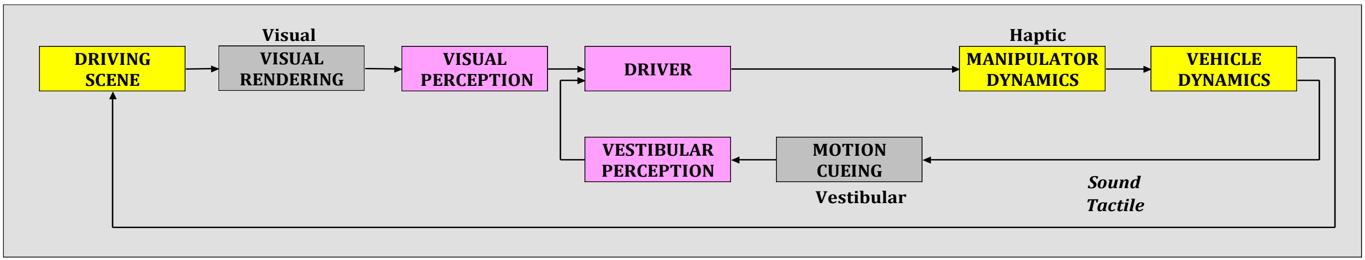

Figure 1. Driver's perception (magenta boxes) in a simulator takes place through cue rendering transfer functions (grey boxes). It is assumed that yellow boxes can be represented veridical in a simulator because those are not the most cost consuming simulator components; motion and visual system are most costly.

characteristics by assessing the ability of the FSTD to support flight crew training/assessment within the operational range of the simulator defined by those characteristics.

In contrast, assessing the merits of a particular car design is generally the responsibility of the vehicle manufacturer, whose interest is in understanding the implications of minor changes in vehicle stability, suspension, assist systems, body re-design, etc. Typical assessments require test drivers to evaluate safe, agreeable and controlled operation of the vehicle based on a perception of the entire driving environment. Theoretically, defining this plethora of tasks in order to, in turn, define an acceptable driving simulator operational range is possible. The cardinal challenge, however, lies in defining "acceptable" fidelity; the focus of this paper.

1.1. Simulator Utility Quantification

Cybernetic driver models have been used to quantify how drivers perceive cues and integrate them to produce vehicle control actions. Even through most tend to exist only for lateral, lane-keeping manoeuvres [see Ste1 for a recent review], such models have previously been used to objectively assess the design of driving simulators for curve negotiation tasks [Dam1].

The drawback of existing driver models is that few explicitly model driver's perception and integration of available cues. Such a low-level perception model is needed to understand how the particular cue-rendering employed by the simulator influences driver behaviour. Figure 1 shows that simulators add extra dynamics into the perception-action loop in the form of cue-rendering transfer function (grey boxes) and therefore force the driver to adapt in order to maintain equivalent performance. To be able to understand and predict the effect of different simulator cue rendering techniques, we need to know how drivers use these cues at the lowest level. We recommend that simulator developers characterize their simulators based on cue rendering transfer functions as a means to report objective simulator cue-fidelity.

Under normal driving conditions drivers learn to use the available multi-modal cues when they provide a benefit to control performance and stability [Pas1]. In the cascade control of the cybernetic driver model, feedback loops of vehicle position, velocity, acceleration and steering torque are present. The driver perceives these different cue channels with different sensory organs and these cues are rendered by the simulator with different transfer functions. Thus if a channel is removed such as motion or steering torque, then those vehicle states can no longer be directly perceived and have to therefore be estimated based on derivatives of other cues. For example, acceleration, which is normally perceived directly with the vestibular organ, can also be perceived by taking derivatives of visual cues. Taking derivatives requires sampling, introducing a delay. Thus removal of a cue that offers direct perception of a vehicle state will introduce a delay in one of the feedback loops. A delay in one of the feedback loops results in less stability can be observed in these data as larger control actions, more corrective control actions and a more intermittent control. The removal of cues shows its effect especially in high bandwidth manoeuvres such as a chicane or double lane change for which visual cues alone are not fast enough to yield sufficient stability [Hos1].

While existing models [Ste1] are certainly suitable to show differences in behaviour caused by different cue rendering techniques by showing different model coefficients for different cue rendering techniques [Dam1], they cannot predict the effect of such different rendering techniques a-priori.

The ultimate goal of our cybernetic driver model is that it can be used as a standalone virtual prototyping tool and for that it is necessary to explicitly model cue perception and integration as well as the performance goals and adaptation mechanisms that drivers use to adapt their behaviour so that the model produces emergent behaviour that matches what is observed in reality. This long term self-organizing model goal will not be discussed any further in this paper.

Driving is not simply a combination of open and closed loop controllers; it also requires learning of more complex control profiles to be able to perform complex manoeuvres such as parking or optimal obstacle avoidance. These manoeuvres cannot be modelled as simple stimulus response controllers but require at least integration of information up to some horizon and shape the control profile to optimize some performance criterion. Normally, models based on optimal preview control [Tom1] are used or a more modern approach based on model predictive control [Kee1]. Our current scientific challenge is to combine perceptual driver models with cue integration and model predictive control models with explicit performance optimization such that the resulting cybernetic model can predict effects of changes in cue fidelity (effect of simulator) or the introduction of a new support system (effect of vehicle).

The current paper focusses on the first practical steps that will ultimately aid car manufacturers to know whether a simulator is suitable for evaluating a particular prototype. For this, we present a mechanism to quantify a simulator's behavioural fidelity.

2. Method

By focusing on just one of the many manoeuvres defined in a typical vehicle's verification programme, vehicle handling through a double lane-change or chicane [ISO 3888-2], this paper attempts to combine ICAO's competency-based approach with cybernetic driver modelling to define a methodology to assess simulator utility for this specific task in virtual vehicle prototyping.

2.1. Cybernetic Driver Model

A cybernetic driver model has been established to describe the transfer functions that map cues (perceptions in the simulator) to control (handling of the vehicle). Focus is directed primarily to visual, vestibular and haptic cues but other domains are also recognized as potentially important in yielding realistic driver behaviour in simulators. The model under development is a cascade controller based on the classic cross-over model applied to vehicle handling (STI Driver Model – McR1), but expanded to both lateral and longitudinal vehicle handling. A simplified version is depicted in Figure 2 for the purpose of highlighting the various components that make up the current version of the model. The model in its current incarnation is a pure open plus closed loop model and does not explicitly include usage of the entire preview nor optimize an extended control profile as is done in optimal control or model predictive control models. These elements are being added later.

The proposed cybernetic model not only models the dynamics of the visual, vestibular and neuro-muscular sensory organs but also their integration into a single internal representation of relevant vehicle states. Most existing models simply assume direct

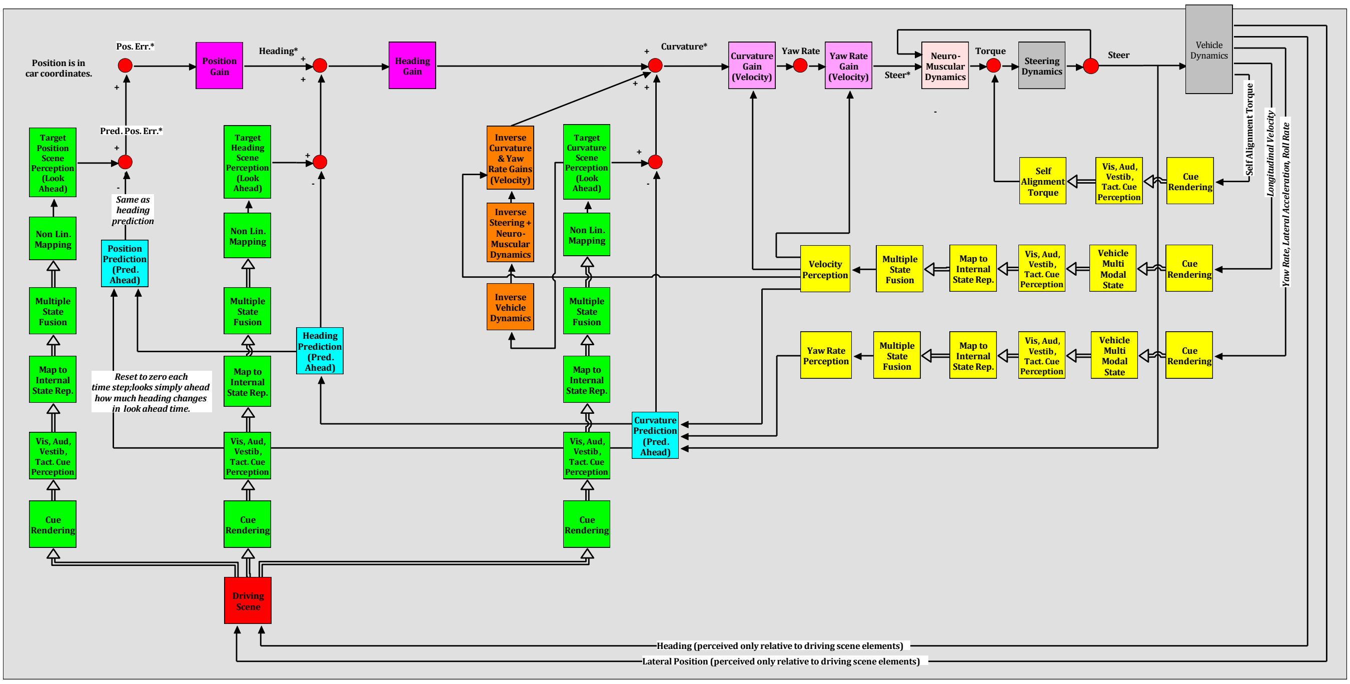

Figure 2. Cybernetic driver model for lateral-control only (for space reasons). See text for detailed explanation of the adopted colour scheme.

perception of these vehicle states and show how model gains change under different conditions but such models do not provide an explicit explanation of the mechanism that results in the final model coefficients; as discussed earlier, such models cannot be expected to predict effects of changes in cue rendering or be used to optimize cue-rendering strategies.

The model in Figure 2 shows several types of boxes each indicated by a different colour:

- The perception of absolute vehicle state fundamentally influenced by cue rendering and cue perception (yellow).
- The perception of relative vehicle state, based primarily on visual environmental cues including preview (green).
- Feed-forward open loop control, representing a driver's internal model relating vehicle control actions to vehicle dynamics (orange).
- Prediction, based on look-ahead time to equalise lags and delays in human/vehicle system (cyan).
- Proprioceptive feedback, modelled as the coupling between the neuromuscular part of the driver and the pedal/steering manipulator dynamics (pink).
- Non-linear control, described as a component of each environmental state perception branch that feeds into the feed forward control path as well as into the error calculation of perceived minus predicted curvature / acceleration (green).

A fully detailed exposition of the model is beyond the scope and spatial constraints of the paper. Here it suffices to state that the sketched cybernetic model is needed for modelling driving manoeuvres such as stopping, lane changing, and obstacle avoidance. The vast majority of existing model focus on car following and gentle radius curve negotiation which can be modelled well without resorting to optimal preview models and a strong use of internal models because of the relatively low bandwidth of the conditions generally studied.

As stated earlier, the target of our cybernetic model development is for it to produce realistic driver behaviour from first principles rather than through explicit identification of model coefficients. In other words, the model should through self-organizing optimization of the balance between performance/safety and effort, be able to match observed driver behaviour in reality (no cu-rendering) and simulator (with cue rendering). An example of such a model for car following in fog is detailed in [Car1]. However, a general full blown self-organizing model is still years removed from maturation but the current research program at U-Leeds with extensive studies comparing real world and simulator driving across a set of basis driving tasks with a limited group of skilled drivers performing all real world and simulator trials is well situated to establish such a model.

2.2. Driving Manoeuvre/Task

The specific driving task targeted in the remainder of this paper, a double lane, is shown in Figure 3. The task was performed in two driving environments with a single driver, one driver in reality and one driver in the virtual conditions of the University of Leeds Driving Simulator, UoLDS [Jam1]. The total length of the high speed chicane (orange dots) is 50m which is half a sinusoid in steering. At 60kph or 17.14mps takes about 3s. Speed was controlled automatically in the UoLDS.

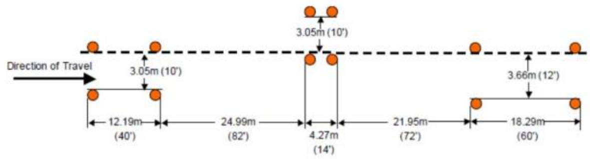

Figure 3: Double lane change cone placement as replicated in the UoLDS.

In reality, the task was performed by a Jaguar Land Rover test-driver in a XF model vehicle on a frozen lake on a proving ground in Sweden. The recorded coefficient of friction of the surface was 0.3 and the task was performed at 60kph without any active vehicle control systems enabled. The driver was instructed to produce the desired target speed which test drivers are highly skilled at.

The same conditions were recreated in the UoLDS and the single driver, experienced with the handling of the simulator under full feedback configuration, undertook the task in three conditions, repeating each four times:

- *Baseline*: simulator operational with full motion and steering torque feedback.
- *NoSteer:* motion system on but without any steering feel provided to the driver.
- *NoMotion:* steering feedback on but without any inertial cues provided to the driver by the motion system.

Here we only report on the performance in the simulator and leave model fitting to a follow-up paper. The main reason for this choice is that the behaviour in the simulator shows fundamentally different behaviour as we discuss in section 4 below.

2.3. Utility Score of Behavioural Fidelity

Behavioural fidelity in this context is defined as the degree to which behaviour in the simulator (UoLDS) during the double lane-change is statistically indistinguishable from the test-track. Evaluation of behavioural fidelity through time-series comparison alone lacks the conclusive insight into the effect of the driving simulator system on the driver. For example, the same level of performance can be achieved with different levels of effort depending on how easy it is to control the vehicle. Hence, three levels of behavioural fidelity assessment are defined, the Utility Triplet.

- *Aggregate Performance* looks at specific metrics that can be extracted from the vehicle state or driver control that quantify performance, risk or effort. This includes spatial and temporal proximity to constraints as well as completion time. Focus is placed on accuracy or the degree to which the task was performed and includes metrics such as standard deviation of steering angle or steering rate. These aggregate metrics can be computed from the available signals without any special decision logic. These aggregate metrics do not really show when and how control is applied.
- *Time Series Comparison* profile driver control actions as a function of time and distance in the manoeuvre, showing when and how control is applied in order to gain insight into the specifics of control. Examples of these metrics are peak to peak analysis in steering rate such as number and magnitude of corrective steering actions, or the lag between control actions and specific vehicle states. These metrics require development of signal specific logic to extract the meaningful time series related metrics.
- *Transfer Function* analyses place focus on perceptual input to control actions rather than vehicle movements, predominantly as time series metrics do not really show what caused the production of the specific control signal profile. In case of the current study, the cybernetic driver models combines open and closed loop control, as well as hard code the availability of different feedback channels (e.g. haptic or vestibular). Human perception and execution are necessarily noisy and thus errors build up even if the driver has a perfect internal model of the environmental constraints and the vehicle. In theory, the driver adapts to yield maximal performance at minimal effort; if this mechanism can be explicitly modelled, then we have made a significant step not only in understanding human drivers but also towards the use of models in virtual prototyping. The metrics here are model coefficients together with estimates of standard error as obtained using the statistical bootstrap method.

To judge a simulator's utility for virtual prototyping, the metrics of all three elements of the utility triplet have to be statistically equivalent; i.e. within normal behavioural variability within and between drivers.

3. Results

Behaviour in the three simulator conditions in the simulator is analysed to establish the impact of motion vestibular feedback and manipulator torque feedback on performance of a double lane change at 60kph. The subject performed each condition 4 times but we only show the last two trials to allow for some behaviour adaptation in the subject.

3.1. Aggregate Performance

The chicane task was performed according to specifications; i.e. no cones were clipped. We also saw that the lower maximum lateral acceleration was observed with full feedback than with either no motion or no steering feedback but, as is often the case, those differences were not as substantial as those observed in the manner in which the driver steered the vehicle to achieve these task performance levels.

3.2. Time Series Comparison (Profiles)

The trajectories in Figure 4 show that they are clustered per condition. We see that the driver steers back sooner when realistic feedback is missing possibly because they over-steer in the first place. Such over-steering is reasonable given the fact that the driver may have expected a build-up of vestibular or steering torque signal that he normally may use to gauge rate and timing of steering actions.

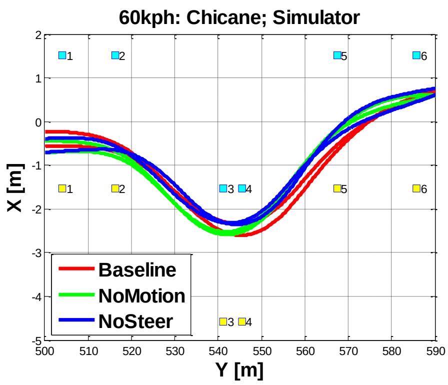

Figure 4. Trajectory of chicane in three simulator configuration conditions.

Such usage of vestibular and haptic cues is not expected to adapt away in 4 trials. Naturally, when the driver is given ample time to adapt, he/she will adopt a new driving strategy that does not rely on those cues. Here we looked at the effect of removing cues on performance.

The steering profiles in Figure 5 do indeed show that the driver steers into the manoeuvre more aggressively (higher peak and rate around 530m) and also steers back more aggressively (around 555m). Because of the overly rapid and strong steering control, the vehicle is perturbed more and the driver has to work harder to correct and re-stabilize the car which is also clearly seen in the greater peaks in the steering rate (bottom panel of Figure 5).

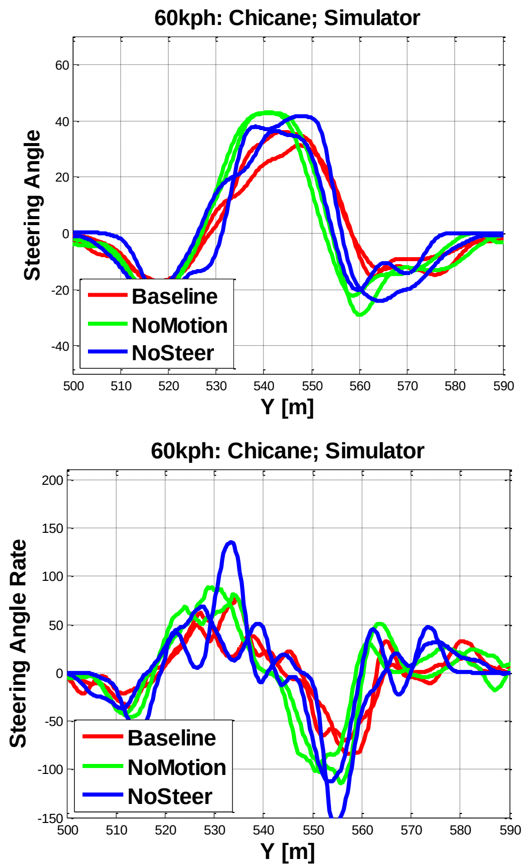

Figure 5. Steering (top) and steering-rate (bottom) profiles as a function of distance down the main axis of the lane change (y-world).

3.3. Time Series Comparison (Metrics)

In order to put quantitative metrics on these time series observations, several metrics specific for the chicane were developed. A sensitive metric is the peak to peak (peak2peak) behaviour in the steering rate because it shows the magnitude of actions (necessary to make the double lane change) and corrections (necessary to stabilize the vehicle) as well as the number of control actions and corrections made. Because we are looking at simulator data, no sensor noise is added and therefore no filtering is needed to eliminate steering rate peaks caused by noise. The resulting metrics are described next and shown in Figures 6 and 7:

- Steering Rate STD (not shown) showing the total power in steering actions and corrections that the driver applies.
- Sum of all absolute magnitudes between successive peaks in the steering rate signal (Figure 6).
- Relationship between the median steering action/correction and the number of steering action/corrections (figure 7).

Figure 6 clearly shows that the total steering-rate-power (std) increases when valuable cues are removed. No motion feedback and no steering feedback both show increased corrective control power as if open loop control was no-longer as effective; this is expected because the driver was not given time to settle into a new open loop control strategy without using motion or steering feedback.

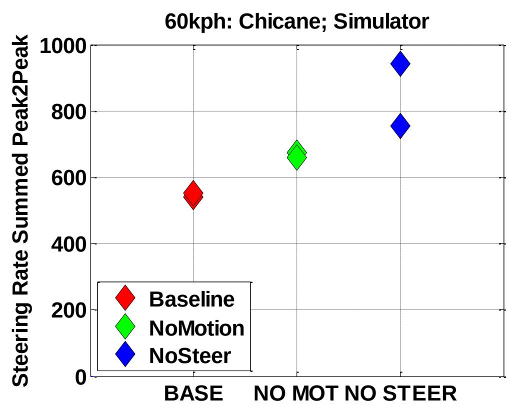

Figure 6. Summation of all absolute peak2peak magnitude changes in steering rate.

Figure 6 shows that the total sum of the absolute value of all the steering corrections (i.e. peak2peak magnitudes in steering rate signal). This does not integrate over time as for an standard deviation but over the number of steering peaks. Figure 6 shows that the NoSteer (blue) condition lies fully above the NoMotion (green) condition suggesting that the driver performs more frequent large corrections without the steering feedback than without the motion feedback; probably because the steering feedback loop is fastest.

Figure 7 shows that the number of steering corrections is highest and weakest when motion and steering feedback are available (red) and that corrections are stronger and less frequent when feedback cues are removed.

This particular fact is discussed below in the context of the cybernetic driver model.

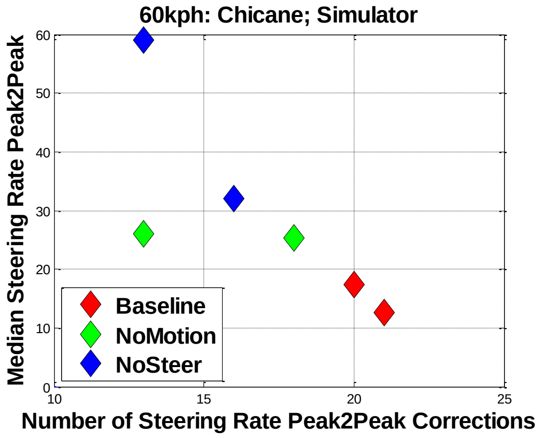

Figure 7. Median absolute peak2peak magnitude changes vs number of peak2peak steering corrections.

3.4. Transfer Function

A most compact and informative quantification of behaviour is through estimation of model coefficients or cost function weights. As detailed in the discussion, further model development to include optimal preview control for a discrete open loop manoeuvre task such as the chicane is needed which remains to be done.

4. Discussion

Metrics should be an embodiment of those task aspects that drivers take into consideration in the learning/adaptation process of arriving at an acceptable control strategy. They are the performance metrics that are fed back to adaptation. It is therefore crucial to establish metrics that are meaningful for drivers as they will ultimately fuel the development of human-like self-adapting models that can be used as powerful virtual prototyping tools; i.e. that do not need simulator or real world data any more.

The time series analysis showed an initial steering overshoot in the no-steer and no-motions conditions suggesting that the driver either had an internal model that included torques/accelerations and/or was expecting a torque/acceleration build-up from the car that did not occur thus resulting in an overshoot.

The driver can of course adapt to a no-steering/no-acceleration feedback condition by simply removing those cues from his perceptual motor control interaction. The question then becomes whether the same performance can be achieved (not expected for high bandwidth manoeuvres simply because deviations from expected vehicle response cannot be detected as quickly and thus a greater error builds up) and whether it is performed with the same controller structure (drivers may adopt a new control strategy to manage the impoverished cue rendering). In either case, the metrics associated with the utility-triplet will differ significantly between reality and simulator.

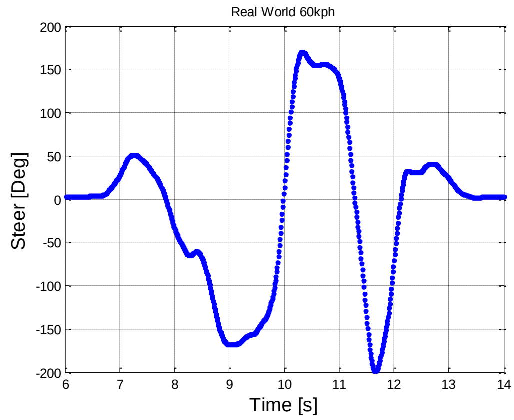

Figure 8. Real world steering angle profile of a chicane manoeuvre at 60kph.

The real-world steering profile as shown in Figure 8 shows a fundament difference with respect to the steering profiles we observed in the simulator (red lines in top panel of Figure 5). The real world steering shows an anticipatory steering action signifying either a swing wide to effectively widen the entry into the chicane or a small shift in weight balance that aids subsequent traction. Such an acausal steering action will not emerge from a pure stimulus response model; it requires a learned behaviour that results from exploration that can only be modelled by optimizing over the entire trajectory; similar to what the driver does over multiple repeated trials. This is one reason why an optimal preview control or model predictive control components has to be part of the final cybernetic model.

At the moment our model does not include such an optimal preview control component and thus it was decided not to show model results but rather focus more on understanding the observed differences in performance between the three simulator conditions.

Because our simulator driver was experienced in driving the simulator with motion and steering feedback enabled, his mental models and internal models were tuned to using these feedback cues. Without torque and acceleration feedback cues the driver has to rely on slow visual feedback cues about vehicle state and movement. Because visual feedback is slow, errors build up over a longer period and therefore to a higher magnitude. This means that the driver will exhibit larger and less frequent corrections when fast feedback is not available. This is exactly what we observed in Figure 7. The fact that corrections are less frequent is partly caused by the extra delay in using visual versus vestibular/torque feedback and partly caused by the fact that Just Noticeable Differences are higher for visual than vestibular/torque feedback.

Over time the diver is expected to adopt a different control strategy but at a high speed of 60kph he is not expected to be able to yield the same level of performance especially when normal perturbations are present such as uneven tracks in the snow or an otherwise uneven road surface. Without natural perturbations, humans are able to perform open loop control very accurately and thus it may appear as if they can yield the same performance in the simulator as in reality even with minimal feedback cues. This is why it is crucial that disturbances experienced in the real world are also represented in the simulator.

5. Conclusion

Understanding the behavioural difference between the three conditions (baseline with motion and steer torque on, no motion, and no steer feedback) requires assessment along each dimensions of the performance triplet. The aggregate performance looks at specific metrics that can be extracted from the vehicle state or driver control that quantify performance, risk or effort. Examples of these metrics are minimum proximity to the cones, standard deviation of steering angle or steering rate. These aggregate metrics can be computed from the available signals without any special decision logic. These aggregate metrics do not really show when and how control is applied. To gain insight into the specifics of control, it is necessary to explore the available time series more deeply. Examples of these metrics are peak to peak analysis in steering rate such as number of corrective steering actions and magnitude of corrective steering actions, or the lag between control actions and specific vehicle states. These metrics require development of signal specific logic to extract the meaningful time series related metrics. These time series metrics do not really show what caused the production of the specific control signal profile; to gain insight into what caused changes in control profiles, it is necessary to look at transfer functions and model coefficients.

The techniques outlined in this paper provide an objective methodology to evaluate the appropriateness of a particular simulator to appropriately characterise a specific driving task. Furthermore, the cybernetic model based approach can also provide insight into the causal mechanisms from cues to behaviour. Such a method can not only identify which modifications to an existing facility are most likely to maximise utility, but also advise on the appropriateness of simulator acquisitions or its potential to perform acceptance tests. To the best of our knowledge, no such driving simulator assessment methodology currently exists. To the question “Are we there yet?” the answer is two-fold. We believe on the one hand that the proposed approach is full of utility but on the other hand we realize that much more test track and simulator research is needed to develop necessary models.

6. References

[Bel1] Bella, F. (2005). Validation of a driving simulator for work zone design. Transportation Research Record, 1937, pp. 136-144.

[Bla1] Blaauw, G.J. (1982). Driving experience and task demands in simulator and instrumented car: a validation study. Human Factors, 24(4), pp. 473–486.

[Car1] Caro, S., V. Cavallo, C. Marendaz, E. Boer, F. Vienne (2009) Can headway reduction in fog be explained by impaired perception of relative motion?, Human Factors: The Journal of the Human Factors and Ergonomics Society, 51(3), pp. 378–392.

[Dam1] Damveld, H.J., Wentink, M., van Leeuwen, P.M. & Happee, R. (2012). Effects of motion cueing on curve driving. Proceedings of the Driving Simulation Conference Europe 2012 (DSC2012), Paris, September 6-7 2012, pp.11-21.

[Hos1] Hosman, R.J.A.W. & van der Vaart, J.C. (1981). Effects of vestibular and visual-motion perception on task performance. Acta Psychologica, 48, pp. 271–281.

[Jam1] Jamson, A.H., Horrobin, A.J. and Auckland, R.A. (2007). Whatever Happened to the LADS? Design and development of the new University of Leeds Driving Simulator. Proceedings of the Driving Simulation Conference North Amercia 2007 (DSCNA2007), Iowa City, September 12-14 2007.

[Kap1] Kaptein, N.A., Theeuwes, J. & van der Horst, A.R.A. (1996). Driving simulator validity: some considerations. Transportation Research Record, 1550, pp. 30-36.

[Kee1] Keen, S.D. & Cole, D.A. (2006). Steering control using model predictive control and multiple internal models. Proceedings of AVEC '06. The 8th International Symposium on Advanced Vehicle Control, August 20-24, 2006, Taipei, Taiwan.

[McR1] McRuer, D.T., Allen, R.W., Weir, D.H., and Klein, R (1977). New results in driver steering control models. Human factors, 1977, 19, 381-397.

[Pas1] Passot, J.B., Luque, N., Arleo, A. (2010): Internal Models in the Cerebellum: A Coupling Scheme for Online and Offline Learning in Procedural Tasks. SAB 2010: 435-446.

[Ste1] Steen, J., Damveld, H.J., Happee, R., van Paassen, M.M. & Mulder M. (2011). A Review of Visual Driver Models for System Identification Purposes. IEEE International Conference on Systems, Man, and Cybernetics (IEEE SMC), Anchorage, October 9-12 2011, pp. 2093-2100.

[Tom1] Tomizuka M (1974), The optimal finite preview problem and its application to man-machine systems. PhD Thesis, Massachusetts Institute of Technology.

REAL VS VIRTUAL DRIVING OR HOW TO IMPROVE THE REALISM OF A DYNAMIC DRIVING SIMULATOR

Anca Stratulat [1], Emmanuelle Diaz [1], Philippe Vars [1], Stephane Masfrand [1], Laurent Leblond [1], Guillaume Gruel [1], Marcelo Martins Meira [1], Florian Savona [1,2], Christophe Bourdin [2]

(1): PSA Peugeot-Citroën
Centre Technique Velizy
Velizy-Villacoublay, France
+33 1 57 59 25 37
E-mail : {ancamelania.stratulat, emmanuelle.diaz, philippe.vars, stephane.masfrand, laurent.leblond, guillaume.gruel, marcelo.martinsmeira, florian.savona}@mpsa.com

(2): Aix Marseille Université, CNRS, ISM
UMR 7287, 13288, Marseille, France

E-mail : christophe.bourdin@univ-amu.fr

Abstract

Most of the dynamic driving simulators are using a constant under-unit scale factor, which is recommended between 0.4 and 0.75 depending on the studies, to produce realistic driving perception. However, other studies on passive driving showed that the scale factor should depend on the level of acceleration, suggesting that a constant scale factor would be less efficient. But none of these studies have validated their results obtained on simulators by comparing them to real driving situations. In our study, we aimed to determine 1/ the best value of the scale factor for the perception of a realistic acceleration, 2/ if this scale factor should be constant or not (evolving with the level of acceleration) by comparing driving behaviours recorded in real and comparable simulated situations. The results show a very small behavioural variability between the real and the virtual driving tasks. The most realistic combination of scale factor and tilt/translation is influenced by the tilt/translation ratio, especially when less tilt is used.

Key words: perceptual validity, longitudinal acceleration, self-motion perception, scale factor, tilt-coordination.

1. Introduction

It is generally accepted that the validity of a driving simulator is based on several aspects: physical, perceptual, relative behavioural and absolute behavioural validity [Rey1]. Still, a motion based driving simulator has a limited physical validity due to its mechanical limits. Therefore, the optimization of the driving simulators should mostly be based on perceptual validity, which should consist in comparing the driver's multisensory perception of self-motion to a real situation. Yet, most of the studies carried out until now were concentrating only on the motion perception in virtual environment, weakening the conclusions on perceptual validity. Nevertheless, it is known that, on dynamic driving simulators, the vehicle motion is overestimated and therefore, a constant under-unit scale factor must be used for the motion cueing algorithms [Gro1]. The paper of Berthoz and colleagues [Ber2] showed that this scale factor should be between 0.4 and 0.75 depending on the studies. However, our previous study on motion perception in driving simulators suggested that this scale factor should not be constant, but adapted to the level of acceleration induced by the driving task [Str2]. Still, scale factor is not the only useful parameter for the simulation of linear accelerations. The tilt-coordination technique, which is used on almost all driving simulators, brings an important benefit for the simulation of strong accelerations. However, there are still some questions regarding the quantity of tilt and translation that should be used in order to produce a realistic acceleration [Gro2, Ber1]. This is due to the fact that the perception of linear acceleration in passive driving seems to be directly influenced by the tilt/translation ratio [Str1]. Nonetheless, there is a perceptual difference between passive and active driving, given the cognitive involvement in the task of the driver during the latter (man-in-the-loop) and the fact that the acceleration is produced by the driver himself, while he's submitted to a predefined profile of acceleration during passive driving. Then, these previous contradictory results concerning the scale factor as well the effect of the tilt/translation ratio have to be accurately questioned in a more systematic way. As a result, we propose to implement a study on active driving that allows us to a/ evaluate the value of the most adapted scale factor b/ determine if the scale factor should be constant or not (evolving with the level of acceleration), c/ evaluate the best tilt/translation ratio for active driving and last, but not least, d/ to compare the induced perceptions of simulated longitudinal accelerations to a similar real car driving task and e/ to validate an experimental design adapted for driving simulation studies. This will allow us not only to answer to the previous questions, but also to define a setting of parameters for the motion cueing algorithm that will improve the realism of our simulator and therefore to reach a perceptual validity.

This study is included in an OpenLab research program, developed in collaboration with the Institute of Movement Sciences of Marseille.

2. Background

Our dynamic driving simulator, Sherpa² [Str1, Str2], like all dynamic driving simulators, needs to use technical artifices in order to simulate a linear acceleration. The first used artifice is a physical one, called scale factor: the real value of the acceleration is reduced by an **under-unit scale factor** (the choice of the scale factor is due to the overestimation of accelerations on dynamic driving simulators [Gro1]):

$$\underbrace{\ddot{x}_t^{Sherpa}}_{\substack{\text{Simulated acceleration}\\ \text{on Sherpa}}} = \underbrace{f(\ddot{x}_t^{MDV})}_{\text{Scale factor}} \times \underbrace{\ddot{x}_t^{MDV}}_{\substack{\text{Real acceleration}\\ \text{output of véhicle dynamics model}}} \quad (1)$$

The second artifice is of psychophysical order and is called tilt-coordination. It uses the tilt of the cabin (and therefore of the subjects) to partly simulate linear accelerations [Gro2]. In order to determine the tilt/translation ratio, we use a parameter called **cut-off frequency**, which defines the limit between the tilt and the translation. From a perceptive point of view, a constant tilt could be perceived as a constant acceleration [Hol1]. The tilt is then produced with an under vestibular threshold angular velocity with the rotation point referred to the head of the driver.

In the literature, the scale factor is traditionally reported as being the most efficient between 0.4 and 0.75. However, multiple driving tests conducted on our simulator show that this value is not adapted to our device, being considered too high. Therefore, in the present study, we try to determine the scale factor and the cut-off frequency that produce a motion perception close to the one perceived during a real driving (baseline condition). The cut-off frequency represents a constant value, but the scale-factor can evolve with the level of acceleration, therefore it is defined as below:

$$f(\ddot{x}_t^{MDV}) = a - b \times \ddot{x}_t^{MDV} \quad (2)$$

, with $f(\ddot{x}_t^{MDV}) \in \Re_+$.

3. Methods

3.1. Subjects

30 persons participated to our study. All subjects were PSA's employees who volunteered for the study.

3.2. Experimental devices

The experimental devices used in the study were the Sherpa² driving simulator [Str1, Str2] and a real vehicle, a Citroën C3 HDI 70CH. The chosen driving situation was the take-off, meaning an acceleration from 0 to 30km/h on a straight road (in-situ of PSA's Velizy Technical Center). The virtual environment used on the dynamic driving simulator was identical to the real driving environment from visual, auditory and vehicle's dynamics point of view.

3.3. Task

The task of the participants was to accelerate from 0 to 30 km/h on straight line (speed limitation to 30km/h), without changing the gear. Once the speed of 30 km/h reached, they had to maintain the speed for 1-2 seconds and then to slowly brake until full stop. No acceleration profile was imposed; the participants were advised to drive in their own "driving style".

Each participant started the test by driving the real vehicle, producing up to 40 accelerations in order to be able to reproduce this acceleration on the dynamic driving simulator. Once they were confident in their repeatability, the subjects were taken on the driving simulator to reproduce the same task, by pairs, using the experimental design described below. At the end of each pair of accelerations, they had to answer to 2 questions: 1/ which acceleration seemed to be more realistic (closer to the real vehicle acceleration)? 2/ which acceleration was stronger?

Before starting to drive the real vehicle or the driving simulator, the participants were submitted to a familiarization phase of about 10 minutes on each device.

3.4. Experimental design

Once arrived on the dynamic driving simulator and after the familiarisation phase, the participants were asked to reproduce the acceleration memorized during the real car driving situation. Each reproduced acceleration was considered to be a test condition, the motion cueing parameters being changed from one condition to another.

The tested conditions were defined by taking into account the cut-off frequency and the parameters *a* and *b* of the linear scale factor (see equation 2). Therefore, the triplet (*a,b,Fc*) represents a test condition. For each variable of the triplet, we chose 2 values:

$$\begin{aligned} a &\in (0.4; 0.5) \\ b &\in (0; 0.05) \\ Fc &\in (0.6; 1.5) \end{aligned} \tag{3}$$

These choices were made by taking into account the physical limitations of the simulator (position, speed, linear and angular acceleration) and on-the-table simulations that were made to verify the correlations of driver's sensations (analysis of acceleration's profile).

The experimental design was a complete-crossed factorial design. The factors are the parameters (*a,b,Fc*) with 2 values for each, meaning 8 test conditions (see table 1).

Table 1. The 8 test conditions.

Condition	a	b	Fc
1	0.4	0.05	0.6
2	0.4	0	0.6
3	0.4	0.05	1.5
4	0.4	0	1.5
5	0.5	0.05	0.6
6	0.5	0	0.6
7	0.5	0.05	1.5
8	0.5	0	1.5

The 8 test conditions were presented in pairs using William's Latin Square, which allowed balancing the order and report effects. The pairs A/B and B/A were balanced over the total panel of subjects. Each participant had $\frac{8 \times 7}{2} = 28$ pairs to test. These pairs were presented to the participants in a pseudo-random order. This experimental design was repeated 3 times by each subject, meaning 84 trials per person.

For the real vehicle, there were 30 subjects x 20 profiles x 3 repetitions = 1800 acceleration profiles. For the driving simulator, there were 30 subjects x 56 profiles x 3 repetitions = 5040 acceleration profiles.

3.5. Data analysis

During each acceleration, on real vehicle and on driving simulator, some objectives measures were recorded: throttle pressure, vehicle speed, displacement time, acceleration profile.

By analysing the acceleration profiles on real and virtual driving, we tried to determine:

- if drivers are able to reproduce the same acceleration profile in time and intensity, from one trial to another, and for both real and virtual driving,
- if drivers are able to reproduce a real acceleration profile on a dynamic driving simulator, independent of the MCA's parameters (triplet (a,b,Fc)),
- if there are several classes of acceleration profiles and therefore several classes of drivers,
- the relationship between the real car and the driving simulator.

Given the non-linearity of an acceleration profile (see fig.1), we calculated a 4-order polynomial trendline for each recorded profile and analysed the maximum point x_m, the corresponded time t_m and the total time t_t (see fig. 1). A phase 1 analysis of these factors was realized in order to underline the abnormal data. A phase 2 analysis was realised in order to define a profile-band that will allow determining the type of a subject for future experiments.

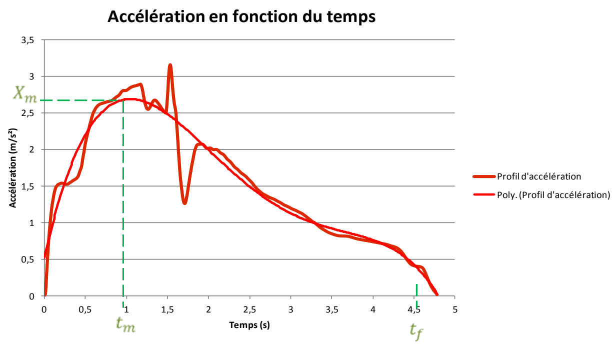

Fig. 1. Example of an acceleration profile.

In parallel, a subjective analysis of participants' responses on driving simulator was realised by using a Bradley-Terry-Luce model [Bra1, Luc1]. The responses for the two questions were analysed separately. For each subject and each pair, we computed a Bradley score that allowed us to determine the discriminant participants. Once the non-discriminant subjects were removed from the panel, a PCA (principal component analysis) was realised in order to evaluate the consensus of the panel and to determine the groups of homogeneous subjects. In the end, ANOVA and Duncan test were realised to determine the test configurations that differentiate from the others, and to determine the influential test factors. A partial eta² was also calculated, which allows determining the influence of one factor when the other factors are controlled. If eta² is around 0.01, there is a small effect of the factor. If eta² is around 0.06, there is a moderate effect of the factor. If eta² is around 0.14 or higher, there is a large effect of the factor.

4. Results

4.1. Descriptive analysis of acceleration profiles on real car and driving simulator

The analysis of the driving simulator's profiles highlighted exploitable and non-abnormal data for 21 subjects (fig.2). The corresponding data were also analysed on the real vehicle, which allowed the comparison between both devices.

By analysing the maximum point of the profile (x_m) and its correspondent time (t_m) (fig.2), 2 main groups of profiles were determined (Group A and Group B) and 3 secondary groups (see fig.3). For each group, a profile-band was computed.

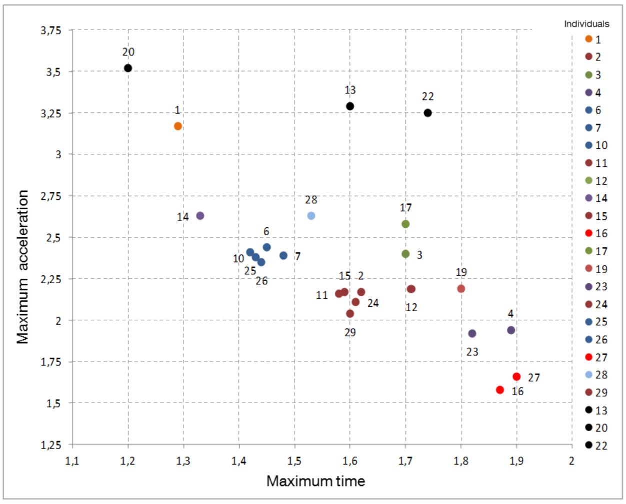

Fig. 2. The mean value of maximum accelerations and their correspondent time for each exploitable subject on driving simulator.

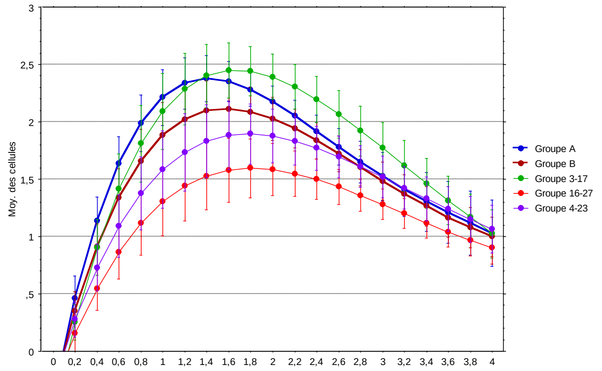

Fig. 3. The groups of acceleration profiles determined on dynamic driving simulator.

The analysis of real vehicle profiles showed a faint influence of the first repetition, which was not observed on the simulator. However, the participants presented a good reproducibility of the individual profiles. On the simulator, there were some atypical individuals, but most of the participants presented a good reproducibility of their profiles. The comparison between the real vehicle and the driving simulator showed that the subjects are able to reproduce their acceleration from real to virtual environment.

4.2. Analysis of subjective responses on driving simulator

4.2.1. Analysis of the realism of the acceleration

The analysis of the individual Bradley score for question 1 (realism of the acceleration) determined 75% of discriminant subjects. The PCA determined 1 group of subjects. The ANOVA and a Duncan test determined a significant influence of the test conditions ($p=0.000$, $F=26.034$), but no influence of the individuals ($p=0.601$). For the test conditions, an influence of the 3 variables (a,b,Fc) was observed, the most influential being the cut-off frequency (Fc) with a partial eta²=0.550. However, an interaction between *a* and *b* was also observed ($p=0.000$, $F=2.769$): the influence of a when $b\neq0$ is weak, while its influence is stronger when $b=0$. There was no interaction between the cut-off frequency (Fc) and the scale factor (a,b) ($p=0.142$ and $p=0.557$). The most realistic conditions were considered to be conditions 1, 5, 2 and 6, for which Fc=0.6 (see fig. 4).

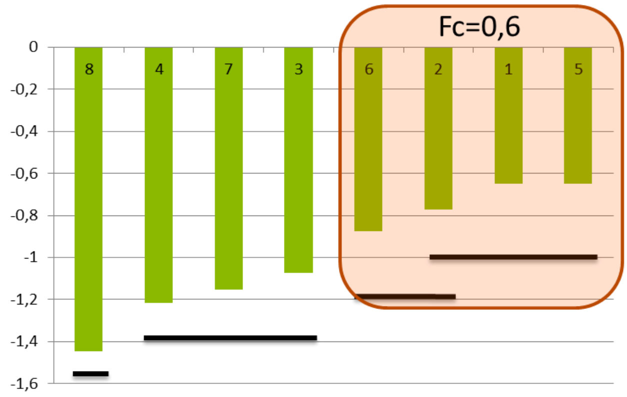

Fig. 4. The classification of test conditions by their realism, from non-realistic (left) to the most realistic (right).

4.2.2. Analysis of the realism of the acceleration

The analysis of the individual Bradley score for question 2 (intensity of the acceleration) determined only 50% of discriminant subjects. The PCA determined 1 group of subjects. The ANOVA and a Duncan test determined a significant influence of the test conditions ($p=0.000$, $F=11.410$), but no influence of the individuals ($p=0.888$). For the test conditions, an influence of the 3 variables (a,b,Fc) was observed, the most influential being b with a partial $eta^2=0.415$. No significant interaction between the 3 variables *a*, *b* and Fc was observed ($p=0.429$ for (a,b), $p=0.273$ for (a,Fc), $p=0.748$ for (b,Fc)). The conditions for which the acceleration was perceived as intensive were the conditions 8, 6 and 4, for which b=0 (see fig. 5).

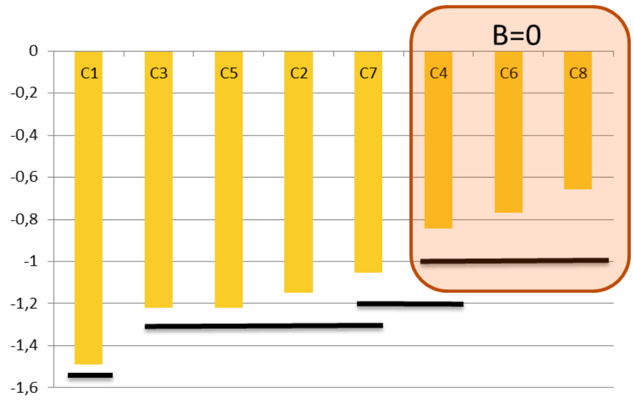

Fig. 5. The classification of the test condition by the perceived intensity of the acceleration: from the less intense (left) to the most intense (right).

5. Discussion

Dynamic driving simulators need to be validated from a perceptual point of view. Through this experiment, we tried to go beyond the previous studies and to compare the perception of acceleration on the simulator with the perception of acceleration on a real vehicle.

Moreover, our study had helped us to validate an experimental design adapted to our driving simulator, but also to validate our Motion Cueing Algorithm.

For the validation of the experimental design, we analysed the acceleration profiles realised on real vehicle and on driving simulator in order to determine if non-expert drivers were able to reproduce the same profile several times, but also if they were able to reproduce it on the simulator. We also wanted to see if there were several classes of drivers according to the acceleration profile and determine a relationship between driver's behaviour on the real vehicle and on simulator by comparing his acceleration profiles.

For the validation of our MCA, we tried to determine the influence and the interaction between the scale factor and the cut-off frequency on the perception of longitudinal acceleration for take-off, in order to obtain a more realistic driving simulator. The results clearly show that the two MCA parameters, scale factor and cut-off frequency, play an important role in the realism of the simulator's motion. However, it seems that the choice of these parameters is not so simple, because it depends on the goal of the simulation.

5.1. Validity of experimental design

The analysis of acceleration profiles determined that there are two main classes of drivers: the drivers that accelerate rapidly and reach a maximum acceleration of 2.5 m/s^2 (mean value) in about 1.4 sec and the drivers that accelerate slower (mean value of 2.1m/s^2) in more time (1.6 sec) (see fig.3). However, the two acceleration profiles are not so different. Moreover, these results showed that the non-expert drivers are able to reproduce the same acceleration profile on real vehicle and on dynamic driving simulator, at least for this specific driving situation, the take-off. This observation underlines the validity of the experimental design built for this study. However, further validations are required for other driving situations, like braking, before generalising the design for all simulations. Moreover, the obtained data represent the baseline for the implementation of a predictable model for driver's profile.

5.2. Realism of the acceleration

In this study, the perceptual validity of Sherpa² was questioned by comparing the real and the virtual driving. The results of this study show that the ratio tilt/translation plays an important role in the perception of a realistic acceleration during active driving. Our results mainly show that it is important to adjust the cut-off frequency so that the level of tilt remains lower than the level of translation, independently of the maximal level of acceleration (see the groups of profiles). Indeed, all of our participants complained of strong tilt during the conditions with Fc=1.5. It confirms the statistical analysis showing that the less realistic conditions were conditions 8, 4, 7 and 3, with Fc=1.5. These results are complementary to the results obtained on passive driving that showed that the tilt/translation ratio was less important than the scale factor, that should be adapted to the level of acceleration (non-constant scale factor) [Str2]. A striking result of our study is that, even in active driving, a non-constant scale factor has to be used in order to achieve a realistic acceleration. Therefore, it is also recommendable to increase b and to reduce a, which means that less jerk should be produced on the motion platform. Indeed, some previous studies showed that the detection of linear motion is based not only on the linear acceleration, but also on the change rate of this acceleration [Gun1, Ben1]. This may be due to the fact that the discrimination threshold of linear acceleration depends on signal’s frequency [Nas1].

5.3. Intensity of the perceived acceleration

Our results showed that 50% of the subjects are discriminants for the second question concerning the perceived intensity of the acceleration. We could then conclude that this kind of evaluation is more difficult to achieve than a comparison with a real acceleration (question 1). This may be due to the fact that the subjects compared two virtual accelerations, which were produced in the same manner (same acceleration profile – see results), but simulated differently (different scale factor and different tilt/translation ratio). Therefore, the perception of acceleration’s intensity could be influenced by the way this acceleration is simulated by the motion platform. The statistical analysis shows that the perception of the motion is mainly influenced by the scale factor, and more specifically, by the b variable. If the scale factor is constant (b=0), the acceleration is perceived as being stronger than in the case where the scale factor evolves with the level of acceleration. Therefore, if we are interested in producing stronger accelerations, it is recommended to reduce b, increase a and Fc, meaning that the scale factor is constant and at a higher value (0.5 in our case) and that we should use more tilt than translation (Fc=1.5). If we are interested in producing a softer acceleration, it is recommended to increase b and reduce a and Fc, meaning that we should use a non-constant scale factor and more translation than tilt (in our case Fc=0.6). This means that the tilt is the motion that induces the “impression” of intensity in the simulation of linear acceleration. This may be due to the fact that the driver perceives the rotation, but it integrates it as part of natural pitch of the car, which corresponds indeed to a stronger longitudinal acceleration.

6. Conclusion

This study showed that the Motion Cueing Algorithm used on Sherpa^2 could be well set-up, if some conditions are met, for realistic take-offs. Therefore, it is important to verify if these conditions are also adapted for other driving situations, for instance, the braking (from 30km/h to full stop). However, we should analyse more deeply the behaviour data collected during this study and make a crossed-analysis between the subjective answers and acceleration profile analysis.

7. References

[Ben1] Benson AJ, Spencer MB, Stott JR. Thresholds for the detection of the direction of whole-body, linear movement in the horizontal plane. In Aviat Space Environ Med 57: 1088 –1096, 1986.

[Ber1] Berger, D., Schulte-Pelkum, J., & Bülthoff, H. Simulating believable forward accelerations on a Stewart motion platform. In ACM Trans. Appl. Percept., 7, 1–27, 2010.

[Ber2] Berthoz, A., Bles, W., Bulthoff, H., Correia Gracio, B., Feenstra, P., Filliard, N., et al. Motion Scaling for High-Performance Driving Simulators. In IEEE Trans. Hum.-Mach. Syst, 43, 265–276, 2013.

[Bra1] Bradley RA, Terry ME. Rank Analysis of Incomplete Block Designs: I. The Method of Paired Comparisons," In Biometrika, vol. 39, no. 3/4, p. 324, Dec. 1952.

[Gro1] Groen, E. L., Clari, M. V., & Hosman, R. Psychophysical thresholds associated with the simulation of linear acceleration. In Proceedings of the AIAA Modeling and Simulation Technologies Conference, 14-17, 2000.

[Gro2] Groen, E., & Bles, W. How to use body tilt for the simulation of linear self motion. In Journal of Vestibular Research Equilib. Orientat., 14, 375–385, 2004.

[Gun1] Gundry A. Thresholds of perception for periodic linear motion. In Aviat Space Environ Med 49(5):679–686, 1978.

[Hol1] Holly JE, McCollum G. The shape of self-motion perception-I. Equivalence classification for sustained motions. In Neuroscience Jan; 70(2):461-86, 1996.

[Luc1] Luce RD, Individual choice behavior; a theoretical analysis. In New York: Wiley, 1959.

[Nas1] Naseri AR. Human discrimination of translational accelerations. In Exp Brain Res, 218:455–464, 2012.

[Rey1] Reymond, G., & Kemeny, A. Motion cueing in the Renault driving simulator. In Vehicle System Dynamics, 34, 249-259, 2000.

[Str1] Stratulat, A., Roussarie, V., Vercher, J.-L., & Bourdin, C. Improving the realism in motion-based driving simulators by adapting tilt-translation technique to human perception. In Proceeding of Virtual Reality Conference, IEEE, 47–50, 2011.

[Str2] Stratulat, A., Roussarie, V., Vercher, J.-L., & Bourdin, C. Perception of longitudinal acceleration on dynamic driving simulator. In Proceedings of Driving Simulation Conference, 2012.

PRESENCE STUDIED IN A DRIVING SIMULATOR

Christophe DENIAUD [1,2], Vincent HONNET[2], Benoît JEANNE[2], Daniel MESTRE[1]

(1): The Institute of Movement Sciences, University Aix-Marseille II, 163 av. de Luminy, 13009 Marseille France. {christophe.deniaud, daniel.mestre}@univ-amu.fr

(2): PSA Peugeot Citroën Route de Gisy 78140 Vélizy-Villacoublay France {christophe.deniaud, vincent.honnet, benoit.jeanne}@mpsa.com

Abstract – In this paper, our ambition is to find a way of measuring “presence” to use it as a measure for ecological validity in driving simulators. The underlying assumption is that a person experiencing a strong sense of presence in the virtual environment will react in this environment as if it would be a real one. We propose to measure "presence" by measuring “attention” toward the driving task". Our objective is to demonstrate that the higher the subject's attention required by the primary driving task will be, the more the spatial presence will be felt. In the experiment we tried to vary "attention" by adding a dual task and by adding traffic and measure driving performance and subjective "presence". The main result is a lack of congruence between subjective and behavioral measures.

Key words: Driving simulator, spatial presence, attention, ecological validity, cognitive involvement

1. Introduction

In the 1960s, driving simulation was mainly used to train specific target audiences such as novice drivers, law enforcement officers and truck drivers [All3]. Since then, many advances have been achieved in terms of computing, visual display and vehicle dynamics rendering [All2]. Driving simulation was originally developed to avoid cost of field studies, allowing more control over circumstances and measurements, and ensuring safety in hazardous conditions [All1]. In the second half of the twentieth century, simulation was being successfully applied to aeronautical, rail and maritime operations. In spite of significant differences, it is interesting to note that the development of driving simulation was based on the development of flight simulation. Driving is a dynamic task with a set of rapid control maneuvers involving critical feedback for avoiding obstacles and preventing crashes [Han9]. Compared to the activity performed by air line pilots, driving involves higher amplitude, and higher frequency cues. The motion feedback doesn’t play a key role for the major part of slow maneuvers performed by civilian pilots. Indeed there is no evidence that motion base-simulators are more efficient than fixed base simulators for training of commercial pilots [Bür6]. Thus there is a stark contrast between driving simulation and flight simulation (Civil aviation only). Compared to an air line pilot, a driver needs a higher degree of motion simulation. That is probably the reason why the use of flight simulators is more than commonplace for pilot training and, conversely driving simulators are not widely used for driver training due to the inherent higher complexity of the driving task. Nowadays driving simulators are usually designed for two purposes: research and training. The simulator is essentially used to place constraints on driver behavior in order to study driver distraction and workload or used as test beds for highway design [Kan14]. The use of a modern advanced driving simulator for human factors research has many advantages such as experimental control, efficiency, expense, safety, and ease of data collection [Nil19]. However, the literature describes some possible disadvantages, i.e. simulator sickness, accurate replication of physical sensations, and most importantly, validity.

2. Ecological Validity

In spite of significant advancements in the physical fidelity of the driving simulation, a lack of realism seems to be always observed in the major part of driving simulator studies [All4]. The most important question is to know in which extent measures from simulation are similar to those obtained in the real world. This multidimensional problem is called simulation validation [Bla5]. This question has been a concern for at least 25 years. Blaauw (1982) defined two types of validity. The first is the absolute validity, it deals with the extent to which a manipulation of a variable in the real world produces the same or equivalent change in the same measure when manipulated in a driving simulator. The second is called the relative validity it refers to the extent to which the direction of change of a variable is in the same direction as a corresponding manipulation and measure in the real world [Kap15]. If absolute validity is obviously desired by researchers, regarding the variability of driver performance, it seems highly unlikely to have an exact correspondence of on-road and simulation measures. Furthermore there is no bad or good simulator from a methodological point of view. The simulation validation seems to be arbitrated between the research issue and how simulators are used to investigate this question. Each simulator must be validated for a specific use. In addition, the question of simulation validation has followed the perpetual development of a significant number of simulator components as computers and various display technologies. That is the reason why, since four decades, simulators have been designed to deliver more and more perceptual cues to the driver in order to reproduce as accurately as possible the experience of driving an automobile. Thus, simulator validity is often addressed in the extent to which a physical variable in a simulator corresponds to its operationally equivalent component in the real world is called Physical fidelity [Lee18]. As previously discussed, simulation validity is multidimensional and can be related to behavioral and physical dimensions [Jam11] but also to the perceived sensation of the subjective experience and objective performance. Indeed, despite significant advancements in the fidelity of the driving experience driving simulator studies continue to be criticized for lack of realism [Goo8]. More specifically, the physical fidelity of the driving experience appears insufficient to overcome criticisms concerning the lack of psychological fidelity [Goo7], defined as the extent to which the risks and rewards of participation in the experiment correspond to real-world risks and rewards [Ran20]. The main problem is that driving experimental studies failed to provide a non-artificial trip purpose which could be able to reproduce drivers' motives inherent to the real driving activity. Generally, it appears that the assessment of the validity of the virtual environment involves the comparison of results obtained from studies conducted in real situations and in virtual environment. However, this comparison is expensive (instrumentation) and complex (strict control of all the events occurring in a real situation). This is probably the reason why questions about the validity of simulators are most often pending [Rei22] and why only few studies on this question can be found.

3. The concept of presence: a methodological alternative to assess the ecological validity in driving simulators

In this paper, a new approach is developed. We propose to understand the behavior similarities between real and virtual environment through the concept of presence which will be clearly explained in the continuation of our lecture. The validity issue requires to not opposite physical validity to psychological validity. The main idea is to find a methodological tradeoff, based on behavioral and psychological considerations in order to investigate the ecological validity of simulators. We argue in favor of a phenomenological approach understanding experience as the source of all knowledge. More specifically, it deals with the necessity to overcome the dualism developed by Descartes assuming that mind and body are not identical. In understanding the legitimacy of our theoretical approach we quickly expose the paradigm of virtual reality upon which the driving simulation also rests. Driving simulation is a historical component of virtual reality, the purpose of which being to enable one person (or more) to develop sensori-motor and cognitive activity in an artificial world [Kem16]. The interaction of a person with the virtual world is a transposition of the perception-cognition-action loop of human behaviour in the real world. Immersion in a virtual world cannot be the same as in the real world [Ijs10] since the user has learned to act naturally in a real and physical world (without, for instance, any delay and/or sensorimotor bias). Thus, immersion, depending on the sensorimotor contingencies permitted by the simulator, is a necessary but not sufficient condition for the expression, within the virtual environment, of a performance that is representative of the actual situation [Lee17]. Facing this problem, a concept emerged in the '80s from the early steps of research about virtual reality. This concept addresses the issue of "ecological" validity of the behaviour observed in virtual environments. It is the concept of presence. This multidimensional concept is considered as the ability of individuals to adopt behavioural patterns similar to that observed in everyday life and therefore as their propensity to respond to various stimuli by a realistic way [Sla25]. Some studies [Joh13, Tic27] already proposed this concept as a tool for assessing driving or railway simulators but only in driving situations generating a state of stress. In studies about presence, finding a consensus about presence conceptualization in order to enhance its operationalization and its assessment [Sla26] seems to be the main challenge. Various attempts have been made to describe this concept. Despite divergences, the major part of publications considers that presence rests on an attentional basis [Reg21, Sch24]. Among the previous attempts to develop a unified approach for spatial presence, a model developed in 2007 caught our attention (see figure1). It is made of two levels: the first level involves the construction of an unconscious mental representation of space (the spatial situational model), allowing in a second level a conscious percept of subjective presence (spatial presence). The novelty of this model is therefore based on the fact that it offers a description of subjective processes involved in the emergence of the feeling of presence. In the MEC model of spatial presence, it clearly appears that the formation of a spatial situational model is a key concept for the emergence of presence.

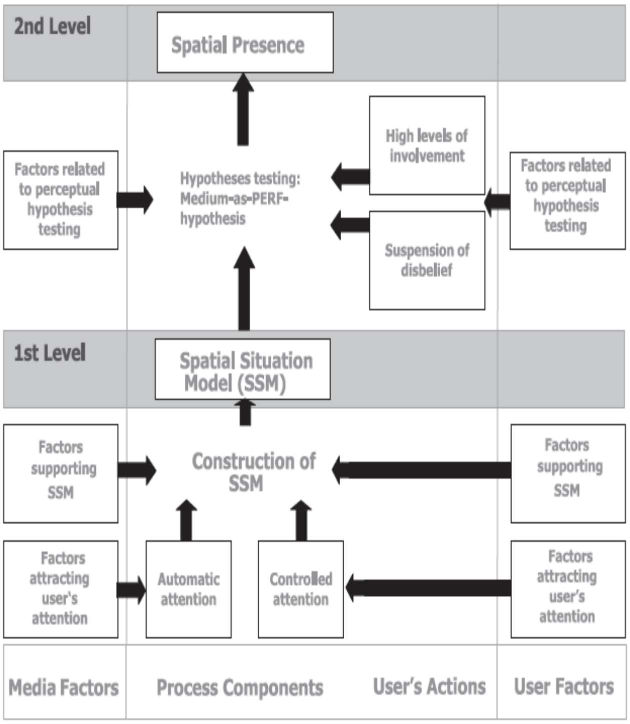

Fig. 1. MEC Model of Spatial Presence

Furthermore we notice that the spatial situational model is clearly the result of automatic and controlled attentional processes. Thus, we decided to modulate experimentally the cognitive load induced during the simulated driving task, in order to generate different attentional states and finally to induce different levels of spatial presence. We crossed the following 2 independent variables: 1) A secondary task (dual-task paradigm), supposed to distract the driver from the primary task (driving) and 2) the presence of traffic on the roadway, supposed to focus the driver's attention toward the primary task. . Our objective was to develop a sensitive measure of presence in order to assess the simulator validity. To do so, we decided to test the attentional assumption developed in the MEC model of spatial presence. According to the two-level model of spatial presence, the measurement of presence can be approached in two different ways [Sch23]. On the one hand, we have to evaluate the behavioral dimension of the activity which describes the first level pretty unconscious. To do so, we analyzed the driving performance. On the other hand, we have to evaluate the conscious subjective experience of physical presence by a qualitative method. We thus used the MEC Spatial Presence Questionnaire (MEC-SPQ).
Our main hypotheses were:

-H1: The vehicle traffic in the virtual world is a positive predictor of the different sections of the MEC -SPQ
-H2: A dual task performed during the driving is a negative predictor of the different sections of the MEC-SPQ

4. Method

4.1. Participants

Twenty experienced car drivers, with at least five years of experience (14 men and 6 women), were divided into four groups, by crossing two independent variables, i.e. a dual task to be performed or not during the experiment and the presence or not of other vehicles' traffic on the road. The age of the participants ranged from 22 to 45 (M=32.8 years, SD=6.45). All were tested on a voluntary basis, having signed an informed consent form.

4.2. Apparatus

The experiment was carried out using the SIM²-IFSTTAR fixed-base driving simulator equipped with an ARCHISIM object database SIM2. The projected display (at 30 Hz) presented a field of view of 150° horizontally and 40° vertically. The simulator's cockpit (see figure2) contained a microcontroller managing a force feedback steering wheel, 3 pedals (accelerator, brake, clutch), a gear box, a display dial (speedometer, a tachometer) and different switches (wipers , lights…). Driving performance was recorded online and stored for offline analysis

4.3. Procedure

In our experiment we used a digital model of the Versailles Satory runway, which is a closed loop of 3.7km, with long straights and corners with different radii of curvature. The first factor was the level of attention induced by the virtual environment with two levels: automated bidirectional traffic or not. The second factor was the level of cognitive involvement induced by the real world with two levels: presence of a dual task or not. The secondary task consisted in launching every minute a digital hourglass by double clicking the mouse of a laptop positioned so that the person had to deport his gaze from the main visual scene. Half of the subjects had to perform the dual task, either in condition "traffic", or in condition "no traffic" on the Satory circuit. It is important to note that this dual task was used as a manipulation device and not as a performance measurement. That is the reason why reaction times were not presented in this paper. Whatever the experimental conditions, each participant had to perform 10 laps with a maximum speed of 110 km/h by respecting the Highway Code.

Table 1. Experimental design

	Dual task	Traffic
Group1	No	Yes
Group2	Yes	Yes
Group3	No	No
Group4	Yes	No

We applied a 2 X 2 factorial design. Four experimental groups of five subjects were thus created (see table1).

4.4. MEC (Measurement, Effects, Conditions) Spatial Presence Questionnaire

After each session an adapted version of the MEC Spatial Presence Questionnaire (MEC-SPQ) [Vor28] was used. As suggested for each scale, we used a 5-point Likert scale ranging from 1 ('I do not agree at all') to 5 ('I fully agree'). We used 4-item scales for the tested dimensions. On the first level, visual spatial imagery (VSI) was assessed with items such as " When someone describes a space to me, it's usually very easy for me to imagine it clearly"; for allocation of attention "I dedicated myself completely to the medium"; for the spatial situational model (SSM) " I was able to imagine the arrangement of the spaces presented in the medium very well". On the second level, higher cognitive involvement (CogInv) was assessed with items such as " I thought most about things having to do with the medium"; for suspension of disbelief (Sod)" I didn't really pay attention to the existence of errors or inconsistencies in the medium". Finally, spatial presence was measured and analysed by the self-location dimension (e.g., «I felt as though I was physically present in the environment of the presentation").

4.5. Driving performance

We analyzed two behavioral variables reflecting the driving performance, i.e. means and standard deviations of speed and of lateral position (SDLP).

5. Results

5.1. MEC spatial presence questionnaire

A mean score was computed for each group for the various dimensions of the MEC SPQ (see figure2). Overall, Whatever the section of the questionnaire, participants reported rather high scores. Specifically, "attention" scale (M= 4.2; SD=0.70) had the highest score while "cognitive involvement" scale (M=3.33; SD=0.95) had the lowest.

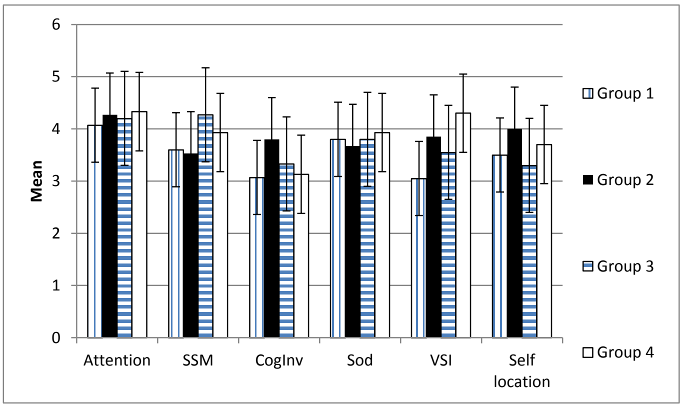

Fig. 2. Mean of MEC Spatial Presence Questionnaire Sections

The generalized linear model was used in order to test our hypotheses, with a 2x2 factorial design and independent groups. Then multivariate analysis of variance (MANOVA) was considered for assessing interaction effects between independent variables.

Table 2. Manova results (statistical significance set at p<0.5)

	Dual Task	Traffic	Dual Task*Traffic
Attention	F=0.24 P=0.63	F=0.09 P=0.77	F=0.01 P=0.92
Spatial Situation Model (SSM)	F=0.58 P=0.48	F=4.13 P=0.06	F=0.26 P=0.62
Cognitive Involvement (CogInv)	F=0.36 P=0.56	F=0.20 P=0.66	F=1.11 P=0.31
Suspension Of Disbelief (Sod)	F=0 P=1	F=0.17 P=0.69	F=0.17 P=0.69
Visual Spatial Imagery (VSI)	F=4.48 P=0.05	F=1.68 P=0.21	F=0.01 P=0.95
Self-Location	F=1.48 P=0.24	F=0.46 P=0.51	F=0.02 P=0.89

From the MANOVA analysis, no interaction effect was observed between the traffic condition and the dual task condition (see Table2). Whatever the experimental condition no significant effect was observed on the various sections of the MEC Spatial Presence Questionnaire. Contrary to what was expected, the dual task and the traffic had no impact on the questionnaire results.

5.2. Driving performance

5.2.1. Lateral position

An interaction effect was first observed between dual task and traffic (F(1, 360)=28.827;p<0.01). Lateral positions of Groups 1 and 2 submitted to traffic were higher than those of groups 3 and 4 not submitted to traffic (see figure 3).

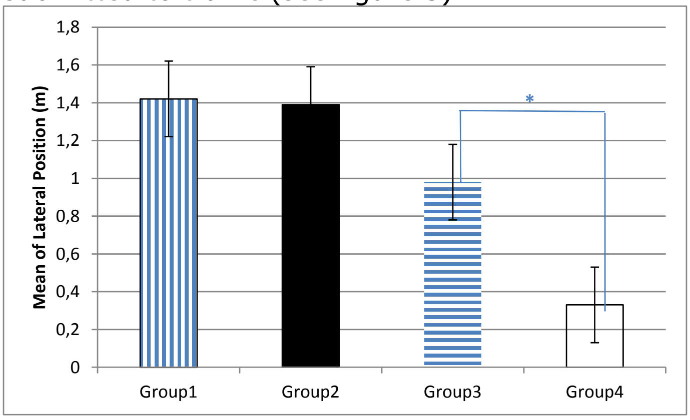

Fig. 3. Mean of lateral position (m)

A dual task effect is also observed in the absence of traffic, (F(1,360)=35.27, p<0.01). Indeed, subjects not submitted to the dual task (Group3) had a higher mean lateral position compared to subjects submitted to the dual task (Group4).

5.2.2. Speed

A dual task effect was observed (F(9,360)=2.33;p=0.012) on 10 laps performed between groups not submitted to the dual task (group 1 and group 3) and groups submitted to the dual task (group 2 and group 4).

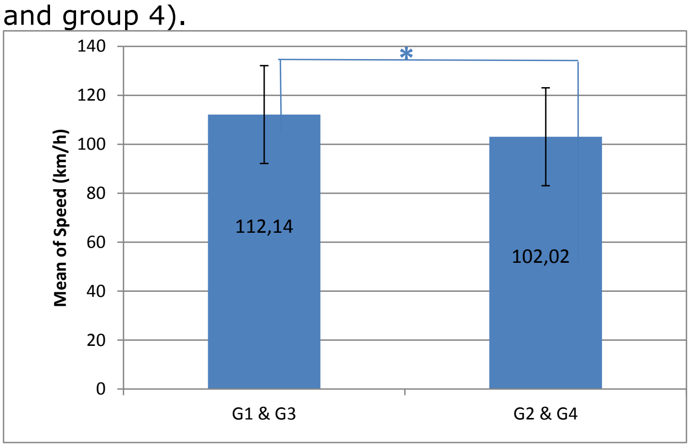

Fig. 4. Mean of speed (km/h)

Subjects not performing the dual task drove faster than others (see figure 4).

5.2.3. SD of lateral position (SDLP)

There was no interaction effect between group and lap variables (F(24,1754)=0.60, p=0.94). However, the group significantly influenced the SDLP (F(3, 1754)=156,39, p<0.01).

Table 3. Mean and SD of SDLP (m)

Groups	Means	SD
G1	0,83	0,52
G2	0,72	0,51
G3	0,84	0,47
G4	1,41	0,57

Over the 10 laps, the group 4 submitted to the dual task without traffic had the higher mean contrary to groups 1, 2, 3 (see table 3)

5.2.4. SD of Speed

There was no interaction effect between group and lap variables (F(24,1754)=0.60, p=0.93). However, the group significantly influenced the SD of speed (F(3, 1754)=41,018, p<0.01).

Table 4. Mean and SD for the SD of Speed (km/h)

Groups	Means	SD
G1	5,07	5,52
G2	7,01	4,74
G3	4,27	3,23
G4	4,58	3,30

Over the 10 laps, the group 2 submitted to the dual task with traffic had the higher mean contrary to groups 1, 3, 4 (see table4).

6. Discussion and conclusions

Results globally showed that whatever the experimental condition, no significant difference was clearly observed for the different sections of our presence questionnaire. Indeed, the vehicle traffic in the virtual world was not a positive predictor of the different sections of the MEC Spatial Presence Questionnaire. The dual task was not a negative predictor of these different sections either. Although the dual task didn’t have a strong effect on the subjective measures of presence, it affected the behavioral measures. As described in the literature [Wit29], low values in driving performance (SD of speed and SDLP) indicated a good steering control and a stable and consistent driving. Indeed, the SD of speed in traffic condition and the SDLP in no traffic condition were higher in dual task than in single task. Drivers submitted to the dual task without traffic drove in the middle of the road (the smallest mean lateral position), which could be interpreted as an efficient strategy but pretty inconsistent with the Highway Code. Similarly, participants submitted to the dual task in traffic condition have tried to reduce their speed as a compensatory strategy to deal with the dual task. Unfortunately, it appeared that they also failed to maintain a stable driving with a lack of speed control (the highest SD of speed). Thus, driving performance seemed to be globally impaired by the dual task. In conclusion, the main outcome was that behavioral measures revealed significant effects of the manipulated variables (traffic and dual task) on driving performance. These behavioral effects showed that participants took into account these variables. However, these effects were not confirmed by subjective reports. One explanation could be that, whatever the current experimental conditions, driving activity did not involve high-level, conscious, cognitive processes. Despite high scores reported through the MEC Spatial Presence Questionnaire, driving was probably more based on a set of procedures or routines. Our experimental conditions might have been insufficient to induce several distinct levels of attention, involvement and suspension of disbelief, leading to several distinct levels of presence (see figure 1). As developed by Schubert [Sch23], in the MEC model, internal factors (such as emotional arousal) are considered as key elements in the emergence of a sense of presence based on controlled attentional processes. Thus, high levels of self-reported presence (positively correlated with behavioral measures) might require to develop more challenging scenarios, in terms of controlled attention, cognitive involvement and more specifically in terms of emotions induced by the media. Actually, participants of driving simulation sessions are clearly aware that they are not exposed to any physical danger. According to Jamson [Jam12], the main problem to be solved is how simulated driving can reach out to them and engage them.

7. Acknowledgments

This work was supported by PSA (Peugeot Citroën) and by University Aix-Marseille II.

8. References

[All1] Allen, R. W., & McRuer, D. T. (1977). "The effect of adverse visibility on driver steering performance in an automobile simulator". 1977 SAE *Transactions* (Vol. 86, pp.1081-1092; SAE Paper 770239). Warrendale, PA: Society of Automotive Engineers.

[All2] Allen, R. W., Stein, A. C., Aponso, B.L., Rosenthal, T.J., & Hogue, J.R. (1990). "A low cost, part task driving simulator based on microcomputer technology". *Transportation Research Record, 1270, 107-113.*

[All3] Allen, R. W. and Jex, H. R. (1980). "Driving simulation – Requirements, mechanization and application." SAE Technical Paper Series Paper number 800448: 1-12.

[All4] Allen, R.W., Mitchell. D.G., Stein, A.C., & Hogue, J. R. (1991)." Validation of real-time man-in-the-loop simulation". *VTI Rapport, 372A,* Part 4, 18-31.

[Bla5] Blaauw, G. J. (1982). "Driving experiments and task demands in simulator and instrumented car". *Human Factors*, 24, 473-486.

[Bür6] Bürki-Cohen, J., & Go, T. H. (2005). "The effect of simulator motion cues on initial training of airlines pilots*".* AIAA-2005-6109. Proceedings of the American Institute of Aeronautics and Astronautics Modeling and Simulation Technologies Conference. San Francisco, CA.

[God7] Godley, S. T., Triggs, T. J. et Fildes, B. N. (2002). "Driving simulator validation for speed research". *Accident Analysis and Prevention*, 34(5):589–600.

[Goo8] Goodman, M., Bents, F. D., Tijerina, L., Wierwille, W. W., Lerner, N., & Benel, D. (1997). "An investigation of the safey implications of wireless communications in vehicles" (DOT HS 808 635). Washington, DC: National highway Traffic Safety Administration, US Department of Transportation.

[Han9] Hancock, P. A. (2008). "The future of simulation". In D. Vicenzi, J. Wise, M. Mouloua, & P. A. Hancock (Eds.), *Human factors in simulation and training* (pp. 169-188). Boca Raton, FL: CRC Press.

[Ijs10] Ijsselsteijn, W. A., de Ridder, H., Freeman, J., & Avons, S. E. (2000, January). "Presence: Concept, determinants and measurement". Paper presented at Photonics West-Human Vision and Elec-tronic Imaging, San Jose, CA

[Jam11] Jamson, A. H. (1999). "Curve negociation in the Leeds Driving Simulator: The role of driver experience". In D. Harris (Ed.), *Engineering psychology and cognitive ergonomics.* (Vol. 3, pp. 351-358). Ashgate.

[Jam12] Jamson SL; Jamson AH (2010). "The validity of a low-cost simulator for the assessment of the effects of in-vehicle information systems", *SAFETY SCI*, 48, pp.1477-1483

[Joh13] Johnson, M. J., Chahal, T., Stinchcombe, A., Mullen, N., Weaver, B. et Bedard, M. (2011)." Physiological responses to simulated and on-road driving". *International Journal of Psychophysiology*, 81(3):203–208.

[Kan14] Kantowitz, B. H. (2001). "Using microworlds to design intelligent interfaces that minimize driver distraction". Proceedings of the first international driving symposium on human factors in driver assessment, training and vehicle design (pp. 42-57). Aspen, CO.

[Kap15] Kaptein, N. A., Theeuwes, J., & Van der Horst, R. (1996). "Driving simulator Validity: Some considerations". *Transportation Research Record*, 1550, 30-36.

[Kem16] Kemeny, A., & Panerai, F.,(2003). "Evaluating perception in driving simulation experiments," Trends in Cognitive Sciences, vol. 7, no. 1, pp. 31–37.

[Lee17] Lee, K. M. (2004). "Presence, explicated". *Communication Theory*, *14* (1), 27–50.

[Lee18] Lee, A. T. (2005)." Flight simulation". Alder shot, United Kingdom: Ashgate.

[Nil19] Nilsson, L., 1993. "Behavioural research in an advanced driving simulator-experiences of the VTI system". Proceedings of the Human Factors and Ergonomics Society 37th Annual

[Ran20] Ranney T. A., Simmons, L. A., Boulos, Z., & Macchi, M. M. (2000). "Effect of an afternoon nap on nighttime performance in a driving simulator". *Transportation Research Record*, 1686, 49-56.

[Reg21] Regenbrecht, H., & Schubert, T. (2002). "Real and illusory interaction enhance presence in virtual environments". *Presence: Teleoperators and Virtual Environments, 11*, 425-434.

[Rei22] Reimer, B., D'Ambrosio, L. a., Coughlin, J. E., Kafrissen, M. E. et Biederman, J. (2006). "Using self -reported data to assess the validity of driving simulation data". *Behavior Research Methods*, 38(2):314–324.

[Sch23] Schubert, T. W. (2009).” A new conceptualization of spatial presence: Once again, with feeling”. *Communication Theory, 19*, 161-187
[Sch24] Schubert, T. (2004). “The sense of presence in virtual environments: A three-component scale measuring spatial presence, involvement, and realness”. *Zeitschrift für Medienpsychologie, 15*, 69-71
[Sla25] Slater, M., Lotto, B., Arnold, M. M. et Sanchez-Vives, M. V. (2009). “How we experience immersive virtual environments : the concept of presence and its measurement”. *Anuario de Psicologia*, 40(2):193–210.Meeting 37 (1), 612–616.
[Sla26] Slater, M. (1999). “Measuring presence: A response to the Witmer and Singer presence questionnaire”. *Presence: Teleoperators and Virtual Environments, 8,* 560-565.
[Tic27] Tichon, J. G. (2007). “Using presence to improve a virtual training environment”. *CyberPsychology &Behavior*, 10(6):781–787.
[Vor28] Vorderer, P, Wirth, W., Gouveia, F. R., F., Saari, T., Jäncke, F., Böcking, S., Schramm, H., Gysbers, A., Hartmann, T., Klimmt, C., Laarni, J., Ravaja, N., Sacau, A., baumgartner, T. & Jäncke, P. (2004). “MEC Spatial Presence Questionnaire (MEC-SPQ):Short Documentation and Instructions for Application”. Report to the European Community, Project Presence : MEC (IST-2001-37661)
[Wit29] Wittmann, M., Kiss, M., Gugg, P., Steffen, A., Fink, M., Poppel, E., Kamiya, H., 2006. “Effects of display location of a visual in-vehicle task on simulated driving”. Appl.Ergon. 37, 187–199.

VALIDATING ON-THE-LIMIT PROPERTIES OF A DRIVING SIMULATOR

M. Hjort[1], S. Kharrazi[1], O. Eriksson[1], M Hjälmdahl[1], J. Andersson Hultgren[1]

(1): Swedish National Road and Transport Research Institute (VTI), Linköping, Sweden
E-mail: mattias.hjort@vti.se, sogol.kharrai@vti.se, magnus.hjalmdahl@vti.se, olle.eriksson@vti.se, jonas.andersson.hultgren@vti.se,

Abstract – The paper describes a validation model for both subjective and objective comparison of on-the-limit properties of a driving simulator. VTI moving base driving simulator, SIM III, has been used with three different versions of VTI's vehicle model, for validation toward field tests involving double lane change manoeuvres. Methods for handling evaluation suggested in the literature were adapted to our circumstances. The results are encouraging, although we found some limitations with respect to the objective evaluations that need to be addressed in future studies.

Key words: Limit handling, driving simulator, vehicle model, double lane change

1. Background

Experiments which study driving and driver behaviour close to the vehicle limit demands reliable models. We anticipate a future increase of studies involving on-the-limit driving due to the introduction of various active safety systems, especially stability control systems. For testing of Active Safety systems, field tests has been dominating, partly because driving simulators often do not perform well enough in situations where the vehicle is close to the handling limit. However, field tests have their share of problems, e.g. repeatability, learning effects, test drivers compared to a population of normal drivers, measurement accuracy etc. The possibility to, in a reliable way, perform such tests in a driving simulator could radically reduce the costs for testing and development. Another example involving on-the-limit handling would be driving in slippery conditions, or tests of different tyre models. However, before conducting simulator tests involving on-the-limit driving, the simulator should be validated with respect to its handling properties. This paper is concerned with developing a methodology for performing such validations.

While the VTI SIM III driving simulator is regarded as realistic for normal driving, on-the-limit driving however, is generally considered to be too easy in the simulator. This paper deals with the problem of improving and validating on-the-limit behaviour of a driving simulator.

A methodology for subjective and objective comparison of handling properties of a real vehicle with those of the driving simulator has been developed and tested. The method, which uses ordinary drivers instead of professional test drivers, is described and its merits and possible flaws are discussed.

Another result is the improvement of the driving simulator. Based on open loop track tests with an instrumented test vehicle, alterations were made to the existing driving simulator vehicle model of VTI SIM III. Two different candidate models were developed, differing mainly in lag times for tyres and suspensions. It was difficult to judge beforehand which of the two models that would produce the best result in the driving simulator, or if they would compare favourably to the existing vehicle model.

Using the double lane change manoeuvre, both the old, as well as the two new candidate vehicle models were compared to reality in driving conditions close to the vehicle handling limit.

2. The VTI Driving Simulator

VTI driving simulator III was used for all experiments. The simulator has been described in detail in [Nor1]. The parameters for the vehicle model represents a Volvo s40 of a model somewhere around year 2000. In 2006 a new tyre model was introduced. The Magic Formula (MF) parameter set that currently is used in the vehicle model of the driving simulator is the result of the EU project VERTEC, which ended 2006. Together with Pirelli, Nokian and other partners, VTI developed MF parameter sets for a passenger car tyre and a heavy truck tyre. Measurements were done on both high friction (dry and wet asphalt, as well as Pirelli's tyre test machine which uses a sand paper surface) and low friction (ice, done in VTI tyre test facility). Each tyre model includes both high and low friction, which in principal could be changed by adjusting the value of the lambda parameter for peak friction.

2.1.The candidate vehicle models

In order to adjust and validate the vehicle model for on-the-limit driving a test vehicle, a Volvo s40 of year model 2000, was acquired. It was fitted with new Pirelli P6000 tyres. Based on open loop measurements with the test vehicle on a dry asphalt test track some adjustments were made to the vehicle model. Primarily the slowly increasing steer and the step steer tests were used in order to capture the steering dynamics of the Volvo. From the results it was clear that the original model, denoted A, was too responsive and a modified candidate model B was constructed.

The main change compared to the original model is that a first order filter has been applied to the steering, introducing a time lag of 500 ms. Other changes involved a slight movement of the centre of gravity, and increased lateral stiffness in the MF parameters.

Since some double lane change tests were also conducted on the test track it was possible to get an indication on how the simulations with model B compared to reality. It was clear that model B accurately captures the first part of the manoeuvre (which is more or less a step steer), but results in excessive lag times for following steering inputs. Thus it was decided to also construct another candidate vehicle model C, which only differed from model B by having a shorter time lag (250 ms).

3. Experiments

The comparison was made using a double lane change manoeuvre both on a test track and in the driving simulator. 7 drivers were included in the study who drove the car in both experiments. The speed upon entering the manoeuvre was predetermined: 55, 60 and 65 km/h. The manoeuvre involved only steering input from the driver. Four repetitions for each speed and driver were carried out.

The number of failed manoeuvres was 7, 8 and 17 in 55, 60 and 65 km/h respectively for the seven drivers on the test track. It showed that the vehicle was on the handling limit already at 65 km/h and there was no reason to try 70 km/h; it would have been beyond the limit and just worn out the tyres.

3.1.Test track

The drivers worked in pairs with the person not driving sitting in the passenger seat and taking notes according to a predefined schema. Measures of interest are pass/fail speed, ease of passing, over- and understeer at various speeds, yaw behaviour, risk of losing control and ease of getting control back. A few test runs was allowed for the driver to adapt to the car, the surrounding track and the cruise control before the experiment started. The car had a GPS speedometer and the driver had plenty of time to set the cruise control before entering the manoeuvre for the first run and could then press resume to get the same speed in the following runs. The car had manual gearbox and the driver was instructed to clutch down at start of the manoeuvre.

When rating, the driver first drove through the manoeuvre twice according to the procedure described above, then stopped and completed the questionnaire. Then two more runs were carried out and the driver went through the questionnaire again, correcting where necessary. The reason for this procedure was that it forced the drivers to think of the attributes that should be rated, what attributes they were certain about and what attributes needed extra attention during the third and fourth run. If needed the driver could choose to carry out more runs, this was however never needed. In total each driver used roughly 40 – 60 minutes for the field test.

The car was the Volvo s40 described above. The air temperature was about +1 C with a mild rain. The asphalt was not new but mostly even with small cracks. The test was made in daylight except for the last driver who finished after the sun had started to set. It should be pointed out that the temperature was below the ideal, and that the driving was not intense enough to keep the tyres warm. This may have made a direct comparison with the driving simulator more difficult.

3.2.Driving simulator

The driving simulator runs were made the day after the field tests. Each test person drove the simulator with all the three versions of the vehicle model and filled in the questionnaire for each model; the order of the vehicle models was randomised and blind to the drivers. The evaluation of the simulator behaviour replicated the evaluation of the vehicle as much as possible using the same manoeuvre and the same questionnaire. However, the simulator questionnaire was complemented with an overall assessment comparing the simulator with the real car with respect to each attribute.

When rating in the simulator the driver was not limited to a certain number of runs through the manoeuvre since it does not take as long time to do an extra run in the simulator as in the field. This meant that the drivers drove a few times until they had a feel for the simulator behaviour, completed the questionnaire, did a few more runs, went through the questionnaire and corrected it where appropriate.

Since the conditions on the test track had been wet asphalt, it was decided to adjust the friction levels of the tyre models to wet asphalt.

4. Evaluation methods

The evaluation aims at verifying that the simulator feels and behaves like a real vehicle when driving on the limit. It was divided into a subjective and objective part as described.

4.1.Subjective evaluation of vehicle behaviour

The subjective evaluation was based on the drivers' ability to rate the vehicles behaviour going through the double lane change manoeuvre. The rating was done using a questionnaire including six different attributes, loosely based on [Pau1]. The attributes were: 1) over- or understeer; 2) controllability; 3) speed of steering response; 4) possibility to repeat manoeuvre; 5) effort of steering; and 6) tail swingout. The response was on a nine grade rating scale with five descriptive words on the scale.

In order to attend to different aspects of vehicle behaviour, the double lane change manoeuvre was divided into three sections: entry, mid and exit. For all three sections the driver should rate the vehicle behaviour according to the six attributes above, meaning that for each speed there were 18 different ratings. The rating was done sitting in the car using a pen and paper questionnaire.

The evaluation is based on the mean ratings for the drivers. Each attribute was analysed in a 3-way ANOVA with driver, speed, section and all 2-factor interactions. The reason for doing this analysis was not to use any inferential statistics but rather to find means adjusted for partial non response (least squares means).

4.2.Objective evaluation of vehicle behaviour

Three different signals has been studied in the objective analysis. The steering wheel angle (SWA) has been regarded as the input signal, and the resulting yaw rate and lateral acceleration are output signals. Comparisons of objective measures were carried out following a proposal by [Ste1]. It uses cross correlation as a limit handling parameter, studying the cross correlation between input signal (steering wheel angle) and various output signals such as lateral acceleration and vehicle yaw rate. A time shift is introduced between input and output signal. The time shift resulting in maximum correlation between input and output signals is defined as lag time. The results are then evaluated in terms of maximum correlation and lag times for various speeds. In addition to the cross correlation analysis, the maximum values of steering wheel angle, lateral acceleration and yaw rate during the double lane change manoeuvre in the vehicle and in the simulator (with the three vehicle models) were studied and compared.

5. Results

5.1.Subjective analysis

The analysis of the vehicle field test, as well as the driving simulator test using the three vehicle models, showed that the six attributes could be paired into three groups where the answers to both attributes in that group showed similar pattern. The paired questions in each group are:

- Group 1:"Did the vehicle oversteer or understeer?" and "How did you experience the vehicles steering response?"

- Group 2:"Did you feel that you had control over the vehicle" and "How did you experience the manoeuvers repeatability"
- Group 3:"How much effort was needed to steer?" and "How much did you experience the tail swingout?"

The average results from group 1 are shown in Fig. 1. Model A does not understeer as much as the Volvo does, especially through the midsection. It is more neutral and stays neutral as speed increases while the Volvo understeers more with higher speed. The steering response is also experienced as quicker for model A. Models B and C, both imitate the behaviour of the Volvo well with regard to level of under/oversteer, as well as steering response changes with increasing speed.

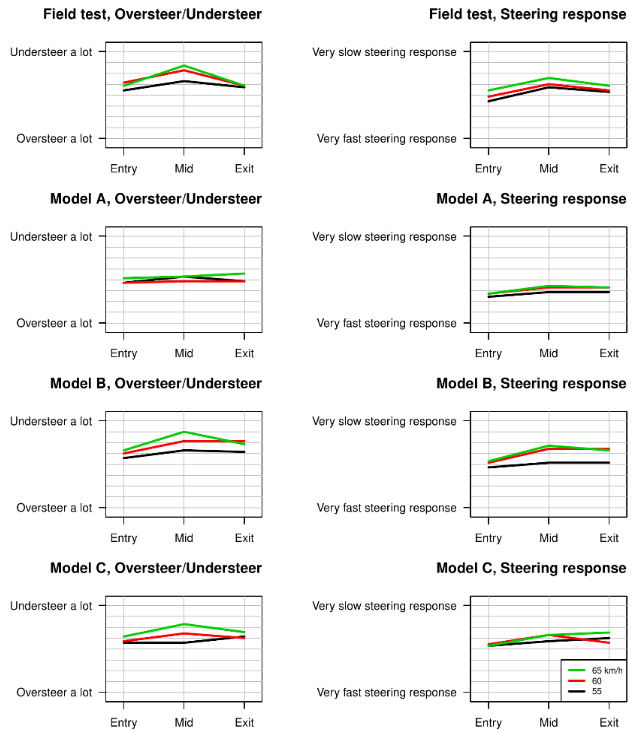

Fig. 1. Subjective evaluation of "oversteer/understeer" and "steering response"

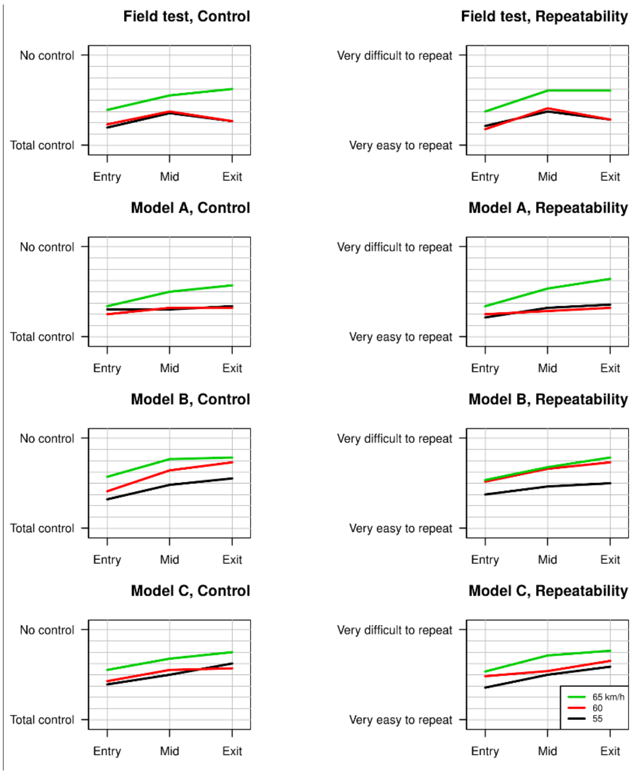

Fig. 2. Subjective evaluation of "controllability" and "repeatability"

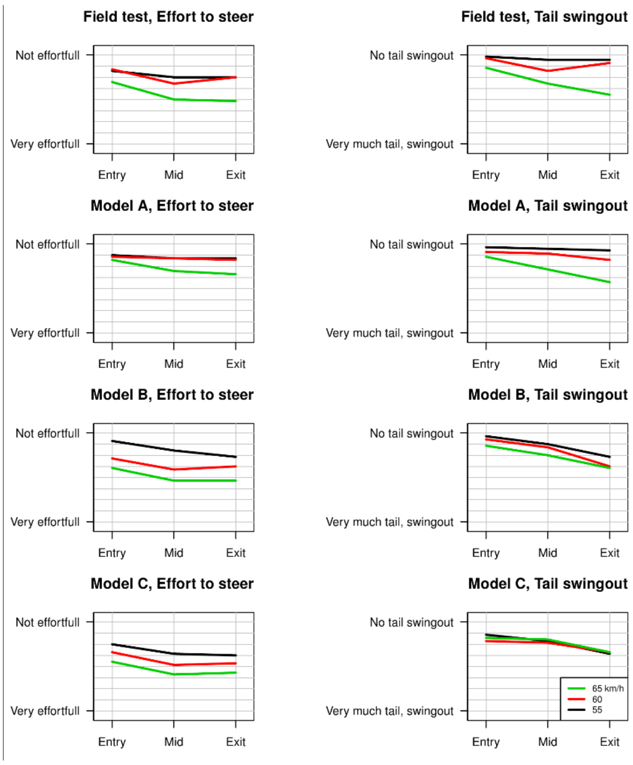

Fig. 3. Subjective evaluation of "Effort to steer" and "tail swingout"

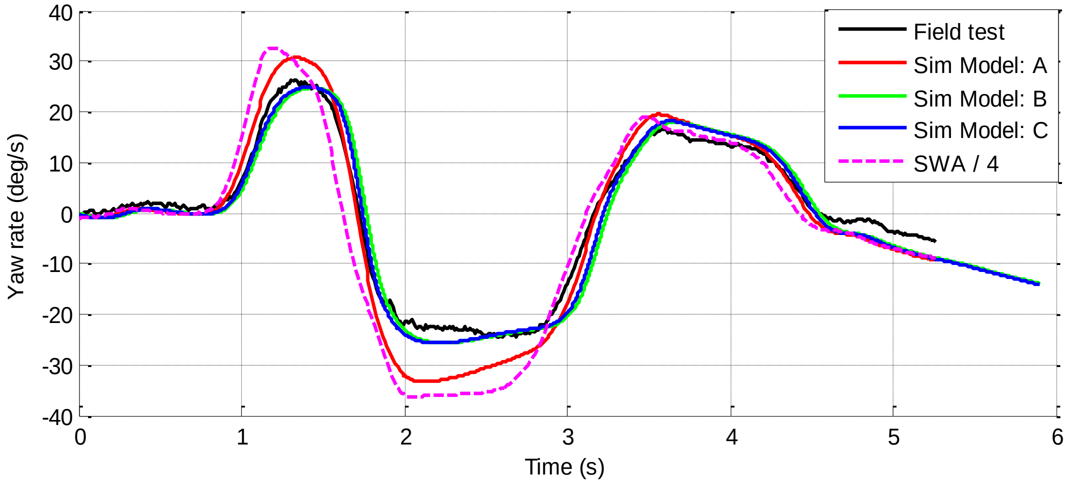

Fig. 4. Steering wheel angle (SWA) and resulting yaw rate in field test and simulations from a single field test drive at 60 km/h.

As shown in Fig. 2, drivers felt they have most control over model A. In fact, the controllability of Model A is ranked higher than the Volvo, especially at low speeds. The tendency for the Volvo at low speeds was that the feeling of control was reduced through the mid-section and regained again at the exit; this was not seen for model A. For models B and C the feeling of control was much lower already at the low speeds and it seems that the limit is reached already at 55 or 60 km/h, since the control is not regained at the exit.

With respect to tail swingout, model A imitates the Volvo rather well, but with a little less swingout at the mid-section at 60 km/h, see Fig. 3. Models B and C have more tail swingout already at lower speeds and there is little effect of increased speed for model B and no effect of increased speed for model C. This can be explained by the fact that the limit is reached already at 55 km/h.

Higher speed results in an increased effort to steer in all models. The increased effort in A is however not of the same magnitude as for the Volvo. This is in line with model A having a higher rating on control and being more neutrally steered. Models B and C require more steering effort at low speeds in comparison with the Volvo.

5.2.Objective analysis

Fig. 4 shows the recorded SWA and yaw rate from a single field test drive. From visual inspection of the curves the time lag between input and output signal seems to be about 0.10 sec throughout most of the manoeuvre. However, there is a discrepancy during the exit part of the manoeuvre when the driver tries to straighten up the car and the time lag is closer to 0.05 sec (occurs between 3.0 and 3.5 sec in the graph).

When the recorded SWA is run through the different driving simulation models the resulting yaw rate curves exhibit a different behaviour. It is clear from the figure that model A is too responsive during the first turn of the manoeuvre, while models B and C are closer to the field test data. On the other hand, during the mid-section when the driver begins to steer back, model A is now in phase with the field test data, while B and C are too slow. Which model that is closest to reality changes along the time line, and it is clear that neither of them accurately captures the dynamics of the manoeuvre. This non-constant time lag effect may pose a problem when using the cross correlation method with a constant time lag for comparing the models.

In Fig. 5 the maximum values of the SWA, lateral acceleration and yaw rate is shown for each test drive – field tests and driving simulator tests combined. It is clear that the peak lateral acceleration level of model A better represents the actual field test conditions in comparison with models B and C. In addition maximum steering inputs are bigger for models B and C, while model A better represents the field tests, which is not surprising considering that model A is more responsive. On the other hand, inspection of the maximum yaw rate shows that models B and C are well in line with the field tests, while model A results in far excessive yaw rate. In essence, models B and C have a general understeer behaviour that is closer to the real vehicle, which is also evident from the subjective evaluation.

The dynamics of the different models compared to the field tests is evaluated using the cross correlation method. The results are shown in Fig. 6. It is clear that for the field tests the correlation between input and output signals is quite high for the lower speed, but becomes increasingly worse as the speed is getting higher, particularly for the yaw rate. Thus, the correlation method needs to be complemented with an additional evaluation tool.

The general impression is that the driving simulator models have lower correlation values than the field test. Particularly model A shows low correlation for lateral acceleration during the limit handling conditions at 65 km/h.

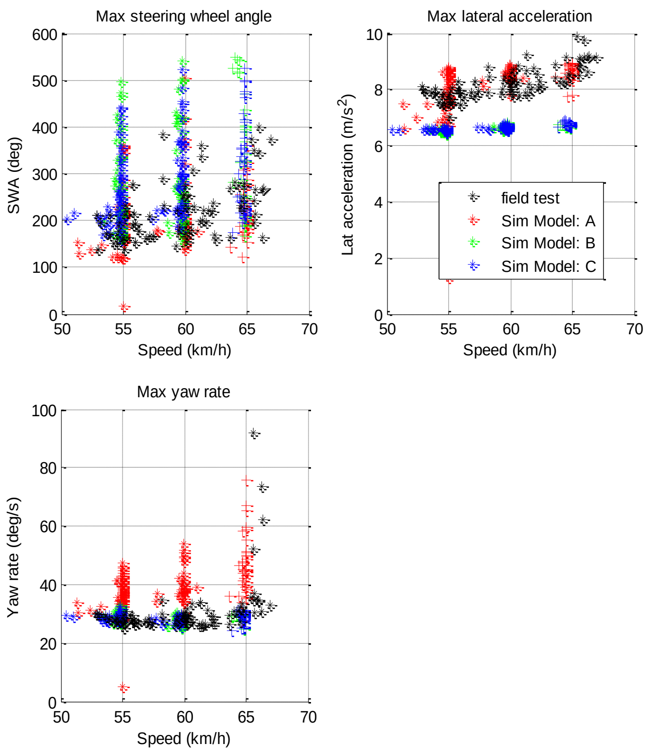

Fig. 5. Comparison of field tests and simulator tests: maximum absolute values of steering input, lateral acceleration and yaw rate.

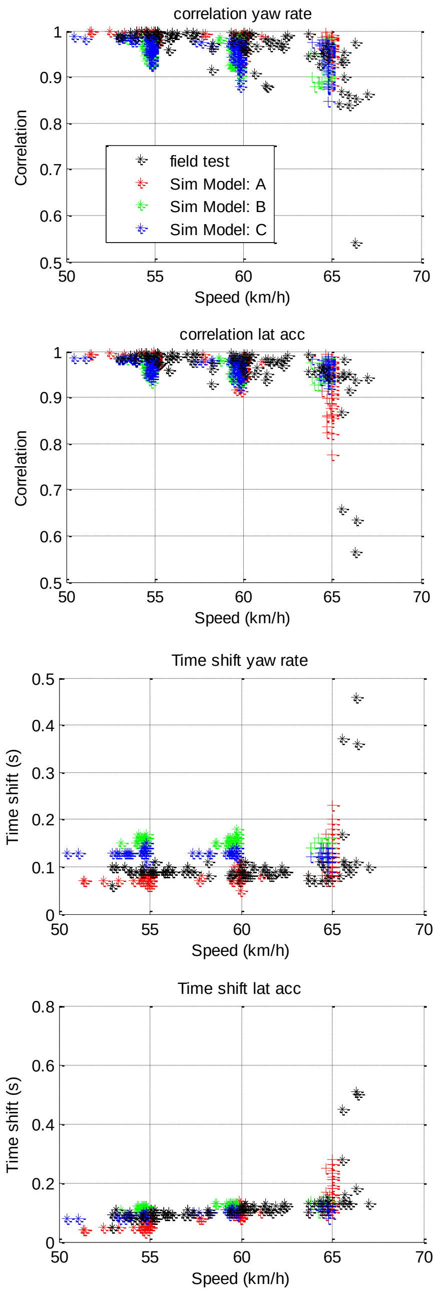

Fig. 6. Comparison of field tests and simulator tests: Correlation between input signal (swa) and output signals (yaw rate and lateral acceleration).

6. Discussion

The subjective evaluation method, used in this study, worked well and did provide useful results. Based on the subjective evaluation the following conclusions were made:

- Model A is more neutral and stable than the Volvo and has a too fast response. It also lacks the nuances that the Volvo has, like the increased understeer through the midsection. In terms of speed–response ratio the model seems to be well calibrated.

- Model B does show some of the nuances that the Volvo has, especially for steering response. There is however a mismatch between the speed–response ratio and model B reaches limit handling at much lower speeds.
- Model C, like model B, has the nuances of the Volvo. Furthermore, it reaches limit handling at higher speeds, compared with model B and is closer to the Volvo.

The rating of the vehicle attributes by the test persons in the subjective evaluation, showed that the attributes can be paired into two groups. This indicates that some attributes can be interpreted as redundant by the test persons based on their level of knowledge about the vehicle dynamics, e.g. a fast/slow steer response was interpreted as over/understeering by some test persons. Accordingly, it can be concluded that the number of questions should be adjusted to avoid redundant questions.

Regarding the objective evaluation, it can be concluded that the cross correlation method can be useful, but needs to be tailored for the application considered in this study. This is due to the fact that the time shift between input and output signals is not constant during the double lane change manoeuvre, complicating the evaluation. One possible solution is to divide the manoeuvre into sections with piecewise constant time lag and utilize the cross correlation method on the individual sections. However, more work is needed to verify this.

In addition to the cross correlation analysis, looking at the peak value of the variables of interest, namely steering wheel angle, yaw rate and lateral acceleration, also helped to identify the possible cause of differences between the simulator performance and the actual vehicle at the limit handling. One of the possible causes of the discrepancy is the tire relaxation length, which is only load dependent in the current vehicle. However, physical tire models, such as the brush model, indicate that a slip angle dependency may also be present.

In summary, this study has helped in understanding how the current vehicle model could be improved for simulating on-the-limit driving, although the method has not yet been fully developed. Both the subjective and the objective parts seems essential for a proper model evaluation. It was shown that the derived vehicle model closer captures the understeer and time lag properties of a real Volvo s40 compared to the original model. Still, additional improvements needs to be made before the model can be regarded as useful for on-the-limit driving situations.

7. References

[Nor1] Nordmark, S., Jansson, H., Palmkvist, G., Sehammar, H., (2004) The new VTI Driving Simulator – Multi Purpose Moving Base with High Performance Linear Motion. *In Proceedings of the Driving Simulator Conference 2004 Paris, 45-55.*

[Pau1] Pauwelussen J.P. "Effect of Tyre Handling Characteristics on Driver Judgement of Vehicle Directional Stability". *Vehicle Performance- Understanding Human Monitoring and Assessment.* Edited by J.P. Pauwelussen. Zwers & Zeitlinger B.B., Lisse, the Netherlands, 1999, pp. 151-176.

[Ste1] Stephens P. and Kohn H.J. "Influence of the Tyre on Subjective Handling at the". *Vehicle Performance- Understanding Human Monitoring and Assessment.* Edited by J.P. Pauwelussen. Zwers & Zeitlinger B.B., Lisse, the Netherlands, 1999, pp. 177-195. Table 1

Colour-Difference Assessment for Driving Headlight Simulation

Quentin Vidal[1,2], Sylvain Michelin[2], Baptiste Laborie[4] and Andras Kemeny[2,3]

(1) : University of La Rochelle
Laboratoire Informatique Image et Interaction
F-17042 La Rochelle Cedex 01
{quentin.vidal,sylvain.michelin}@univ-lr.fr

(2) : Technocentre Renault
Technical Center for Simulation
1 avenue du Golf, F-78288 Guyancourt
{quentin.vidal,andras.kemeny}@renault.com

(3) : Arts et Métiers ParisTech
Laboratory of Immersive Visualization
151 Boulevard de l'Hôpital, F-75013 Paris
{andras.kemeny}@ensam.eu

(4) : OKTAL
19 Boulevard des Nations Unies
F-92190 Meudon, France
{baptiste.laborie-renexter}@renault.com

Abstract – In high quality driving simulation applications, such as headlight simulation, colorimetric validity is essential. In virtual testing of headlight systems, it is important that the WYSIWYG (What You See Is What You Get) paradigm is respected for product quality headlight assessment. Indeed, if a slightly reddish orange colour is displayed instead of the typical orange of halogen lighting, the effect for driver comfort or traffic safety can be critical. The lighting specialist should accept a headlight which doesn't have the right colour.

Previous studies have shown that there is a significant colour difference between virtual and real environments. Nevertheless, in virtual headlight testing the rendered colour fidelity has to fit industrial assessment. This study therefore deals with the colour-difference perceptibility that is the ability of an observer to detect a difference between two colours and, more precisely, on the acceptability of the perceived difference.

We propose in this paper a psychophysical function for colour difference acceptability which fits well with the measured data. The colour acceptability function was implemented in a driving simulator for high validity headlight assessment. Driver acceptability experimentation was carried out using Renault's headlight driving simulation equipped with a full-cab and a 210° cylindrical display screen.

Key words: Colour-Difference Acceptability, Virtual Reality, Psychophysical Threshold.

1. Introduction

1.1. Purpose

Virtual environments are gaining widespread acceptance as a tool for assessing the quality of physical prototype such as vehicle headlights. In a context of high quality simulation applications, it is essential that a displayed colour is as near as possible to the real one. Indeed, if a slightly reddish orange colour is displayed instead of the typical orange of halogen lighting, the effect for driver comfort or traffic safety can be critical. The lighting specialists should accept a headlight which doesn't have the right colour.

Previous internal investigation has shown that a significant colour difference exists between virtual and real environments. In a critical application such as the evaluation of vehicle headlights, the acceptability of that difference as to be evaluated.

1.2. Related works

1.2.1. Colour perception

For the human colour perception, the CIE (*Commission Internationale de l'Eclairage*) has defined two widely used colour spaces: CIELAB and CIELUV [CIE1]. Both spaces are derived from the CIE XYZ colour space and are known to be pseudo-uniform which mean that the perceived difference between two colours depends on their locations in that space.

Because of this non-uniformity, the computation of the perceived difference in the CIELAB space has evolved. The first metric ΔE^*_{ab}, released in 1976, is define as the

Euclidean distance. This formulae has been succeeded by three other reputed metrics: ΔE^*_{CMC}, ΔE^*_{94} [CIE1] and ΔE^*_{00} [Sha1]. Those new metrics introduce application-specific weights which are unknown for our application. That's why, when the notion of difference appears in this article it refers to the first metric.

Using the ΔE^*_{ab}, it is often considerate that the JND (Just Noticeable Difference) is 1 unit which means that no difference can be seen between two colours if the difference between them is under that value [Kan1] [Mah1]. Later, using the ΔE^*_{94}, Gibson *et al.* [Gib1] found acceptable a characterized display that has a mean prediction error of 1.98.

Due to the variety of observers, the difference acceptability is harder to define. Abrardo *et al.* [Abr1] evaluated the VASARI scanner and classified a difference between 1-3 as "very good quality", 3-6 as "good quality", 6-10 as "sufficient" and over 10 as "insufficient". Hardeberg [Har1] defines a rule of the thumb where the difference is "acceptable" if it's between 3 and 6. Lastly, Thomas [Tho1] extended Hardeberg's rule by taking into account the difference between an expert and a consumer.

1.2.2. Psychophysical methods

For the determination of a correlation between a physical stimulus (objective) and the perception of it (subjective) a psychophysical task have to be made. In this psychophysical experiment where a series of colours tests are compared with a reference, a threshold can be computed from the statistical count of accepted and non-accepted colour differences [Lab1].

Among the existing methods, Ehrenstein *et al.* [Ehr1] made a classification of those which have proven to be most useful in that research field: *method of adjustment*, *method of limits*, *method of constant stimuli*, *adaptive testing*, *forced-choice methods*.

Four of the five previous methods can only be used for the determination of a threshold between two categories and cannot be adapted for the determination of an acceptability rate which is dependant of the consumer's will. In this kind of context, the method of the constant stimuli had to be selected [Wic1].

Furthermore, for the evaluation of the colour acceptability another aspect have to be taken into account. Indeed, when asked to provide a visual judgment, an observer may interpret the acceptable colour-difference, depending upon the intended or anticipated end use of the product. Thus colour-difference acceptability results from a compromise between the process outcome and the customer expectations [Lab1].

2. Experiments

In this section, we describe two different experiments that were conducted with two objectives: (1) allowed us to compute a psychological function which relates the percentage of acceptability in function of a colour difference to a reference, and (2) compute a threshold between acceptability and unacceptability of a difference in an expert population.

The experiments took place in the lighting simulator at Renault where all the light/screen were turned off. The observer sat on the driver's sit at a distance of 3.5 meters of the screen. At that distance, with A4 patches and following the recommendation of Schanda [Sch1], the standard 10° observer was used for the colour space transformations.

For those two experiments, the observer was invited to report his degree of satisfaction on the colours similarity via a man-machine interface. He has to make his decision between four semantic categories: "Very Satisfied", "Satisfied", "Not Satisfied", "Very Unsatisfied". To understand this scale, instructions were given before the test: "Very Satisfied means that no difference can be seen and Very Unsatisfied when the difference is much too far. For the other values, imagine that you order a car or a cloth with a specific colour and you get the other one. Would you accept this difference?".

2.1. Experiment n°1

In front of the observer nine patches were disposed on the screen. During the test a computer program was responsible to randomly enlighten, via a calibrated sRGB projector Barco's Galaxy NW-12 with a gamma of 2.2 and a D65 white point, one of those patches and display a virtual colour next to it (ref. section Patch selection). Usually, for comparison of two colours a grey background is used [CIE2], for our application we used the mean colour of the rendered scene because it's in that condition that the headlights are evaluated.


a

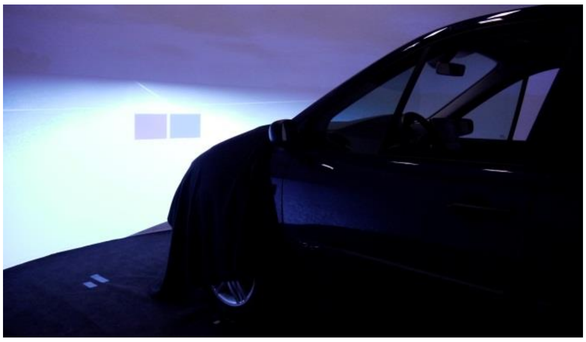
b

Fig. 1. Experimental condition for: a - experiment n°1, b – experiment n°2

To limit the experiment duration, the observer had to take his decision about the difference in less than ten seconds. Such a time was chosen because in this time the observer can see the two patches, think if he accepts or not the difference and validate the answer. If he weren't able to make his decision during that time, the program passes to another patch.

The chosen population for this experiment was composed by 10 women and 27 men both aged 25-50. All participants had normal colour vision tested with the Ishihara's colour deficiencies test and no one had experience with the colour management.

2.2. Experiment n°2

The aim of the second experiment is to evaluate/validate the result of the first experiment. In that purpose, the experiment was lead under the virtual environment SCANeR™ (i.e. the environment used by Renault lighting specialist). Under this environment, two patches were disposed on the road and were uniformly enlighten by the car headlights.

Using the staircase method [Ehr1], the observer had to accept or not the difference between those two patches. If he accepts, the difference increase otherwise it decrease. At the beginning, the two patches were widely separated (ΔE^*_{ab} of 20) which force the expert to reject this first value. The initial value of the step was set to ΔE^*_{ab} of 4 and progressively reduced to 0,125 (to compute a precise thresh the step is divided by two at each reversal).

In this experiment, the population was composed by three colour expert from Renault (design direction). Two works on the industrial quality validation and the other one on the colour & material expert assessment. Because of the expert nature of the population, it's considered, as a predicate of this experiment, that their results should be highly closed among themselves and the result not dependant of the number of participants.

2.3. Patch selection

2.3.1. Physical patches

The physical patches use in this experiment come from the Natural Colour System®© and are guaranteed not to exceed $\Delta E^*_{CMC} =$ 0.8. Those patches were selected because they fit the specification of the white lamps for road vehicles [AFN1] and they're in the sRGB gamut which correspond to the projector's gamut (see Fig. 2). The nine chosen patches of this evaluation are selected because: six of them correspond to the headlight gamut boundary and three to the colour coordinates of the three mains lamps used in the Renault's headlight (LED, Halogen and Xenon).

2.3.1. Virtual patches

For the determination of the acceptability threshold, it is important to know the difference between the physical patch and the virtual one. With the $L^*a^*b^*$ value of the real patch the sRGB value can be computed following [CIE1]. However, because of the reflectivity of the screen, the colours seem different. Equalization had to be made and was validated by two colours experts (1 designer and 1 doctor in vision science).

Because of the non-uniformity of the CIELAB space, the distance from which everybody find the difference "Very Unsatisfied" have to be compute. For that point the staircase method [Wic1] have been used for the four judgements directions of each patch.

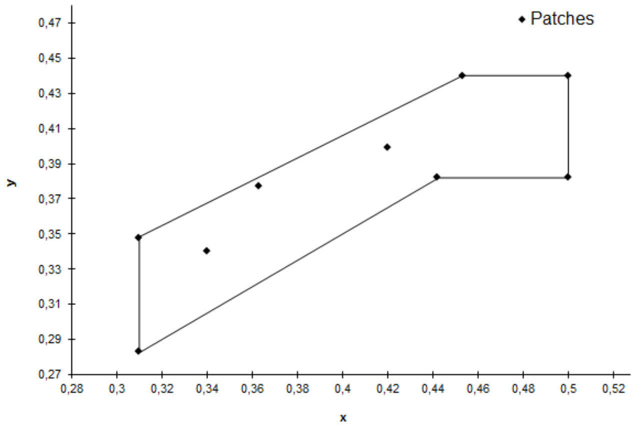

a

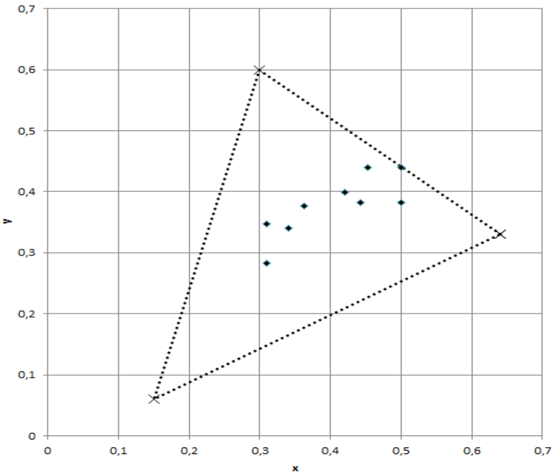

b

Fig. 2, Patches xy coordinates in: a – headlight gamut [AFN1], b – sRGB gamut

Once the maximum distance D_{max} is obtained, for each direction, the set can be divided in six equal parts. Each distance δ lies in $1 \leq \delta \leq D_{max}$. From that distance and the L_{ab} value of the reference patch, the new values are computed using the CIELCH space. For each distance in chroma, the new values C_{dist} are computed by adding to the initial Chroma value C_{init} the distance δ (see Eq. 1). For the difference in hue, it isn't possible to directly use the distance; it has to be converted in an angle using the law of cosine. For this, an isosceles triangle is considered (because the Chroma needs to be constant). Once the difference angle α computed, the hue value h_{dist} is calculated by adding α to the initial hue h_{init} (see Eq. 2).

$$C_{dist} = C_{init} + \delta \tag{1}$$

$$\alpha = arccos\left(\frac{2\times C_{init}^2 - \delta}{2\times C_{init}^2}\right) \quad h_{dist} = h_{init} + \alpha \tag{2}$$

3. Results

3.1. Psychophysical function fitting

The psychophysical function is often represented by a two-parameter function F, which is typically a sigmoid function, such as the Weibull, logistic, cumulative Gaussian, or Gumbel distribution [Wic1]. This kind of shape is explained by the fact that the more a stimulus is close to a reference the more people don't see any difference and accept it. In our case, the function that best describes our distribution is the logistic one (see Fig. 3).

The overall results for the function fitting is presented on Table 1 and, as expected, the parameters alpha and beta are different for each patch and for each axis. This is explained by the non-uniformity of the CIELAB-space and by the used metric.

Despite that, the function fitting is strongly correlated to the real data with only 6 of the 36 values under 0.95, a mean coefficient of determination of 0.97, a standard deviation of 0.02 and a minimum value of 0.8988.

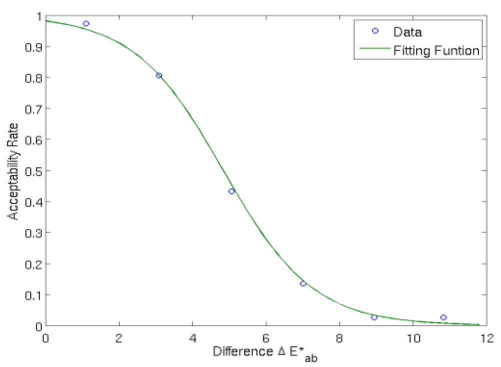

a

$$F(x) = \frac{1}{1 + \exp(\beta \times x + \alpha)}$$

b

Fig. 3. Sigmoid function: a – Fitting of the logistic function (green curve) with the acceptability rate data (blue dot), b – Equation of the logistic function

Table 1. Psychophysical coefficient α, β and the coefficient of determination R^2 for each axis of each patches.

		1	2	3	4	5	6	7	8	9
Chroma -	α	4.1185	4.4624	3.3926	3.0079	4.5274	2.817	3.6273	2.5825	3.1449
	β	-0.5894	-0.9198	-0.7189	-0.3520	-0.5736	-0.2690	-0.9331	-0.8178	-0.8178
	R^2	0.9915	0.9958	0.9921	0.9842	0.9831	0.9110	0.9852	0.9651	0.9760
Chroma +	α	3.1157	2.6065	2.6974	2.5026	2.3688	2.0838	2.0182	4.0595	3.2351
	β	-0.6943	-0.6008	-0.4561	-0.3258	-0.3614	-0.0982	-0.4161	-0.6794	-1.4235
	R^2	0.9725	0.9764	0.9762	0.9650	0.9683	0.9191	0.9542	0.9885	0.9764
Hue -	α	6.9637	4.1312	3.5242	3.8316	2.8139	3.2619	3.9539	4.2934	7.5371
	β	-2.1862	-0.7898	-0.8104	-0.7154	-0.5679	-0.5716	-0.5716	-0.9310	-1.2043
	R^2	0.9782	0.8988	0.9907	0.9459	0.9881	0.9866	0.9985	0.9126	0.9910
Hue +	α	2.0519	3.9824	4.0638	2.4571	2.9708	4.1719	4.4488	1.8822	2.3237
	β	-0.9979	-0.6461	-0.8694	-0.7159	-0.5748	-0.5201	-1.1804	-0.8674	-0.8310
	R^2	0.9875	0.9611	0.9850	0.9738	0.9119	0.9913	0.9913	0.9691	0.9864

Even if the data were highly correlated to the real data some psychological function had to be remove from the set. That's the case for the patch n°6 where its acceptability percentage doesn't go below 25% and moves back up at the maximal difference. Because of the patch position on the sRGB gamut (see Fig 2.a) this result could have been predicted. Indeed, this patch was on the border of the gamut and the computation of the new colours using the Eq.1 and 2 generates colour that cannot be displayed by the projectors.

From that result and the knowledge that most of the time, a threshold measured with the method of constant stimuli is defined as the intensity value that elicits perceived responses on 50% of the trials [Ehr1], it's possible to reverse the function F(x) for having the acceptable difference in function off the acceptability rate (see Eq 3.).

$$x = \frac{\ln\left(\frac{1}{F(x)} - 1\right) - \alpha}{\beta} \qquad (3)$$

3.2. Expert's validation

Like expected from an expert population, their responses for the colour difference acceptability test are closely connected with a mean standard variation of 0.49 which is under the just noticeable difference of the colour perception [Kan1]. This first result shows that the experts are agreed amongst themselves which validate our predicate for this experiment.

From the computed expert acceptation threshold and the function giving the percentage of colour-difference acceptability in the normal population, it's possible to know how are situated the expert population compared to the normal one (see Table 2).

This data set shows that Renault's colour experts do not accept a colour difference when 71.3% of the normal population accepts it. However, it seems that some values of the set are significantly different of the others (like the patch n°5 with the negative hue).

For cutting-off highly influential values, it is supposed that the acceptable difference for the expert population match a particular percentage in the normal one. In such a case, we can model the problem by a linear regression with a null slope and a y-intercept equal to the mean of the set.

The outlier suppression is performed using the Cook's distance which measures the effect of deleting a given observation. If the distance D_i is over the constant $4/n$ (with n the number of observation), a closer examination of the data have to be made [Bol1].

This test reveals that a particular attention had to be made concerning three data (bold values in Table 2). After a measure session it appears that, for those data, we were not able to reproduce the right colour . Removing those data enables us to know that the expert population does not accept a colour-difference when 76% of the normal one accepts it.

Table 2. Naïve population acceptability rates in function of the expert acceptable difference.

	1	2	3	4	5	7	8	9
Chroma -	96.74%	90.59%	88.35%	77.25%	73.18%	84.67%	84.56%	75.06%
Chroma +	88.23%	73.19%	77.43%	74.42%	70.66%	69.07%	90.67%	53.21%
Hue -	75.79%	90.43%	62.11%	82.74%	19.06%	56.94%	93.86%	96.90%
Hue +	66.68%	91.84%	73.43%	56.02%	11.04%	26.64%	59.80%	51.00%

Table 3. Colour-difference acceptability.

	Expert		Naïve
	Mean ΔE^*_{ab}	Max ΔE^*_{ab}	Mean ΔE^*_{ab}
$\Delta E^*_{ab} \leq 1$	Good	Good	Good
$1 < \Delta E^*_{ab} \leq 3.1$	Acceptable	Good	Good
$3.1 < \Delta E^*_{ab} \leq 4.8$	Unacceptable	Acceptable	Acceptable
$\Delta E^*_{ab} > 4.8$	Unacceptable	Unacceptable	Unacceptable

4. Discussion

The first experiment shows that the computed s-shaped curves are strongly correlated to the data with a mean coefficient of determination of 0.97. Like we expected, because of the non-uniformity of the CIELAB-space the coefficients of each curve are different. Another interesting thing which will not be discussed here is that instead of separating the hue/chroma into a negative and a positive, it was also possible to take the whole hue/chroma data and fits a Gaussian curve.

The second experiment indicates that for a high quality application such as the headlight assessment, the common 50:50% threshold [Ehr1] isn't optimal. Indeed, colour expert from Renault find unacceptable a colour difference when 76% of the normal one accepts it. With this value and the equation 3, the corresponding value of the colour-difference is computed and the following table constructed.

The values 3.1 and 4.8 are respectively computed using the 76% and 50% of acceptability rates. For the expert population, in addition to the mean difference, the maximum difference is added. Indeed, the global scene can have a good representativity but cannot display correctly the road line marking colour which is used by the headlight expert for assessing the headlight quality.

5. Conclusion

In this paper, we present a method for assessing the acceptability of a colour-difference of a driving car simulator. In that purpose, we have lead two psychological experiments; the first one with naïve people and the second one with colour expert from Renault. Those experiments enable us to construct a colour-difference acceptability scale which directly reflects the perception of the observers (expert and non-expert).

Besides, we found that a significant difference exist between the naïve and the expert population, this result is in agreement with a previous study lead by Shamey *et al.* [Sha2] where they found a significant difference between the two populations in the assessment of small colour differences. This difference, can be explained by the fact that expert are accustomed to this task and have an *a priori* knowledge on what they accept or not [Mil1].

A limit to our method is the use of the old metric ΔE^*_{ab}, a future work would be to determine the best colour-difference metric for a driving car simulator. Another improvement point would be the use of more colours in the experiment. Indeed, nine colours are enough for the evaluation of the headlight rendering but in a more complex scene there are more colours which lead us to the evaluation of more colours.

Another interesting point that wasn't discuss here is that our data can also be approximated by a Gaussian curve which isn't centred on $\Delta E^*_{ab} = 0$. This means that the observer finds a colour slightly different better than the same colour.

6. References

[Abr1] Abrardo A., Cappellini V., Cappellini M. and Mecocci A., "Art-works colour calibration using the VASARI scanner.", *Color Imaging Conference, IS&T - The Society for Imaging Science and Technology*, 1996, pp. 94-97.

[AFN1] Association Française de Normalisation, "Lamps for road vehicles - Dimensional, electrical and luminous requirements", *AFNOR pub.*, NF EN 60809/A4, 2009.

[Bol1] K. A. Bollen and R. W. Jackman "Regression Diagnostics An Expository Treatment of Outliers and Influential Cases", Sociological Methods & Research, 1989, 13(4), pp 510-542.

[CIE1] International Commission on Illumination, "Technical Report – Colorimetry", *Pub. 15:2004 3rd ed,* ISBN 3-901906-33-9, 2004.

[CIE2] International Commission on Illumination, "Parametric effects in colour-difference evaluation", *Pub. CIE 101-1993*, ISBN 978 3 900734 38 1, 1993.

[Ehr1] Ehrenstein W. H. and Ehrenstein A., "Psychophysical Method", *Modern Techniques in Neuroscience Research*, Chap. 43, 1999.

[Gib1] Gibson J. E., Fairchild M. D., "Colorimetric characterization of three computer displays (LCD and CRT)", *Munsell Color Science Laboratory Technical Report*, 2000.

[Har1] Hardeberg J. Y., "Acquisition and reproduction of colour images: colorimetric and multi-spectral approaches", *Master Thesis at Ecole Nationale Supérieure des Télécommunications*, 1999.

[Kan1] Kang. H. R., "Color Technology for Electronic Imaging Devices", *SPIE Optical Engineering Press.*, 1994.

[Kem1] Kemeny A., Combe E. and Posselt J., "Perception of Size in Vehicle Architecture Studies*", Proceedings of the 5th Intuition International Conference*, 2008.

[Lab1] Laborie B., Viénot F., Langlois S., "Methodology for constructing a colour-difference acceptability scale", *Journal of Ophthalmic and Physiological Optics*, 2010, 30(5).

[Loo1] Loomis J. M. and Knapp J. M., "Visual perception of egocentric distance in real and virtual environment", *Virtual and Adaptive Environments*, 2003, pp. 21-46.

[Mah1] Mahy M., van Eycken L. and Oosterlinck A., "Evaluation of uniform color spaces developed after the adoption of CIELAB and CIELUV", *Color Research and Application*, 1994, 19(2), pp. 105-121.

[Mil1] Miller A.M., "The Magical Number Seven, Plus or Minus Two: Some Limits on Our Capacity for Processing Information", *The Psychological Review*, 1956, vol. 63, pp. 81-97.

[Tho1] Thomas J. B., "Colorimetric characterization of displays and multi-display systems", *Master Thesis at University of Bourgogne*, 2009.

[Sch1] Schanda J., "Colorimetry: Understanding the CIE system", *John Wiley & Sons*, ISBN 9780470175620, 2007.

[Sha1] Sharma G., Wu W. and Dalal E. N., "The CIEDE2000 Color-Difference Formula: Implementation Notes, Supplementary Test Data, and Mathematical Observations", *Color Research & Applications*, 2004, 30(1), pp. 21–30.

[Sha2] Shamey R., Cardenas L. M., Hinks D. and Woodard R., "Comparison of naïve and expert subjects in the assessment of small color differences", *Journal of the Optical Society of America,* 2010, 27(6), pp. 1482-1489.

[Wic1] Wichmann F. A. and Hill N. J., "The psychometric function: I. Fitting, sampling, and goodness of fit", *Perception & Psychophysics*, 2001, 63, pp. 1293-1313.

VARIABLE ROLL-RATE PERCEPTION IN DRIVING SIMULATION

Paolo Pretto [1], Alessandro Nesti [1], Suzanne Nooij [1], Martin Losert [1,2], Heinrich H. Bülthoff [1,3]

(1) Max Planck Institute for Biological Cybernetics, Dept. Human Perception, Cognition and Action
E-mail: {paolo.pretto, heinrich.buelthoff}@tuebingen.mpg.de

(2) University of Tübingen, Dept. Psychology

(3) Korea University, Dept. Brain and Cognitive Engineering

Abstract – In driving simulation, simulator tilt is used to reproduce linear acceleration. In order to feel realistic, this tilt is performed at a rate below the tilt-rate detection threshold, which is usually assumed constant. However, it is known that many factors affect the threshold, like visual information, simulator motion in additional directions, or active vehicle control. Here we investigated the effect of these factors on roll-rate detection threshold during simulated curve driving.

Ten participants reported whether they detected roll in multiple trials on a driving simulator. Roll-rate detection thresholds were measured under four conditions. In the first condition, three participants were moved passively through a curve with: (i) roll only in darkness; (ii) combined roll/sway in darkness; (iii) combined roll/sway and visual information. In the fourth condition participants actively drove through the curve.

Results showed that roll-rate perception in vehicle simulation is affected by the presence of motion in additional directions. Moreover, an active control task seems to increase the detection threshold, i.e. impair motion sensitivity, but with large individual differences. We hypothesize that this is related to the level of immersion during the task.

Key words: Motion Cueing, Motion Perception, Tilt-coordination, Driving simulation

1. Introduction

In dynamic vehicle simulation, motion cueing algorithms (MCAs) aim to adapt the original vehicle motion to the limited capabilities of simulators, while preserving at the same time the perceptual realism of the simulation. The goal of MCAs is therefore to transform the linear and angular accelerations of the simulated vehicle into translations and rotations of the motion platform, such that perceptually equivalent specific forces and rotations are provided to the driver.

Most MCAs are based on washout filters, which split the input linear accelerations into high-frequency and low-frequency components. The high-frequency components are integrated to produce the translational motion of the platform, while the low-frequency components are reproduced by tilting the platform [Nah1]. The tilt of the platform is used by MCAs to simulate sustained accelerations (otherwise not reproducible) exploiting the so-called tilt-coordination technique [Ben1, Gro1]. This is one of the most used "perceptual tricks" in motion cueing, which relies on the tilt-translation ambiguity [Ang1]. Indeed, under certain conditions the simulator tilt can be perceived as linear acceleration, as the reorientation of the body with respect to gravity causes the sensation of being forced into (or away from) the seat. This illusion occurs because different combinations of linear accelerations and static body tilt result in similar gravito-inertial forces acting on the humans inertial sensory systems (primarily vestibular and somatosensory). This is particularly effective when concurrent translational motion is visually presented [Gro1]. The tilt-coordination technique exploits the inability of humans to resolve the tilt-translation ambiguity, and use simulator tilt to induce the illusory perception of sustained linear acceleration [Sta1].

However, the illusion is spoiled if the platform tilt is detected by the driver. This happens when the tilt velocity exceeds the perceptual threshold, inducing the sensation of rotational motion and resolving the ambiguity. Therefore, to preserve the realism of the simulation, a rate limiter saturates the platform tilt-rate below perceptual threshold. A commonly used saturation value is 3 deg/s [Gro1].

Tilt-rate detection threshold is usually measured in darkness [Soy1, Zai1]. Yet, it is known that motion perception thresholds can vary in the presence of visual information [Gro1, Val1], simulator motion in additional directions, i.e. increased motion complexity [Zai1], active vehicle control [Hos1, Dev1, Nes1], or even cognitive expectations [Wer1]. All these factors are actually present in a typical driving simulation. Still, most of current MCAs assume constant tilt rate thresholds, often derived from studies where simple motion stimuli were investigated. Therefore, a better understanding of how motion complexity, visual information and active control affect the perception of simulator motion may help in improving the efficiency of tilt-coordination techniques.

In this study, we investigated for the first time in the same experiment (using the same simulator and methodology for all experimental conditions), the effect of each of these factors on roll-rate detection threshold during simulated curve driving.

2. Method

2.1. Setup

The experiment was conducted on the CyberMotion Simulator (CMS) at the Max Planck Institute for Biological Cybernetics. The CMS was developed as an alternative to traditional dynamic simulators based on hexapod systems [Nie11]. It is a 8-dof serial robot, where a 6-axes industrial robot manipulator is mounted on a linear rail and equipped with a motorized cabin at the end effector (figure 1, top). The cabin is equipped with a stereo projection system and mounting possibilities for haptic control devices used for flight and driving simulation (figure 1, bottom). In the driving configuration it is equipped with force-feedback steering wheel (Sensodrive GmbH, Germany) and pedals, and a large projection screen (160 x 90 deg FoV) with two WUXGA (1920x1200 pixels) projectors. For this study, the motion was generated using a classical washout filter, adapted to the cylindrical workspace of the CMS [Rob1]. No linear rail was used and the lateral motion was mapped into a circular trajectory [Nes1]. The vehicle dynamics and the visualization environment were provided by the simulation software CarSim (Mechanical Simulation, Michigan, US). The visual scene resembled a flat skidpad, and no roll-motion was present other than the one originating from the car suspensions.

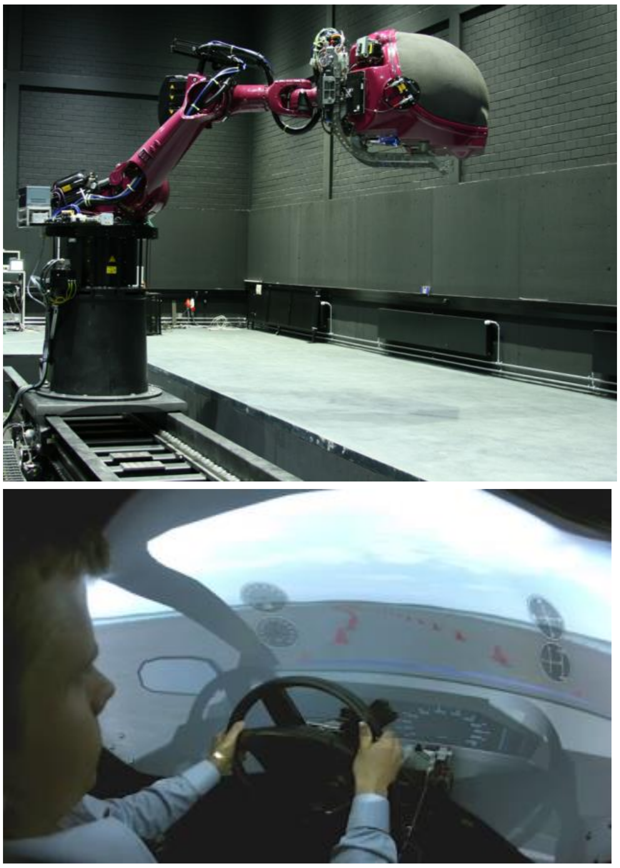

Fig. 1. The Max Planck Institute CyberMotion Simulator: exteriors (top) and cabin interior (bottom).

2.2. Experimental manipulations

The rate limiter of the tilt (roll) channel of the washout filter was manipulated during this experiment. Roll-rate detection thresholds were estimated under four conditions:

- “Roll”: roll only in darkness;
- “+Sway”: combined roll/sway in darkness;
- “+Visual”: combined roll/sway and visual information whilst passively moved through a curve;
- “+Active”: combined roll/sway and visual information whilst actively driving around a curve.

An overview of the experimental conditions is provided in Table 1.

Table 1. Experimental conditions

	“Roll”	“+Sway”	“+Visual”	“+Active”
Roll	present	present	present	present
Sway	absent	present	present	present
Visual	absent	absent	present	present
Active	absent	absent	absent	present

2.3. Procedure

Ten participants (three females), aged between 25 and 36 (mean = 29, SD = 3.5) took part in the experiment. All had a valid driving license for at least three years and self-reported regular car usage. The experiment was divided into four sessions, over different days. Each session started with three practice trials to familiarize the participant with the task. When the participant initiated a trial by button press, the car accelerated automatically on a straight road until a constant speed of 70 km/h was reached. The speed was maintained constant throughout the whole trajectory. During the acceleration phase, the surround scene and the layout of the curve were visible in all conditions (figure 1, bottom). Before entering the curve section, the screen turned to black in conditions "Roll" and "+Sway"; while in conditions "+Visual" and "+Active" the outside view remained visible. The car progressed through the curve automatically (conditions "Roll", "+Sway", and "+Visual") or with the heading actively controlled by the participant (condition "+Active"). At the end of the curve the road was straight again (no active control required) and the following question appeared on the screen: "Did the car tilt (Y/N)?" The participant indicated the answer by pressing a button accordingly. When the answer was given the car decelerated and the simulator was brought back to the starting position for the next trial.

Thresholds were measured by iteratively adjusting roll-rate saturation value according to the Single Interval Adjustment Matrix (SIAM) procedure [Kae1, She1]. In 50% of the trials, the tilt coordination path of the MCA was active (roll motion present), while in the other 50% tilt coordination was disabled (roll motion absent). Additional roll-motion of the car (e.g. suspensions) was not cued. The trials were randomly interleaved. The participants had to correctly identify whether the roll was present by answering the question above. The adjustment matrix of the four possible outcomes was set up to induce a neutral response criterion: the answer "yes" in presence of roll (hit) decreased the roll-rate saturation value for the next trial of one step size; the answer "no" in absence of roll (correct rejection) left the roll value unaltered; the answer "yes" in absence of roll (false alarm) increased the next roll value of two step size; the answer "no" in presence of roll (miss) decreased the roll rate of one step size for the next trial. The SIAM is given in short form in Table 2.

Table 2. Single Interval Adjustment Matrix

Motion Stimulus	Answer: "Yes"	Answer: "No"
Roll	Hit [-1]	Miss [+1]
No Roll	False Alarm [+2]	Correct Rejection [0]

Since in the "Roll" condition the thresholds were expected to be the lowest, the initial roll rate was 6 deg/s, with an initial step size of 1 deg/s. For all other conditions the initial rate was 12 deg/s and the step size was 2 deg/s. The step size was halved every 4 reversals of the resulting staircase (figure 2). The session was terminated after 12 reversals, where a reversal is a change in the staircase direction from decrease to increase or vice versa. The threshold was then computed as the average roll rate over the last 5 reversals. An example of the resulting staircase profile is shown in figure 2.

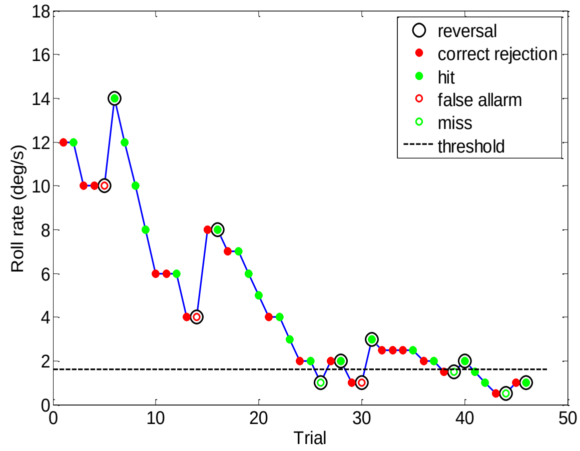

Fig. 2. An example of staircase from the study (condition "+Sway"). The initial roll rate was 12 deg/s, with initial step size 2 deg/s, which was halved to 1 deg/s after four reversals and to 0.5 deg/s after 8 reversals. The staircase was terminated after 12 reversals and the last five were averaged to compute the threshold (dashed line).

After each session, participants filled out a questionnaire to indicate their subjective ratings about mental demand, level of concentration, ability to maintain a constant level of attention, level of frustration, physical comfort and simulation realism on a 9-point rating scale (Table 3).

Motion sickness questionnaires were also collected for all participants after each experimental session [Ken1]. In every session, the level of sickness was monitored every 10 minutes using a numerical score, based on the scale used by Golding and colleagues [Gol1]. A typical session lasted about one hour.

Table 3. Rating Scale

Item #	Question
1	"Overall mental demand"
2	"Average level of concentration"
3	"Ability to keep concentration"
4	"Level of frustration"
5	"Physical comfort"
6	"Feeling of being in a car"
7	"Quality of lateral motion: strength"
8	"Quality of lateral motion: timing"

3. Results

In the following sections we report the results of the three types of measures that were collected during the experiment: perceptual thresholds for roll-rate, objective measures of the driving behavior, and subjective ratings of the task attentional demand and the level of immersion in the simulation.

One participant did not complete condition "+Visual" due to mild symptoms of motion sickness. Therefore, the corresponding staircase stopped after 7 reversals (31 trials), of which the last five were used to calculate the threshold. Two participants did not fill out the questionnaire at the end of a session. The missing values were replaced by the average score of the other participants in the same condition, and included in the analysis of subjective ratings.

3.1. Perceptual thresholds

Mean detection threshold for roll-rate increased from 0.7 deg/s with roll only (condition "Roll") to 6.3 deg/s in active driving (condition "+Active"), while mean threshold was 3.9 deg/s and 3.3 deg/s in conditions "+Sway" and "+Visual" respectively (figure 3, blue line). A repeated-measures analysis of variance (ANOVA) indicated a significant effect of the four conditions on the roll-rate detection threshold ($F(3,27) = 5.49$, $p < 0.05$). Post hoc test with Bonferroni adjustment for multiple comparisons revealed a significant difference between condition "Roll" and conditions "+Sway" and "+Visual", which did not differ from each other. For condition "+Active", large differences between participants were observed: for some the threshold did not increase from passive to active driving, while for others about 3 times higher threshold was measured. A cluster analysis (k-means clustering) of the thresholds distribution in condition "+Active" revealed that thresholds values could be divided into two clusters: "High Threshold Cluster" and "Low Threshold Cluster", respectively indicated by black and red lines in figure 3.

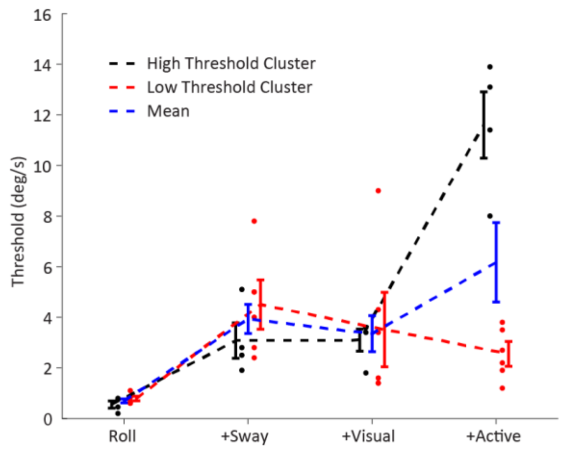

Fig. 3. Roll rate detection thresholds. Global mean (blue line); mean thresholds for participants who showed increment in condition "+Active" (black line); mean thresholds for participants who showed no increment in condition "+Active" (red line). Error bars indicate ±1 SEM.

3.2. Behavioral measures

During the trials of condition "+Active", steering wheel commands and car position were continuously recorded. These data where analysed to find evidence of the above reported differences in motion sensitivity.

Neither steering wheel angle and associated variance over time, nor the car position on the track and associated variance over time showed significant differences between the two clusters of participants. An inspection of the power spectral density (PSD) of the steering wheel commands also indicated no qualitative differences in driving behaviour between the two clusters.

We did not find any significant differences in driving behaviour for all the considered objective measures. This clearly indicates that the differences in roll-rate detection thresholds between the two clusters cannot be related to different driving styles, or to different motion profiles experienced by the participants.

3.3. Subjective ratings

In the active driving condition ("+Active"), participants with high thresholds (low sensitivity) reported a lower level of immersion (question 6 "Feeling of being in a car") than participants with low thresholds (better sensitivity), as shown in figure 4.

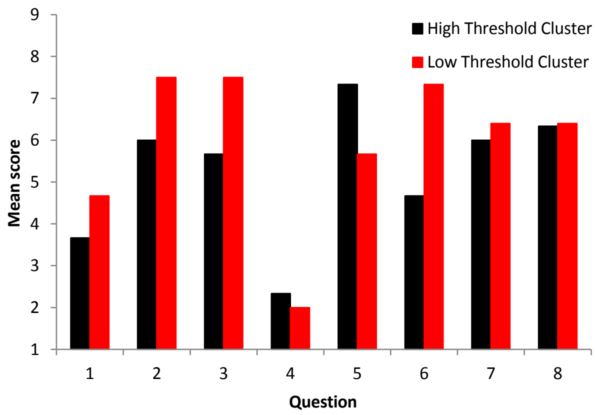

Fig. 4. Mean rating scores.

The Pearson's correlation coefficient calculated on the rating scores resulted in a significant negative correlation between the "Feeling of being in a car" (question 6) and the roll-rate thresholds ($r = -0.72$, $n = 10$, $p < 0.05$). This indicates that participants who experienced a lower feeling of immersion in the simulation also showed a lower sensitivity for roll rate, and were unable to notice the rotation of the platform up to 12 deg/s on average (figure 3). All other questions did not show any significant correlation with the threshold clusters.

Overall, the feeling of being in a car increased significantly ($F(3,27) = 6.58$, $p < 0.01$) from the condition in which roll motion was presented in darkness ("Roll") to the conditions where active control was available ("+Active"), as shown in figure 5.

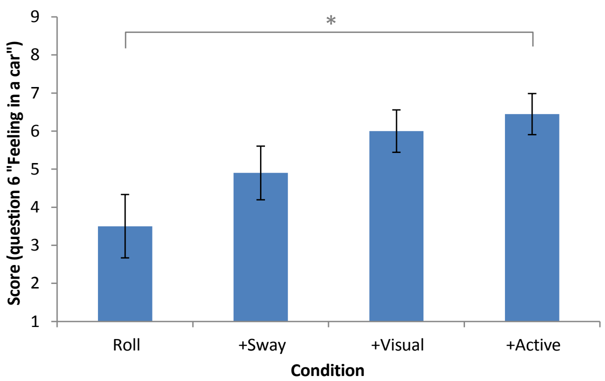

Figure 5. Mean score at question 6 "Feeling of being in a car" for different conditions. Error bars indicate ±1 SEM.

4. Discussion

The purpose of the study was to investigate the effect of different sensory and cognitive factors on motion sensitivity in a driving simulation. We measured detection thresholds for roll rate in darkness, with additional lateral motion, with available visual motion information, and in conditions that closely resemble an actual driving scenario, in which a driver actively controls the vehicle.

We found that thresholds significantly increase when translational motion (sway) is added to rotational motion (roll). This result essentially replicates what was previously reported by Zaichik et al. [Zai1]. Visually suppressing the roll did not increase the thresholds further, but led values comparable to those reported by Groen et al [Gro1]. Our study extends the validity of previous results by allowing a direct comparison of the measured thresholds, since all the conditions were tested here using the same participants, motion stimuli, platform and methodology.

Interestingly, the addition of incongruent visual information did not affect further the detection threshold. Indeed, the visual motion information during the experiment showed a lateral translation with no roll, which was actually present in the inertial motion stimulation due to tilt-coordination. We confirm again the results of previous literature [Gro1], which indicated in about 3 deg/s the pitch rate detection threshold for incongruent visual-inertial stimulation during passive motion.

Up to now, this value was widely adopted within the driving simulation community and used as a reference for the tilt rate limiter in the washout algorithms responsible for tilt-coordination. However, one should consider that this value was measured during passive motion. In other words, this value refers to the motion sensitivity of a passenger, not a driver. Since it is reasonable to expect a further decrease in sensitivity during an active task [Hos1], we measured the threshold during active driving, with the intent of providing the community with a more realistic value to be used in simulation. The result replicates our previous finding, indicating an average roll rate detection threshold of approximately 6 deg/s [Nes1]. However, here we found that two clusters better describe the thresholds for roll in active driving conditions. The "low threshold" cluster showed no difference in threshold between the passive and active driving simulation (approximately 3 deg/s), while the "high threshold" cluster showed a significant increment: roll rate of 12 deg/s was required to perceive a body rotation to the side while driving.

Despite the small size of the sample, we found also a significant negative correlation between the threshold clusters in condition "+Active" and the feeling of being in an actual car. Thus, lower sensitivity for roll rate correlates with a lower level of immersion in the simulation. Conversely, a better feeling of being in an actual car correlates with a higher sensitivity for rotational rates. We hypothesize that sensitive drivers ("low threshold") take advantage of a better feeling of immersion, and can maintain their sensitivity even when their attention is diverted to the driving task, with complex and rich multisensory stimulation. This suggests that a realistic driving simulation, in which drivers have active control over the vehicle, helps the sensitive drivers to better understand the characteristic vehicle motion. As a consequence, drivers concentrate more on the relevant motion aspects, and maintain a high sensitivity. On the other side, one could be overwhelmed by the richness of the simulation and the effort required in controlling the vehicle. This would prevent the driver to reach a sufficient level of immersion. The consequence would be a distribution of the attentional resources over multiple cues, with a reduced level of attention to the relevant motion aspects, and an increased threshold.

The driving simulation community should carefully evaluate the importance of our findings when transferring the results from simulator studies to production cars. Indeed, recruiting simulator users with low motion sensitivity (high threshold) would increase the perceptual workspace of the simulator, as higher tilt rate saturation values would be accepted. However, our study shows that drivers with low sensitivity also report a lower feeling of immersion, with potential negative impact on the validity of the results for safety and training applications.

Future studies should address more specifically the cause of individual differences in motion sensitivity during active driving simulation. The relationship between subjective feeling of immersion and individual motion sensitivity should be also further investigated. For this, the development of novel and robust method for measuring immersion, perhaps based on perceptual judgments [Wal1], would be highly beneficial. This will improve our understanding of human motion perception and the reliability and validity of simulator studies for real world applications.

5. Conclusion

In this study we investigated how roll rate detection threshold during lateral motion is affected by motion in multiple directions, concurrent visual information, and active control task. Indeed, motion in different directions, multisensory visual-inertial stimulation and vehicle control activities are actual parts of a typical driving simulation. Thus, the question is particularly relevant for the development of efficient motion cueing techniques in driving simulation, in order to ensure the best use of the simulator workspace and provide the user with a realistic driving experience.

The main results indicate that roll rate perception is affected by the combination of different simulator motions. Furthermore, for some drivers an active control task seems to increase detection threshold for roll rate, i.e. impair motion sensitivity; while for others the threshold remain unaffected by the additional attentional load.

We hypothesize that an active control task may induce a better feeling of immersion and a better understanding of the vehicle relevant motion. If this does not occur, however, the overall complexity of the simulation may cause motion sensitivity to decrease.

6. References

[Ang1] Angelaki, D. E., & Yakusheva, T. A. How vestibular neurons solve the tilt/translation ambiguity. Comparison of brainstem, cerebellum, and thalamus. Annals of the New York Academy of Sciences, 1164: 19–28, 2009.

[Ben1] Benson A. J., Spencer M. B., Stott J. R. R. Thresholds for the detection of the direction of whole-body, linear movement in the horizontal plane. Aviat Space Environ Med 57: 1088–1096, 1986.

[Bos1] Bos J. E., & Bles W. Theoretical considerations on canal-otolith interaction and an observer model. Biol Cybern 86: 191–207, 2002.

[Dev1] De Vroome, A. M., Valente Pais, A. R., Pool, D. M., Van Paassen, M. M., & Mulder, M. Identification of Motion Perception Thresholds in Active Control Tasks. In Proceedings of the AIAA Modeling and Simulation Technologies Conference and Exhibit, 2009.

[Gol1] Golding, J. F., Mueller, A. G., & Gresty, M. A. A motion sickness maximum around the 0.2 Hz frequency range of horizontal translational oscillation. Aviation, Space, and Environmental Medicine, 72(3): 188–192, 2001.

[Gro1] Groen E. L., & Bles W. How to use body tilt for the simulation of linear self motion. Journal of Vestibular Research: Equilibrium & Orientation, 14(5): 375–385, 2004.

[Hos1] Hosman R. J. A. W., & van der Vaart J. C. Vestibular models and thresholds of motion perception. Results of tests in a flight simulator (No. LR-265). Delft University of Technology, Department of Aerospace Engineering, 1978.

[Kae1] Kaernbach, C. A single-interval adjustment-matrix (SIAM) procedure for unbiased adaptive testing. The Journal of the Acoustical Society of America, 88(6): 2645–2655, 1990.

[Ken1] Kennedy R. S., Lane N. E., Berbaum K. S., Lilienthal M. G. Simulator Sickness Questionnaire: An Enhanced Method for Quantifying Simulator Sickness, 1993.

[Nah1] Nahon, Meyer A., & Lloyd D. Reid. Simulator Motion-Drive Algorithms - A Designer’s Perspective. Journal of Guidance, Control, and Dynamics 13(2): 356–362, 1990.

[Nes1] Nesti A., Masone C., Barnett-Cowan M., Robuffo Giordano P., Bülthoff H.H., & Pretto P. Roll rate thresholds and perceived realism in driving simulation. Driving Simulation Conference, Paris, 2012.

[Nie1] Nieuwenhuizen, F. M., & Bülthoff, H. H. The MPI CyberMotion Simulator: A Novel Research Platform to Investigate Human Control Behavior. Journal of Computing Science and Engineering, 7(2): 122–131, 2013.

[Rob1] Robuffo Giordano P., Masone C., Tesch J., Breidt M., Pollini L. and Bülthoff H.H. A Novel Framework for Closed-Loop Robotic Motion Simulation - Part II: Motion Cueing Design and Experimental Validation 2010. IEEE International Conference on Robotics and Automation (ICRA 2010), IEEE, Piscataway, NJ, USA, 3896-3903, 2010.

[She1] Shepherd, D., Hautus, M. J., Stocks, M. A., & Quek, S. Y. The single interval adjustment matrix (SIAM) yes–no task: an empirical assessment using auditory and gustatory stimuli. Attention, Perception, & Psychophysics, 73(6): 1934–1947, 2011.

[Soy1] Soyka F., Giordano P. R., Beykirch K., & Bülthoff H. H. Predicting direction detection thresholds for arbitrary translational acceleration profiles in the horizontal plane. Experimenal Brain Research 209(1): 95–107, 2011.

[Sta1] Stanton, Neville A. Advances in Human Aspects of Road and Rail Transportation. CRC Press, 2012.

[Val1] Valente Pais, A. R., Mulder, M., van Paassen, M. M., Wentink, M., & Groen, E. L. Modeling Human Perceptual Thresholds in Self-Motion Perception. Presented at the AIAA Modeling and Simulation Technologies Conference and Exhibit, American Institute of Aeronautics and Astronautics, 2006.

[Wal1] Wallis, G., & Jennifer T. Predicting the Efficacy of Simulator-Based Training Using a Perceptual Judgment Task Versus Questionnaire-Based Measures of Presence. Presence: Teleoperators and Virtual Environments 22(1): 67–85, 2013.

[Wer1] Wertheim, A H, Mesland B S, & Bles W. Cognitive Suppression of Tilt Sensations during Linear Horizontal Self-Motion in the Dark. Perception 30(6): 733–41, 2001.

[Zai1] Zaichik L., Rodchenko V., Rufov I., Yashin Y., & White A. Acceleration perception. Collection of Technical Papers, edited by AIAA Modeling and Simulation Technologies Conference, 4334: 512–520, 1999.

[Zup1] Zupan L. H., Merfeld D. M., & Darlot C. Using sensory weighting to model the influence of canal, otolith and visual cues on spatial orientation and eye movements. Biol Cybern 86: 209–230, 2002.

Simulation sickness comparison between a limited field of view virtual reality head mounted display (Oculus) and a medium range field of view static ecological driving simulator (Eco2)

Baris Aykent [1], Zhao Yang [1], Frédéric Merienne [1], Andras Kemeny [1,2]

(1) : Arts et Métiers ParisTech, CNRS 6306 Le2i Institut Image
2 Rue Thomas Dumorey
71100 Chalon-sur-Saône France
Phone: +33 (0) 385 909 860
Fax: +33 (0) 385 909 861
b.aykent@gmail.com
{zhao.yang,frederic.merienne, andras.kemeny}@ensam.eu

(2) : Technical Centre for Simulation, Renault
TCR AVA 013
1, avenue du Golf
78288 Guyancourt Cedex
Phone: +33 (0) 176 851 985
Fax: +33 (0) 176 890 774
{andras.kemeny}@renault.com

Abstract – In this article, an experimental procedure is presented in order to evaluate the role of having HMD oculus and (Eco2 driving simulator) in terms of driving simulation sickness. The driving simulation sickness is investigated with respect to SSQ (simulator sickness questionnaire) and vestibular dynamics (head movements) of the driver participants for a specific driving scenario. The scenario of driving task is created by using open source "iiVR (institut image virtual reality)" software which is developed by Institut Image Arts et Métiers ParisTech. The experiments are executed in static mode for the driving simulators.

Key words: Driving simulation, simulation sickness, virtual reality, field of view, visuo-vestibular cues

1. Introduction

The driving simulators are getting more and more benefited to evaluate the vehicle dynamics, advanced vehicle control systems such as ESP, ABS, ACC, etc.… Powertrain systems (such as gasoline, diesel internal combustion engined, hybrid or electric vehicles) for the first prototypes of the new developed cars. Not only the vehicle concepts but also the driver behavior are of interest. In general, there are two different types of driving simulators as [Ayk1, Ayk2]:

- static driving simulators (without motion platform or motion platform is inactivated)
- dynamic driving simulators (with motion platform or motion platform is activated)

In driving simulation, simulation sickness is an inevitable topic to study further on and therefor it is required to develop systems and/or methods to decrease it.

An important issue to deal with, in terms of driving simulation sickness, is the transport latency. In moving based driving simulators with fixed visual systems, a compensation of display system is essential to provide a visual stability for the driver. A delay in visuo-inertial cues shrinks the coherence and might induce a bias (incoherence) in the driver's behaviour. Even though drivers are able to compensate those delays and to ensure the control of the car, those latencies have to be declined. A simple linear prediction model was shown inappropriate. Transfer functions based algorithms of the motion platform were revealed to be more efficient to detract this delay [Kem1, Dag1].

Motion cueing algorithms are used to represent the physical motion at dynamic simulators. The results of a multi-partner European collaborative project were described, which examined different scale factors in a slalom-driving maneuver. The results from four comparable experiments at driving simulator, which were acquired with 65 subjects, denote a predilection for motion scale factors below 1, within a wide range of acceptable values (0.4-0.75). However, so much reduced or absent motion cues significantly degrade the driving performance [Ber1].

"CAVE" is a multi-sided box with displays on each surface used in virtual reality (VR) environments. It has been sufficient and enough for so long as the "immersive" simulation of VR resulting from the inadequate head-mounted displays (HMDs) in that domain [Man1 , Sha1, Tos1, Kim1]. However, current HMDs are able to compete with many CAVEs and actually have started to take over them [Hav1].

A study had been made in order to compare the levels of presence and anxiety in an acrophobic environment that was visualized by using a computer automatic virtual environment (CAVE) and a head-mounted display (HMD) [Jua1]. In that environment, the floor was falling away and the walls were rising up. So as to specify whether any of these two visualization systems provoke a greater sense of presence/anxiety in non-phobic users, the experiments for the two visualization systems had been performed to compare their influences on the subjects.

Twenty-five participants had joined in the study of [Jua1]. After having used each visualization system (HMD or CAVE), the participants had been asked to complete an adapted Slater et al. questionnaire [Sla1, Jua1], and a *t* test had been utilized to the registered data for assessing whether a significance in difference of the yielded results. According to [Jua1], the CAVE induces a more elevated level of presence in users. The mean score had been 5.01 (where 7 is the maximum value), which had been more elevated than the score obtained using the HMD which had been 3.59. The *t* test had also revealed that there had been significant statistical differences. The anxiety stage had also been examined at different times during the experiments. The results emphasize that both visualization systems provoke anxiety, however that the CAVE provokes anxiety more than the HMD does. The animation in which the floor fell away was the most important reason that had caused a higher provocation of the anxiety. [Jua1].

In our study, the effect of using Oculus Rift HMD and the Eco2 driving simulator has been discussed.

2. Methods and materials

Fig. 1. Oculus rift HMD in driving simulation experiments

Fig. 2. Eco2 driving simulator in driving simulation experiments

The aim of the experiments is to differentiate the influence of having HMD oculus and the Eco2 driving simulator for the driving simulation aspect and to compare the convergence to the reality for each condition. Hence, a scenario has been created in the software iiVR that enables generating a specific driving incidence. The scenario is composed of several roundabouts and curvatures.

Fig.1 illustrates the playseat low cost static driving simulator with use of HMD Oculus and the computer screen also depicts the driver view of the driving scene during the operation by the driver, whereas Fig. 2 indicates a real-time driving experiment in the ECO_2 driving simulator.

For each type (HMD and Eco2 simulator), the vestibular dynamics related motion sickness (objective metrics) and the psychophysical situations (subjective measures through questionnaires) of the drivers' are measured. Fig. 2 also illustrates the sensor that is used to measure the head (vestibular related) dynamics data (attached to the headphone from right).

The effect of having a different visual interface is explained statistically for the driving simulation and the proximity to the reality for the subjects who participated in the experiments.

3. Objective measures

The dynamic information of vehicle and movement of head are all recorded in files. By building a model of Simulink, we could get the acceleration of vehicle and head (vestibular). In order to evaluate the conflict of these two accelerations as longitudinal and lateral, Pearson correlation and Mann-Whitney U test are employed in Matlab.

Pearson correlation between sets of data is for measuring how related they are, which is to show the linear relationship of two sets of accelerations. In Pearson correlation, two values are presented in final calculation results: in Matlab, [r, p] = corrcoef (X, Y), in which r is coefficient of correlation; p is the probability; X and Y are respectively the matrix of accelerations of vehicle and head. If r is between 0.5 and 1.0 or -0.5 and -1.0, that means high correlation; otherwise low correlation. If r is 0.0 to -1.0, there is a negative correlation.

In order to analyze the significance in differences between the head and vehicle data, another analysis method (bilateral Mann-Whitney U test) is used in Matlab. Mann-Whitney U test can evaluate two sets of data without condition on sample size. In Matlab, [p, h, stats] =ranksum (X, Y), p value is the probability; h indicates a rejection or accept of the null hypothesis; stats includes information about the test statistic. Therefore if $p > 0.05$ or h=0, null hypothesis is accepted, in other words, there is no significant difference between two sets of data. If $p < 0.05$ or h=1, null hypothesis is rejected, in other words, there is a significant difference between two sets of data.

4. Subjective measures

The subjective measure is to conduct a questionnaire for subject at the end of each driving simulation phase. These issues are related to the subject feelings. Questions focus on the degree of experienced nausea, possible dizziness, headaches, fear, uneasiness…etc. Table 1 lists the questions in this report after each driving phase. The purposed questionnaire in this report has been built and modified from the following articles [Ken1, Kim2, Xse1]. Different from the questions in resources above, in this report two questions about the visual and immersive quality of scene are included. The questionnaire permits to evaluate the disorientation and the response range from 1 to 10, which is a modified SSQ (simulator sickness questionnaire) from 1 to 4 (SSQ). Our range allows more possible choice.

Table 1. List of questions

Questions	Expression of question
Q1	Have you felt nausea?
Q2	Have you felt dizziness?
Q3	Have you felt eyestrain?
Q4	Have you felt headache?
Q5	Have you felt mental pressure?
Q6	Have you felt fear when you face the critical situation?
Q7	Have you felt uneasiness?
Q8	How do you evaluate the visual quality?
Q9	How do you evaluate the immersive quality?

The subject had to answer each of these questions with a value. This value should reflect psychophysical perception of the experiment (1: too little, 10: too strong for the questions 1 to 7; 1: very bad, 10: very good for the questions 8 and 9). Subsequently, these values were statistically analyzed.

Before the subject answers these questions, they should have firstly written down some personnel information, which allows analyzing the data more deeply. Here is the list these questions: *your name; your age; driving experience; type of driving license; experience of game playing (first-person); experience of virtual reality (VR)*.

In all subjects, 12 of them are men and 2 are women. Age varies from 20 to 36 (Mean ± SD = 24.4. ± 2.3; SD: standard deviation) 6 of them do not play first-person game, 4 of them sometimes play and 4 of them often play. 9 of them have no experience of virtual reality and 5 of them often work in VR environment.

5. Results

We want to explain our results about the study, which is related to comparison between Oculus HMD and Eco2 simulator. The MATLAB/Simulink is used to calculate the data and present the results.

5.1. Results of objective analysis

Fig. 3 presents a protocol of vehicle speed with respect to time. The speed condition in the experiments is maximum 60 km/h.

Fig.4 describes the vehicle trajectory during the experimental phase.

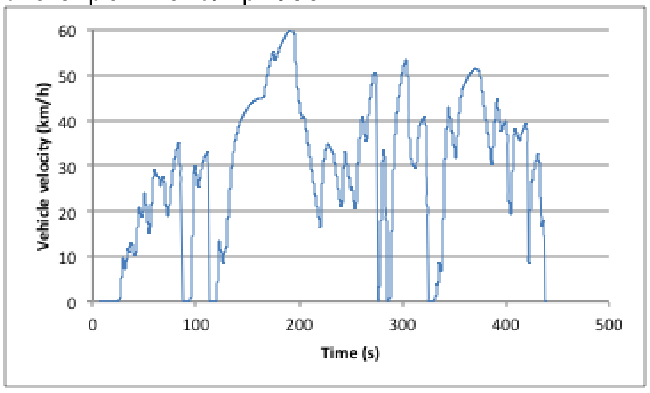

Fig. 3. Vehicle velocity

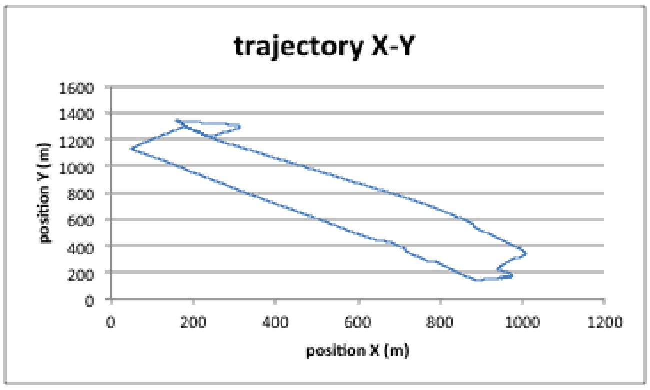

Fig.4. Trajectory X-Y of the vehicle for the experiment protocol

For Oculus, Fig. 5 and Pearson correlation show that there is a significant negative correlation between a_{x_veh} (longitudinal vehicle acceleration) and a_{x_vest} (head dynamic) ($r(14)= -0.2729$ and $p=0.0000$). This means that Oculus has a trend for increase in simulator sickness in longitudinal acceleration.

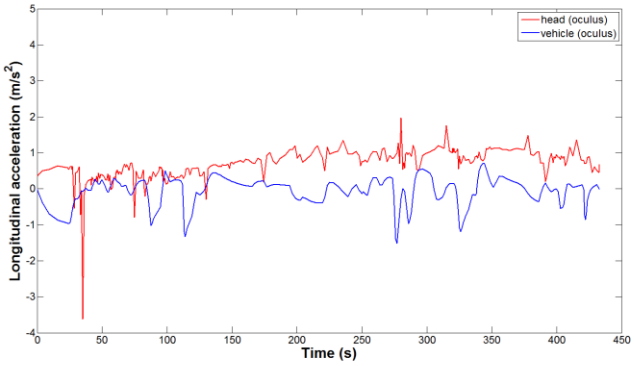

Fig. 5. Longitudinal acceleration of vehicle and vestibular of Oculus in real-time (m/s^2)

Fig. 6 indicates the result of bilateral test of Mann-Whitney U: U(14); h=1, $p=3.0795\times10^{-243}$. Zval: 33.3068. Ranksum: 1370364. This means there is a significant difference between a_{x_veh} and a_{x_vest}.

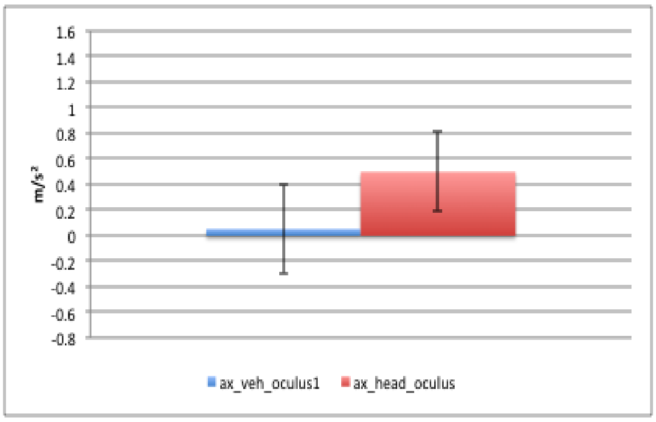

Fig. 6. Longitudinal acceleration of vehicle and vestibular of Oculus in real-time (m/s^2)

For Eco2, Fig. 7 and Pearson correlation show that there is a significant positive correlation between a_{x_veh} and a_{x_vest} ($r(14)=0.2512$ and $p=0.0000$). This means that Eco2 has a trend to avoid simulator sickness in longitudinal acceleration.

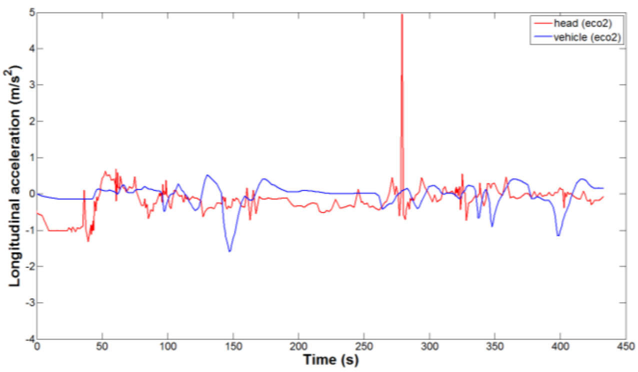

Fig. 7. Longitudinal acceleration of vehicle and vestibular of Eco2 in real-time (m/s^2)

Fig. 8 indicates the result of bilateral test of Mann-Whitney U: U(14); h=1, $p=2.0730\times10^{-13}$. Zval: 7.3440. Ranksum: 1046600. This means there is a significant difference between a_{x_veh} and a_{x_vest}.

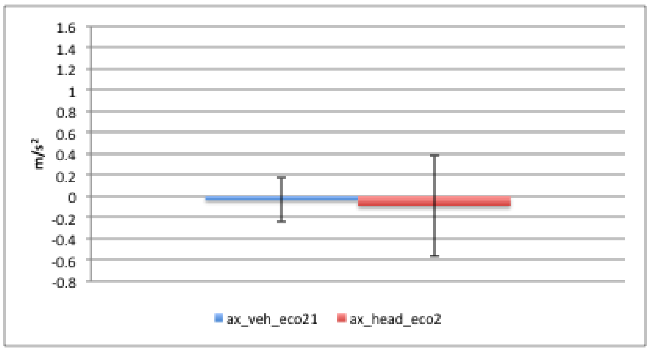

Fig. 8. Longitudinal acceleration of vehicle and vestibular of Eco2 in real-time (m/s^2)

For Oculus, Fig. 9 and Pearson correlation show that there is a significant negative correlation between a_{y_veh} (lateral vehicle acceleration) and a_{y_vest} (head dynamic) (r(14)= -0.4093 and p=0.0000). This means that Oculus has a trend to raise simulator sickness in lateral acceleration.

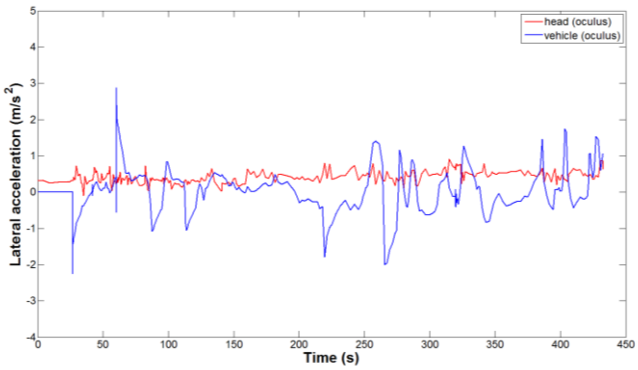

Fig. 9. Lateral acceleration of vehicle and vestibular of Oculus in real-time (m/s^2)

Fig. 10 indicates the result of bilateral test of Mann-Whitney U: U(14); h=0, p=0.3687. Zval: 0.8989. Ranksum: 966227. This means there is no significant difference between a_{y_veh} and a_{y_vest}. (Avoidance of simulator sickness)

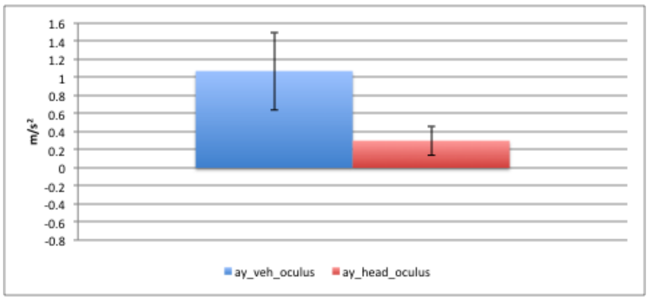

Fig. 10. Lateral acceleration of vehicle and vestibular of Oculus in real-time (m/s^2)

For Eco2, Fig. 11 and Pearson correlation show that there is a significant positive correlation between a_{y_veh} and a_{y_vest} (head dynamic) (r(14)=0.2855 and p=0.0000). This means that Eco2 has a trend to avoid simulator sickness in lateral acceleration.

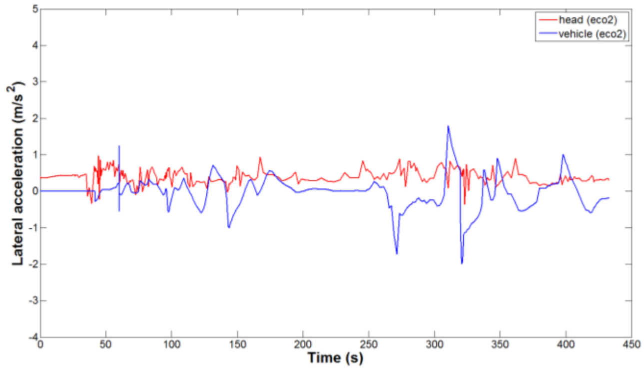

Fig. 11. Lateral acceleration of vehicle and vestibular of Eco2 in real-time (m/s^2)

Fig.12 indicates the result of bilateral test of Mann-Whitney U: U(14); h=1, $p=2.6036\times10^{-177}$. Zval: 28.3911. Ranksum: 1309026. This means there is a significant difference between a_{y_veh} and a_{y_vest}.

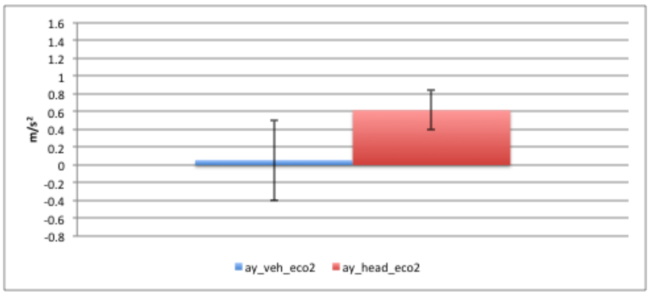

Fig. 12. Lateral acceleration of vehicle and vestibular of Eco2 in real-time (m/s^2)

5.2. Results of subjective analysis

Fig.13 presents the results of subjective evaluation that has been accomplished according to the self-report of the participants just after each experiment session.

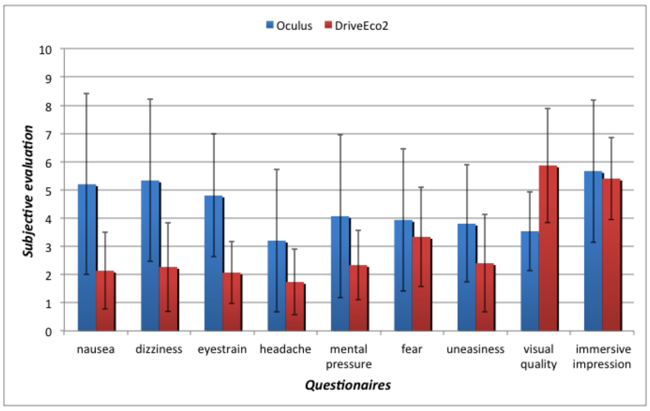

Fig. 13. Subjective evaluation

Q1) Nausea (1: too little, 10: too strong): (U(14), $p=0.012<0.05$)

There is a significant difference between Oculus and Eco2 with respect to feeling of nausea. Nausea with Oculus is significantly stronger than Eco2.

Q2) Dizziness (1: too little, 10: too strong): (U(14), $p=0.005<0.05$)

There is a significant difference between Oculus and Eco2 with respect to feeling of dizziness. Dizziness with Oculus is significantly stronger than Eco2.

Q3) Eyestrain (1: too little, 10: too strong): (U(14), $p=0.002<0.05$)

There is a significant difference between Oculus and Eco2 with respect to feeling of eyestrain. Eyestrain with Oculus is significantly stronger than Eco2.

Q4) Headache (1: too little, 10: too strong): (U(14), $p=0.082>0.05$)

There is no significant difference between Oculus and Eco2 with respect to feeling of headache. Headache with Oculus is non-significantly stronger than Eco2.

Q5) Mental pressure (1: too little, 10: too strong): (U(14), $p=0.142>0.05$)

There is no significant difference between Oculus and Eco2 with respect to feeling of mental pressure. Mental pressure with Oculus is non-significantly stronger than Eco2.

Q6) Fear (1: too little, 10: too strong): (U(14), $p=0.657>0.05$)

There is no significant difference between Oculus and Eco2 with respect to feeling of fear. Fear with Oculus is non-significantly stronger than Eco2.

Q7) Uneasiness (1: too little, 10: too strong): (U(14), $p=0.097>0.05$)

There is no significant difference between Oculus and Eco2 with respect to feeling of uneasiness. Uneasiness with Oculus is non-significantly stronger than Eco2.

Q8) Visual quality (1: very bad, 10: very good): (U(14), $p=0.005<0.05$)

There is a significant difference between Oculus and Eco2 with respect to visual quality. The visual quality of Eco2 is significantly better than Oculus.

Q9) immersive impression (1: very bad, 10: very good): (U(14), $p=0.798>0.05$)

There is no significant difference between Oculus and Eco2 with respect to immersive impression. The immersive impression of Oculus is non-significantly better than Eco2.

6. Conclusion

We compared the longitudinal and lateral accelerations of vehicle and head. The feelings after experiments are also analyzed by Mann-Whitney U test and Pearson correlation methods to evaluate the significant difference.

Deviation between vehicle and head accelerations depends on the scale factor (vertical to horizontal field of view) and especially the limited field of view static driving simulator. If it had a broader horizontal field of view, the simulation sickness when going from 60° to 150°, would probably be doubled the rate of simulator sickness (40° vertical – Eco2 very low).

For Oculus, these two longitudinal accelerations of vehicle and head are significantly different according to Mann-Whitney U test and Oculus has the trend to increase simulator sickness due to Pearson correlation; these two lateral accelerations of vehicle and head have no significantly difference according to Mann-Whitney U test and Oculus has the trend to rise simulator sickness due to Pearson correlation.

For Eco2, these two longitudinal accelerations of vehicle and head are significantly different according to Mann-Whitney U test and Eco2 has the trend to avoid simulator sickness due to Pearson correlation; these two lateral accelerations of vehicle and head have significantly difference according to Mann-Whitney U test and Eco2 has the trend to avoid simulator sickness due to Pearson correlation.

For the feelings of nausea, dizziness and eyestrain, there are significant difference between Oculus and Eco2; Oculus can cause more sickness than Eco2.

For the feelings of headache, mental pressure, fear, uneasiness and immersive impression, there are no significant differences between two simulators. From the average value of each feeling, we can see that Oculus cause more sickness than Eco2.

For the visual quality, there is significant difference between Oculus and Eco2; Eco2 is much better than Oculus in visual quality.

In conclusion, Oculus HMD can cause more sickness in driving simulation than medium FOV system such as Eco2 driving simulator though this type of HMD may provide better immersive impression than medium large FOV display systems.

7. References

[Hav1] Havig, P., McIntire, J., & Geiselman, E. (2011, May). Virtual reality in a cave: limitations and the need for HMDs?. In *SPIE Defense, Security, and Sensing* (pp. 804107-804107). International Society for Optics and Photonics.

[Jua1] Juan, M. C., & Pérez, D. (2009). Comparison of the Levels of Presence and Anxiety in an Acrophobic Environment Viewed via HMD or CAVE. *Presence: Teleoperator and Virtual Environments*, *18*(3), 232-248.

[Sla1] Slater, M., Usoh, M., & Steed, A. (1994). Depth of presence in virtual environments. *Presence*, *3*(2), 130-144.

[Man1] Manek, D. (2004). *Effects of visual displays on 3d interaction in virtual environments* (Doctoral dissertation, Virginia Polytechnic Institute and State University).

[Sha1] Shapiro, M. (2006). *Comparing user experience in a panoramic HMD vs. projection wall virtual reality system*. tech. rep., Sensics, Inc.

[Kim1] Kim, K., Rosenthal, M. Z., Zielinski, D., & Brady, R. (2012, March). Comparison of desktop, head mounted display, and six wall fully immersive systems using a stressful task. In *Virtual Reality Short Papers and Posters (VRW), 2012 IEEE* (pp. 143-144). IEEE.

[Tos1] Tossavainen, T. (2004). Comparison of CAVE and HMD for visual stimulation in postural control research. *Studies in health technology and informatics*, 385-387.

[Ayk1] Aykent, B., Merienne, F., Guillet, C., Paillot, D., & Kemeny, A. (2014). Motion sickness evaluation and comparison for a static driving simulator and a dynamic driving simulator. *Proceedings of the Institution of Mechanical Engineers, Part D: Journal of Automobile Engineering*, 0954407013516101.

[Ayk2] Aykent, B., Merienne, F., Paillot, D., & Kemeny, A. (2013). The role of motion platform on postural instability and head vibration exposure at driving simulators. *Human movement science*.

[Ken1] Kennedy R.S., Lane N.E., Berbaum K.S., and Lilienthal M.G.. Simulator sickness questionnaire: An enhanced method for quantifying simulator sickness. The international journal of aviation psychology, 3(3):203–220, 1993.

[Kim2] Kim MS, Moon YG, Kim GD, and Lee MC. (2010). Partial range scaling method based washout algorithm for a vehicle driving simulator and its evaluation. International Journal of Automotive Technology, 11(2): 269–275.

[Xse1] XSens Technologies BV 15. Mti and mtx user manual and technical documentation. document mt0100p, revision o., 2010.

[Dag1] Dagdelen M, Reymond G, Kim GD, and Kemeny A. (2002). Analysis of the visual compensation in the Renault driving Simulator. Proceedings of the Driving Simulation Conference, Paris, September 2002. pp 109-119.

[Kem1] Kemeny A. (2014), From driving simulation to Virtual Reality, VRIC 2014, Laval Virtual, pp. AE2, 1-5.

[Ber1] Berthoz, A. , Bles, W. ; Bulthoff, H.H. ; Correia Gracio, B.J. ; Feenstra, P. ; Filliard, N. ; Huhne, R. ; Kemeny, A. ; Mayrhofer, M. ; Mulder, M. ; Nusseck, H.G. ; Pretto, P. ; Reymond, G. ; Schlusselberger, R. ; Schwandtner, J. ; Teufel, H. ; Vailleau, B. ; van Paassen, M.M. ; Vidal, M. ; Wentink, M. High-performance motion cueing for driving simulators to Motion scaling for high-performance driving simulators, Human-Machine Systems, IEEE Transactions on, Volume:43 Issue:3.

How much visual attention does braking require? A study of the effect of memory of the scene on driver's braking behaviour

Mehdi Saffarian [1], John W. Senders [1]

(1) : 5 King's College Road, Department of Mechanical and Industrial Engineering, University of Toronto, Toronto, ON M5S 3G8, Canada
416 946-5413 (P), 416 978-7753 (F)
{mehd.saffarian, johnw.senders}@ utoronto.ca

Abstract – Braking is a common activity of driving. An important question as yet remains unanswered: how much attention, both visual and mental, is required to execute a correct braking response? We measured drivers' abilities to stop accurately at visually pre-designated positions. We compared performances in two conditions: with and without continued visual input during the braking action.

We found that drivers' responses differ as a function of temporal demand. When the temporal demand is high, drivers use visual information after the brake onset to adjust the braking effort. When the visual information is available, drivers brake faster, shorter and harder. Drivers' brake timing was least effective to control the distance when the temporal demand was low and visual was occluded during braking.

Key words: driver behaviour, braking control, occlusion technique, visual information, attention, distance perception.

1. Introduction

Roads present a myriad of opportunities for collision. Cars can run into each other; they can go off the road; they can hit other objects on the road. Braking is possibly the most common activity that drivers use to avoid collision [Mal1, Gik1]. By braking, drivers can control the speed and maintain an appropriate distance from the other objects on the road; hence braking reduces the probability of collision. While proper braking can save lives and limbs, improper braking can escalate the risk of collision: for example, if a driver brakes too hard in a highway lane, he increases the risk of rear-end collision by increasing the speed difference between his car and the following vehicle. In contrast, if a driver does not brake hard enough or early enough at a signalled intersection, he can block the intersection and increase the risk of collision.

Despite its fundamental role in driving safety, drivers' braking behavior is not well understood. Like other locomotion tasks, brake theories are based on the principle that a driver uses visual information of the motion of other vehicles to regulate his own motion. Current theories of braking assume drivers perceive possible collisions and, based on this information, change or maintain the course of motion to avoid a collision [see Lee1, Yil1, And1]. These theories propose that a driver's action is an almost automatic response of human motor system when the magnitude of certain visual parameters passes a threshold. The driver's role is to close the control loop and compensate the deviation from this threshold. These theories assume that during braking, drivers can perceive and use the parameters such as speed differential, distance or rate of visual expansion to control their braking response.

Although these theories describe how drivers can use the perceived information, they are less clear on how drivers actually behave [Gre1]. It is assumed that driver's decision to brake and the resulting braking pattern depends on driver's perception of changes in the driving scene, and on whether these changes require braking. Lack of attention and lack of skill are proposed as the main human causes of motor vehicle accidents. In case of braking, it is not known how these two factors interact with each other and shape the driver's response. Is braking a tacit skill that drivers execute with minimum dependency on feedback during its execution, or do drivers depend on the visual information to brake properly during the course of braking?

Driving is considered mainly as a visual task. Some research claims that the visual channel accounts for 90% of the information acquired and used in driving [Siv1]. Most of the previous research on driving behaviour in general, and braking behaviour in particular, has been focused on predicting the behaviour based on the state of the traffic percieved in the front road. Drivers can use vision to estimate position and velocity, and to a lesser degree to estimate their acceleration and deceleration, particularly at lower levels of deceleration. However, previous research in human perception suggests that the perceptual world of human is different from the physical world. The visual space perception law of distance (and size) proposes the relation between the physical and the percieved world [Gli1]. Gilinsky's empirical theory formulates the perceived distance (d) as a function of real distance (D):

$$\frac{d}{D} = \frac{A}{A+D} \tag{1}$$

This relation can have a serious safety implication for driving and for our understanding of how drivers use visual information to control speed and distance with brake systems. It suggests that drivers perceive a world with more compressed distances relative to the reality. It also states that the greater distance, the greater the shortening. The maximum limit of the perceived distance is captured by A, which is an idiosyncratic parameter. If it holds in driving, Glisnky's hypothesis suggests that a drivers' visual system is equipped with a safety mechanism that magnifies the collision hazard and actually reduces the collision risk.

In this work, we have investigated whether Glisnky's hypothesis can explain drivers' braking behaviour in a simulated driving situation. In an experiment, we asked drivers to execute a series of braking maneuvers requiring a stop at a predefined spot on the road. The tasks were executed in a driving simulator where there were no driving hazards. It was expected that in scenarios with no visual input during the brake, drivers brake harder and quicker since they must rely on the shortened perceived distance at the start of the braking task.

Former experiments have shown the capabilities of drivers to perform some driving tasks in the absence of vision using preview or anticipation information [God1]. The vision channel may not be available for a short period of time during driving tasks, as drivers may not pay attention to the road scene or the visual scene maybe blocked by conditions such as rain, fog or smoke.

The need for vision in performing these tasks arises from the unpredictability and the consequent uncertainty that exists in driving environments. The time available to execute a maneuver can have a significant impact on the driving performance. The modified Fitt's speed-accuracy tradeoff predicts that the accuracy of a response is proportional to the magnitude and inversely proportional to the speed of that response. Braking tasks can occur at different driving speeds and at different amount of time available to respond. As the final question of this work, we wanted to know how driver braking pattern changes for different available braking time. Driver motor acuity in performing a braking task without seeing the driving scene during the brake is investigated. The hypothesis is that the lack of visual feedback degrades the braking performance more as the temporal demand of a braking event decreased. The basis for this hypothesis is that in braking events with low temporal demand, drivers have sufficient time to regulate the brake and use visual information to control the braking force. In sudden braking drivers highly dependent on their motor skill and may not use visual information to adjust their braking response. In the other word, when it comes to sudden braking, braking blindly may suffice.

2. Method

Driver perception input and control output were measured during braking events with different urgencies. It was assumed that drivers would devote their full attention (as required in a typical driving task) during the experiment: the attention level was not manipulated, nor was the effect of surprise tested.

2.1. Driving simulator

The experiment was carried out in a fixed-based NADS minisim driving simulator; the simulator provides a 130 degrees horizontal by a 24 degree vertical field of view at 48'' viewing distance. It mimics the sound of the vehicle and the surroundings using two speakers at the front. The roadway vibration is simulated using a speaker located below the driver's seat. The brake and gas pedals, the steering wheel, the automatic gearshift, and the seat are the same as those in an actual vehicle. The simulator measures both driver inputs and telematic data of the vehicle and surroundings at a rate of 60 Hz.

2.2. Participants

For this experiment, 24 participants (19 men and 5 women) with a valid Ontario Class G driving license were recruited from the University of Toronto community. All the participants provided written informed consent and were compensated with a payment of CDN $25. On average, the participants were 27 year old (SD=5years) and had obtained their (first) driving license 9 years previously (SD=5.1years). Four participants had used a driving simulator in the past. Based on the frequency and amount of driving, it was inferred that the majority of the participants (17 out of 24) drove at least once per week for more than 10 km, and 21 participants drove more than 1000 km per year; only one participant drove less than 100 km on an annual basis. During the experiment, the participants drove in cruise control mode before carrying out the braking tasks, and thus previous experience in using cruise control could have an effect on performance. Thirteen participants had used cruise control more than 1-2 times per year.

2.3. Experimental setup

Each participant completed a series of questionnaires, driving simulator tests and work load assessments (Fig. 1). In a simulator setting, the performance of the participants during a series of braking events was compared between the conditions that the information of the driving scene is present or absent. The time available for braking was changed by manipulating the trigger time of the braking event. The participants were instructed to 1) stop the vehicle by braking at a certain position on the road indicated by a circular patch with a drum at either side of the road (Fig. 2); and 2) maintain the vehicle in the centre of the road.

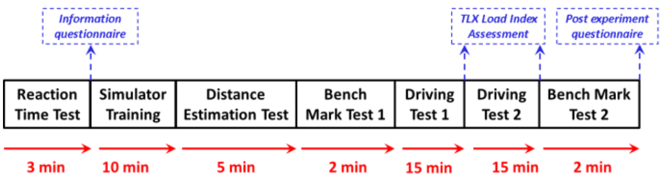

Fig. 1. Timeline of different stages of the experiment

Drivers were asked to respond "at" or "after" a fixed time before reaching to the stop target. The speed and path of the driving is kept constant; drivers drove at 60 mph and on a straight road. Half the participants were instructed to start braking right after hearing the beep or seeing the occluded scene; the other half were free to start braking at any time after the occlusion or beep sound. The participants were instructed not to pump their brakes.

Fig. 2. View of the stopping target

2.4. Reaction Time Tests

The visual and auditory reaction times of the participants were measured using two separate tests [Att1]. Each test consisted of 10 trials, among which the first five trials were used as practice runs. In the visual reaction time test, the participants had to click on the screen as soon as they saw a green balloon appeared. The balloon is always the same size and appears at the same location. In the auditory reaction time test, the participants had to click on the screen as soon as they heard a beep. For both tests, the interval between the start time of the trial and the projection of either the beep sound or the balloon were changed among trials.

2.5. Dependent Variables

For the driving tests, the descriptive statistics (means and standard deviations of the participant responses) of the following variables were calculated:

2.5.1. Vehicle control activity

Brake response time (T_{RT} *; s)*: The time between the start of occlusion or beep sound and the initial brake input of the participant. T_{RT} is a measure of reaction time of the participants to the brake events of this experiment.

Maximum brake force ($F_{\max}$ *; lb)*: The maximum brake force that the participant applies on the brake pedal in a braking event. Low $F_{\max}$ values correspond to normal, modulated braking behaviour, whereas higher $F_{\max}$ values show the shift of braking behaviour towards slam on the brake.

Maximum brake force Time ($T_{\max}$; s): The time between the start of occlusion or beep sound and the moment that the maximum brake force was applied by the participant.

Average brake force (F_{avg}; lb): The average of the brake force that the participant applies on the brake pedal during a braking event.

2.5.2. Driving performance

Distance gap (D; ft): The difference between the final stopping position of the vehicle and the position of the stopping target on the road. The distance gap is an indicator of the driver's performance in stopping at the pre-determined position.

2.5.3. Non-driving perception and reaction time performance

Distance estimation error (E; %): The distance estimation error is the ratio of the difference between the estimated and the projected distances to the projected distance. The average and standard deviation of E indicate the accuracy and the reliability of the distance perception by the participants in the simulator environment, respectively.

Auditory and visual reaction time (RT^a, RT^v; seconds): RT^a and RT^v measure the reaction time of the participants to an standard auditory and visual stimuli (see Section 2.4).

2.5.4. Data analyses

The dependent variables were measured during each braking event: after the occlusion or beep tone trigger until the moment that participant stopped the simulated car. The differences between conditions were compared using a mixed between-within analysis of variance (ANOVA) test. There were two within and one between subject factors. The within subject factors were Time to Arrival (T) with four levels of 2, 4, 6 and 8 seconds, and the existence of visual information after the initiation of braking (V) with two levels: with and without occlusion. The between subject factor was the two driver's group (G): group 1 (G1), who were told to start braking any time after the braking event triggered and group 2 (G2), who were asked to start braking right after the event trigger.

3. Results

3.1. Reaction time and distance perception in the simulator

Descriptive statistics of reaction time, distance error estimate and the distance limit parameter of the Glinsky's model (see Equation 1) are reported in Table 1. Results of independent t-tests found no significant differences between the estimated parameters of G1 and G2 participants.

Table 1. Mean (and standard deviation) of reaction time and perception parameters of participants

RT^a	RT^v	E	A
212.6 (48.2)	304.5 (54.5)	70 (16)	45.08 (32.43)
t(118)=0.23 p=0.59	t(118)=0.73 p=0.77	t(477)=3.13 p=1	t(10)=5.45 p=1

3.2. Vehicle control performance

Fig. 3 results show that the response time of the participants increase as the TTA of the braking event increases, F (3,66) =26.24, p<.000. There is also a significant main visual information effect: F (1,22)=6.12, p<.05. Over all, the brake reaction time is faster in the scenarios with occlusion than that of the scenarios without occlusion.

Considering the standard deviation of the response time, there are two main effects of G: F(1,22)=7.94, p<.01, and TTA: F(3,66)=17.32, p<.000. All participants show less consistent reaction time at longer levels of TTA. Overall, G2 participants possess more consistent reaction time. There is also a significant G × T interaction effect: F(3,66)=4.29, p<.01. This shows that as the TTA increases, G1 participants adapt a wider range of reaction time compared to the G2 group, whose reaction time is tied to the start of the braking event.

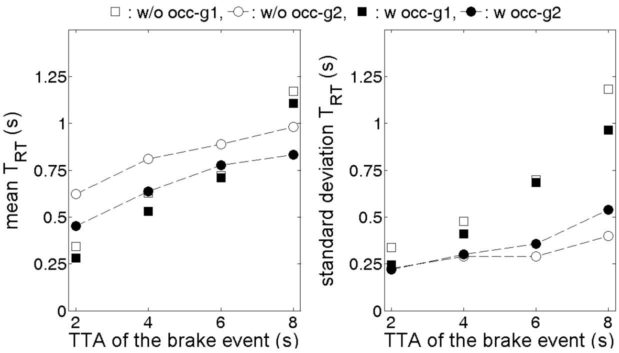

Fig. 3. Mean (left) and standard deviation (right) of the brake response time

The results of the maximum brake force (Fig.4) indicate significant effect for both main factors of visibility: F (3,66) =16.91, p<.001, and time to arrival: F (3,66) =68.36, p<.000. The maximum brake force decreases as the TTA increases. The maximum brake force is also larger when there is no occlusion. There is also a significant V × T interaction effect, F (3,66)

=11.41, p<.000. This means that the maximum brake force decreases faster for the scenarios without occlusion than that it does for with occlusion scenarios.

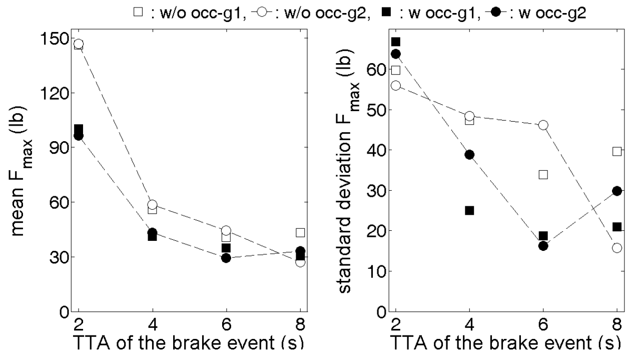

Fig. 4. Mean (left) and standard deviation (right) of the maximum brake force

The maximum brake force time (Fig. 5) reveals significant main effect of TTA: F (3,66) =56.42, p<.000, and interaction effect of V × T: F (3,66) =90.29, p<.000. This suggests that as the TTA of a braking event increases, the maximum brake force occurs later during the brake execution. However, for the scenarios with occlusion the pace of the peak braking force delay increase slows down at longer TTAs. For without occlusion scenarios, the maximum brake force delay increases for longer TTAs. Considering the standard deviation of the maximum brake force, V × T interaction is the only significant effect: F (3,66) =5.04, p<.005. The standard deviation results of the maximum brake force time show only one significant effect of TTA: F (3,66) =14.19, p<.000. As the TTA increases, the time of the maximum brake force varies more.

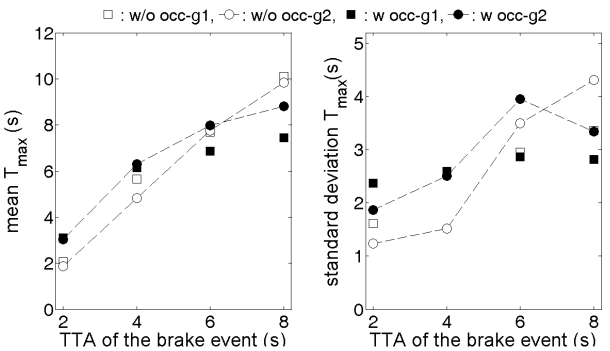

Fig. 5. Mean (left) and standard deviation (right) of the maximum brake force time

For the average brake force (Fig. 6) there are significant effects of visibility: F (1,22) =8.57, p<.01, TTA: F (3,66) =79.86, p<.000 and V × T interaction: F (3,66) =15.06, p<.000. The average is calculated for the moments that the brake pedal is pressed. The results show that the average brake force decreases with the increase in the TTA levels. On average, participants also exert lower force levels on their brake pedals during the scenarios with occlusion than they do in the scenarios without occlusion. The difference between the average braking forces exerted in these two scenarios decreases as the TTA increases.

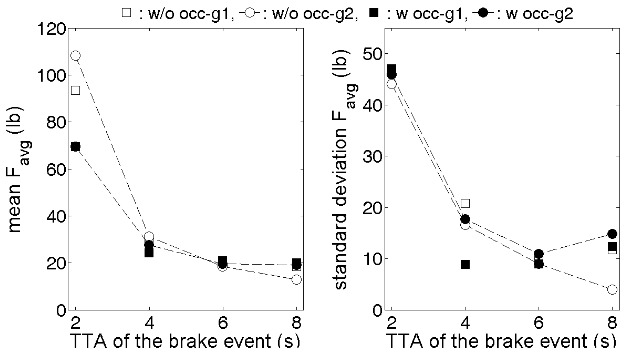

Fig. 6. Mean (left) and standard deviation (right) of the average brake force

The standard deviation results for the average braking force show two main T and V significant effects. Participants average brake force is more consistent with the presence of visual information: F (1,22) =4.96, p<.05 and with the increase in TTA: F (3,66) =28.59, p<.000. There is also a significant V × T interaction effect: F (3,66) =2.81, p<.05. For the scenarios without occlusion, the standard deviation of the average braking force of the participants as the TTA increases. For the occluded scenarios however, the standard deviation of the braking force increases at TTA=6s and 8s.

3.3. Driving performance

Fig. 7 shows the results of the distance gap achieved when the participants stop at the target. TTA is found as the only main factor with significant effect: F(3,66)= 67.14, p<.000. Participants stop after the target at shorter TTAs and before the target at longer TTAs. The V × T interaction effect is also significant: F(3,66)= 30.90, p<.000. The distance gap increases at a significantly higher rate for the with occlusion scenarios than it does for the without occlusion scenarios.

The standard deviation results reveals two main significant effects of TTA: F(3,66)=25.59, p<.000 and V: F(1,22)=12.49, p<.005. As the TTA increases, participant distance gap response varies more. The distance gaps for the occluded scenarios are also less consistent than they are for the scenarios without occlusion. There are also two significant interaction effects of G × T: F(3,66)=3.35, p<.05 and V × T: F(3,66)=7.24, p<.000. G1 participants show more consistent responses than G2 at the TTA=2s. This trend reverses at longer TTAs. The inconsistency of the responses at higher distances increases at higher rate for the scneraios with occlusion compare to the ones without occlusion.

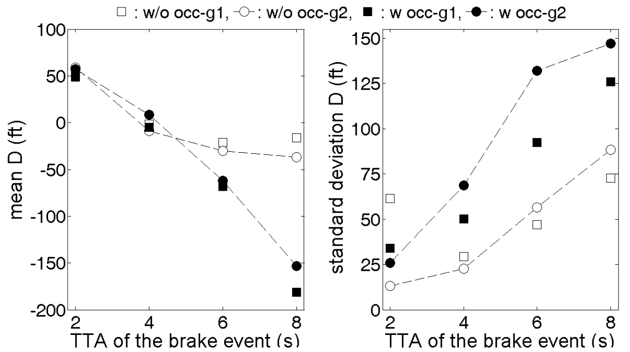

Fig. 7. Mean (left) and standard deviation (right) of the distance gap

3.4. Analysis of braking duration

The results of the brake duration (Fig. 8) reveal only one main factor with significant effect: F(3,66)= 101.72, p<.000. The brake duration increases as the TTA increases. The V × T interaction effect is also significant: F(3,66)= 15.57, p<.000. The braking duration increases at faster rate for scenarios without occlusion than it does for the occluded scenarios. There is also a significant G × T interaction effect: F(3,66)= 7.69, p<.000. The braking duration is similar for both G1 and G2 at shorter TTAs of 2s and 4s. However, at higher TTAs the duration differs between the two groups, with the G1 duration being higher. The standard deviation trend shows that as the TTA increases, the consistency in response decreases for both groups of participants and in both scenarios. However, this trend found not to be significant.

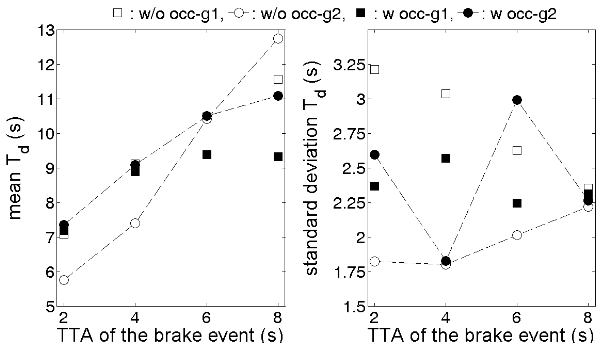

Fig. 8. Mean (left) and standard deviation (right) of the braking duration

The force characteristic of the brake pedal is divided into five different ranges. The relative duration of the braking force ranges exerted by each participant is calculated to quantify the braking patterns of the drivers under with and without occlusion conditions. Table 2 lists the ranges and the corresponding duration parameters. Each duration is calculated as a percentage of the total braking time (Figures 9 and 10).

Table 2. Brake force ranges

<20lb	20–40 lb	40–60 lb	60–80 lb	>80 lb
$T^d_{<20}$	T^d_{20-40}	T^d_{40-60}	T^d_{60-80}	$T^d_{>80}$

An ANOVA analysis revealed that there is a significant TTA effect for all ranges of the brake force (p<.000). Specifically, it was found that the shorter the TTA, the greater the proportion of more severe braking.

Visual information found to be significant for $T^d_{>80}$: F(1,22)= 11.75, p<.005. The amount of severe braking is significantly higher for the scenarios without occlusion.

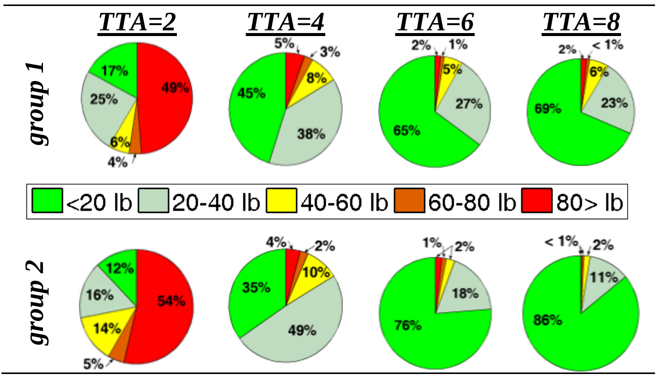

Fig. 9. Time ratios of brake force ranges for without occlusion scenarios

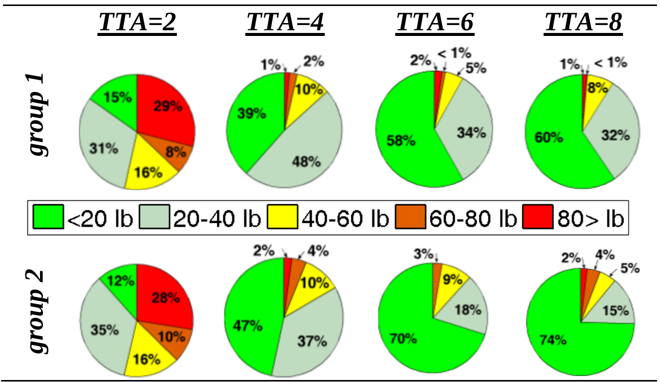

Fig. 10. Time ratios of brake force ranges for with occlusion scenarios

For $T^d_{80>}$, there is a significant V × T interaction effect: F(3,66)= 11.98, p<.000; For shorter TTAs (TTA=2s and 4s) $T^d_{80>}$, the ratio of the most severe braking range, is higher for scenarios without occlusion. There is a significant V × T interaction effect for T^d_{60-80}: F(3,66)= 2.76, p<.05; The share of T^d_{60-80} for the occluded scenarios is larger than it is for the non-occluded scenarios. Finally, there is a significant interaction effect of G × T: $F(3,66)= 3.95$, $p<.05$ for $T^{d}_{<20}$. Most notably, the share of $T^{d}_{<20}$ increases faster for G2.

4. Discussion and Conclusion

As the urgency of a braking event increases, drivers are expected to press the brake pedal more rapidly and more forcefully. The result of this experiment shows that occlusion does not significantly change the reaction time of participants regardless of the urgency of braking events. However, the results suggest that compared to the occluded scenarios, participants press the brake pedal harder during the scenarios without occlusion. This effect is evident for both the average and the maximum brake forces of the events with TTA=2s. Occlusion also moderates the rate at which the braking force increases when the available braking time is short. The maximum braking force in the occluded scenarios occurs later during the braking events with shorter TTAs than it does in the scenarios without occlusion. Over all when the time to brake is short, participants brake with less maximum force and for longer period during the scenarios with occlusion than they do during the without occlusion scenarios. The results of the distance gap indicate that the performance degrades at events with longer TTAs. For those events, drivers are less capable to stop at the target during the occluded scenarios than they are in the non-occluded scenarios. This result indicates that participants use visual information to control the distance when they have more time available to execute the brake and are far from the stopping target.

These findings reveal some important aspects of drivers braking behaviour. First, they show that occlusion degrades the flexibility of drivers in using the full range of the braking force when the temporal demand is high. Affordance control of brake proposes that actors keep a safe region between ideal acceleration and maximum acceleration to ensure safe braking is possible [Faj1]. Second, the result of this experiment suggests that the lack of visual information after the brake onset reduces the maximum brake force threshold used by drivers, especially in braking events with high temporal demand. The results also show that as the urgency increase, participants brake longer when the visual information is not available. In the occluded scenarios, drivers brake less severely and adapt larger distance gaps than they do in without occlusion scenarios. This can be explained by the perceived visual distance of the stopping target during the distance estimation test (Fig. 11).

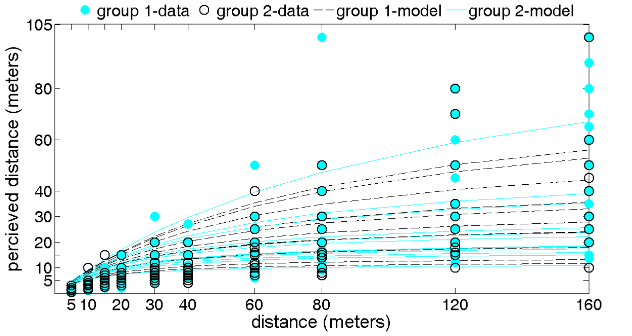

Fig. 11. Perceived vs. projected distances in the NADS minisim simulator, Dot lines are the Glinsky distance estimation model for each participant

For longer TTAs, drivers are far from the stopping target at the initiation of braking. Under these conditions, the distances at the start and in the early stages of the brake fall within the perception limits predicted by Glinsky's Equation (1). If the participants do not pump the brakes, they build up the maximum braking force early in the brake execution. Perceiving the target at a far distance significantly decreases the duration of the brake and slows down the rate that participants exert the braking force. In the non-occluded scenario, participants can regulate the force to stop at the stopping target as they approach the target.

These findings imply the potential benefit for driving information systems that assist drivers to look at the scene shortly before and during the brake. We also showed that the driver's perception of space may limit their performance. Based on the integrated relationship between time and space in driving, any driving assistance systems that provides timing advice should examine the usability of such advice at the given location.

5. References

[And1] Andersen, G. J., & Sauer, C. W., Optical information for collision detection during deceleration. In Advances in Psychology. 135: 93-108, 2004.

[Att1] Attentional reaction time, http://cognitivefun.net/ Accessed, March 27th, 2014.

[Faj1] Fajen, B.R., Calibration, information, and control strategies for braking to avoid a collision. Journal of Experimental Psychology: Human Perception and Performance. 31(3): 480-501, 2005.

[Gki1] Gkikas, A., Richardson, J. H., & Hill, J. R., A 50-driver naturalistic braking study: overview and first results. Contemporary Ergonomics. 423-431, 2009.

[Gil1] Gilinsky, A., Perceived size and distance in visual space. Psychological Review. 460-482: 58(6), 1951.

[God1] Godthelp, J., (1985), Precognitive control: open- and closed-loop steering in a lane-change manoeuvre. Ergonomics. 1419-1438: 28(10), 1985.

[Gre1] Green, M., Forensic vision with application to highway safety. Chapter 16: Collision Analysis. 2008.

[Lee1] Lee, D. N., A theory of visual control of braking based on information about time to collision. Perception. 437-459: 5, 1976.

[Mar1] Malaterre, G., Ferrandez, F., Fleury, D., & Lechner, D., Decision making in emergency situations. Ergonomics. 643-655: 31(4), 1988.

[Siv1] Sivak, M., The information that drivers use: is it indeed 90% visual? Perception. 1081-1089: 25(9), 1996.

[Yil1] Yilmaz E. H., & WarrenW. H., Visual control of braking: a test of the tau hypothesis. Journal of Experimental Psychology and Human Perception Performance. 996–1014: 21, 1995.

ROLL TILT THRESHOLDS FOR 8 DOF DRIVING SIMULATORS

Zhou FANG[1], Florent COLOMBET[2], Jean-Christophe COLLINET[1], Andras KEMENY[1]

(1): RENAULT, Virtual Reality and Immersive Simulation Center,
TCR AVA O 13, 1 avenue du Golf,
78288 Guyancourt
{zhou.fang, jean-christophe.collinet, andras.kemeny}@renault.com

(2): THEORIS
103 rue La Fayette
75010 Paris
+33(0) 1 53 25 02 32
florent.colombet@theoris.fr

Abstract –The tilt coordination technique is used in driving simulation for reproducing a sustained linear horizontal acceleration by tilting the simulator cabin. The rotational motion must be slow to remain under the perception threshold and thus be unnoticed by the driver.

However the acceleration to render changes fast. Between the slow rotational motion limited by the tilt threshold and the fast change of acceleration to render, the design of the coupling between motions of rotation and translation plays thus a critical role in the realism of a driving simulator. This study focuses on the acceptance by drivers of 8 different configurations for tilt restitution, for a slaloming task. Results show what thresholds have to be followed in terms of amplitude, rate and acceleration.

Key words: Driving simulator, Motion cueing algorithm, Explicit MPC algorithm, Tilt coordination technique, Scaling factor

1. Introduction

The role played in automotive industry by driving simulators is increasingly important. During the design phase, they allow testing new advanced driver assistance systems (ADAS)such as ACC, AEBA, etc. by studying driver's behaviour. They also allow testing the car's handling, ride comfort, drivability, behaviour, performance or fuel consumption without having to build a physical prototype. The 0.2Hz slalom is one of the most common scenarios performed for handling test. For Renault Company, being able to perform this test on a driving simulator could have a large number of interests in terms of cost and delay reduction. Unfortunately, the level of lateral acceleration rendered in simulation during this test is not enough according to professional test pilots who interpret the driving simulator feeling tightly connected to the driving commands, including the vehicle speed. Actually, the available X-Y rails strokes (5.2 meters) of the ULTIMATE simulator appear to not be enough to render the needed acceleration level. This is why we are focusing our research on the implementation of the tilt coordination technique in the motion cueing algorithm of the ULTIMATE simulator.

More generally, a sustained lateral acceleration is essential for the driver like in a curve for example [Rey1]. In this case, the obtained results could also be applied to perform the tilt-coordination task.

After presenting the tilt coordination technique and the difficulties generally encountered when using it in driving simulation, we will see that some thresholds needed for its implementation on a motion cueing algorithm remain unclear. Our experiment aims at comparing eight parameters configurations to see the acceptance of drivers and then determine what acceleration levels can be reached with the tilt coordination technique for the slalom test.

1.1. Tilt coordination technique

Accelerations are perceived by the human body mainly by the inner ear [Gra1]. The vestibular system is composed of the otholitic system and the semicircular canals. The first is sensitive to the linear accelerations while the seconds are sensitive to the angular accelerations. However the otholitic system presents a perception ambiguity: it cannot differentiate a horizontal acceleration from the gravity component due to an inclination around a horizontal axis. This ambiguity is thus used in motion cueing strategies to render a part of the vehicle accelerations by tilting the simulator cabin and is known as tilt coordination technique (Fig. 1). This rotation has to be done at a slow tilt rate to remain under the semicircular canals perception threshold. Visual rendering of the simulation has also to be compensated if the display screen is not fixed to the cabin.

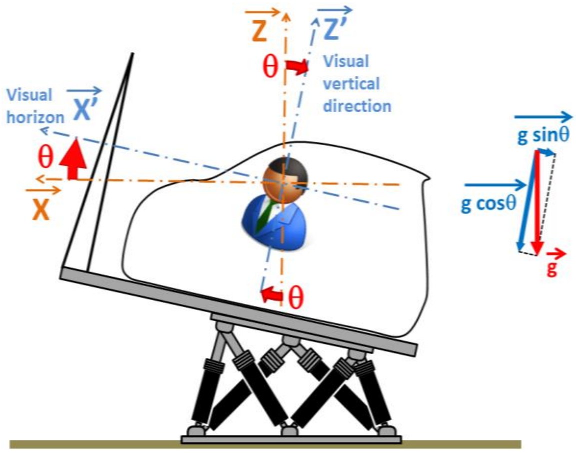

Fig. 1. Illustration of the tilt coordination technique. By tilting the simulator cabin of an angle θ, the component g*sinθ of the gravity may be interpreted by the driver as an horizontal acceleration.

Knowledge about rotation motion perception appears thus as primordial for the use of the tilt coordination technique, especially the detection threshold. According to the particular dynamics response of the inner ear semicircular canals model, Guedry [Gue1] has traced a relationship between the rotational acceleration and the time exposed to the excitation for the detection threshold. The theoretical model is correlated by Meiry's experience data and gives, e.g., a rotational acceleration threshold of about 8°/s² for 0,2s exposure and of 0.3°/s² for 10s exposure. Based on the step excitation and the canals' dynamic model, Mulder [Gue1] has adopted a rotational rate approach. He has proposed a perceived tilt rate perceived law and given a tilt rate threshold of about 2°/s which is independent of tilt acceleration. This low tilt threshold seems a reasonable value for general purpose driving simulation in the case of very low simulator's linear motion [Cha1]. By mean of a robotic simulator, Nesti *et al.* [Nes1] have showed with dynamic driving scenario and linear-tilt motion, that the roll rate threshold can be raised to a much higher value (about 5.2°/s) and suggested a high tilt rate threshold of 6°/s.

1.2. Problem

The tilt coordination technique appears thus to be quite difficult to implement in a motion cueing strategy for driving simulation. On one hand rotational motion has to be limited in terms of amplitude to avoid phase lag and in terms of rate and acceleration to avoid being noticed by the driver. On the other hand we need to tilt the cabin as much and as fast as possible to render an equivalent acceleration as high as possible. The motion cueing strategy has then to use a compromise between these two situations and unfortunately literature does not provide consistent thresholds values, and knowing which levels to use remains unclear.

For example by a simple sinus signal consideration for a 0,2Hz slalom scenario and assuming that no phase lag exists between reference and tilt signals, the relationship between the tilt level and the thresholds can be written in Table 1. If we choose to limit the tilt angle to 5°, the maximum equivalent acceleration we can provide is then 0.86 m/s². To reach this level when performing slalom at 0.2Hz, we will then have to rotate the cabin at a maximum tilt rate of 6.3 °/s and at a maximum tilt acceleration of 7.9 °/s². We see then that even with low levels of equivalent accelerations rendered with the tilt coordination technique, the theoretical perception thresholds are overtaken.

Table 1. Relationship between the tilt levels (amplitude, rate and acceleration) for a 0.2 Hz slalom scenario ($\omega=2\pi f=1.2566$ rad.s^{-1}).

Max tilt level (θ_{max})	Max equivalent linear acceleration ($g.\sin\theta_{max}$)	Max tilt rate ($\omega.\theta_{max}$)	Max tilt accel. ($\omega^2.\theta_{max}$)
3°	0.51 m/s²	3.8°/s	4.7 °/s²
5°	0.86 m/s²	6.3°/s	7.9 °/s²
8°	1.37 m/s²	10°/s	12.6 °/s²

It is found that in the case of multi-sensory stimulations, perception thresholds are modified in comparison of single sensory stimulation [Ber1, Nes1]. We think that if the rotational motion is accompanied with linear motion, perception thresholds could be higher. We aim then to determine what the acceptable thresholds for tilt acceleration and tilt rate are in an 8 DOF simulator. In the case of a slalom where lateral acceleration will be rendered both by linear acceleration and tilt coordination, is it possible to obtain a higher combined rendered level by overcoming the traditional thresholds?

2. Motion cueing algorithm

2.1. Renault ULTIMATE simulator

We intend to conduct our experiment on the high-performance dynamic ULTIMATE simulator [Dag1] at Renault Virtual Reality and Immersive Simulation Centre (VRISC) (Fig. 2). First developed in 2001, the simulator has been renewed in 2011 [Sch1] and consists now of a closed cabin based on a Renault Twingo 2 car which has been lightened and instrumented. Inside the cab, transmission is carried out using a manual gearbox, and a system of sound synthesis is used to reproduce engine noise and the audio environment for an interactive vehicle. Active steering force feedback is computed by a proprietary model and reproduced by a SENSO-Wheel system. The SCANeR© Studio 1.2 software package is used with a real-time version of the MADA (Advanced Modelling of Vehicle Dynamics) vehicle dynamics software, developed by RENAULT. The visual environment is displayed on a cylindrical screen (radius 1.9 m) thanks to five single-chip DLP projectors (Projection Design F12), each with a resolution of 1980 x 1080. The system covers a horizontal field of view of 210°.

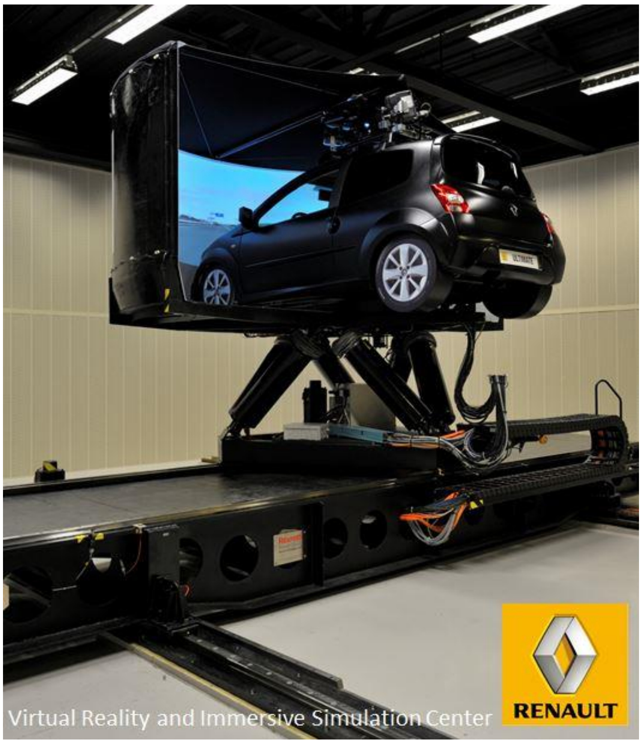

Fig. 2. Renault ULTIMATE driving simulator at Virtual Reality and Immersive Simulation Centre.

The cabin is mounted on a large X-Y table and a hexapod motion system to render physical accelerations and rotations. Table 2 presents the physical capabilities of the motion system.

Table 2. Physical capabilities of Renault ULTIMATE simulator

	Stroke	Speed	Accel.
X Rail	± 2.6 m	± 2.0 m/s	± 5.0 m/s²
Y Rail	± 2.6 m	± 3.0 m/s	± 5.0 m/s²
X Axis	± 0.28 m	± 0.7 m/s	± 7.5 m/s²
Y Axis	± 0.26 m	± 0.7 m/s	± 7.5 m/s²
Z Axis	± 0.20 m	± 0.4 m/s	± 5.0 m/s²
H Axis	± 15 °	± 40 °/s	± 300 °/s²
P Axis	± 15 °	± 40 °/s	± 300 °/s²
R Axis	± 15 °	± 60 °/s	± 600 °/s²

2.2. MPC-based motion cueing algorithm

The motion cueing algorithm is in charge of computing the physical displacements of the simulator cabin as a function of the simulated vehicle motion. It has to realize a compromise between rendering the vehicle accelerations (in terms of driver perception) and keeping the simulator within its physical limits. The algorithm used on the ULTIMATE simulator is a MPC-based (Model Predictive Control) motion cueing algorithm as described by Fang [Fan1]. Compared with classical or LQR optimal filters' approaches, the MPC integrates directly the system constraints into its optimization process, and then gives a real optimal solution and hardly needs the tuning process to check the workspace limits and the driver's perception thresholds.

In the motion cueing process, acceleration rendering with the tilt coordination technique has been added and is performed as a priority. The equivalent acceleration thus rendered is then subtracted to the vehicle acceleration before being rendered with the rails.

Tilt rotation thresholds (in terms of amplitude, rate and acceleration) are explicitly taken into account in the optimization process of the algorithm. Different configuration sets can be used and the possibility to switch online from one to another has been implemented. In this case, a transition phase between the two configurations is performed during 5 seconds.

We can also specify that rotation motions are rendered around the driver's head centre. Both vehicle and tilt coordination rotations are computed around this particular point. Specific modules are in charge of realizing the change of coordinates from the rotation point of the hexapod to the driver's head by adding linear motions (on the hexapod and not on the XY rails).

2.3. Tilt scaling factor

It is found that without any restriction the rendering by tilt coordination technique could induce a phase lag between the reference signal and the input signal of the linear restitution. It could thus lead into a global rendering worse than without tilt coordination. The solution we brought to this particular issue was to add an amplitude reduction of the reference signal (only for the tilt restitution part). In order to preserve at best the original signal profile, the scaling has been done with a hyperbolic tangent function as described in Eq. 1:

$$Y_{tilt\_ref} = Acc_{max} * \tanh(Y_{ref} / (K * Acc_{max})) \qquad (1)$$

where $Acc_{max} = g*\theta_{max}$ and K is a form factor. K varies from 3 to 6 depending on the maximum roll angle and roll rate.

3. Experimental protocol

3.1. General purpose

We aim at determining the acceptable tilt coordination parameters for lateral acceleration rendering during slalom. Table 3 details the 8 compared tilt configurations in terms of maximum tilt angle, tilt rate and tilt acceleration.

Table 3. Compared tilt configurations

Configuration	1	2	3	4
Max tilt angle [°]	3	4	5	5
Max tilt rate [°/s]	5	4	4	5
Max tilt accel. [°/s²]	8	8	8	12
Configuration	5	6	7	8
Max tilt angle [°]	5	5	6	6
Max tilt rate [°/s]	6	6	6	7
Max tilt accel. [°/s²]	15	60	60	60

We varied the maximum tilt angle from 3 to 6°, the maximum tilt rate from 4 to 7°/s and the maximum tilt acceleration from 8 to 60 °/s². In fact 60 °/s² is never reached because maximum angle or maximum rate is reached first (it is observed that a more reasonable limit value is about 20-30°/s). So the 60 °/s² constraint can be seen as non-constraint instead. The purpose of the value is only for safety matters.

3.2. Road description

The road used for this experiment is a straight portion of a double-lane motorway. This portion is visually realistic and there was no traffic.

Orange cones were dispatched on the road so that the driver can perform slaloms. In total 16 groups of 9 cones were disposed on the road every 1250 m (Fig. 3). For each slalom, the distance between the cones (62.5 m) ensuresthat when driving at 90 km/h the slalom is performed at a 0.2 Hz frequency (Fig. 4).

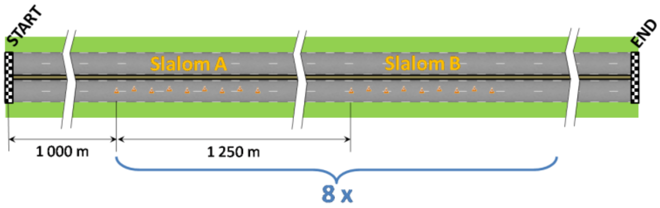

Fig. 3. Illustration of the road used for the experiment.

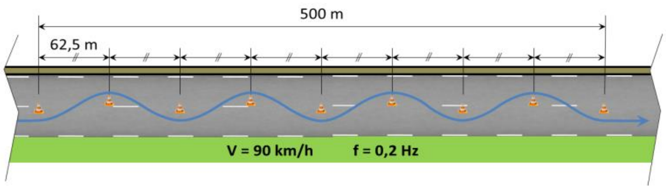

Fig. 4. Detailed illustration of the disposition of cones for one of the 16 slaloms. Cones are separated by 62.5m thus when driving at 90 km/h, the sinus trajectory is performed at a 0.2 Hz frequency.

3.3. Protocol

After presentingthem the simulator and the purpose of the experiment, subjects were proposed to perform a familiarization driving in which they could perform 4 slaloms: the 2 first with no tilt and the 2 others with tilt rendering.

For the experiment, there were 16 slaloms to perform in total. The slaloms were paired (1A/1B, 2A/2B, 3A/3B, ...). For each "A" slalom, no tilt coordination was done. For each "B" slalom, one of the 8 configurations (parameters set, see Table 3) was used for tilt rendering. Subjects were asked to drive at a constant 90 km/h speed in order to obtain a lateral acceleration around 3 m/s² when slaloming. In order to focus on the slalom performing and the motion rendering, subjects were asked to enable the cruise control. It ensured also that all drivers performed the experiment at the exact same speed. Finally, subjects were asked to verbally indicate after every "B" slaloms if they had found the motion rendering acceptable or not.

Eight volunteer subjects have participated to the experiment. Table 4 presents the configurations order for the 8 participants. We used a counterbalanced Digramlatin square in order to avoid rank effects (a given configuration is only once in a particular position) and report effects (any configuration is followed or preceded only once by each of the 7 other configurations).

Table 4. Configurations order for the 8 participants

Subject	Configurations order							
#1	1	8	2	7	3	6	4	5
#2	2	1	3	8	4	7	5	6
#3	3	2	4	1	5	8	6	7
#4	4	3	5	2	6	1	7	8
#5	5	4	6	3	7	2	8	1
#6	6	5	7	4	8	3	1	2
#7	7	6	8	5	1	4	2	3
#8	8	7	1	6	2	5	3	4

4. Results

4.1. Results analysis

Fig. 5 presents an example of lateral motion rendering with rails only ("A" slaloms). The vehicle lateral acceleration is represented by the solid line. We can see that the lateral acceleration rendered by the Y rail (dashed line) does not follow the reference signal every time. The rail stroke forces the cabin to slow down and approach to the limited ~~come back to the neutral~~ position.

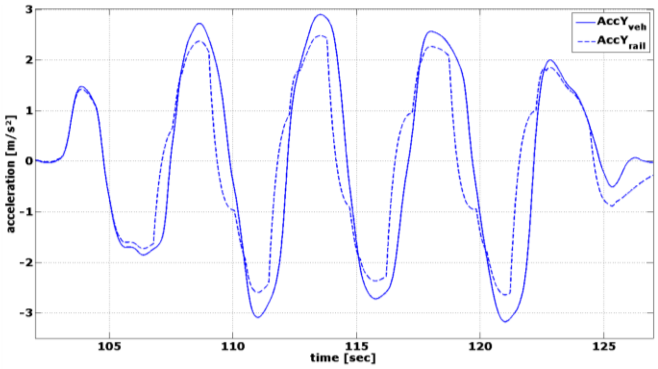

Fig. 5. Example of lateral restitution with rails only (without tilt)

On the other hand, Fig. 6 presents an example of lateral motion rendering with combined linear motion (Y rail) and tilt coordination technique ("B" slaloms). The vehicle lateral acceleration is represented by the solid blue line. The dashed red line is the equivalent acceleration rendered by tilt coordination. The solid red line is the acceleration rendered by the Y rail. And finally the dashed blue line is the combined rendered acceleration. The corresponding roll tilt angle, tilt rate and tilt acceleration are presented in Fig. 7. The configuration used for this particular slalom was the first (see Table 3). We can see tilt rate limited to 5°/s and tilt acceleration limited to 8°/s².

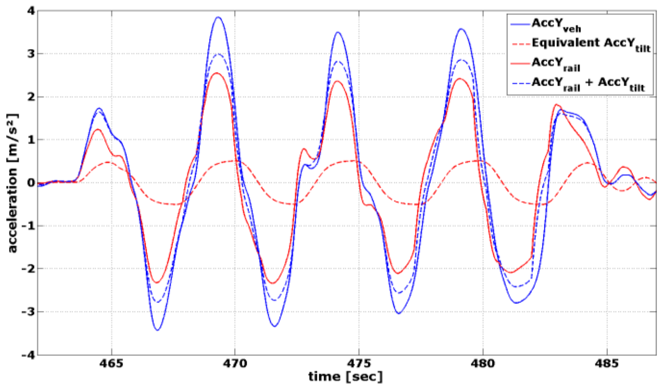

Fig. 6. Example of lateral rendering with combined rails and tilt coordination technique.

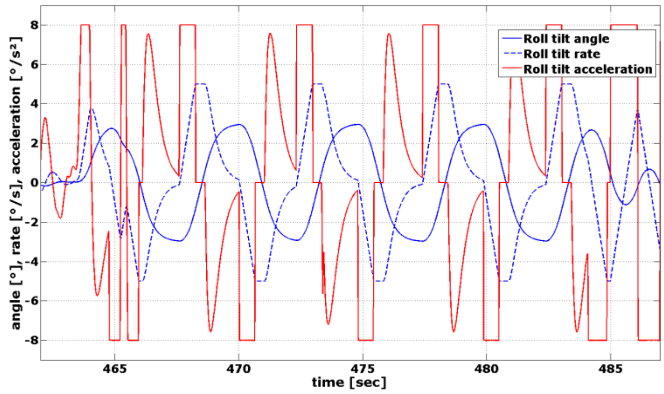

Fig. 7. Example of roll tilt angle, rate and acceleration for a slalom. The corresponding configuration is #1.

We can see on Fig. 6 the interest of tilt coordination. The combined rendered acceleration is closer to the vehicle acceleration than without tilt (Fig. 5).

Concerning subjects verbal answers, Table 5 presents the results of the 8 subjects (A = acceptable, NA = non-acceptable).

Table 5. Acceptance results of the 8 participants

Config.	1	2	3	4	5	6	7	8
Subj. 1	A	A	A	A	A	A	A	A
Subj. 2	A	A	NA	A	A	A	NA	NA
Subj. 3	A	A	A	A	NA	A	A	NA
Subj. 4	A	A	A	A	A	A	NA	NA
Subj. 5	A	A	A	A	NA	NA	NA	NA
Subj. 6	A	A	A	NA	A	NA	A	NA
Subj. 7	A	A	NA	NA	A	NA	NA	A
Subj. 8	A	A	A	A	NA	A	NA	NA

Except from subject 1, all drivers were able to notice a difference between configurations. From Table 5, we can trace the graph on Fig. 8 showing the percentage of acceptance for each configuration.

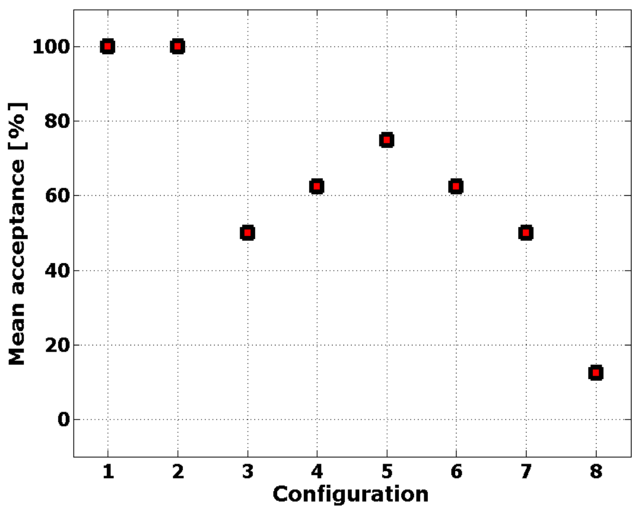

Fig. 8. Mean acceptance answer of the 8 subjects for each configuration.

4.2. Results discussion

What appears on Fig. 8 is that 100% of the subjects accepted the configurations 1 and 2. And if we exclude subject 1 who judged all configurations acceptable, none of the 7 other drivers judged the configuration 8 acceptable.

This shows that with the correct parameters (configuration 1 and 2), it is possible to use tilt coordination in terms of drivers acceptability, thanks to the coordination between tilt orientation and rails displacement. But what appears also is that tilt coordination cannot be used "too much". Results of the configuration 8 show clearly that: by using too high thresholds values, we can render higher levels of acceleration but no driver finds it acceptable in terms of perceived motion.

Finally for configurations 3 to 7, tilt coordination is accepted on average by 60% of the drivers (50% if we exclude subject 1). More subjects are needed if we would like to determine the 50% acceptance threshold but we think that limiting tilt in order to ensure that 100% of drivers accept it would be preferable, even if it doesn't allow rendering more than a 0.7 m/s² equivalent acceleration.

5. Conclusion and perspectives

We have presented a study on the use of tilt coordination technique for lateral acceleration rendering in the case of slalom performing, situation in which the tilt coordination technique is generally not recommended for an 8DOF driving simulator. We had to add an amplitude reduction (with a tanh function see Eq. 1) of the vehicle acceleration to reduce phase lag with the equivalent acceleration rendered by tilt.

Results show that if maximum tilt angle remains under 5 °, maximum tilt rate under 5 °/s and maximum tilt acceleration under 8 °/s² at the same time, every driver find it acceptable. And on the opposite, if both maximum tilt angle is beyond 6 ° and tilt rate beyond 7 °/s, no driver will find it acceptable.

What really is the cause of the non-acceptance by drivers remains yet unclear. Is it tilt amplitude, tilt rate, tilt acceleration or combined effects? Our results do not allow us to conclude. However they allow us to confine the values for our future experiments. For example we could keep tilt angles and rates at low levels and increase maximum reachable tilt acceleration to study its impact on drivers.

Are these results transposable? It is not a simple question. As reported by Chapron*et al.*[Cha1], the tilt perceived threshold varies according to the linear motion. In the experimental 0.2Hz slalom scenario, the tilt angle is nearly phased with linear motion, but tilt rate and tilt acceleration have respectively about 90° and 180° (opposite phase) phase lag. It could be considered as a rather bad situation to deduce high tilt rate and tilt acceleration thresholds. As a consequence, we think that in other driving situations, the values determined in our experiment could be transposable if the frequency of lateral accelerations remains under 0.2 Hz. For a slalom test beyond this level, tilt rate and acceleration levels may not be high enough to produce a significant tilt angle underphase lag constraint between the reference signal and the tilt angle. Moreover, tilt coordination becomes less necessary when frequency increases, because the higher the slalom frequency, the higher the lateral acceleration level which can be reproduced by linear motion if the simulator's frequency bandwidth allows to.

Concerning the transferability of our results for pitch tilt rendering, we presume that it is highly possible. In fact tilt detection thresholds for pitch and roll are often almost equal in literature.We have already implemented an MPC algorithm to render longitudinal motion by taking into account the rail linear acceleration level and the simulated vehicle's pitch rate. A good feedback has been obtained from internal professional drivers. However we intend to conduct an experiment similar to this one and quantify more precisely the tilt pitch tuning parameters.

6. References

[Ber1] Berthoz A., Bles W., Bulthoff H., Correia Gracio B., Feenstra P., Filliard N., Huhne R., Kemeny A., Mayrhofer M., Mulder M., Nusseck H.G., Pretto P., Reymond G., Schlusselberger R., Schwandtner J., Teufel H., Vailleau B., van Paassen M.M., Vidal M., Wentink M., "Motion Scaling for High-Performance Driving Simulators", 2013, *IEEE Transactions on Human-Machine Systems*, 43 (3), pp. 265-276.

[Cha1] Chapron T., Colinot J.P., "The new PSA Peugeot-Citroën Advanced Driving Simulator – Overall design and motion cue algorithm", 2007, *DSC North America 2007 Proceedings*.

[Dag1] Dagdelen M., Berlioux J.-C., Panerai F., Reymond G., Kemeny A., "Validation process of the ULTIMATE high performance driving simulator", 2006, *Proceedings of Driving Simulator Conference 2006*

[Fan1] Fang Z., Kemeny A., "Review and prospects of Renault's MPC based motion cueing algorithm for driving simulator", 2014, *DSC Europe 2014 Proceedings*, Paris, France

[Gra1] Graf W., Klam F., "Le système vestibulairee : anatomie fonctionnelle et comparée, évolution et développement", *Comptes Rendus Palevol* 5, no. 3-4 (2006): 637-655.

[Gue1] Guedry F.E., "Psychophysics of vestibular sensation". In: Kornhuber HH (ed) *Handbook of Sensory Physiology*, 1974, Vol. VI/2. Springer Verlag, Berlin, Heidelberg, New York, pp 3-154

[Jam1] Jamson A. H. J. , "Motion Cueing in Driving Simulators for Research Applications", PhD Thesis, University of Leeds, Nov. 2010

[Lew1] Lewis J. R., "Pairs of Latin Squares that produce digram-balanced Greco-Latin designs: BASIC Program", *Behavior Research Methods, Instrument & Computer*, 1993, Vol. 25, No. 3, pp 414-415.

[Nes1] Nesti A., Masone C., Barnett-Cowan M., Giordano P.R., Bülthoff H. H., Pretto P., "Roll rate thresholds and perceived realism in driving simulation", 2012, *DSC Europe 2012 Proceedings*, Paris, France

[Rey1] Reymond G., Kemeny A., Droulez J., Berthoz A., "Role of lateral acceleration in driving: experiments on a real vehicle and a driving simulator", 2001, *Human Factors* 43(3): pp 483-495.

[Sch1] Schill V, Schulz T., Kemeny A., Collinet J.-C., Legrand O., Deborne R., "Renewal of the Renault Ultimate Simulator", 2012, *DSC Europe 2012 Proceedings*, Paris, France

[Str1] Stratulat A.M., Roussarie V., Vercher J.-L., Bourdin C., "Perception of longitudinal acceleration on dynamic driving simulator", 2012, *DSC Europe 2012 Proceedings*, Paris, France

THE INFLUENCE OF LATERAL TILT/TRANSLATION, ROLL AND YAW SCALE FACTORS ON DRIVING PERFORMANCES ON AN ADVANCED DYNAMIC SIMULATOR

Florian Savona [1,2], Anca Stratulat [1], Emmanuelle Diaz [1], Vincent Honnet [1], Gilles Houze [1], Philippe Vars [1], Stéphane Masfrand [1], Vincent Roussarie [1], Christophe Bourdin [2]

(1) : PSA Peugeot Citroën, Centre Technique de Vélizy, Route de Gizy 78943 Vélizy-Villacoublay Cedex France, +33 1 57 59 25 37
E-mail : {florian.savona, ancamelania.stratulat, emmanuelle.diaz, vincent.honnet, gilles.houze, philippe.vars, stephane.masfrand, vincent.roussarie}@mpsa.com

(2) : Aix-Marseille Université, CNRS, ISM UMR 7287, 13288 Marseille, France, +33 4 91 17 22 52
E-mail : {florian.savona, christophe.bourdin}@univ-amu.fr

Abstract – The present study investigates the importance of lateral acceleration, roll angle and yaw acceleration as scale factors (motion gains) on these components, in the driving perception and behavior in curve. Recent study advises to use down scale-factors (0.4-0.75) on the three car lateral motions felt in curve. In the current study, we used the same slalom task, and increased the range of lateral acceleration produced by the slalom, as the scale factors. The principal result is that the lateral motion gain has to decrease with the increase of lateral acceleration, in order to improve the perception and the driving performance. Concerning the roll motion gain, we advise to use it with a unit gain whether the quantity of lateral acceleration. However, the important of yaw motion is more controversial, it only seems to facilitate the driving control, at less in this slalom task.

Key words: Lateral acceleration, scale factors, multisensory perception, driving performance, tilt-coordination.

1. Introduction

On dynamic driving simulators, the motion perception is produced by stimulating the vestibular and somatosensory systems in addition to the visual system [Kem1]. However, the intricacy of the multisensory stimulations undergone when driving a car makes the optimization of the motion based simulators quite complex. For instance, it has already been proven that the motion on driving simulator is overestimated when simulated at 1-to-1 rate [Gro2], [Str3], [Str4] and that the inertial magnitude (gain) and the way (distribution between tilt and translation) to reproduce a positive or negative acceleration e.g. take-off or braking, is highly dependent on the level of the simulated acceleration [Ber5], [Str4].

For turning manoeuvers, the control of the simulator appears to be even more complex than for longitudinal manoeuvers because, in addition to lateral acceleration, yaw and roll motions of the car have to be simulated. The main source of information on which the driver bases his manoeuvers is the lateral acceleration. Indeed, the driver controls his speed or trajectory to keep this acceleration in a comfortable range and to insure a safety margin [Fel6], [Rey7]. In most dynamic driving simulators, simulation of the lateral acceleration is produced by using tilt coordination technique (lateral translation and roll tilt). However, in natural driving and for simulation, rotational components i.e., roll and yaw movements, are also associated to steering behavior of the car during cornering. This very last component, that is yaw motion, seems to be an influent component for realistic driving simulations. Indeed, recent studies [Dam8], [Hog9] have confirmed that a yaw component associated to the other lateral acceleration components (translations and/or roll) leads to better driving performances and improve motion perception, than when it is absent. In addition, Berthoz et al. (2013)

[Ber10] proposed that motion scale factors (for lateral and rotational acceleration) have to be comprised within the range 0.4-0.75. One limitation of this study is that the gain of linear translations, roll movements and yaw movements and their relationships were not systematically varied for different levels of acceleration.

To go further, the present study, conducted on the dynamic driving simulator Sherpa² by PSA, is focused on cornering manoeuvers. It aims at systematically revisiting the gains of the three lateral motion components (lateral, yaw and roll movements) for several levels of lateral accelerations. In order to evaluate the individual effects of the three parameters on the driving behavior, we chose a slalom driving task.

Through subjective and objective analyses, we seek to identify and quantify the major sources of movements for perception and driving performance in cornering and to identify the best set of parameters according to the level of acceleration to simulate. A precise cartography of the settings of the dynamic driving simulators will make it more realistic in a wider range of lateral accelerations. We make the hypothesis that the motion gains on the different parameters are not necessarily linked [Cor11], [Dag12], and could be different depending on the level of lateral acceleration to be simulated.

2. Methods

2.1. Participants

27 volunteers (2 women and 25 men), aged between 22 and 49 (mean age: 28) participated in the study. All were PSA's employees who volunteered for the study, and none had significant experience of the simulator (average dynamic driving simulator experience less than 1.5 hours).

2.2. Experimental devices

SHERPA² is a dynamic driving simulator equipped with a hexapod and an X-Y platform (10 x 5 m). The cell placed on the hexapod contains a half-cab Citroen C1 fully-equipped (2 front adjustable seats, seat belts, steering wheel, pedals, gearbox, rearview mirror and side-view mirrors) where the driver is sitting. The motion limits of the hexapod are ±30 cm, ±26.5 cm and ±20 cm, on X, Y and Z respectively [Cha13]. The rotational movements are limited to ±18 deg, ±18 deg and ±23 degrees, on pitch, roll and yaw respectively. The X-Y motion platform can reproduce linear movements of 10 and 5 meters. The maximum longitudinal and lateral acceleration is 5 m/s², and is actually produced by combination of tilt and translation (termed "lateral motion" in this paper).

2.3. Experimental Scenario

The vehicle dynamics model (car dynamic and audio) tuned for the present experiment was a Peugeot 208 1.4 HDi. The visual scene consisted in a straight two-lane road (road width: 8m). Guardrails were placed at both sides of the road to delimit the allowed maximum excursion of the car. The slalom driving scenario consisted of a series of 8 pylons separated by a constant distance (for a given condition). In addition, multiples mini-cones were used to represent the optimal sinusoidal pathway (Figure 1). The pylons were alternately placed 0.9 m to the right and left side of the road centerline. Sinusoidal magnitude was always 2m, the sinusoidal pathway was forming by two mini-cones path of 2m of width. The velocity of the car was regulated to 70 km/h. By adjusting the distance separating two pylons, we imposed the theoretical lateral acceleration, while keeping constant the longitudinal velocity of the car, the lateral pylons placements as well as the magnitude of sinusoidal pathway. Hence, we designed three different slaloms scenario leading to 3 theoretical lateral accelerations i.e., 1, 2 and 4m/s², corresponding to a pylons spacing of 86.39, 61.09 and 43.19 meters respectively. The equation enabling to compute theoretical lateral acceleration was borrowed from Grácio et al. (2011) [Grá14].

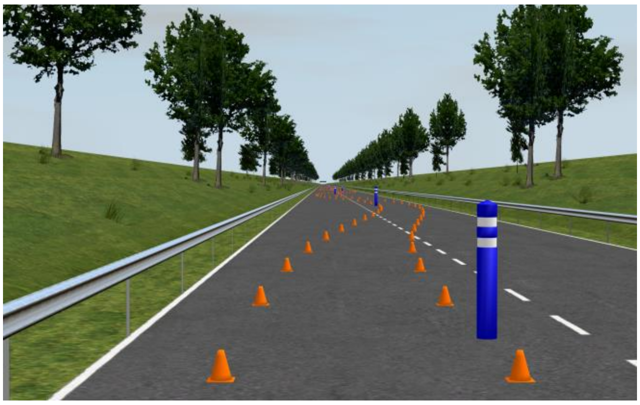

Figure 1. Visual environment of slalom task.

2.4. Task

Drivers were asked to perform a slalom course on the dynamic driving simulator in following the mini cones path, without touching any pylons or going out of the road (no damage on the car). The run was realized in cruise control at the constant speed of 70 Km/h. Nonetheless, to activate the cruise control, participant had to accelerate himself to 30 Km/h.

2.5. Experimental Design

For each level of lateral acceleration (1, 2 and 4 m/s²), we manipulated the scale factors (0 0.2 0.4 0.5 0.6 0.8 1 depending on the slalom scenario) of the 3 motion components (lateral tilt-translation; yaw and roll movements) leading to a total of 25 different conditions (Table 1). Each participant realized 3 trials per conditions for a total of 75 trials divided into two sessions to avoid fatigue effect. The overall trials were organized by using a central composite experiment design [Tin15]. The choices of scale factors (or motion gains) were made by taking into account the physical limitations of the simulator (position, speed, linear and angular acceleration). During the first session, realized the morning, participants first started with a simulator familiarization phase (10min of rural drive in dynamic simulator) and a learning slalom phase (one trial for each slaloms without motion). This first session was continued with twenty-five trials of a same slalom (same level of acceleration). The second session, performed the afternoon (of the same day), included another learning slalom phase along with the 50 resting trials. The order of slalom was balanced over the total panel of participants. The orders of stimuli were presented using William’s Latin Square, which allowed balancing the order and report effects. The use of a central composite experiment design enable to obtain a maximum information in a minimum experience, and to build a model estimating nonlinear effects. Furthermore, at the end of each trial, the participants answered a couple of questions to provide us with information about their subjective perception of the realism of the vehicle behavior and the facility of the task (Table 2). In addition, their motion sickness level was monitored throughout the experimentation by using a motion sickness questionnaire (MSSQ) [Cor11].

Table 1. The 25 motions conditions for each specific slalom. The motions conditions varied according to different gains (scale factors) applied to the three simulator motion components. Slalom 1, 2 & 3 respectively correspond to 1, 2 and 4m/s² slalom levels. The condition number 20 corresponds to the actual Sherpa² configuration.

	Gain Lateral motion acceleration			Gain Roll angle	Gain Yaw acceleration
Slalom	**1**	**2**	**3**	**1, 2 & 3**	**1, 2 & 3**
Condition					
1	0.2	0.2	0.2	0.2	0.2
2	0.8	0.8	0.6	0.2	0.2
3	0.2	0.2	0.2	0.8	0.8
4	0.8	0.8	0.6	0.8	0.8
5	0.2	0.2	0.2	0.2	0.2
6	0.8	0.8	0.6	0.2	0.8
7	0.2	0.2	0.2	0.8	0.8
8	0.8	0.8	0.6	0.8	0.8
9	0	0	0	0.5	0.5
10	1	1	0.8	0.5	0.5
11	0.5	0.5	0.4	0	0.5
12	0.5	0.5	0.4	1	0.5
13	0.5	0.5	0.4	0.5	0
14	0.5	0.5	0.4	0.5	1
15	0.5	0.5	0.4	0.5	0.5
16	0.5	0.5	0.4	0.5	0.5
17	0.5	0.5	0.4	0.5	0.5
18	0.5	0.5	0.4	0.5	0.5
19	0.5	0.5	0.4	0.5	0.5
20	-1	-1	-1	-1	-1
21	0	0	0	0	0
22	1	1	0.8	1	1
23	1	1	0.8	0	0
24	0	0	0	1	0
25	0	0	0	0	1

2.6. Data analysis

During the driving task, some vehicle and simulator dynamics variables e.g. lateral acceleration, steering wheel angle, lateral position were recorded. All these measurements were used to conduct an objective analysis of the driver’s behavior. From the steering wheel angle, we can compute the steering wheel reversal rate. The steering wheel reversal rate (SWRR) is a performance indicator that quantifies the amount of steering corrections, and enables to determine the effort required to accomplish a certain task [Fee16]. This metric measures the frequency of steering wheel reversals larger than a finite angle, or *gap*. The magnitude of this gap, the *gap size*, is thus a key parameter for this metric [Öst17]. In the present study, the number of reversals per slalom course was counted. To this end, the steering signal was filtered with a second-order low-pass Butterworth filter with a cutoff frequency depending on the slalom level i.e., 0.6, 2 and 5 Hz for the 1, 2 and 4m/s² slalom levels respectively. The algorithm for detection of reversal was extracted from the "Reversal Rate 2" in the Östlund's study (2005), and a difference greater than or equal to 2° (*gap size*) indicates one reversal.

The driving accuracy was quantified as lateral deviation from the reference trajectory (center of mini cones path) and computed as Root Mean Squared Error (RMSE) of the vehicle path [Pre18].

The subjective and objective data were analyzed with the software NEMRODW, which enables to construct experimental plans, and the analysis of experimental results. A principal component analysis (PCA) was realized for all kind of variables (subjective and objective) in order to determine if there was a consensus among subjects. PCA were realized with the software SPAD 7.

Table 2. Two 11 points qualitative scale.

Not Realistic 0	1…9	Very Realistic 10

1-Assessing the quality of realism of vehicle behavior

Not Easy 0	1…9	Very Easy 10

2-Evaluate the facility of achieving slalom

3. Results

3.1. Subjective analysis

3.1.1. Motion Sickness

During the experiment, four subjects felt motion sick and were not able to finish all experimental conditions (MISC ≥6). Three of these participants felt motion sick during the higher slalom level and following to higher lateral acceleration gains (condition 10, 22 or 23 in Table 1). The remaining twenty-three subjects were able to conduct the experiment without serious motion sickness (average MISC = 0.78 ± 1.2).

3.1.2. Realism of Vehicle Behavior

Following to PCA, no consensus among participants was found, so we centered the data, and realized a hierarchical clustering to identify homogeneous groups of subjects: 2 groups were identified. We analyzed the experimental results for the two groups separately. The analysis of model coefficient enabled us to determine the optimal motion configuration. The coefficient are named as follow: "B0" is the model's constant, "B1" is the linear coefficient applied to lateral motion gain, "B2" is the linear coefficient applied to roll gain, "B1-1" is the square coefficient of lateral motion gain.

For the first slalom level (1m/s²), and for the two groups, the lateral motion was a significant factor for both groups, and roll motion was a significant factor for the second group. The model coefficients are presented in the Table 3 for the 2 groups.

Table 3. Model's coefficient and significance for both groups G1 and G2, concerning the realism of vehicle behavior for the first slalom.

Name	G1 Coeff	Sign	G2 Coeff	Sign
B0	7.756	<0.01***	6.889	<0.01***
B1	-0.374	0.518***	1.174	<0.01***
B2	-0.081	48.5	0.405	2.13*
B1-1	-1.227	<0.01***	-4.5	0.05***

According to G1 answers, the experimental model asses as more realistic a motion configuration with: lateral motion gain = 0.5, roll motion gain = 1, and yaw motion gain = 0.

According to G2 answers, the best set of parameters concerning the realism is: lateral motion gain = 0.85, roll motion gain = 1, and yaw motion gain = 0. The Fig. 2 shows a 2D representation of experimental model of Lateral and Roll motion gains for the realism of vehicle behavior in the first slalom and according to G2. In this figure, the yaw motion gain is fixed to 0, because it do not significantly influences the results, but a best result is obtained if it equal 0.

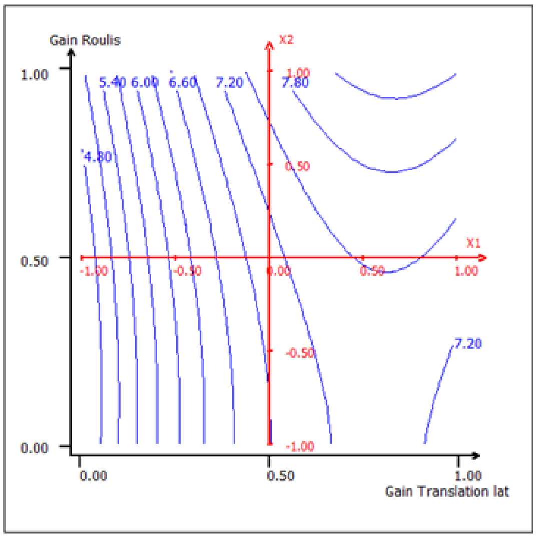

Fig. 2. 2D representation of experimental model for the realism of vehicle behavior, for the 1st slalom and 2nd group.

For the second slalom, the only significant factor was the lateral motion (p<0.01), for both group. In the third slalom, and G1, the significant factors were: the lateral motion (p<0.01), as the roll and yaw motion, the lateral motion-yaw motion interaction and the roll-yaw motion interaction.

The Fig. 3 presents the most realistic lateral motion gains, according to the two groups. The lateral motion gains are digressive for both groups. Note that, yaw motion = 0 was still computed by the model as giving best results for both groups and all slaloms, but was only a significant factor for G1 in the third slalom. For both groups, a roll motion gain of 1 always gives a best result in all slaloms.

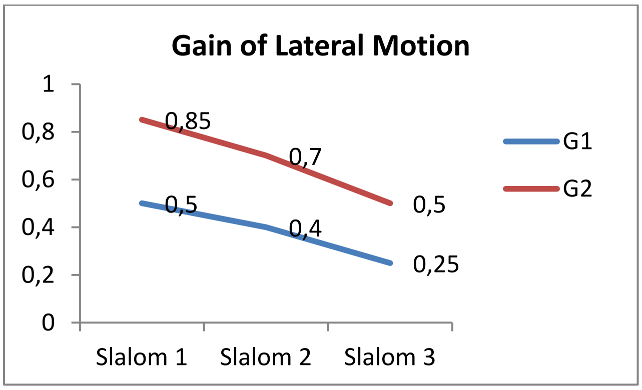

Fig. 3. Best Lateral motion gains according to the two groups and the three slaloms.

3.1.3. Facility of Achieving Slalom

In the first slalom, for judging the facility of achieving slalom, no difference was found between all configurations. The first slalom was certainly too easy to realized, and so drivers had not need to external help to realized the task, and inversely, did not feel perturbed by motions.

In the second and the third slalom, a consensus was found between the participants, so one groups was used to compute the experimental model. The only significant factor was the lateral motion (p<0.01), for the second and the third slalom. The best motions gains are presented in the Table 4.

Table 4. Best motion gains to the second and the third slalom, concerning the facility of achieving slalom.

	Gain Lateral Motion	Gain Roll	Gain Yaw
Slalom 2	0.2	0.3	0
Slalom 3	0	1	1

Contrary to the first slalom, participants found the second and the third slalom less easy, notably with lateral motion gain superior to 0.2 in the second slalom and superior to 0 in the third.

3.2. Objective Analysis

3.2.1. Steering-Wheel Reversal Rate

The PCA revealed a consensus among the participants, for all slalom levels. Hence, the 23 participants were analyzed together, for the three experimental models. The significant factor was the lateral motion gain for all slalom level.

For the first slalom level, the results show that number of reversals decreases with an increase in lateral motion gain, and so that more steering correction was required for a reduced lateral motion gain (Figure. 4)

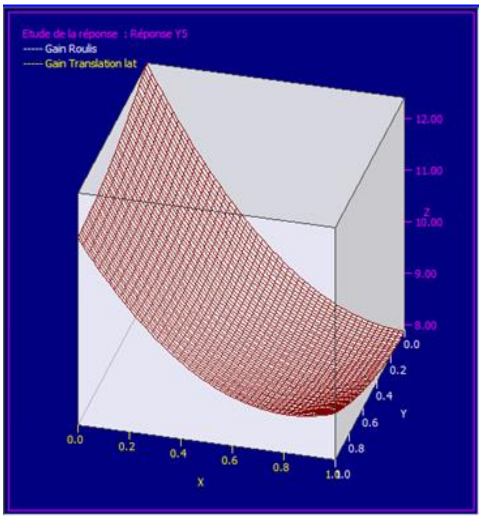

Figure. 4. 3D representation of response surface for the SWRR variable and for the first slalom.

The Figure. 4 shows that the roll motion gain is not very important, however, best result was obtained for a roll motion gain of 0.

Contrary to the first slalom, in the second and in the third, a best model is obtained with a roll motion gain of 1. However, as for the Realism variable, the best lateral motion gain decrease with the increase of lateral acceleration. The yaw motion effect, although not being significant for the model, give a better result with a motion gain of 1 (Table 5).

Table 5. Best motion gains to the SWRR variable and for the three slaloms.

	Gain Lateral Motion	Gain Roll	Gain Yaw
Slalom 1	1	0	0
Slalom 2	0.5	1	1
Slalom 3	0.25	1	1

3.2.2. Path Root Mean Square Error

As for the previous variable, one group was kept for the model construction. No difference was found between the motion configurations for the first and the second slalom. Maybe the mini cones path was very helpful to accurate drive. Nonetheless, differences were found in the third slalom (4m/s²). The significant factor was again the lateral motion gain.

The experimental model found two configuration settings, giving the same performance (Table 6).

Table 6. Best motion gains to the RMSE variable for the third slalom.

Slalom 3	Gain Lateral Motion	Gain Roll	Gain Yaw
1st configuration	0.25	1	0
2nd configuration	0.35	0 or 1	1

The Figure. 5 shows the results for the second configuration (0.35 lateral motion gain), as we can see, extreme lateral motion gains decrease the drive accuracy.

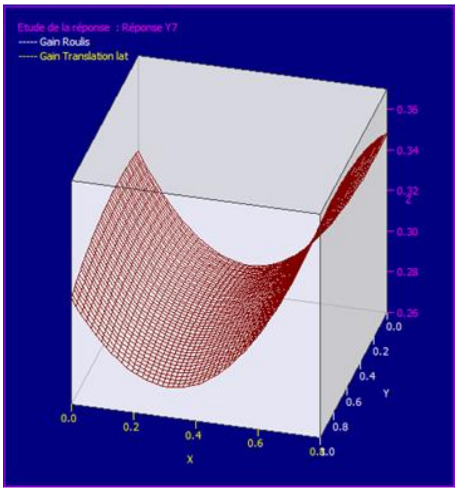

Figure. 5. 3D representation of response surface for the RMSE variable, for the third slalom and the second configuration.

4. Discussion of Results and Conclusion

Previous researches in dynamic driving simulator, advise to use under-unit scale factors in cornering, in order to improve perception and driving behavior [Fee16], [Pre18], [Fee19] and [Fil20]. The present research aims to develop knowledge of driver perception and simulator setting in curve. The slalom task was already validated by several studies, however, these studies did not question if preferred motion gains could evolve as function of slalom intensity, i.e., several lateral accelerations.

We asked drivers to assess the quality of realism of vehicle behavior and the facility of achieving slalom. For the first question, we found that the more important factor is the lateral motion gain i.e., the quantity of lateral acceleration produced by the simulator and felt by the driver. Two groups emerged and were analyzed separately. Despite the fact that the two groups preferred different motion gains, the experimental model showed a roll motion gain = 1, is evaluated as more realistic. Similar results were found in a previous research [Dag12] but with expert drivers, which was not the case in the current study, where the population was "normal" drivers. Our driving simulator reproduces exactly the roll angle and its derivates, and is temporally coherent with the visual roll. Absolute threshold of roll motion is around 2°/s [Ben21], hereby; the roll velocity could attempt this threshold from the second slalom. Thus, a roll motion with downscale factor is not forcedly felt by the driver.

Surprisingly, the yaw motion influences very little the final perception, maybe its intensity was not felt or masked by the two others component i.e., the lateral and roll motion, more works are required to elicit this point.

The more important result concerns the lateral motion gain, which is digressive for both groups with the increase of lateral acceleration. Although we asked participants to evaluate the realism of vehicle behavior, it is not impossible that a "comfort level" was also evaluated. Higher lateral amplitude can be more uncomfortable, so the decrease of lateral motion gain could be due to the decrease of discomfort. Nevertheless, we use the tilt coordination technique for the reproduction of lateral acceleration, it is also possible than the tilt is easier perceived with the increase of lateral acceleration. A previous study [Nes22] showed that limit of lateral tilt (before to be perceived as a tilt and no a lateral acceleration), is higher for active drivers than for passive passengers [Gro2]. This research advised to limit the tilt to 6°/s, twice the limit found for passive subjects. In our study, for the second and third slalom and for the higher lateral motion gains, the lateral tilt could attempt 14° of inclination and an angular velocity of 12°/s (limit fixed by our motion cueing algorithm or MCA). These magnitudes are higher than recommended by the Nesti's et al. study [Nes22], and higher than the threshold of roll tilt [Bri23]. Hence, more investigations are required to definite the tilt limits of our simulator, whether in velocity or total angle.

Concerning the subjective perception of facility, we also found a decrease of lateral motion gain with the increase of slalom level. Drivers found more difficult to realize the second and the third slalom for configurations with lateral motion gains higher than 0.2 and 0 respectively. The increase of discomfort is probably one cause.

Nonetheless, as showed by the objective analysis of steering-wheel corrections and lateral deviations, lateral motions gains inferior to 0.2 is not advised. Except the first slalom, where a lateral motion gain of 1 enables optimal steering, the driving accuracy for the two others slaloms is better with lower lateral motions gains. However, a lateral motion gain of 0 is not recommended in order to improve driving performances and accuracy, as shown by the RMSE variable (Table 6). A previous research [Fee16] showed a decrease of steering correction with the increase of lateral motion gain. Nevertheless, they analyzed only one level of slalom (1.2m/s²). Hereby, we show that with the increase of lateral acceleration (and so the slalom level), the effort required to accomplish the slalom is more important whit a unit or near unit lateral motion gain.

In order to improve the driver's perception and control performances, it is recommended to setup the MCA with a decreasing lateral motion gain, while keeping the roll gain to 1 and yaw motion gain to 0

5. Conclusions

If the lateral motion seems to have the most influence in the perception of lateral acceleration on dynamic driving simulators, surprisingly, the roll and the yaw motions are less influential than expected. However, given the results of previous studies, we should investigate more closely this matter in order to better understand the interaction between these 3 motion components from a perceptive point of view.

6. References

[Kem1] A. Kemeny et F. Panerai, « Evaluating perception in driving simulation experiments. », *Trends Cogn Sci*, vol. 7, n° 1, p. 31–37, janv. 2003.

[Gro2] E. L. Groen et W. Bles, « How to use body tilt for the simulation of linear self-motion », *J. Vestib. Res. Equilib. Orientat.*, vol. 14, n° 5, p. 375-385, 2004.

[Str3] A. Stratulat, V. Roussarie, J.-L. Vercher, et C. Bourdin, « Improving the realism in motion-based driving simulators by adapting tilt-translation technique to human perception », 2011, p. 47-50.

[Str4] A. M. Stratulat, V. Roussarie, J.-L. Vercher, et C. Bourdin, « Perception of longitudinal acceleration on dynamic driving simulator », présenté à Proceeding of the Driving Simulation Conference 2012, Paris, France, 2012.

[Ber5] D. R. Berger, J. Schulte-Pelkum, et H. H. Bülthoff, « Simulating believable forward accelerations on a stewart motion platform », *ACM Trans. Appl. Percept.*, vol. 7, n° 1, p. 1-27, janv. 2010.

[Fel6] E. Felipe et F. Navin, « Automobiles on Horizontal Curves: Experiments and Observations », *Transp. Res. Rec.*, vol. 1628, n° 1, p. 50-56, janv. 1998.

[Rey7] G. Reymond, A. Kemeny, J. Droulez, et A. Berthoz, « Role of lateral acceleration in curve driving: driver model and experiments on a real vehicle and a driving simulator », *Hum. Factors*, vol. 43, n° 3, p. 483-495, 2001.

[Dam8] H. J. Damveld, M. Wentink, P. M. van Leeuwen, et R. Happee, « Effects of Motion Cueing on Curve Driving », présenté à Proceeding of the Driving Simulation Conference 2012, Paris, France, 2012.

[Hog9] J. H. Hogema, M. Wentink, et G. P. Bertollini, « Effects of Yaw Motion on Driving Behaviour, Comfort and Realism », présenté à Proceeding of the Driving Simulation Conference 2012, Paris, France, 2012.

[Ber10] A. Berthoz, W. Bles, H. H. Bulthoff, B. J. Correia Gracio, P. Feenstra, N. Filliard, R. Huhne, A. Kemeny, M. Mayrhofer, M. Mulder, H. G. Nusseck, P. Pretto, G. Reymond, R. Schlusselberger, J. Schwandtner, H. Teufel, B. Vailleau, M. M. (René) van Paassen, M. Vidal, et M. Wentink, « Motion Scaling for High-Performance Driving Simulators », *IEEE Trans. Hum.-Mach. Syst.*, vol. 43, n° 3, p. 265-276, mai 2013.

[Cor11] B. J. Correia Grácio, J. E. Bos, M. M. Paassen, et M. Mulder, « Perceptual scaling of visual and inertial cues: Effects of field of view, image size, depth cues, and degree of freedom », *Exp. Brain Res.*, vol. 232, n° 2, p. 637-646, nov. 2013.

[Dag12] M. Dagdelen,, J.-C. Berlioux, F. Panerai, G. Reymond, et A. Kemeny,, « Validation Process of the Ultimate high-performance driving simulator », présenté à Proceeding of the Driving Simulation Conference 2006, Paris, France, 2006.

[Cha13] Chapron, Thomas et Colinot, Jean-Pierre, « The new PSA Peugeot-Citroën Advanced Driving Simulator Overall design and motion cue algorithm », présenté à Proceeding of the Driving Simulation Conference 2007, North America, Iowa City, 2007.

[Grá14] B. J. C. Grácio, M. Wentink, et A. R. Valente Pais, « Driver Behavior Comparison

Between Static and Dynamic Simulation for Advanced Driving Maneuvers », *Presence Teleoperators Virtual Environ.*, vol. 20, n° 2, p. 143-161, avr. 2011.

[Tin15] W. Tinsson, « La notion de plan d'expérience », in *Plans d'expérience: constructions et analyses statistiques*, vol. 67, Berlin, Heidelberg: Springer Berlin Heidelberg, 2010, p. 3-37.

[Fee16] P. Feenstra, R. van der Horst, B. J. C. Grácio, et M. Wentink, « Effect of Simulator Motion Cuing on Steering Control Performance: Driving Simulator Study », *Transp. Res. Rec. J. Transp. Res. Board*, vol. 2185, n° -1, p. 48-54, déc. 2010.

[Öst17] J. Östlund, B. Peters, B. Thorslund, J. Engström, G. Markkula, A. Keinath,, D. Horst,, S. Juch, S. Mattes, et U. Föhl., « Driving Performance Assessment—Methods and Metrics. », Report AIDE IST-1-507674-IP (D 2.2.5). European Union, 2005.

[Pre18] P. Pretto, H.-G. Nusseck, H. Teufel, et H. H. Bülthoff, « EFFECT OF LATERAL MOTION ON DRIVERS' PERFORMANCE IN THE MPI MOTION SIMULATOR », présenté à Proceeding of the Driving Simulation Conference 2009, Monaco, Europe, 2009.

[Fee19] P. Feenstra, M. Wentink, B. Correia Grácio, et W. Bles, « EFFECT OF SIMULATOR MOTION SPACE ON REALISM IN THE DESDEMONA SIMULATOR », présenté à Proceeding of the Driving Simulation Conference 2009, Monaco, Europe, 2009.

[Fil20] N. Filliard, B. Vailleau, G. Reymond, et A. Kemeny, « COMBINED SCALE FACTORS FOR LATERAL AND YAW MOTION RENDERING », présenté à Proceeding of the Driving Simulation Conference 2009, Monaco, Europe, 2009.

[Ben21] A. J. Benson, E. C. Hutt, et S. F. Brown, « Thresholds for the perception of whole body angular movement about a vertical axis. », *Aviat Space Env. Med*, vol. 60, n° 3, p. 205–213, mars 1989.

[Nes22] A. Nesti, C. Masone, M. Barnett-Cowan, P. R. Giordano, H. H. Bülthoff, et P. Pretto, « Roll rate thresholds and perceived realism in driving simulation », présenté à Proceeding of the Driving Simulation Conference 2012, Paris, France, 2012.

[Bri23] L. Bringoux, Sž. Schmerber, V. Nougier, G. Dumas, P. A. Barraud, et C. Raphel, « Perception of slow pitch and roll body tilts in bilateral labyrinthine-defective subjects. », *Neuropsychologia*, vol. 40, n° 4, p. 367–372, 2002.

COPING WITH COMPLEX DRIVING SCENARIOS: EXPLORATORY SCENARIO DESIGN

Julian Schindler 1, Tobias Hesse 1

(1) : German Aerospace Center, Lilienthalplatz 7, 38108 Braunschweig, Germany
+49-531-295-3510
{julian.schindler, tobias.hesse}@dlr.de

Abstract – The design of current scenarios in driving simulators can already be very challenging. It is assumed that new components of driving simulation, like coupling of simulators or the introduction and addressing of additional agents (e.g. pedestrians, cyclists or communicating infrastructure like Road Side Units) will aggravate this problem. Therefore, the issues of current scenario design have been analysed and recommendations have been extracted leading to a new suggested approach of scenario design. This new approach is driven by tools promoting the collaboration of the people involved in scenario design. Being part of a PhD thesis, this paper describes both the process and the needed tools, focussing on the operation of a multi-touch table guiding through the design.

Key words: Exploratory Scenario Design; driving simulation; collaborative platform, multi-touch table.

1. Introduction

Performing simulator studies in driving simulators is motivated by very different things, from functional testing via psychological testing to training or plain demonstration of technology. Driving simulators therefore make use of driving scenarios with different content, but mostly consisting of phases of free driving in traffic flows which should be as realistic as possible interrupted by phases with special behaviour of any involved agents. An agent could be movable like cars, trucks, cyclists or pedestrians, but also stationary like a traffic light or a Road Side Unit. The special behaviour of an agent, e.g. a strong braking of a car ahead of the ego vehicle, is used to force a special behaviour of the ego driver, e.g. by utilizing the function to be tested.

Olstam & Espié [Ols1] already described the alternation of the phases by introducing the Theater Metaphor, in which phases of "Everyday life" driving are interrupted by phases in which the automated road users have to follow certain manuscripts with special behaviour ("Play" on the "Stage"), see Figure 1.

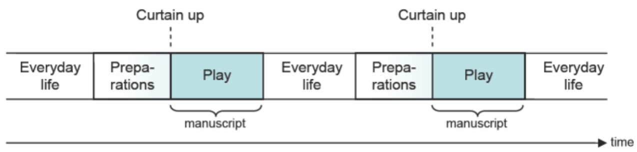

Fig. 1. Theater Metaphor by Olstam & Espié [Ols1]

In order to produce comparable results, the "Play" phases must consist of very well defined traffic behaviour leading to a strong behavioural restriction of all the involved agents, manifested in the presence of a manuscript. This contrasts to the mostly unrestricted "Everyday life" driving phases, in which all the agents may only be restricted in following road traffic regulations and optionally some additional advices by the study instructors like maintaining a minimum speed.

Therefore, a "Preparation" phase is needed used to migrate all acting agents from free driving to a well-defined starting behaviour, e.g. a defined position with a defined speed and acceleration, when the "curtain goes up" and the "Play" phase begins.

It is mandatory in the scenarios that these transitions have to take place unrecognizable by the ego driver, because the driver gets a pre-warning to the upcoming event when the behaviour of the involved agents changes too much or is not fully comprehensible to the ego driver. Therefore, the behaviour of the agents in the "Preparation" phases must be restricted as well, by providing limits of possible behaviours (e.g. a maximum acceleration) in the manuscript.

This results in manuscripts consisting not only of trivial information like the number of cars, used car models and the sometimes trivial special behaviour in the "Play" phases, e.g. the braking of a car ahead, but also consisting of fairly unknown parameters for the phase transitions in the "Preparation" phases and in some "Play" phases. Sometimes the value of parameters is unknown, but sometimes even selecting the right parameter is an issue. As a result, the parameters are frequently guessed, and therefore mostly not optimal. This introduces the following issues:

(1) The traffic situation and its parameters must be adapted iteratively in order to make a good look-and-feel.

(2) A wide range of situations must be tested to guarantee a smooth transition to the "Play" phases and the occurrence of the "Play" phases in any precondition.

In addition to this, scenarios are becoming more and more complex, as e.g. sophisticated Advanced Driver Assistance Systems (ADAS), the interaction between different kinds of agents or even the interaction between the drivers (and not the vehicles they are in) may be tested. Sometimes, on top of this, these tests also cover more complex sensor simulations, or Vehicle-to-Infrastructure/Vehicle-to-Vehicle (V2X) communication, probably resulting in additional complexity of the manuscripts.

As described in [Fis1], DLR's Institute of Transportation Systems (ITS) currently has many different simulators and test vehicles in service which may also be coupled so that various test drivers can participate in one scenario of the above mentioned complexity in the so called "Modular and Scalable Application Platform for ITS components" (MoSAIC). MoSAIC enables many new kinds of scenarios, but introduces the complexity of getting not only the automated agents to the correct positions and velocities in the "Preparation" phases, but also the human ones. As human drivers represent subjects in studies, they can mostly not be advised to follow many extra rules. Therefore, the human drivers have to be influenced by the surroundings, e.g. traffic lights, automated road users, or instructed human drivers, again resulting in a higher complexity of the manuscripts with lots of parameters not known in the beginning.

The problem now is that the scenario design process in companies or institutes in general, i.e. the process for specifying the manuscript, is very often not tailored for iterations or multiple test cases, esp. not in the case of rising complexity. Although there might not exist any specified process for this in many institutes or companies operating driving simulators, the generation of the manuscripts commonly follows a requirement-driven approach. This means, as shown in Figure 2, that the basic idea and the goals of a scenario are analysed in a first step in order to get a catalogue of requirements. The requirements are afterwards transferred into a rough plan of the scenario and the following creation of the 3D model and the implementation of the scenario. After the implementation, the scenario is getting tested. As this is a well-known procedure in other disciplines like systems or software engineering, it can be found that there are many parallels to common process models, esp. the Waterfall Model [Roy1]. The only main difference to this model is that refinements can be done by restarting any of the phases directly instead of moving up phase by phase. In addition to the often criticised linearity of this model, e.g. by [Liv1] or [Boe1], scenario design is very often challenged by the existence of two parties: One party – mostly consisting of people from the domain of psychology (esp. when performing psychological studies) – is analysing the needs of the scenario and describing the requirements of it. In the following, we therefore call this party the "requesters". The other party is responsible for the implementation (the "implementers") and therefore this party consists of people trained in the operation of manuscript editors or driving simulators. So both parties may lack a lot of knowledge of the other party, often leading to the specification of incomplete requirements and to the implementation of scenarios not complying with the initial needs.

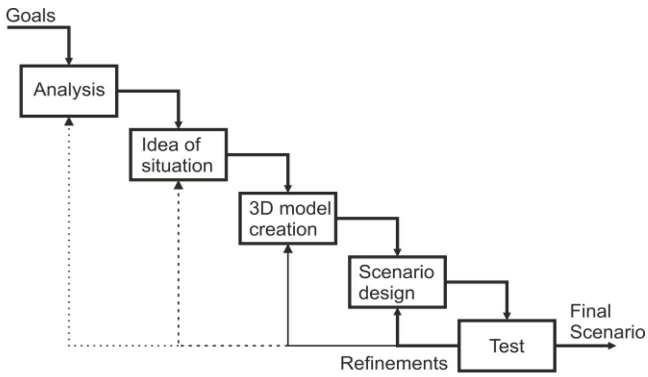

Fig. 2. Waterfall-like approach of common scenario design

As a result, the testing of the scenario script very often fails, and large refinements of the scenario design have to be performed. Due to the waterfall-like structure of the process, these refinements are expensive and time consuming. Catalogues of requirements have to be adapted, the meaning of situations have to be explained.

There are several possibilities to cope with the occurrence of these iterations: On the one hand by changing the process and on the other by using proper tools. This paper addresses both, by introducing a new scenario design process and tools for enabling it.

2. Ideas for a better process

As mentioned before, the missing tailoring to possible iterations is not a new phenomenon, but has been widely discussed in systems or software engineering. So it is not surprising that various approaches exist for solving this issue, e.g. prototyping [Flo1 or Ril1] or the spiral model of Boehm [Boe1] (which is also based on the prototyping approach).

In prototyping, the goal is the creation of horizontal prototypes (e.g. mock-ups without function) or vertical prototypes (e.g. parts of the complete target system) which can be tested by users before the complete system has to be built. Furthermore it describes how to get closer to a final product, e.g. by rapid, evolutionary or incremental prototyping [Ril1].

Adapted to the scenario design this means that the target scenario needs to be decomposed into smaller parts, which can be implemented in a prototypic way. As a "scenario mock-up without functionality" can only be hardly imagined, we classify scenario prototypes as vertical prototypes. They therefore represent a part of the whole scenario, e.g. one special situation during one "Play" phase. The kind of the prototypes may be rapid (meaning that a developed prototype may be thrown away after instantiation) or evolutionary (meaning that a developed prototype will get more and more precise in each iteration). As a result, several prototypes may exist for the several parts of the scenario which can be merged into one scenario as done in the incremental prototyping [Ril1].

One major problem of scenario design is that parameters like acceleration or time-headways, or the limits of parameters, very often must be guessed or approximated iteratively, as their effect can only hardly be imagined. A misfit can only be recognized when testing the prototype in action. The same is true for the creation of a good look-and-feel in the "Preparation" phases, where a wide range of initial conditions has to be tested. In some situations not only the approximation of the value of any parameter, but the choosing of the correct parameter itself is already challenging. Both aspects in general are addressed in the field of exploratory research [Ste1]. This research has also been applied to the development of ADAS as "exploratory design"; see [Fle1] or [Sch2]. In the exploratory design, the complete space of design possibilities, the "Design Space", is reduced systematically in iterations in order to find an optimal design. It makes use of a method called the "integrated testing" where design alternatives get tested step by step by driving in a simulation before any line of code has been written.

It therefore makes use of a tool called the "Theater System" [Sch1], in which one ADAS designer playing the role of a potential user of a future ADAS is sitting in a simulator with active inceptors (steering wheel, pedals or side-sticks). The active inceptors are coupled to a second set of inceptors, operated by another designer playing the system, the so called *confederate*. The confederate now can directly ask how e.g. a haptic feedback should feel like while driving through the situation. As the inceptors are coupled, the driver can directly feel the actions of the confederate. Iteratively the designers may also change their roles and can therefore express their intentions directly. When a good solution has been found for any tiny step, this step is implemented quickly, and directly validated in the simulation. Thanks to tool support the implementation can be done (mostly) in seconds, so that crisp ADAS designs can be reached very fast.

The approach of integrated testing would strongly benefit the scenario design, as it enables quick iterations of prototyping with high performance and emerging scenarios of high quality.

Nevertheless, the general prototyping approach only describes how to get to a final product in smaller iterative steps, but it does not define the means used for the creation. As described, there often are two parties involved in the scenario design process, the "requesters" and the "implementers", both often with different backgrounds. Bringing both parties closer to each other would largely benefit the design process. The party of the "requesters" can be seen as "users" in a wider sense, as they want to use the scenario for the performing of their studies. Therefore, when using the term of "user", an analogy to systems engineering can easily be found, esp. by looking at Participatory Design (PD) [Ken1], where users are directly integrated in the design of systems. This has already been done in ADAS design by the “Theater System”, as a potential user can directly participate instead of a designer playing the role of him. As the changing of the roles is still possible, the designer is able to directly feel the interaction a potential user has in mind.

The participation of the “users” is a very valuable step in systems engineering. Nevertheless, it is criticised to be possibly ineffective, as the users cannot be professionals and therefore lack knowledge and tend to reinvent the wheel. Kensing and Blomberg [Ken1] state that “…design professionals need knowledge of the actual use context and workers [i.e. users in this context] need knowledge of possible technological options”.

Applied to scenario design user participation as stated in PD would mean to simply let the psychologist create the scenario alone. Although scenario design has changed a lot in the last years from plain scripting to the common use of scenario editors with Graphical User Interfaces (GUI), using those tools and knowing about all the implemented features is still not fully intuitive and needs to be trained. So indeed this option would be ineffective.

The ineffectiveness in general is a well-known problem already addressed in systems engineering, e.g. in the Cooperative System Development Process (CESD) [Gro1], where “existing technological concepts and systems […] can be brought in as thought-provoking artefacts in cooperative workshops extending the participants’ understanding of alternatives as well as current practice”. Applied to scenario design this would mean to show the users the alternatives they have when designing the scenario.

But Grønbæk et al. [Gro1] also go a little further: “To design cooperatively, to develop visions of technology in use, it is important to give these visions a form that allows users to apply their knowledge and experience as competent professionals in the process.”

Kensing and Blomberg [Ken1] therefore interpret the mentioned form as the requirement of “access to adequate prototyping tools” leading to the statement that “the development of tools and techniques is a key focus for PD projects”. Applied to the scenario design this means that using special tools beyond any GUI scenario editor may enable a better cooperation between professionals and users, i.e. implementers and requesters. Proper Tools may benefit the whole process of scenario generation. These tools should bring the requester and the implementer closer together so that on the one hand the requester understands which possibilities and short-cuts exist when designing scenarios and on the other hand the implementer gets a better understanding of the broader context of the scenario and the reasons for the specified requirements.

Ideally, these tools will also support the former mentioned approach of integrated testing.

In summary, a new process for scenario design therefore should cope with the following three basic recommendations for complex scenario design:

(1) Prototypes for each part of a scenario should be created instead of complete scenarios
(2) Prototypes should be created in quick iterations, best in a form of integrated testing, as this enables the exploration of various parameters and alternatives, promising scenarios of high quality.
(3) Requesters of the scenario should participate in the scenario design actively, best by cooperating directly with the implementers. This is reached by the introduction of proper tools.

One suggestion for such a scenario design is described in the following.

3. The Exploratory Scenario Design Process

The Exploratory Scenario Design Process as shown in Figure 3 starts in the same way as regular processes, i.e. by the initial definition of the goals of the target scenario. These goals then have to be transformed into a rough idea, how a test scenario might look like. The transformation is done in an analysing phase by a decomposition of the goals into use cases, user stories and single requirements. In this context, use cases describe the general situation, e.g. being on a two-lane highway with a speed limit of 120 km/h and mixed traffic of low density.

User stories than describe the individual things happening in the use cases, e.g. a close overtaking of a slower truck when there is upcoming traffic in the blind spot of the ego car. Each “Play” phase consists of one or more consecutive user stories.

In this example, an emerging requirement would be that there is a slower truck in the lane of the ego car. Another would be that in that precise moment there has to be another car in the blind spot.

When the requirements have been specified, they are transferred into a basic idea of how the final scenario might be composed. Afterwards, a phase of preparation is started. In this phase, e.g. the 3D model of the virtual landscape is generated and a set of road users of the needed type and density is provided to the streets in order to make the desired look-and-feel of everyday life situations.

The resulting basic scenario is afterwards set up in the simulator. In order to reduce artefacts of different simulators, the target simulator should be the one where the study will take place, if possible.

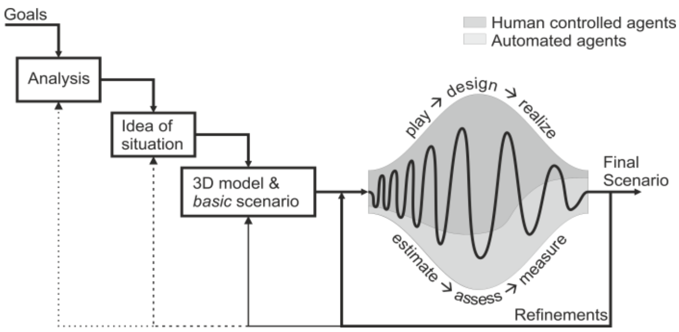

Fig. 3. Exploratory Scenario Design

As shown in Figure 3, at this point the integrated testing is started. As analogy to the "Theater System" approach when designing ADAS online in the simulation, the same can be done in the design of scenarios. The different agents involved in a situation can be controlled manually by connecting additional control entities like simulators or simple game wheels to the target simulator. In this way, humans play the interaction between the vehicles on the track before any single line of scenario code has to be written. When the involved persons agreed on a played situation, the scenario script is created directly from the manually driven test runs.

The exact procedure of the integrated testing in the scenario design is as follows:

First, the basic scenario is loaded and it is jumped to the time and/or place where the first "Play" phase is supposed to happen. Each of the agents which are going to play a specific role in the first user story of this phase, including the ego car in the targeted scenario and any other agent, is assigned to a manual driver and a control entity. One of the drivers may also be the requester of the scenario, who now has the direct ability to show his intentions. Afterwards, the scenario is started and the movements of all agents are recorded.

One special thing about the recording is that not only the trajectory of the agents is recorded but also events like indicator signals or inceptor movements. When a user story has been recorded, it can be replayed. The recording may be discarded and repeated when somebody (and esp. the requester) is not satisfied with the result.

In case of full satisfaction the recorded data is analysed by software. This step is necessary because a simple replaying of the trajectories during the study will not serve all possible behaviours of the ego drivers in the study. Just imagine a fast driving and a slow driving participant in a study: When cars simply follow trajectories the resulting situation will be completely different, as the behaviour of each agent has an impact on the behaviour of the others. Therefore, the data esp. of the movable agents must be brought to a more abstract level. This is done by categorizing the data into driving manoeuvres. Afterwards, the events not fully complying with the currently driven manoeuvre are marked. The manoeuvres and the marked events per agent are presented in form of a timeline of the run in a graphical way. An example for this with three agents is shown in Figure 4: All involved movable agents are classified as driving in the manoeuvre "follow lane" at the beginning (t_0). When the blue car – let us say18.3 meters in front of the red car - started to brake, the driver of the red car did a movement of the steering wheel resulting in a swerving of his car. The swerving does not comply with the manoeuvre and therefore it gets marked (the highlighted red area shortly before t_1). Afterwards, the red and green car continue driving, the blue one has stopped (t_2).

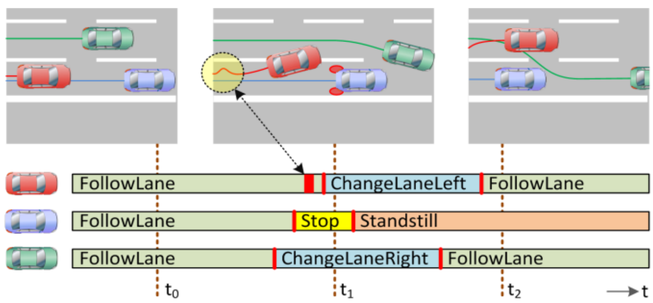

Fig. 4. Example of a scenario analysis output. Situations are marked where car behaviour changes. The upper images show how the situations and the just driven trajectories looked like at the given timestamps of t_0, t_1 and t_2. The yellow circle highlights a marked swerving situation just before t_1.

The people involved in the scenario design now have the direct ability to discuss the events. Events occurring unintendedly can be unmarked. All the other events have to be linked to triggers. Triggers can be any logical combination of one or more other events, manoeuvre changes or any thresholds of any other available parameter, e.g. distances/time headways/time to collisions to other agents or infrastructure, durations, indicator signals etc.

In the above example, the scenario designers may decide if the swerving has been intended or not. When it has been intended, it has to be linked to one or more triggers, possibly to the braking of the car ahead and the distance to it. Also the manoeuver changes have to be linked to certain triggers. Additionally, the triggers can be specified with tolerances or limits of thresholds. E.g. "braking" may be defined as "braking with more than 0.4g" or "distance" may be defined as "between 10 and 30 meters".

Furthermore, not only the trigger itself can be specified with tolerances; also the event happening because of the trigger may be performed with tolerances adapting to the surrounding. In the example, you may link the amplitude of the swerving to the width of the current lane. Another example would be the linking of the length of a triggered lane change (like the ones of the red and green car in the example) to the surrounding traffic situation.

The setting of triggers has to be done for all the not movable agents as well. Traffic light phases may be linked to events happening in the simulated world or simply to timing models.

The general advantage of the abstraction is that the intended behaviours of the agents can be separated from the unintended easily. The key-behaviour in the scenario is extracted and uncoupled from trajectories, allowing a range of initial situations to be tolerated for triggering. The abstraction of the situation furthermore enables the transferability of manually driven scenarios to automated car behavior, a necessary step for creating a script of the scenario. Driving the situation manually gives a good overview on the parameters to choose as triggers and their values.

Each user story of each "Play" phase, i.e. each situation or prototype, can be recorded consecutively in this way.

Nevertheless, sometimes situations occur, where more agents are involved than simulators or controllers are available. In this case, another way of scenario creation must be chosen, as parallel driving is not possible. This can be done by either manually script parts of the scenario so that some of the agents are controlled automatically, or by recording the behavior sequentially, or by switching between the currently controlled agents while recording.

When all situations of a scenario meet the requirements, the whole scenario script is generated, so that it can be used by single ego drivers. This procedure is also applicable for scenarios with multiple ego drivers or agents of different type.

In any case, a crisp scenario design will emerge after a short phase of preparation, as parameters and thresholds are not needed to be guessed, but are directly tangible in the simulation. Requesters of scenarios can directly feel how parameters must be chosen to create a desired output.

Therefore, the mentioned approach already copes with the three basic recommendations for complex scenario design. Nevertheless, it might be difficult for the design team to keep track on the proceeding of the scenario creation. Additionally, it would be beneficial if the scenario designers are able to discuss the recorded scenarios in detail in a collaborative way, something not so easy in the limited room available in some driving simulator cabins. Furthermore, not enough control entities might be available.

To account on these issues it is proposed to make use of an additional tool, described in the following.

4. A Multi-Touch-Table as central tool in the Exploratory Scenario Design Process

A new tool has been created to cope with the mentioned issues. It has been found (see [Sch3] for details) that the ideal basis for such a tool is a multi-touch-table showing bird views on the scenario. At DLR ITS an Ideum MT 55" Multi-Touch-Table with a maximum of 32 possible parallel touch points has been chosen for this task.

The software running on the table is a self-developed scenario editor with a graphical user interface focussing on maximum collaboration and intuitive control. In Figure 5, the table is shown running attached to the three small simulator entities of the DLR ITS MoSAIC Laboratory. Up to six bird-views of the situation are shown on the table in parallel, each of it centring on a freely selectable agent of the scenario. Each bird-view can be controlled by using standard gestures as known from current smart-phones, e.g.

zooming with two fingers moving away from each other, rotating with two fingers doing a circular movement.

Fig. 5. Scenario preparation around the Multi-Touch-Table at the DLR MoSAIC Lab

Additionally, it is possible to control the centred agents directly on the table. The controlling of movable agents is possible in three ways according to the three hierarchical layers of the driving task from Donges [Don1]: It is possible to specify and change the route of each agent (navigational layer), to change the actually driven manoeuver (guidance layer), and to directly control the movements of the agent (control layer). The route of each road user can be specified by dragging waypoints into the scenery. Manoeuvers are switched by selecting them in a small menu displayed near the car. The direct control is done in the following way as shown in Figure 6: first, one finger is put on the displayed agent who has to be controlled. Afterwards, another finger is put where it is supposed to head. This second point is also the neutral position for acceleration, so moving the fingers apart will accelerate the agent, moving them towards each other will cause deceleration.

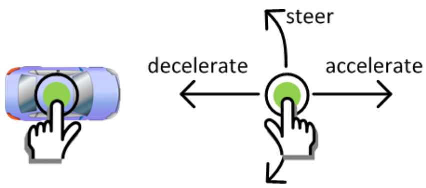

Fig. 6. Controlling a moving agent with touch gestures

Agents which are not movable are controlled similar as the controlling of manoeuvers, i.e. by small menus, e.g. showing the phases of the traffic lights.

Another aspect of the multi-touch table is that it allows the controlling of the scenario recording and basic functionality like 3D model loading, vehicle insertion etc. Therefore, dialog-boxes and menus are shown on the screen. Due to the fact that the designers are supposed to stand around the table, the position and even the orientation of the menus had to be freely adjustable. Because of this, each menu can be picked, rotated and resized with the former introduced gestures known from smart phone interaction. This makes it possible to work on a menu and to "hand it over" to another person on the other side of the table. As all the standard windowing toolkits (at least FLTK, GTK, QT) do not have the ability to perform such actions easily, it has been chosen to create a new toolkit based on osgwidgets, a part of OpenSceneGraph [Wan1]. The creation of the windowing toolkit has been discussed in detail in [Hes1].

The same menu structure can be used to directly access and manipulate all available parameters of the agents, e.g. by smoothing the recorded values, setting some initial speeds, selecting the 3D model of the agents, or by introducing threshold values etc.

Finally, the output of the scenario recording can be displayed similar to the example in Figure 4. As described, the manoeuvres and the events per agent are presented in form of a timeline of the run. The discarding, the setting of triggers of events or the modification can be done graphically on screen. The resulting script can be exported into a human-readable XML scenario script files and used for testing in the simulator.

The multi-touch table application is currently (May 2014) under development. The work on the windowing toolkit and the support of multi-touch gestures is already finished, the implementation of the scenario recording and analysis has just started and is targeted to finish by the end of 2014. Therefore, the approach of Exploratory Scenario Design has not been tested practically in any project, and there is currently no data on increasing efficiency available. As soon as the tool development is finished, the performance will be measured.

5. Conclusion

This paper has described the issues of current scenario design and the assumed aggravation of them in the near future. A new approach, the Exploratory Scenario Design, has been introduced which focusses on the direct integration of the people normally only creating requirements for scenarios into the process of the detailed design of the scenario itself. It has been shown that the methods of prototyping and "integrated testing" used in the Exploratory Scenario Design are strongly benefitting the design of complex driving scenarios in terms of time needed for the preparation and quality of the resulting scenario. Furthermore, the integration of a multi-touch table as central tool and enabling technology for the Exploratory Scenario Design has been introduced and described in detail, including some of the available multi-touch gestures.

The utilization of the design process, the methods and the proposed tools will enable the coping with complex driving scenarios of all kinds in the upcoming future.

6. References

[Boe1] Boehm, B.W. "A Spiral Model of Software Development and Enhancement" In: *IEEE Computer*, Vol. 21, Issue 5, pp. 61-72, 1988

[Don1] Donges, E. "Aspekte der aktiven Sicherheit bei der Führung von Personenkraftwagen". In: *Automobil-Industrie*, Volume 27, pp. 183–190, 1982.

[Fis1] Fischer, M., Richter, A., Schindler, J., Plättner, J., Temme, G., Kelsch, J., Assmann, D., Köster, F. "Modular and scalable driving simulator hardware and software for the development of future driver assistance and automation systems", Paper submitted to the *Driving Simulation Conference*, 2014.

[Fle1] Flemisch, F., Schindler, J., Kelsch, J., Schieben, A., Damböck, D. "Some Bridging Methods towards a Balanced Design of Human-Machine Systems, Applied to Highly Automated Vehicles"*. Applied Ergonomics International Conference*, Las Vegas (USA), 2008

[Flo1] Floyd, C. "A systematic look at prototyping". In: *Approaches to prototyping*. Springer Berlin Heidelberg, pp 1-18, 1984.

[Gro1] Grønbæk, K, Kyng, M., Mogensen, P. "Toward a Cooperative Experimental System Development Approach". In Kyng, M., Mathiasen, L. (Eds.): *Computers and Design in Context*, MIT Press, pp. 201-238, 1997

[Hes1] Hesse, S. "Development of a Graphical User Interface for the Explorative Design of Driving Scenarios", Bachelor thesis, 2014.

[Ken1] Kensing, F., Blomberg, J. "Participatory Design: Issues and Concerns". In: *Computer Supported Cooperative Work*, Vol. 7, Kluwer Academic Publishers, pp. 167-185, 1998

[Liv1] Liversidge, E., "The Death of the V-Model", 2005, Available at http://www.harmonicss.co.uk/index.php/hss-downloads/doc_download/12-death-of-the-v-model, Last accessed May 2014

[Ols1] Olstam J., Espié, S. "Combination of autonomous and controlled vehicles in driving simulator scenarios". In Andrea Benedetto (Ed.): *Advances in Transportation Studies*, University Roma Tre (21), pp. 23–32, 2010.

[Ril1] Riley, D. D. "Software Lifecycle Models". 2010, Available at cs.uwlax.edu/~riley/CS741Sum10/lectures/2_LifeCycles.pdf, Last accessed May 2014

[Roy1] Royce, W. "Managing the development of large Systems". In: *IEEE Wescon*, pp 1-9, 1970.

[Sch1] Schieben, A., Heesen, M., Schindler, J., Kelsch, J., Flemisch, F. "The theater-system technique: agile designing and testing of system behavior and interaction, applied to highly automated vehicles". In Albrecht Schmidt (Ed.): *1st International Conference on Automotive User Interfaces and Interactive Vehicular Applications*, pp. 43–46. 2009

[Sch2] Schindler, J., Temme, G., Schieben, A., Flemisch, F. "Exploratory design of a highly automated system for entering the expressway". In: de Waard, D., Axelsson, A., Berglund, M., Peters, B., Weikert, C. (Eds.): *Human factors. A system view of human, technology and organisation*. Maastricht: Shaker Publishing, pp. 201–216, 2010.

[Sch3] Schindler, J., Kelsch, J., Heesen, M., Dziennus, M., Temme, G., Baumann, M. "A Collaborative Approach for the Preparation of Cooperative Multi-User Driving Scenarios". In: *10. Berliner Werkstatt Mensch-Maschine-Systeme*, Berlin, Germany, 2013.

[Ste1] Stebbins, R. A., ed. "Exploratory research in the social sciences". Vol. 48, Sage, 2001.

[Wan1] Wang, R., Qian, X. „OpenSceneGraph 3 Cookbook", Packt Publishing, 2012.

EFFECTS OF HAPTIC VERSUS VISUAL MODALITIES WHEN COMBINED WITH SOUND IN FORWARD COLLISION WARNINGS

Mikael Ljung Aust[1]

(1) Volvo Cars Safety Centre
Volvo Car Corporation
SE-405 31 Göteborg, SWEDEN
Phone: +46 31 59 63 52
E-mail:
mikael.ljung.aust@volvocars.com

Abstract - The Crash Warnings Interface Metrics study showed that seat belt pretensioning in Forward Collision Warning (FCW) situations reduced driver response times significantly. This study examined whether that effect is limited to haptic belts, or is a general effect of haptic warnings. 48 participants received FCWs in critical lead vehicle braking situations while doing a visual distraction task. Three FCW types were tested. A warning sound was combined with either seat belt jerks, a brake pulse or a visual warning in a head up display. All FCWs made drivers abort the distraction task and look up. Furthermore, combining sound with seat belt jerks or a brake pulse lead to significantly faster response times than combining the sound with a visual warning. These results indicate that faster response times may be typical for haptic warnings in general. They also suggest that future FCWs should include a haptic modality to improve driver performance.

Keywords: forward collision warning, haptic warnings, driver distraction, brake response time, simulator event design

1 Introduction

For a Forward Collision Warning (FCW) system to be effective, the warning it issues has to (re)direct the driver's attention to the forward roadway and make him/her respond appropriately in typical pre-crash situations. Numerous studies have been carried out to understand the extent to which different FCWs succeed in doing so [Abe1, Abe2, Abe3, Che1, Jam1, Kra1, Sco1, Ler1].

One outcome of these previous studies is that presenting the FCW in more than one modality, for example by combing an auditory and a visual warning, elicits quicker responses than single modality warnings.

The question that follows is of course which modalities to combine. In a recent paper [Sch1], Euro NCAP indicated that it will require FCWs to be loud and clear, which suggests a combined auditory/visual warning. However, other combinations may elicit even quicker response times.

In the Crash Warnings Interface Metrics (CWIM) report [Ler1], all FCWs that included seat belt pretensioning gave faster driver responses than those that did not. However, as that study did not include other haptic alternatives, it was not possible to conclude whether this was a general effect of adding a haptic modality, or a specific effect of using seat belt pretensioning to warn.

The present study aimed to address this particular question, i.e. whether adding a haptic modality is generally beneficial or if the effects are limited to seat belt pretensioning only.

The study tested three different FCW types. All had the same auditory warning but differed in their additional modality. The first added seat belt pretensioning to the sound, the second a brake pulse and the third a visual warning in a head-up display (HUD).

One more topic, regarding response validity, was also addressed in the study. Among others, the recent 100 Car Naturalistic Driving study [Din1] has shown that real world situations where FCW would be useful, i.e. where emergency braking is required to avoid collision with a lead vehicle, typically occur very unexpectedly from the driver's point of view.

To properly replicate these real life scenarios in an experimental setting, and thus get a valid assessment of whether a particular FCW would help or not, each simulated critical event should therefore ideally come as a complete surprise to the test person. This is very difficult to achieve, and a key challenge for simulator study design [Lju1]. In the present study, the magnitude of potential expectancy effects was studied by including a second repetition of the critical scenario.

2 Method

A critical lead vehicle braking event including a visual driver distraction task was implemented in a moving-base simulator.

2.1 Participants

48 subjects, 15 women and 33 men participated in the study. All subjects had normal or corrected-to-normal vision, and had held a driver's licence for more than 5 years with a total driving experience of at least 50 000 km. All participants also had previous experience of the driving simulator, because they were recruited from a larger pool of previous participants. However, none of the subjects had previous experience of FCW, and they were not informed about there being FCW in the vehicle. Each subject was given 30 € for their participation.

2.2 The driving simulator

A high-end moving base driving simulator, located at VTI, Linköping, Sweden, was used. The vehicle mock-up was a Saab 9-3 Sport sedan MY 2003 with automatic transmission. The visual system consists of 3 DLP projectors (1280x1024 pixels) providing a 120 degrees forward field of view. Edge blending and geometrical correction is provided by a dedicated graphics card. There are 3 LCD displays incorporated into the rear view mirrors for rearward views. Sound from vehicles, road and wind is simulated and presented via the in-vehicle speaker system. The moving base has three parts: a linear sled, a tilt motion system and a vibration table. The sled can provide linear motion with an amplitude of ± 3.75 m at speeds up to ± 4.0 m/s and accelerations up to ± 0.8 g. The tilt motion system can produce pitch angles between - 9 degrees and + 14 degrees and roll angles of ± 24 degrees. The vibration table gives ± 6.0 cm in vertical and longitudinal movement, with a maximum roll angle of ±6 degrees and pitch angle of ± 3 degrees.

2.3 Event design

The lead vehicle braking event took place on a simulated 4-lane divided motorway with 2 lanes in each direction, in daylight conditions and with no precipitation (dry surface), with a moderate density of ambient traffic travelling in the opposite direction to the subject vehicle (henceforth referred to as SV), and some slower moving traffic travelling in the same direction as the SV. Subjects were instructed to maintain the posted speed limit of 90 kph. The lead vehicle in the two conflict scenarios (henceforth referred to as the Principal Other Vehicle, POV) was always of the same model and colour in order to keep brake light contrast constant.

The primary task was to drive on a motorway for approximately 30 minutes. The participants were instructed to drive as they normally would under similar circumstances and keep the speed limit (90 km/h). There was oncoming traffic at an average rate of three vehicles per minute and other cars overtook the participants once a minute on average. They also caught up with slower vehicles which they had to overtake on average once every two minutes.

A key goal for the study was to assess braking performance in kinematic conditions sufficiently critical to elicit true emergency braking reactions. As discussed at greater length in [Eng1], this is challenging since drivers tend to adapt their behaviour in anticipation of critical events.

For this study, a scenario previously shown to be effective in tricking subjects into violating their safety margins [Lju2] was used with slight modifications. The SV initially travels in the right lane at speed v_1 (self-paced). The POV overtakes in the left lane at speed v_2, and then at a time headway of 0.9 seconds moves back into the right lane. The POV then continues to move away from the SV at speed v_2 until it reaches a time headway of 1.5 seconds. Here, POV speed is first instantaneously set to SV speed minus 5 m/s, and then the POV brakes at a rate of 0.55 g. To keep the time from when the POV starts to change lanes until it is in braking position constant across variations in SV speed, the POV speed was continuously adjusted to a predetermined fraction (1.15) of SV speed.

2.4 Visual distraction tasks

To make the drivers look away from the forward roadway from time to time, they were from time to time instructed to carry out certain in-vehicle tasks, including phone dialling, radio tuning and changing the sound settings. A special visual distraction task from Ford's VIRtual Test Track EXperiment (VIRTTEX) [Lju2] was also used. In this task, drivers are prompted to read back a sequence of 5 numbers (randomized single digits between 1 and 9) appearing on a display positioned far down to the right (approximately 45 degrees down angle). Each number is shown for 0.3 seconds with 0.2 seconds of blank screen in between, creating a total task duration of 2.3 s. It was during this special task that the critical event was triggered. To motivate drivers to complete the numbers task, they were told that their responses would be randomly checked for correctness. Each task was initiated by a pre-recorded voice message instructing the driver task what to do and the details of the tasks.

Drivers were prompted to initiate a task on average once every 2 minutes of the drive. In the lead vehicle braking events, task initiation was automatically triggered based on POV position to ensure that the distraction task overlapped with the POV braking event.

2.5 The Forward Collision Warnings

The FCW was given in three ways, by combining a warning sound with either seat belt pretensioning, a brake pulse or a visual display. The belt pretensioning consisted of 5 belt jerks of 150 ms duration with 150 ms pause between each jerk. The visual warning was given by flashing a series of LED-lights mounted on the dashboard, projected upwards. When lit, the LEDs are not directly visible to the driver, but their light is reflected in the windscreen, conceptually mimicking the effect of flashing lead vehicle brake lights. Each visual warning consisted of six of 125 ms duration with 125 ms intervals in between. The auditory warning consisted of a sound very similar to the one developed in the CAMP project for FCW [Kie1], which is used in all Volvo Cars with FCW up to MY2013. The sound was presented at 74.5 dB A. The Brake Pulse took the form of a triangular deceleration pulse of 400 ms duration with a peak value of 2,2 m/s^2.

The study used the FCW warning algorithm described in [Jan1], which is similar to the improved CAMP algorithm [Kie2]. Due to the event dynamics described above, the triggering threshold was reached almost immediately upon POV brake onset. The FCW was thus issued on average 300 ms after POV brake onset.

2.6 Experiment design

FCW type was included as a between-subject variable while event exposure was a within subject variable. All subjects were exposed to two critical lead vehicle braking events that were intermingled with non-braking events, where a similar POV did overtake without braking, and non-critical braking events, where a similar POV overtook and then turned on the brake lights without decelerating, but the FCW was made to trigger anyway. There was a total of 24 events along the route. First came 15 non-braking events, then the first critical event. Then came two non-critical braking events intermingled with 5 non-braking events. Last, the second critical event occurred. The first three minutes of the drive did not include any events. The entire drive took 27 to 30 minutes to complete.

2.7 Dependent variables

A number of dependent variables were defined to characterise the process of responding to the braking POV. *Gaze Response Time* represents the time from POV brake onset to the first driver glance on the forward roadway, i.e. when the driver looks up from the visual distraction task screen. For eye-tracking, a four-camera system running Smart Eye Pro 5.9 was used.

Accelerator release time represents the time from POV braking onset until the driver has released the accelerator pedal fully. In this study, negative accelerator release times were allowed, to capture any expectancy effects especially in the second critical scenario.

Response time represents the time from POV braking onset to initiation of a driver response. Response times were determined by first calculating *Brake* and *Steer onset times*. The driver’s response time was defined as the shortest of these two times.

2.8 Procedure

To minimise any initial expectations of critical events, the subject was told that the purpose of the study was to collect general data on normal driver behaviour for later use in other projects. The subject was instructed to drive as s/he normally would, with no extreme manoeuvres, and to maintain the posted speed of 90 kph.

Before commencing the practice drive, the subject practiced all in-vehicle tasks until s/he felt comfortable doing them. Then followed a ten minute practice drive. The practice drive did not include any braking or steering events of critical character, only normal steering and two instances of normal braking to a full stop. Towards the end of the test drive the subject again practiced the secondary tasks, until s/he felt comfortable performing the task while driving.

After the drive, the experimenter revealed the true purpose of the study. Subjects were debriefed and an interview was conducted.

3 Results

Data was subjected to a 3*2 mixed ANOVA with Condition (FCW type) as between-subjects factors and Exposure (First and second critical event) as a within-subjects factor. Data was analyzed with the SPSS general linear model using type III sums of squares.

3.1 Response times

The average Gaze Response Time (GRT) was about 570 ms, and this was similar across all FCW types and events, i.e. there were no main effects of either FCW type or Exposure.

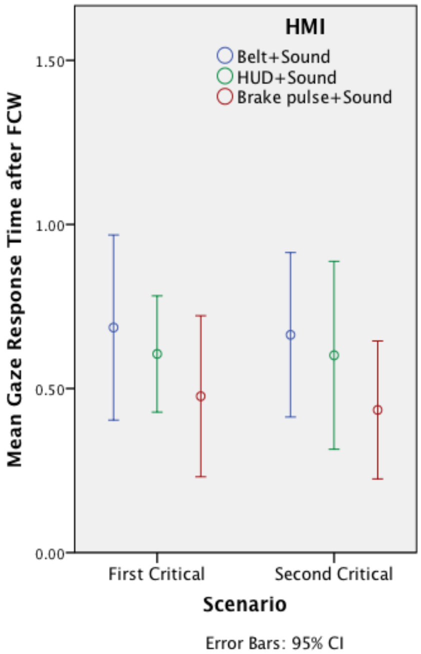

Figure 1: Average gaze response times per FCW type and scenario

There was a main effect of FCW type for Accelerator Release Time (ART) ($F(2, 44)=5.2$, $p=.01$). Pairwise comparison of the FCW types within each scenario showed that drivers with Belt/Sound warning and Brake Pulse/Sound warning released the accelerator approximately 300 ms faster than drivers with HUD/Sound in the first scenario, though these differences were not statistically significant ($p=.232$ and $p=.146$ respectively). In the second scenario, drivers with Belt/Sound were 350 ms faster than drivers with HUD/Sound ($p=.024$) and drivers with Brake Pulse/Sound ~280 ms faster than drivers with HUD/Sound (not significant).

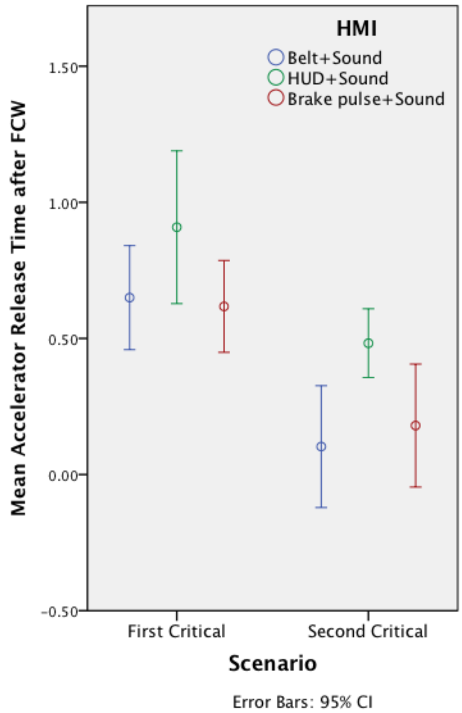

Figure 2: Average accelerator release times per FCW type and scenario

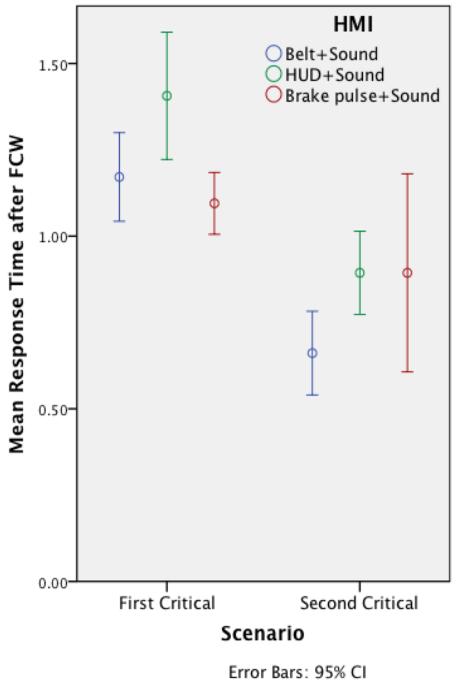

Figure 3: Average response times per FCW type and scenario

There was a main effect of FCW type for Response Time ($F(2, 43)=6.8$, $p<.004$). Response times were significantly reduced with ~440 ms in the second scenario ($F(1, 44)=44.9$, $p<.001$). Also, ART variability did increase with repeated exposure, due to occurrences of anticipatory responses (negative ART values).

Pairwise comparison of the FCW types within each scenario shows that drivers responded to both Belt/Sound and Brake Pulse/Sound approximately 300 ms faster than to HUD/Sound in the first scenario ($p=.016$ and $p=.024$ respectively). In the second scenario, drivers with Belt/Sound were 200 ms faster than drivers with HUD/Sound ($p=.024$) and drivers with Brake Pulse/Sound ~100 ms faster than drivers with HUD/Sound (not significant). Response times were also significantly reduced with ~440 ms in the second scenario ($F(1, 43)=137.9$, $p<.001$).

In terms of avoidance type, braking was the predominant maneuver. Only one driver did steer to avoid collision. Over the full event series, there was one collision.

4 Discussion

The results for GRT shows that all FCW types were effective in redirecting the driver's attention back to the forward roadway, i.e. all FCWs made the drivers look up from the visual distraction task. Regarding differences between the FCWs, the groups who received a haptic warning in combination with the sound both showed significantly faster response times than the group who got the auditory/visual warning.

This indicates that the faster driver responses with seat belt pretensioning found in [Ler1] may be typical for haptic warnings in general and may not restricted to seat belt pretensioning only. The response time difference found in this study is roughly of the same magnitude as found in [Ler1], so this study can be said to corroborate those findings.

This indicates an interesting route for future research, which is to go deeper into the possible underlying mechanisms whereby a haptic input leads to a faster "situation check" on behalf of the driver. It also suggests that future FCWs could benefit from including a haptic modality to improve driver performance even further.

The second topic for the study was to investigate whether a truly surprising event could be created. In the first scenario, when drivers looked back to the road after the warning, the situation was perceived as critical enough to elicit an emergency response, and the response time magnitudes are in line with those for really unexpected events [Gre1]. The scenario design thus was successful in creating a truly surprising event.

In the second scenario however, both RT and ART were significantly shorter, with magnitudes in line with those for drivers who know something will happen, but not what it is [Gre1]. The presence of negative ART values also suggest that some drivers began to adopt more proactive response strategy, e.g. releasing the accelerator already when the POV changed lane. The second event can therefore not be classified as truly surprising.

Two caveats regarding the study should be mentioned. First, drivers were not encouraged to practice braking in the test drive, to avoid inducing motion sickness. No artefacts were expected from this, as feedback from previous studies in this simulator indicate that braking is perceived as normal and realistic right from the start. However, the lack of braking practice may have influenced the results in some way.

Second, the drivers were completely naive to FCW, i.e. did neither know that the vehicle was equipped with a warning system nor had any previous experience with similar systems. This may not be fully realistic, since real-world drivers with FCW in their vehicles would have developed a stronger association between warning and response over time, and hence may respond faster or differently in this type of scenario.

5 References

[Abe1] Abe, G., & Richardson, J. (2005). The influence of alarm timing on braking response and driver trust in low speed driving. *Safety Science, 43*, 639-654.

[Abe2] Abe, G., & Richardson, J. (2006a). Alarm timing, trust and driver expectation for forward collision warning systems. *Applied Ergonomics, 37*, 577-586.

[Abe3] Abe, G., & Richardson, J. (2006b). The influence of alarm timing on driver response to collision warning systems following system failure. *Behaviour and Information Technology, 25*, 443-452.

[Che1] Cheng, B., Hashimoto, M., & Suetomi, T. (2002). Analysis of driver response to collision warning during car following. *JSAE Review, 23*, 231-237.

[Din1] Dingus, T. A., Klauer, S. G., Neale, V. L., Petersen, A., Lee, S. E., Sudweeks, J., Perez, M. A., Hankey, J., Ramsey, D., Gupta, S., Bucher, C., Doerzaph, Z. R., Jermeland, J., & Knipling, R. R. (2006). The 100-Car Naturalistic Driving Study, Phase II – Results of the 100-Car Field Experiment. In. Cambridge: U.S. Department of Transportation, John A.Volpe National Transportation Systems Center.

[Eng1] Engström, J., & Ljung Aust, M. (2011). Adaptive behaviour in the simulator: Implications for active safety system evaluation. In D. Fisher, M. Rizzo, J. Lee & J. Caird (Eds.), *Handbook of Driving Simulation for Engineering, Medicine and Psychology*: CRC Press.

[Gre1] Green, M. (2000). How long does it take to stop? Methodological analysis of driver perception-brake times. *Transportation Human Factors, 2*, 195-216.

[Jam1] Jamson, A. H., Lai, F. C. H., & Carsten, O. M. J. (2008). Potential benefits of an adaptive forward collision warning system. *Transportation Research Part C: Emerging Technologies, 16*, 471-484.

[Jan1] Jansson, J. (2005). Collision avoidance theory with application to automotive collision mitigation. Dept. of Electrical Enginering Univ., Linköping.

[Kie1] Kiefer, R., LeBlanc, D., Palmer, M., Salinger, J., Deering, R., & Shulman, M. (1999). *Development and validation of functional definitions and evaluation procedures for collision warning/avoidance systems*. Crash Avoidance Metrics Partnership, National Highway Traffic Safety Admin.

[Kie2] Kiefer, R., Shulman, M. A., Deering, R. K., Palmer, M. D., LeBlanc, D. J., Flannagan, C. A. C., & Cassar, M. T. (2003). *Forward collision warning requirements project: refining the CAMP crash alert timing approach by examining "last-second" braking and lane change maneuvers under various kinematic conditions*.

[Kra1] Kramer, A. F., Cassavaugh, N., Horrey, W. J., Becic, E., & Mayhugh, J. L. (2007). Influence of age and proximity warning devices on collision avoidance in simulated driving. *Human Factors, 49*, 935-949.

[Ler1] Lerner, N., Jenness, J., Robinson, E., Brown, T., Baldwin, C., & Llaneras, R., (2011) Crash Warning Interface Metrics Final Report. DOT HS 811 470a. NHTSA.

[Lju1] Ljung Aust, M., Engström, J., & Viström, M. (2013) Effects of forward collision warning and repeated event exposure on emergency braking. Transportation Research Part F: Traffic Psychology and Behaviour. Volume 18, Pages 34–46.

[Lju2] Ljung, M., Blommer, M., Curry, R., Artz, B., Greenberg, J., Kochhar, D., Tijerina, L., Fagerström, M., & Jakobsson, L. (2007). THE INFLUENCE OF STUDY DESIGN ON RESULTS IN HMI TESTING FOR ACTIVE SAFETY. In *20th International Technical Conference on the Enhanced Safety of Vehicles*. Lyon, France: National Highway Traffic Safety Administration.

[Sch1] Schram, R., Williams, A., Ratingen, M. (2013) Implementation of Autonomous Emergency Braking (AEB), the Next Step in Euro NCAP's Safety Assessment. Paper Number: 13-0269, proceedings of The 23rd International Technical Conference on the Enhanced Safety of Vehicles (ESV) Seoul, Republic of Korea, May 27-30, 2013.

[Sco1] Scott, J. J., & Gray, R. A. (2008). Comparison of Tactile, Visual, and Auditory Warnings for Rear-End Collision Prevention in Simulated Driving. *Human Factors, 50*, 264-275(212).

DRIVER DISTRACTION AMONG COMMERCIAL VEHICLE OPERATORS: A STUDY USING A DRIVING SIMULATOR TO ENHANCE CONTROL

Ronald W. Tarr[1] & Eric Paul Totten[2]

(1) : 3100 Technology Parkway, Orlando, FL. 32826; Institute for Simulation and Training
405-882-1391
rtarr@ist.ucf.edu

(2) : 3100 Technology Parkway, Orlando, FL. 32826; Institute for Simulation and Training
407-882-1323
etotten@ist.ucf.edu

Abstract – Driver distraction continues to be a topic that is regularly at the forefront of public discussion concerning safety on America's roads and highways. This paper reports the simulator application and experimental design for a study sponsored by the U. S. Department of Transportation's Federal Motor Carrier Safety Administration, which attempted to create a unique approach to studying driver distraction among CMV operators. The results of the study found that engaging touchscreen devices (MP3 players) led to over three times the level of cognitive distraction, while cell phones caused two to three times greater cognitive distraction than the baseline scenario. In addition, the study validated previous scholars' research claims about the usefulness of driving simulators and provided next steps for future research efforts.

Key words: Distracted Driving, Driving Simulation, Commercial Motor Vehicles

1. Introduction

This paper explores a study performed at the University of Central Florida's Institute for Simulation and Training. This study developed a method for quantifying how different distractors affect driving performance. The researchers specifically measured changes in driving performance resulting from internal and external distractors to the vehicle. This study uses two different electronic devices as internal distractors and when external distractors were present, researchers used three types of external distractions—two work zones and an accident—to affect the driving performance of CMV Operators. The following sections will describe the developed research methods and the utilized distracted driving performance measures.

2. Background

Distraction was identified by the U.S. Department of Transportation in the late 1970s as a "contributing factor to motor vehicle crashes in reviews of accident causation" [Tre1, Zai1, Jon1]. In 2000, the National Highway Traffic and Safety Administration (NHTSA) expanded on this assertion with updated studies employing advanced statistical and technological analysis. The NHTSA went as far as to say that, "driver inattention is one of the most common causes of traffic crashes" [Ran1]. The level of distracted driving related crashes remains consistent over the past two decades. Articles from over a decade ago attempted to place the number of reported crashes caused by driver distraction to be around 25% of all accidents [Zai1, Ran1]. with other works asserting the number is between 35-50% [Sus1, Wan1].

Different avenues of research into distracted driving abound such as analytical statistical investigations of crash reports, naturalistic, and simulation-based studies. These research methods produced a greater understanding of the three main types of distractions that occur while operating a motor vehicle: visual, cognitive, and manual. Visual distraction is any observation that takes your attention off the task of driving. Cognitive distraction is mental processes that distract you from driving and slows your reactions. Lastly, manual is any action that takes your hands off the wheel. Numerous studies point out that all of these distractions reduce driving performance, leading to traffic collisions [Cai1, Hor2, Str1, Str2, Str3, Str4].

Virtual reality investigatory approach became more common a decade ago and uses driving simulators to place participants in realistic yet safe experiments. Driving simulators are able to prompt participants with multiple distractions in an unlimited number of environments, without exposing participants to actual dangerous situations. Works involving driver simulators proved the viability of using simulators as a tool to view risky behaviour among participants [Gre1, Fis1, Pra1, Cha1, Mut1].

3. Methods

The research team conducted the project with 27 Commercial Motor Vehicle (CMV) operators as our participants. All participants were required to have their Commercial Driver's License (CDL) a minimum of two years. Unexpectedly, the participants on average had their CDL's for twenty years. Subsequently, the participants had over a combined 500 years of driving experience. The participants had an average age over 35 years old, consisted primarily of male drivers, and employed by a variety of companies in the greater Central Florida area.

4. Measures

The researchers used five measures to analyse the participants driving performance. The driving performance measures were: hazardous speed, dangerous braking, collisions, lane deviations, and off road. Each occurrence of the aforementioned measures counted as one performance error point. Tabulating each type of five measures separately, researchers summed the five measures into a total performance error for each scenario per participant. The measures were dictated by the legal definitions found in the 2012 Florida Drivers Handbook [Fla1].

Researchers also included a demographic and study experience survey to catalogue participants' reaction to the simulation.

5. Equipment

5.1. Driving Simulator

Since the participants in this experiment were highly trained and experienced professionals, the research team decided to use a high fidelity driving simulator to provide realistic feedback. The driving simulator used was the L-3 Mark III, which features a motion platform with six degrees of freedom, two LCD side mirrors, and three projectors creating life size images in front of the fully functional truck cabin. The simulator's high fidelity combined with the safety procedures allowed for a low rate of simulation sickness among this group of experienced professionals.

5.2. Hand-Held Devices

All participants used the same touchscreen Mp3 player, which researchers provided. To mitigate any confounds that might arise from varying touchscreen Mp3 players; the researchers preloaded an iPod Touch. This touchscreen Mp3 player was loaded with a variety of song tracks and organized them into specific playlists. In scenarios 3 and 7, participants followed embedded instructions from the songs, which told the participants various tasks to perform on the Mp3 player. In scenarios 4 and 8, participants selected from a set of songs to have playing during the experiment. The demographic survey asked a several questions, which allowed researchers to determine each participant's familiarity. In the results section, the researchers discuss the effect of iPod ownership within the sample.

This study also required the use of a cell phone and since participants were already learning to manipulate the touchscreen Mp3 player, researchers allowed them to use their personal cell phone. All of the participants used only the phone function of the cell phone in this research. Researchers did not allow participants to use "hands free" devices, Bluetooth, or phone accessories in this research. Participants made phone calls to the researchers, and other times the participants received phone calls from the research team at predetermined positions.

5.3. EEG/ECG

To assist in further study of the experimental scenarios, the research team used a ten channel dual machine "B-Alert" Electroencephalogram (EEG) and Electrocardiography (ECG) made by ABM. The data and findings from this equipment will be addressed in another paper.

5.4. Video Recordings

To capture the driving performance of the participants the research team recorded several videos for each scenario. The cameras recorded a video of the participants inside truck cabin and a video of the room surrounding the simulator while driving. Additionally, the research team recorded a helicopter view of the participant's truck inside the computer simulation. The researchers used these videos to obtain the participants performance error scores.

The researchers digitally recorded videos of the experiment to a secure drive to promote green and sustainable research. The videos were all simultaneously recorded in real-time and saved between scenarios. This allowed the research team to see and hear the participants during the entire experiment. To communicate with the participants the research team used a strategically placed hand radio to give instructions. The cameras and radio functioned as an intercom system, which also increased the study's safety protocol for the drivers. A team member was standing by at the back of the room to render immediate assistance as added safety.

6. Design

The research team developed computer simulations in L-3 Scenario Builder for the experimental scenarios. Each of the eight scenarios simulates the same stretch of a highway with additional traffic present but none entering or exiting the roadway. To minimize fatigue, each scenario contained only two distraction areas. Researchers would implement the variables only within these three separate areas on the highway. The external distractions included common aspects of work zones with different looking traffic. The participants began by merging onto the highway, which was always in the same direction to preserve the same level of task complexity. To keep the effect of the external scenes balanced the number of stationary vehicles, moving vehicles, lights, and pedestrians were equal in both kinds of work zones. The work zones used features observed from real scenes that follow in accordance with Florida State law. The MPH was displayed on screen, and collisions resulted in a temporary text notification on the screen and driving continued.

Table 1: Scenario Configuration

	Distraction Area 1	Distraction Area 2
Scenario 1 (Control)	➢ No external distractors ➢ No internal distractors	➢ No external distractors ➢ No internal distractors
Scenario 2	➢ No external distractors ➢ Received Phone Call	➢ No external distractors ➢ Returned Phone Call
Scenario 3	➢ No external distractors ➢ Active Mp3 use only	➢ No external distractors ➢ Active Mp3 use only
Scenario 4	➢ No external distractors 1. Silenced Mp3 music 2. Received Phone Call 3. Resumed Mp3 music	➢ No external distractors 1. Silenced Mp3 music 2. Received Phone Call 3. Resumed Mp3 music
Scenario 5	➢ Work Zone (construction)2 ➢ No internal distractors	➢ Work Zone (vehicle accident)1L ➢ No internal distractors
Scenario 6	➢ Work Zone (construction)1R ➢ Received Phone Call	➢ Work Zone (vehicle accident)1L ➢ Returned Phone Call
Scenario 7	➢ Work Zone (construction) 1L ➢ Active Mp3 use only	➢ Work Zone (construction)2 ➢ Active Mp3 use only
Scenario 8	➢ Work Zone (construction)1R 1. Silenced Mp3 music 2. Received Phone Call 3. Resumed Mp3 music	➢ Work Zone (construction)1L 1. Silenced Mp3 music 2. Returned Phone Call 3. Resumed Mp3 music

7. Results

The data summary includes an analysis of the survey data and driving performance error data. Participants filled out a demographic survey at the beginning of the experiment. The demographic survey gathers relevant characteristics about the participants. This includes driving experience and experience with the internal distraction devices. Additionally, researchers administered a repeated Participant Assessment Survey to obtain feedback about the experiment.

These surveys showed that participants enjoyed the experience and felt immersed in the simulation due to the fidelity of the experiment.

Previous studies, like Chisholm and Horrey's works, show that touchscreen Mp3 players and cell phones [Chi1, Hor1, Hor2] are detrimental to driver performance and attention. In this study, researchers expressed decreases in participants' performance as increases in performance errors.

Hypothesis-1: Distractions will, on average, cause a significantly higher number of driving errors than when no distractions are present.

Hypothesis-2: Multiple distractions will cause significantly more errors on average.

Hypothesis-3: Internal distractors such as the cell phone and Mp3 player will cause significantly more driving errors than external distractions such as work zones.

8. Data Analysis

To guard against practice effects, learning curve, or fatigue, the researchers randomized the sequence of the scenarios for each participant in order to counterbalance the study. The research team established a naming convention of "Run number" that represents the order of the scenarios. Each participant started the experiment on Run 1 and ended on Run 8, although to the research team each run was a different scenario. To keep track of which scenario was happening and in what order, the team created a table style list for each participant. These tables listed the run numbers sequentially and aligned them with the corresponding scenarios.

Multiple t-tests compared the chronological sequence of the scenarios. Researchers wanted to see if there is any significant difference, increase, or decrease in the average of errors between run 1 through run 8. For instance, the tests results show that there is no sufficient evidence to conclude that the total average of errors in run 1 and run 8 are statistically different (t-value=-1.17, p-value=0.249), neither increased from run 1 to run 8 (t-value= -1.17, p-value=0.124) nor decreased from run 1 to run 8 (t-value= -1.17, p-value=0.876). The results delineate the availability of a significant fatigue bias or a learning factor. The average number of errors per run is shown in FIGURE 1.

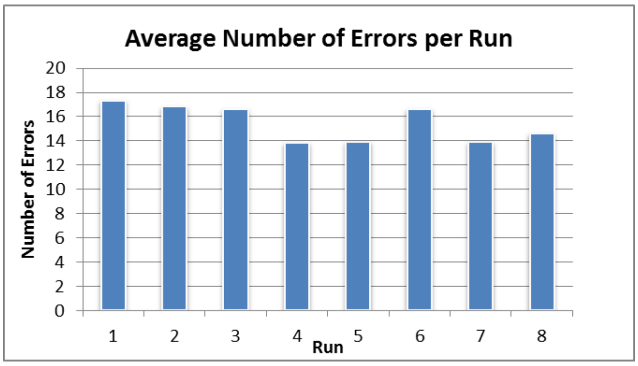

Figure 1: Average Number of Errors per Run

Scenarios 2-8 contained the three distracting factors (cell phone, touchscreen Mp3 player, and an external events) and their combinations. FIGURE 2 is a bar graph of the average of the total number of driving errors per scenario and variance.

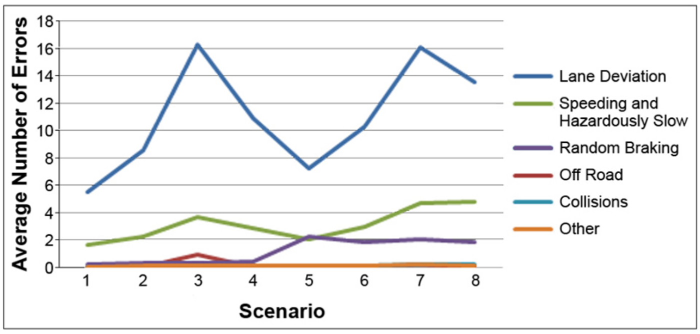

Figure 2: Average Total Errors per Scenario

Before comparing the scenarios, a review of the residuals showed the data after a natural logarithm transformation follows a normal distribution. A multiple one way within subject ANOVA tested for the existence of a significant difference between the eight scenarios. The ANOVA results revealed that at least one scenario was significantly different from the rest of the scenarios (F-value=25.23, p-value=0.000).

Knowing there are some statistical differences within the data set, several comparisons of the eight scenarios were conducted for significances. To account for the overall probability of type I error, multiple Tukey's test comparisons were employed on a 95% confidence level, the results were as follows:

Hypothesis-1 is supported by comparisons one through eight, which means every distractor, internal and external, caused a significantly higher average number of driving errors than driving without a distractor.

Hypothesis-2 is inconclusively supported by comparisons nine, ten, and eleven, meaning the presence of multiple distractors does not always result in more distraction.

Hypothesis-3 is inconclusively supported by comparisons twelve, thirteen, and fourteen, meaning internal distractors are not always higher than internal distractors.

9. Discussion

Compared to scenario 1, all distractors including the combination of distractors (scenarios 2-8) resulted in significantly more errors during the driving task. This suggests that compared to having no distractors, driving errors will increase with the addition of a cell phone, Mp3 player, external event, or any combination of the three. Moreover, in scenario 3 and 7, participants were required to interact actively with an Mp3 player, as opposed to simply listening or turning the volume up and down. The sustained use of an Mp3 player showed the highest error rates. Researchers have attributed these deficits in driving performance to the prolonged glances away from the road required to manipulate an Mp3 player [Chi1, Din1]. Additionally, this finding is congruous with previous research that more complex Mp3 player tasks decrease driver performance when compared to less complex Mp3 player tasks [Chi1].

This study was not without complications and challenges. One such limitation was the inability to garner a larger sample size of commercial motor vehicle operators. Expert drivers in the field are limited in number and their time is expensive. Additionally, representatives from the Florida Trucking Association expressed concern over possibility of negative consequences to the industry participation associated with academic studies. Though a few participants had only two years of driving experience, the average years of experience across participants was twenty years. Despite the variance, results from the control scenario (scenario 1) were similar, validating that the expertise of the sample group was homogenous. In addition, this effort was proposed as a two year effort but due to contract issues, it was only granted 13 months, resulting in limited outreach and follow up effects of driver awareness.

10. Conclusion

It should be noted that many studies have questioned the viability of using simulators when the topic concerned driver training, distracted driving, and other topics. Chan et al., noted.

"Simulators measure driving performance, what the driver can do. However, safety is determined primarily by driver behaviour of what a driver chooses to do. It is exceedingly unlikely that a driving simulator can provide useful information on a driver's tendency to speed, drive while intoxicated, run red lights, pay attention to non-driving distractions or not fasten a seat belt [Cha1]."

Although this study measured the CMV operator's performance, there is a high correlation between what drivers can do versus what they choose to do [Cha1]. This study focused on what professional drivers can do while behind the wheel of a motor vehicle. To influence and change behaviours' of a driving community, the authors believe that distracted driving studies should be accompanied by awareness campaigns that include outreach to influence not just CMV operator behaviour but the general public as well. This study showed that very experienced drivers are clearly distracted by such behaviours/events, even though many people believe they can do these things and NOT be distracted adversely.

The experiment was conducted in a safe, controlled environment, which compared the effect of being distracted to the non-distracted scenario. The team found that manipulating a touchscreen Mp3 player device is approximately three times more distracting among CMV operators. In addition, the team found that engaging with multiple tasks while driving is approximately two to three times more distracting than non-distracted driving among CMV operators.

The results of this investigation have shown that the use of a cell phone, the use of a touchscreen Mp3 player, the presence of external distraction, or any combination of the three causes increases in driving performance errors. Performance measures suggested the largest performance deficiencies come from actively using a touchscreen Mp3 player. This study combined aspects of previous experiments expressed in the literature review and focused on a key demographic. The combined aspects of the previous research were the most relevant to the studied demographic, which ensured that the project would be as realistic and useful as possible. The challenge of distracted driving continues to be a concern for overall traffic safety. As such, additional research is strongly encouraged.

11. References

[Cai1] Caird, J.K., Willness C.R., Steel P., & Scialfa., C. (2008). A meta-analysis of the effects of cell phones on driver performance, Accident Analysis and Prevention, 40, 1282-1293.

[Cha1] Chan, E., Pradhan, A. K., Pollatsek, A., Knodler, M. A., & Fisher, D. L. (2010). Are driving simulators effective tools for evaluating novice drivers' hazard anticipation, speed management, and attention maintenance skills? *Transportation Research Part F* 13, 343-353.

[Chi1] Chisholm, S. L., Caird, J. K., & Lockhart, J. J. (2008). The effects of practice with MP3 players on driving performance. *Accident Analysis and Prevention*, 40(2), 704-713.

[Din1] Dingus, T. A., Antin, J. F., Hulse, M. C., & Wierwille, W. W. (1989). Attentional demand requirements of an automobile moving-map navigation system. *Transportation Research Part A*, 23A(4), 301–315.

[Fis1] Fisher, D. L., N. E. Laurie, R. Glaser, K. Connerney, A. Pollatsek, S. A. Duffy, and Brock, J. (2002). Use of a fixed-base driving simulator to evaluate the effects of experience and PC-based risk awareness training on drivers' decisions. Hum Factors 44(2):287-302.

[Fla1] Florida Department of Highway Safety and Motor Vehicles, Florida Driver's Handbook (2012) Accessed June 1, 2012, http://www.flhsmv.gov/handbooks/EnglishDriverHandbook.pdf

[Gre1] Greenberg, J., Tijerina, L., Curry, R., Artz, B., Cathey, L., & Kochhar, D. (2003). Driver distraction: Evaluation with event detection paradigm. *Transportation Research Record: Journal of the Transportation Research Board* (1843), 1-9.

[Hor1] Horrey, W. J., & Wickens, C. D. (2006). Examining the impact of cell phone conversations on driving using meta-analytic techniques. *Human Factors*, 48(1), 196-205.

[Hor2] Horrey, W. J. & Wickens, C. D. (2007). In-vehicle glance duration: Distributions, tails and a model of crash risk. Transportation Research Record, 2018, 22-28.

[Jon1] Jones, J. L. (2010). Traffic crash statistics report 2009: A compilation of motor vehicle crash data from Florida crash records database. Florida Highway Safety and Motor Vehicles. Tallahassee, FL. http://www.flhsmv.gov/hsmvdocs/CS2009.pdf

[Mut1] Muttart, J. W., Fisher, D. L., Knodler, M., & Pollatsek, A. (2007). Driving without a clue: evaluation of driver simulator performance during hands-free cell phone operation in a work zone. *Transportation Research Record: Journal of the Transportation Research Board*. 2018(9-14).

[Par1] Parker, Jr., M. R. (1997). Effects of Raising and Lowering Speed Limits on Selected Roadway Sections. Publication No. FHWA-RD-97-084. U.S. Department of Transportation, Washington D.C.

[Pra1] Pradhan, A. K., Hammel, K. R., DeRamus, R., Pollatsek, A., Noyce, D. A., Fisher, D. L. (2005). Using eye movements to evaluate the effects of driver age on risk perception in a driving simulator. Human Factors, 47 (4), 840-852.

[Ran1] Ranney, T.A., Mazzae, E., Garrott, R., Goodman, M.J. (2000). "NHTSA Driver Distraction Research: Past, Present, and Future." Washington D.C.

[Str1] Strayer, D. L. & Johnston, W. A. (2001). Driven to distraction: Dual-task studies of simulated driving and conversing on a cellular phone. Psychological Science, 12(6), 462-466. http://www.psych.utah.edu/AppliedCognitionLab/PS-Reprint.pdf

[Str2] Strayer, D. L., Drews, F. A., & Johnston, W. A. (2003). Cell phone-induced failures of visual attention during simulated driving. Journal of Experimental Psychology: Applied, 9(1), 23-32. http://www.cellphonefreedriving.ca/media/failures_of_visual_attention.pdf

[Str3] Strayer, D. L. & Drews, F. A. (2004). Profiles in Driver Distraction: Effects of Cell Phone Conversations on Younger and Older Drivers. Human Factors: The Journal of the Human Factors and Ergonomics Society, 46(4), 640-649. http://trb.metapress.com/content/d1m049h9745u0qh8/fulltext.pdf

[Str4] Strayer, D. L. & Drews, F. A. (2007). Cell phone-induced driver distraction. Association of Psychological Science, Vol. 16, No. 3, 128-131.

[Sus1] Sussman, E. D., Bishop, H., Madnick, B., & Walter, R. (1985). Driver inattention and highway safety. Transportation Research Record, 1047, 40-48.

[Tre1] Treat, J. R., Tumbas, N. S., McDonald, S. T., Shinar, D., Hume, R. D., Mayer, R. E., Stansifer, R. L., & Castellan, N. J. (1979). Tri-Level study on the causes of traffic accidents: Final Report, Volumes I and II. U.S. DOT HS-805-086, (NTIS PB 80-121064).

[Wan1] Wang, J., Knipling, R. R., & Goodman, M. J. (1996). The role of driver inattention in crashes; new statistics from the 1995 Crashworthiness Data System. Proceedings of the 40th Annual Association for the Advancement of Automotive Medicine, Vancouver, British Columbia, Canada.

[Zai1] Zaidel, D. M., Paarlberg, W. T., & Shinar, D., (1978). Driver performance and individual differences in attention and information processing. Volume1: Driver Inattention. Institute for Research in Public Safety, DOT-HS-803 793.

Motion Rendering

AN ALGORITHM FOR FALSE CUE REDUCTION AND PREPOSITIONING

IG Salisbury [1], DJN Limebeer [1]

(1) : University of Oxford, Department of Engineering Science,
Parks Road, Oxford, UK, OX1 3BN
Phone: 018652 {83172,73810}
E-mail: {ingrid.salisbury,david.limebeer}@eng.ox.ac.uk

Abstract – This paper studies the utility of numerical optimal control (NOC) in the driving simulator motion cueing problem. In this way it is possible to examine how workspace limits affect the cueing signal. A comparative study against Linear Quadratic Gaussian (LQG) and model predictive control (MPC) algorithms shows that false cues are a result not only of platform physical limitations, but also the methods themselves. A scheme is then devised whereby miscues can be manipulated to achieve small acceleration signals that are independent of the onset cueing. The concept is initially tested in a numerical optimal control framework, and having improved the miscue performance, a similar approach is applied to the other algorithms. These new methods produce attenuated miscues, facilitate stronger onset cueing and make better use of the workspace.

Key words: Motion cueing, numerical optimal control

1. Introduction

The critical limitations of all driving simulators are the bandwidth and workspace constraints of the motion platform. Moving platforms simulators were introduced to stimulate the drivers' inertial sensors (vestibular system), thus enhancing the realism of the driving experience and providing a better understanding of the vehicle's behaviour during braking and cornering.

The exact replication of the vehicle's accelerations is prevented by the motion platform constraints. Hence, motion cueing algorithms were developed to determine a simulator reference that approximates the acceleration and thereby improves the simulation.

There are various motion cueing design techniques, the oldest being the classical frequency-shaping algorithm. In this approach the vehicle accelerations are high-pass filtered to generate simulator references. From a workspace perspective the lower frequency motions that correspond to large displacements are removed. With appropriate filter parameter choices, the platform excursions will remain within the limits, although this is only achieved indirectly. From a driver's perspective the initial changes in acceleration, such as at the onset of braking, are important for understanding the vehicle behaviour. The lack of sustained cues later in a manoeuvre is relatively less critical.

Another widely used algorithm is based on LQG theory and includes a model of the human vestibular system. The resulting high-pass filter is designed to minimise the difference between the acceleration sensed by a car driver and driver in the simulator. A more recent approach uses MPC to determine the simulator input reference, while simultaneously reducing perceived acceleration error and directly respecting the workspace constraints.

All of these established approaches have common features: an onset cue, an acceleration washing and a false cue (acceleration in the wrong direction) that prevents the platform hitting the workspace limits. While broadly similar, the methods differ in relation to the detailed production of the above behaviours. An aim of this paper is to determine how the resulting cueing signal is affected by the algorithm choice and platform constraints. Additionally, there should be an identification of the limitations caused by each of these two factors.

In order to compare these methods, a baseline system that determines the 'best achievable' cues for a given platform, is needed. To this end, numerical optimal control is used to determine an open-loop acceleration input for the simulator over a typical driving scenario. This system is not constrained to be linear or causal, and from the result, it is possible to understand the relationship between the platform constraints and the achievable cues/miscues. In the NOC formulation the workspace constraints are recognised explicitly. The NOC results can then be used as a basis for comparison with the other methods and through this, the underlying limitations of each approach can be identified and understood.

This should provide clarity with regards to the available room for improvement and provide insight into how better cueing can be achieved.

These ideas are then used to develop a new strategy that aims to improve the false cue characteristics of more traditional algorithms. An initial study is conducted in the NOC framework, and given the promising results, a similar approach is implemented for the MPC and LQG cases.

The paper is laid out as follows: In Section 2 the various cueing techniques are described. In Section 3 the results of the non-linear optimal control are examined and then compared with the other algorithms. In Section 4 the new technique is described for each method with comparative results provided.

2. Problem Background

The driving simulator involved in this research is used in Formula 1 racing applications. Race driving is characterised by large-magnitude accelerations that cannot be reproduced or sustained in a confined simulator environment. As a result, the motion cueing problem is challenging and critical, since only a small portion of the actual acceleration is supplied to the driver, and the quality of the simulation is heavily reliant on how this is determined.

A commonly employed technique in road car and flight simulators is tilt-coordination. This uses pitch and roll angles to provide a feeling of sustained acceleration in lateral and longitudinal directions. This, however, only applies when the platform can be rotated sufficiently slowly. A second feature of race driving is the fast dynamics, which render this technique useless, further increasing the difficultly of the problem.

Despite the numerous complications associated with the closed-circuit racing context, there are also some advantages. For a given track, the accelerations on each lap are similar, since the drivers tend to be consistent in terms of their driving. This results in a high level of predictability, a characteristic that lends itself to prepositioning [Wei1]. This technique allows the platform to be moved towards an extreme of the workspace (instead of washing out to the centre) in preparation for the next manoeuvre (e.g. braking or strong lateral acceleration); this effectively doubles the available workspace.

Finally, the test drivers themselves are highly skilled, and will tolerate a lack of realism. However, there are cues they need to understand the car behaviour, and it is important that these are delivered.

2.1. Simulator Platform

A conventional 6 degrees-of-freedom (DOF) hexapod is used in this application. It is moved by changing the length of the legs, and the physical constraints of the system (acceleration, velocity and displacement) arise from the specifications of these actuators.

In motion cueing, it is necessary to examine whether an acceleration trajectory demand exceeds the platform's capability. To achieve this, movements in an inertial reference frame need to be transformed into corresponding changes in the leg lengths. The development of these kinematic equations can be found in [Hel1], and the resulting hexapod model is used in the algorithms.

3. Motion Cueing Algorithms

3.1. Linear Quadratic Gauss

The application of LQG theory to the design of motion cueing filters was developed by [Siv1], [Rei1] and [Tel1]. The details of this method are described in those papers, and consequently only a brief summary is provided here.

The human vestibular system can be modelled as a transfer function that takes as input the experienced accelerations, and produces as output the driver-perceived accelerations. In motion cueing the aim is to make the difference between the acceleration sensed by the simulator driver and that sensed by a driver in a real-car as small as possible. However, since the simulator has physical limits, only a fraction of the car's acceleration can be reproduced. A linear filter, *F(s)* is used to process the vehicle acceleration to produce a simulator motion demand. The LQG approach computes the optimal *F(s)* such that the difference between the output of the real car and simulator drivers' vestibular models is minimised. The LQG cost function is defined as follows:

$$J=E\int_{t_0}^{t_f}(a_s^T R_1 a_s+v_s^T R_2 v_s+s_s^T R_3 s_s+e^T R_4 e)dt, \qquad (1)$$

where a_s, v_s and s_s are simulator acceleration, velocity and displacement, respectively, and e is the error in the perceived acceleration. The inclusion of these four terms, requires the LQG to minimise both simulator motion and vestibular error simultaneously. By tuning the weights in the cost function (using trial-and-error), a compromise between these contradictory aims can be found such that the simulator stays within the workspace bounds.

3.2. Model Predictive Control

The use of MPC in motion cueing is described in detail in [Gar1],[Bas1],[Dag1], and, as before, only the pertinent points are provided here.

MPC involves the formulation of an optimisation problem, with constraints, that is then converted into a quadratic programming (QP) problem and solved using any number of techniques.

The core of any optimisation problem is the cost function, which is given in (2). The input *u(t)* is the simulator acceleration demand, and this is to be determined by the solver. The vector *y(t)* is defined in (4), and *R* and *Q* are weighting terms.

$$\min_{u(t)}\ y(t)^T R y(t) + u(t)^T Q u(t) \qquad (2)$$

Subject to

$$x(t+i+1) = Ax(t+i) + Bu(t+i) \quad i = 0..H_P \qquad (3)$$

$$y(t+i) = x(t+i) - x_{ref}(t+i) \quad i = 0..H_P \qquad (4)$$

$$x_{ref}(t+i) = x_{ref}(t) \quad i = 0..H_P \qquad (5)$$

$$u_{MIN} \le u(t+i) \le u_{MAX} \quad i = 0..H_U-1 \qquad (6)$$

$$v_{MIN} \le v_{PLAT}(t+i) \le v_{MAX} \quad i = 0..H_P \qquad (7)$$

$$s_{MIN} \le s_{PLAT}(t+i) \le s_{MAX} \quad i = 0..H_P \qquad (8)$$

$$u(t+i) = 0 \quad i = H_U..H_P \qquad (9)$$

The first constraint (3) represents the system dynamics, and contains the vestibular system and linearised platform models. From the input (platform acceleration: *u(t)*) the system states (*x(t)*) can be computed. These include the sensed acceleration in the simulator, the vestibular states and the velocity and displacement of the platform actuators.

The vector *y(t)* is representative of the output to be minimised and is calculated as the difference between the system states and a given reference ($x_{ref}(t)$). This reference contains the vestibular states, accelerations sensed in the real car, and components that correspond to the actuator neutral velocity (i.e. *0 m/s*) and length.

A non-zero output therefore occurs when the sensed accelerations do not match, and the platform moves, thus, similar to the LQG approach, both perception error and platform motion are penalised.

A reference acceleration signal is required over the control horizon (H_P). Either a prediction of the future acceleration is needed, or, this can be assumed constant, as given in (5).

Constraints (6), (7) and (8) are a direct result of the actuator acceleration, velocity and displacement limits.

Finally, the input *u(t)* is computed over the control horizon (H_U, where $H_U \le H_P$) and is then assumed to be zero over the rest of the prediction horizon (9).

The optimisation problem is solved at every time step, but only the input computed for the current step (*i=0*) is applied to the simulator.

3.3. Numerical Optimal Control

3.3.1. Theory

An optimal control calculation computes the state and control vectors associated with a system in order to minimise a performance index [Bet1]. The cost can be expressed in Bolza form, and is given by:

$$J = \Phi(t_0,x(t_0),t_f,x(t_f)) + \int_{t_0}^{t_f} l(t,x(t),u(t))dt. \qquad (10)$$

The system constraints are described by:

$$\begin{cases} \dfrac{dx}{dt} - f(t,x(t),u(t),p) = 0 \\ g(t,x(t),u(t),p) = 0 \\ h(t,x(t),u(t),p) \le 0 \\ g_b(x(t_0),x(t_f),u(t_0),u(t_f),p) = 0 \end{cases} \qquad (11)$$

where $t_0 \le t \le t_f$ is the optimisation interval with t_f either fixed, or free to be optimised and $x(t) \in R^n$ and $u(t) \in R^m$ are the state and control vectors respectively. The vector-valued function $f(\cdot) \in R^n$ describes the system dynamics. The vector functions $g(\cdot) \in R^{n_g}$, $h(\cdot) \in R^{n_h}$ and $g_b(\cdot) \in R^{n_{g_b}}$ define the equality, inequality and boundary constraints for the system. The scalar function $l(\cdot)$ is the stage cost that is a function of the state and the controls.

Direct methods are used to convert the infinite-dimensional optimal control problem into a finite-dimensional optimisation problem with algebraic constraints; a nonlinear programming problem (NLP). In this application GPOPS II is used to solve the NOC problem.

3.3.2. Application to Motion Cueing

The motion cueing optimal control problem is defined with the following performance index and constraints:

$$J = \int_{t_0}^{t_f} (\hat{a}_{ref}(t) - \hat{a}_{sim}(t))^2 dt \qquad (12)$$

Subject to:

$$\dot{x} = Ax(t) + Bu(t) \qquad (13)$$

$$a_{MIN} \leq u(t) \leq a_{MAX} \qquad (14)$$

$$v_{MIN} \leq v_{act}(t) \leq v_{MAX} \qquad (15)$$

$$s_{MIN} \leq s_{act}(t) \leq s_{MAX} \qquad (16)$$

The control input, $u(t)$, is the simulator acceleration and is constrained by the actuator capabilities (14). This acceleration demand is used to compute the system states, $x(t)$, from the system dynamics described in (13), which include the vestibular model, and the nonlinear hexapod kinematic equations. The actuator velocity and displacement are therefore components of the state and can be limited in (15) and (16). The acceleration sensed in the simulator $\hat{a}_{sim}(t)$, required in cost function, is also a system state.

Finally, a reference which is the sensed acceleration in a real car, $\hat{a}_{ref}(t)$, is required over the optimisation interval (for example a lap of a race track). The optimal control calculation computes the simulator motion demand over the interval in order to minimise the integral of the squared perception error.

4. Comparison of Cueing Techniques

Each of the above algorithms is implemented for the longitudinal freedom during a typical braking manoeuvre. The results from these are discussed, beginning with the numerical optimal control as a basis for comparison.

4.1. Numerical Optimal Control

The simulator acceleration demand computed by the NOC solver is shown in Figure 1 together with the corresponding platform velocity and displacement. The platform has been constrained to begin the manoeuvre at the front of the workspace and end it at the rear; effectively prepositioning it. The acceleration signal will produce the minimum error as defined in the cost function, and it is in no way constrained to be a linearly filtered version of the reference.

This result can be used to draw conclusions about the effects of the workspace on the cueing fidelity. Firstly, by observing the velocity signal, it can be seen that this, and not the displacement, limits the duration of the acceleration signal; the velocity limit is reached before the workspace limit. Secondly, the

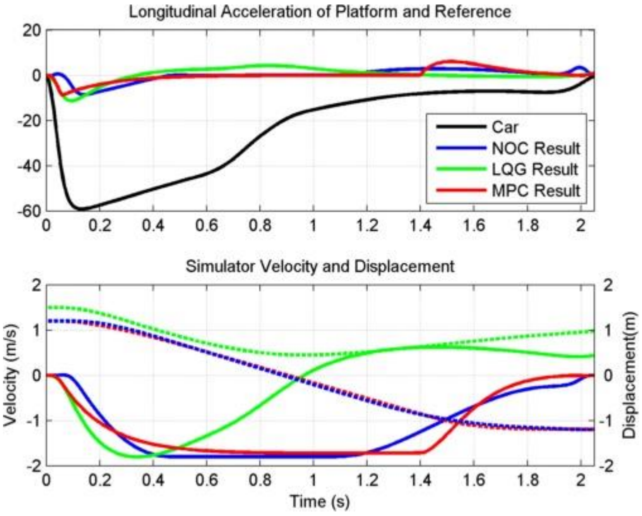

Figure 1 Simulator acceleration, velocity and position (dotted lines) demands computed by the three algorithms.

miscue to slow the platform is delayed until the braking acceleration has decreased in magnitude. This will result in minimal acceleration error and the platform will not violate the constraints.

4.2. Linear Quadratic Gauss

The results of the LQG approach vary depending on the values of the weighting parameters. Adjusting these values is used not only to constrain the platform to move within the workspace, but also to shape the acceleration signal in terms of strength and duration of onset cue. In order to compare the result with the NOC, the LQG is tuned to have a similar cue to the optimal control; the results are shown in Figure 1.

During the onset cue, the velocity once again approaches the constraint. It does not reach the limit however, because the LQG method is difficult to tune to use the full workspace exactly. After numerous iterations it is possible to design filters that come close to the workspace boundary.

In the position demand, some prepositioning was assumed, and the platform is placed initially at the front of the workspace.

The primary difference between the results of the two methods lies in the shape, and timing of the miscue. The LQG miscue immediately follows the onset cue and is of a higher magnitude than the NOC. The shape and duration of this false cue are a direct result of using a linear washout filter. This miscue cannot be adjusted without changing the shape of the onset cue as well. The stronger miscue results in the platform velocity being quickly reduced to zero, and the platform not utilising the full workspace to slow down.

4.3. Model Predictive Control

The MPC cueing problem has more parameters that require adjusting in the tuning process, since not only the weighting vectors can change, but also the length of the control and prediction horizons.

Figure 1 shows the results of the MPC with a control horizon equal to a prediction horizon of 20ms. Since the platform bounds are included as limits in the problem, the workspace is fully utilised.

The results of this are similar to the NOC solution, which is to be expected. If it is assumed that the reference signal is known for the duration of the braking manoeuvre and the control and prediction horizons are set to the whole length of this, the two problems become equivalent (when the plant is linear). The MPC approach differs from the NOC because the look ahead is limited, and the reference is assumed constant in the future.

The key factor in the MPC framework is that the time over which the input is determined can be less than the time over which the system dynamics are solved. So, in an extreme example, if the control is only computed at one time step, and the prediction horizon is 10 steps, then the only way the QP solver can minimise the cost is by changing the input at the first step. During braking, the perception error is minimised by demanding the maximum allowable acceleration at the first time step. Changing the length of the prediction horizon will affect how soon the MPC will determine that the velocity constraints are going to be violated, and this affects how sharply the acceleration is washed out. By adjusting the two horizon lengths the onset cue can be tuned to be both strong and smooth.

Once the platform has reached its maximum velocity, that constraint becomes active and there is no means to reduce the error. At this point, slowing the platform will only increase the perception error, so it is undesirable.

When the platform approaches the edge of the workspace the displacement constraint also becomes active and the platform has to be slowed down. The length of the prediction horizon determines how soon the platform starts decelerating, and the length of the control horizon affects how strong the miscue is. If the control horizon is short with respect to the prediction horizon, then naturally a strong miscue is needed since the input is only non-zero for a fraction of the prediction horizon.

Unfortunately, a longer prediction horizon that will improve the miscues will necessarily also affect the onset cue – making it weaker. Thus, a compromise is needed to produce a good onset cue and an acceptable miscue.

4.4. Remarks

The comparative study of these 3 motion cueing algorithms has made certain things apparent. Firstly, the shape and strength of the miscue is dominated by the platform velocity constraint. This physical limit cannot be avoided and so the onset can be made stronger, but then must be shorter to prevent the platform velocity saturation.

Secondly, the miscues that slow the platform as it approaches the limits are a by-product of the technique employed. Neither LQG nor MPC achieve as smaller miscue as the NOC method. This highlights the need for an alternative miscuing strategy, since it is physically possible to improve them.

Considering these two issues in turn: during onset cueing the aim is to reduce the perception error, however, during miscuing the platform acceleration should be minimised. Ideally, these two problems should be addressed separately so that they can be tuned and adjusted independently. The next section of this work examines the implementation of this idea in the various strategies to determine if, through this, the false cues can be noticeably improved.

5. New Miscuing Strategy

5.1. Numerical Optimal Control

5.1.1. Implementation

The NOC method is the easiest framework in which to implement changes in the cueing strategy, and analyse what improvements can be made that are physically possible. Consequently, the new miscuing idea is applied and tested first in this approach.

A new performance index is given in (17). This function is time-varying and non-linear.

$$J = \int_{t_0}^{t_f} (\beta e^2 w(t) + a_{sim}^2 (1 - w(t)))dt \qquad (17)$$

$$w(t) = \frac{1}{2}(1 + \operatorname{atan}(-k(t - t_0))) \qquad (18)$$

The function *w(t)* is a smooth switch that changes from 1 to 0 at time t_0. The sharpness of the switch is controlled using the parameter *k*. The term *(1-w(t))* is the inverted switch, i.e. it starts at zero and switches to 1 at t_0. The first term in the cost function contains the product of the perception error and the switch, and the second term, the product of the acceleration and the inverted switch. By defining the cost as such, during the first t_0 seconds of the manoeuvre, only the perception error will be minimised, but after t_0 seconds, the perception error will be ignored and the platform acceleration minimised. The weighting term β is included to place more importance on the onset cueing than the miscuing; the resulting miscue should not be considered when designing the onset cue – only the velocity constraint should affect how the cue is shaped.

5.1.2. Results

The results of the braking manoeuvre applied to the newly defined optimal control are shown in Figure 5 below. The onset cue was designed to be strong, reaching the maximum platform acceleration, and the switching time was chosen to be after the velocity limit was saturated.

The improvement in the acceleration miscue is apparent. The acceleration signal is very smooth and the miscue achieves a maximum value of $2m/s^2$. This false cue can be further reduced by removing the constraint that the platform must finish at the rear of the workspace; however, the prepositioning characteristic is more desirable than the slight improvement.

Based on the success of this, the idea was then applied in the MPC and LQG approaches.

5.2. Model Predictive Control

5.2.1. Implementation

In order to improve the false cueing characteristics in the MPC framework the problem needs to be reformulated. At first it seems sensible to make adjustments to the MPC cost function to minimise only acceleration not perception error during miscuing.

However, as mentioned previously, the choice of horizons affects the shape, magnitude and duration of the miscue. As also noted, the horizon cannot be tuned for best miscue without changing the onset cue. Unless, at different times in the braking manoeuvre, the horizons are changed.

The principle is to complete the braking onset cue, and then, once the platform has reached the maximum velocity, the horizons are changed and the control input computed for this adjusted problem. This approach has numerous advantages. The MPC problem does not need to be reformulated as the cost function does not change, and it allows the miscue and onset cues to be tuned independently.

5.2.2. Result

Figure 5 shows the result of changing the horizons during the manoeuvre. The onset cue has been tuned for a stronger deceleration and the false cue has been tuned to be small in magnitude. It is worth noting that if the prediction horizon is too long during the miscue phase then the platform will not fully utilise the workspace.

5.3. Linear Quadratic Gauss

5.3.1. Available Miscue Reduction Techniques

In the context of the LQG and classical filtering approaches other techniques have been developed to reduce the miscues. [Rey1] introduced an additional non-linear gain in the classical approach that reduced the magnitude of the miscues. This is powerful in the classical context where washout is performed by a subsequent filter. However, in the LQG method if the false cues are only gain reduced, then the platform will not stop. This can be remedied by adding an additional washout filter; however, any additional filtering will necessarily affect the onset cues as well. The aim needs to be to not only reduce the gain of the miscues, but also increase the duration and make full use of the available workspace.

5.3.2. Implementation

As it was concluded before, it is not possible to have one filter that is tuned to give both good onset and false cues. There are different requirements during each phase, so the LQG method is now extended to include two filters. The first is optimised to reduce sensation error during the onset cue and the other aims to reduce the acceleration during the false cueing stage. The first filter is designed using the standard LQG approach, and the second is detailed below.

The objective during the miscuing phase is to move the platform to a target position (in preparation for the next manoeuvre), and finish with zero velocity. This can be achieved with a simple controller that feeds back the displacement error and the velocity. This formulation will drive the position to the given reference and the velocity to zero. A diagram of the controller is given in Figure 3 (this also includes bumpless transfer compensation that is still to be explained). The two error signals are gained and summed to produce the acceleration reference. This is described by the Eq. 19, where a_{out}, v_{out} and s_{out} are the platform acceleration, velocity and displacement demands respectively; s_{ref} is the desired platform position and K_1 and K_2 are the feedback gains.

$$a_{out} = K_1(s_{out} - s_{ref}) + K_2(v_{out}) \qquad (19)$$

Finally, it is not recommended simply to switch between two filters, because at a given time there is no guarantee that the states are the same, so there is a 'bump' in the output signal during switching. This is a well-documented problem and is overcome by using a bumpless-transfer scheme. The idea of this is to include feedback around each of the filters that causes the inactive filter output to track that of the active filter. So, when switching occurs, both filters have the same output and no bump appears. The complete switching system is shown in Figure 2, and the details of the two bumpless transfer filters are described below.

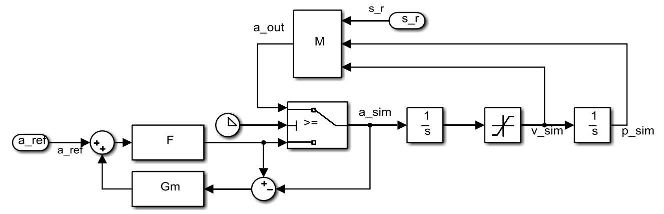

Figure 2 Complete scheme with LQG filter (F), bumpless transfer filter (Gm), and controller M(s) that contains bumpless transfer feedback.

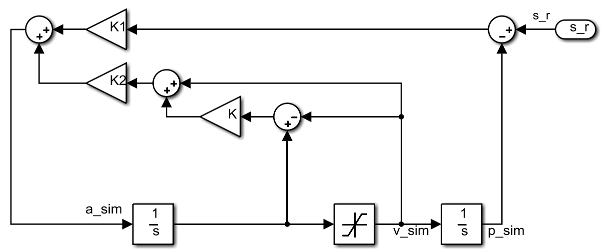

Figure 3 Diagram of controller to slow and preposition platform, with bumpless transfer compensator (K).

The first problem is to ensure that the miscue controller tracks the LQG filter output. The inputs to the controller are velocity and position, and the output is acceleration, which can be integrated to give velocity. It is therefore required that the velocity signal of the miscue controller be the same as the platform velocity when the LQG filter is active. This is achieved using a simple form of bumpless-transfer [Edw1], the implementation of which is shown in Figure 3. The difference between the controller and simulator velocities is gained and added to the feedback loop, adjusting Eq. 19 to:

$$a_{out} = K_1(s_{out} - s_{ref}) + K_2(v_{out} + K(v_{out} - v_{LQG})) \qquad (20)$$

This mechanism has an additional advantage. The output of the controller may produce velocity demands that exceed the platform limits, by including this additional feedback when the velocity saturates the controller output is forced to match the saturated signal and thus the platform acceleration demand remains sensible.

A similar mechanism is required for the LQG filter so that when it is switched back in there is no bump. The simple gain technique did not produce satisfactory results, so an $\mathcal{H}_\infty$ optimisation framework, as introduced and described by [Edw1], was employed to design the feedback.

The bumpless transfer system is described by Figure 4, where a_{sim} is the simulator acceleration demand, a_{out} is the output acceleration of the LQG filter $F(s)$ and a_{ref} is the input acceleration. The aim is to design a filter $G_m(s)$ that minimises the error between the output acceleration and the actual platform acceleration. To formulate a sensible $\mathcal{H}_\infty$ problem it is appropriate to minimise both the error and the output from the $G_m(s)$ filter [Edw1].

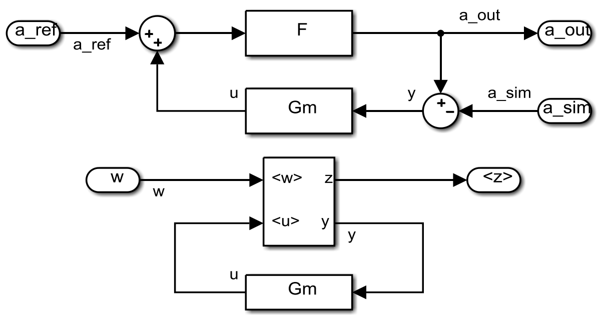

Figure 4 Bumpless transfer feedback filter scheme, and the system recast in generalised regulator form.

This problem can be recast in a generalised regulator format, where:

$$z = \begin{bmatrix} z_1 \\ z_2 \end{bmatrix} = \begin{bmatrix} \lambda(a_{out} - a_{sim}) \\ \beta u \end{bmatrix} \qquad (21)$$

$$y = a_{out} - a_{sim} \qquad (22)$$

And w and u are given by :

$$w = \begin{bmatrix} a_{ref} \\ a_{sim} \end{bmatrix} \qquad (23)$$

$$u = G_m(a_{out} - a_{sim}) \qquad (24)$$

The resulting plant matrix P is given as:

$$P = \left[\begin{array}{cc|c} \lambda F(s) & -\lambda & \lambda F(s) \\ 0 & 0 & \beta \\ \hline F(s) & -I & F(s) \end{array}\right] \qquad (25)$$

From this formulation the optimal filter $G_m(s)$ can be found using standard robust control algorithms. The parameters λ and β are used to weight the relative importance of the error and the magnitude of the output from the filter.

5.3.3. Results

The results from this approach are given in Figure 5, and show an improved miscue, and consequently, workspace usage.

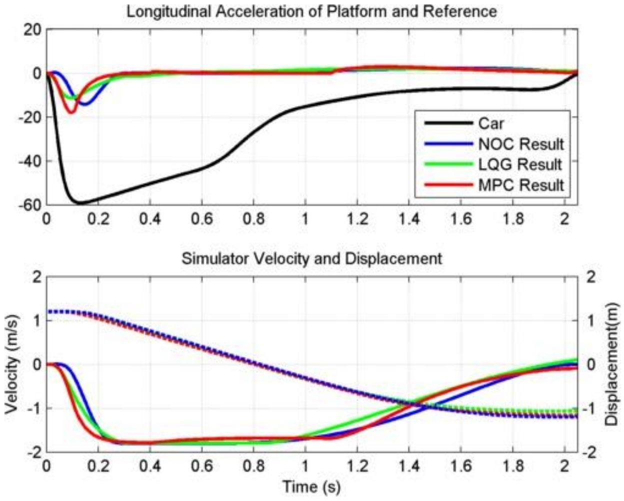

Figure 5 Simulator acceleration, velocity and position (dotted lines) demand calculated using the 3 methods with improved miscues.

6. Future Work

These techniques, having achieved good results in 1DOF, now need to be extended to multiple degrees of freedom.

In the LQG and MPC cases, this needs to be applied in real-time. This requires additional pre-processing of the track to estimate when the respective filters or horizons should be used.

Finally, once implemented on the simulator the driver response will be the ultimate assessment of the improvement.

7. Conclusion

The use of numerical optimal control as a baseline system proved effective in determining the possible areas of improvement in the motion cueing. It was shown that although false cues are physically necessary, the magnitude and duration are a side-effect of tuning for good onset cues, and they can be improved while still respecting the platform physical limits.

A need was identified for methods to separate the onset and false cue phases so that they can be tuned independently, rather than at the expense of each other.

Different means of achieving this were suggested and tested for each algorithm. The results showed a marked improvement in the false cues, and allowed the desired cues to be tuned for a stronger onset.

8. References

[Bas1] Baseggio M. et al. An MPC approach to the design of motion cueing algorithms for driving simulators. In 14th International IEEE Conference on Intelligent Transportation Systems Washington, DC, USA. 2011.

[Bet1] Betts J.T. Practical Methods for Optimal Control Using Nonlinear Programming. Advances in Design and Control. Society for Industrial and Applied Mathematics, 2001.

[Dag1] Dagdelen M. et al. Model-based predictive motion cueing strategies for vehicle driving simulators. In Journal of Control Engineering Practice. 17:955-1003, 2009.

[Edw1] Edwards C., Postlethwaite I. Anti-windup and bumpless transfer schemes. In Automatica, 34:2, 199-210, 1998.

[Gar1] Garrett N.J.I., Best M.C. Model predictive driving simulator motion cueing algorithm with actuator-based constraints, Vehicle System Dynamics: International Journal of Vehicle Mechanics and Mobility, 51:8, 1151-1172, 2013.

[Hel1] Helinski A.L. Dynamic and kinematic study of a Stewart platform using Newton-Euler techniques. Technical report, U.S. Army Tank-Automotive Command, 1990.

[Rei1] Reid L.D., Nahon M.A. Flight simulation motion-base drive algorithm: Part 1 - developing and testing the equations. Technical Report UTIAS Report No. 296, Institute for Aerospace Studies, University of Toronto, Toronto, Canada, 1985.

[Rey1] Reymond G., Kemeny A. Motion Cueing in the Renault Driving Simulator, Vehicle System Dynamics: International Journal of Vehicle Mechanics and Mobility, 34:4, 249-259, 2000.

[Siv1] Sivan R., Ish-Shalom J., Huang J. An optimal control approach to the design of moving flight simulators. In IEEE Transactions on Systems, Man and Cybernetics. Vol:12, Issue:6:818-827, 1982.

[Tel1] Telban R.J., Cardullo F.M. Motion cueing algorithm development: Human-centred linear and non-linear approaches. Technical report, State University of New York, 2005.

[Wei1] Weiss, C. Control of a Dynamic Driving Simulator: Time-Variant Motion Cueing Algorithms and Prepositioning. Diploma Thesis. Deutsches Zentrum für Luft und Raufahrt. 2006

The Effect of Motion Cueing on Simulator Comfort, Perceived Realism, and Driver Performance during Low Speed Turning

Gary Bertollini [1], Yi Glaser [2], Joseph Szczerba [3], Ron Wagner [4]

(1) General Motors Research and Development, VSR Laboratory, 30500 Mound Rd., Warren, Michigan, USA, +1 586 9864212, gary.p.bertollini@gm.com

(2) General Motors Research and Development, VSR Laboratory, 30500 Mound Rd., Warren, Michigan, USA, +1 586 4040519, yi.glaser@gm.com

(3) General Motors Research and Development, VSR Laboratory, 30500 Mound Rd., Warren, Michigan, USA, +1 586 651 3844, joseph.f.szczerba@gm.com

(4) Dynamic Research Inc., 355 Van Ness Ave., Torrance, California, USA, +1 310 2125211, rcw@dynres.com

Abstract - The purpose of this work is to verify the ability of the General Motors Research driving simulator motion system to:

- Mitigate simulator induced discomfort felt during high yaw rate turning maneuvers such as those experienced while turning in an intersection
- Improve subjective rating of fidelity and objective performance measures

A pilot study was conducted to measure the effect of limited displacement and 1:1 yaw motion cues on simulator induced sickness, perceived realism, and driver performance. Three levels of motion cues (No-motion, Hexapod/No-Yaw, Hexapod/ 1:1 Yaw) were manipulated. Dependent measures included subjective assessment of realism of the simulated vehicle; self-reported discomfort; and objective measures of driver input and vehicle response.

Results indicate that the current configuration of the driving simulator is effective in generating motion cues to improve driver performance during intersection turning. For simulator sickness and realism, however, we did not find any statistical effect of motion cueing.

Key words: driving simulator, yaw table, motion cueing, driver behavior, simulator sickness.

1. Introduction

Up to recently, most of the driving simulator studies conducted at General Motors Research (GMR) utilized highway driving scenarios which were not problematic with respect to simulator discomfort, but new investigations increasingly require lower speed maneuvers such as those found in parking or city driving scenarios. As a result of this, there has been a marked rise in simulator discomfort incidents.

Some recent studies indicate that providing a large displacement yaw degree-of-freedom may provide some benefit in driving simulation during low speed driving maneuvers such as turning at intersections. Maurant and Yin [Mau1] demonstrated that a turning cabin reduces optical flow during turns and theorized this accounted for the reduced simulator discomfort measured when compared to a similar turning condition in a non-moving cabin. Similarly, Yoichi and Nobuyuki [Yoi1] found reduced simulator discomfort and improved driver sighting behavior during intersection turns with a rotating cabin compared to the fixed-base condition. Yamaguchi et. al. [Yam1] found lowered position and directional variability with a turning cabin in a slalom maneuver, and Hogema et. al. [Hog1] concluded large yaw motion improves driver behavior as well as realism during low speed turning.

In an attempt to improve participant comfort for these types of maneuvers, a motion system was implemented at GMR with a unique motion and visual system design combination incorporating a large yaw displacement capability. The design consists of a full vehicle cabin mounted on a small displacement hexapod which is supported by a large displacement yaw table. The motion system is centered within a 12 foot diameter projection screen.

The intent of this pilot work is to refine a study design to measure the effect of the GMR driving simulator (GMRDS) motion system cue capability on induced sickness, perceived realism, and driver performance. This pilot manipulates three levels of simulator motion cues (No-motion, Hexapod/No-Yaw, Hexapod/1:1 Yaw) experienced by test participants while recording dependent performance and subjective measures.

2. Prior literature

Recent published studies provide mixed results regarding the effects of driving simulator motion cueing on simulator study participants. Although these studies are difficult to aggregate because of differences in each study's simulator design, the study purpose, conditions explored, and methodology used; they do provide evidence that it is possible to measure effects of motion on perceived realism of the simulated vehicle response, induced simulator sickness, and driver performance.

2.1. Perceived realism

Most studies investigating perceived realism have concluded that realism is enhanced with motion. When perception is integrated from multiple sensory channels it provides a more accurate perception of the real world environment [Sto1]. Essential to this is that the simulator must accurately correlate motion cues with the visual and auditory systems to effectively convey the proper experience to the user [Ber1].

In a study comparing four motion conditions while driving a curved road at a constant speed, an effect was demonstrated on perceived sense of simulator realism [Dam1]. Additionally, an investigation on the effect of motion control algorithms on vehicle following behavior yielded a result that all study participants felt the motion conditions provided a higher degree of realism in the simulated vehicle response than the no-motion condition [Col1]. Furthermore, another study found an effect of motion on subjective assessment of realism while steering into and out of a curve, accelerating and braking [Wen1]. Lastly, an investigation was conducted on detection thresholds for roll tilt coordination. One of the findings was that supra-threshold roll ~~rates~~ levels were judged as more realistic [Nes1]. However, in a research study using two levels of yaw motion in lane change and 90 degree turning maneuvers, no effect from yaw motion was found for realism [Hog2].

2.2. Induced sickness

Simulator sickness has an adverse effect on human behavior and can yield outcomes such as dizziness, fatigue or nausea. The most widely accepted explanation is that simulator induced sickness (SIS) is created from the mismatch between received sensory messages to those that are expected through experience [Rea1], although this theory has exceptions [Bos1].

Visual cueing alone, such as in fixed-based simulators, can induce sickness [McC1]. The addition of motion cues is thought to improve this condition. However, even advanced motion-based simulators can lead to sickness if the visual information does not correspond to the information induced on the vestibular system [Cas1].

Recent studies conducted to evaluate motion cues and their effect on simulator sickness have had varying results. In a comparison of similar studies conducted on Ford Motor Company's fixed based and motion simulators, a lower incidence of simulator discomfort (measured using Kennedy's simulator sickness questionnaire, SSQ) was reported for participants in the motion-based simulator as compared to those driving the fixed-based simulator [Cur1]. Another investigated the effect of yaw motion on driver assessment of induced sickness using a questionnaire administered before and after participants drove right and left turns. It was found that drivers reported higher degree of comfort in the yaw motion condition [Mou1]. It was further found that subjective reports of simulator discomfort decreased in turns for participants in a turning cabin as opposed to a fixed based cabin [Asa1].

Other studies, however, have not achieved a reduction in simulator sickness with the presence of motion. For example, when studying yaw and no-yaw motion in a lane change and 90 degree turning maneuvers, no effect was found for the level of simulator sickness [Hog1]. Additionally, an investigation including a motion sickness evaluation given at the beginning and end of a city circuit consisting of four 90 degree turns yielded no effect for induced sickness. Moreover, Wentink et. al. found that the classical motion algorithm control condition rated lower than the rumble-only condition [Wen1].

The measurement of simulator sickness in the referenced studies seems problematic for several reasons. The effect of simulator design characteristics on SIS is a confounding factor. Secondly, Kennedy has found that at least 40% of participants had never reported any sickness symptoms [Ken1]. As such, these participants don't provide an effective population for inclusion in a study on SIS. A similar point can be made for the type of driving task used in a discomfort study; a non-demanding task (such as freeway driving) may not provide enough stimulus to induce discomfort.

On the other hand, using extremely sensitive subjects, or an extreme task would induce carryover effects from one condition to the next; or worse, lost/excused subjects. The ideal situation in terms of experimental efficiency, is using a subject who is slightly sensitive to discomfort symptoms, does not adapt to the discomfort response, and a simulated driving task that is only demanding enough to induce minor discomfort.

Lastly, the statistical methods used on Kennedy's SSQ scores are debatable. In this paper we conducted nonparametric analysis on percentile scores. In contrast, most prior studies treated the scale variable of the raw scores as a continuous variable, which may be problematic.

2.3. Driver performance

Performance measures are crucial to provide a quantitative assessment of driver capability and the qualification of vehicle systems. The addition of motion cues has been shown to improve driver performance, however, not all studies support this finding.

One study assessed the contribution of motion during braking and cornering maneuvers [Sie1]. This study found that during braking, motion cueing resulted in lower deceleration rates as compared to a no-motion condition. Braking behavior was also stabilized in contrast to the no-motion condition where drivers modified/adapted their braking behavior over time. The authors also found that longitudinal motion resulted in lower mean velocities and that lateral motion had an effect on lateral lane position for the maneuvers investigated.

An additional report contained two experiments exploring the effect of motion cues on specific performance measures used for in-car device evaluation [Gre1]. In the first experiment drivers operated radio, climate control, and telephone features while driving on a typical interstate road and steering against a disturbance function. In this experiment, interaction effects were noted for lane violations and a heading error metric between motion and vertical vibration conditions. In the second experiment, subjects drove four motion conditions while conducting a lane position change and regulating against a disturbance function. Heading and path error was higher in the No-motion condition. Interestingly, the effect of motion diminished for some motion levels, indicating partial motion may be as efficient as full in terms of effect.

Further studies noted difference in driver performance measures during an intersection turning maneuver. Drivers had lower steering, yaw rate, lateral acceleration, mean speed, and braking levels when yaw cueing was present [Hog1].

An equal number of recent studies, however, found that motion cues have no effect on driver performance. One study which investigated motion effects during curve negotiation with a steering disturbance showed no significant difference between motion conditions on the driver's performance measures [Dam1]. Another investigation that studied the effect of motion on vehicle following behavior found no effect on driver performance measures [Col1]. Additionally, no effects of motion cues on driver performance were obtained on intersection and curve negotiation, braking, or acceleration behaviors [Wen1].

2.4. Summary and hypothesis

Although each study discussed above was different in many ways (i.e. apparatus, study purpose, conditions explored, and methodology), most found evidence of an effect of motion on perceived realism. Fewer studies found evidence to indicate that motion cueing lowers simulator induced sickness, while only half of the referenced studies found evidence of an effect of motion on driver performance measures.

In summary, there is evidence supporting a role of motion cueing in improving perceived realism and driver performance, and in reducing simulated induced sickness. Some inconsistency in the literature may be attributed to shortcomings in methodology.

The GMRDS has a design configuration that:

- Separates the projection system and screen from the motion system, thereby eliminating mass and providing opportunity for high bandwidth motion response in a small space
- Stacks the hexapod on a yaw ring to reduce complexity of kinematic control and potential cueing artifacts because the rotational dynamics are isolated from hexapod translations
- Provides 1:1 driver yaw motion without using the image generator to rotate the virtual road image. This produces a smoother rendering of close road objects that are rotating with respect to the driver. The four meter projected image distance from the driver's eye essentially displays the road scene at infinity for comfortable driver eye convergence and accommodation

To examine the effect of motion cueing on perceived realism, induced sickness and driver performance, we applied three levels of motion (No-motion, Hexapod/No-Yaw, Hexapod/1:1 Yaw). We hypothesized that:

- Participant comfort will be improved by providing large yaw motion during low speed cornering over a no-yaw condition
- Limited displacement motion will improve perceived realism over a no-motion condition
- Both motion conditions will show an effect on the obtained performance measures compared to a no-motion condition

The following provides the methodology and results of a pilot study conducted to explore measuring the benefit of the motion system utilized in the GMRDS.

3. Apparatus

The GMRDS provides 360x30 degree roadway view to the driver located in a modified full vehicle compartment as shown in Fig. 1. Haptic feedback is provided at the pedals and steering controls by a three channel control loading system.

Fig. 1. Driving simulator (access door in cab exchange position).

The vehicle compartment is located on 7 DOF motion system that consists of a limited displacement hexapod mounted on a large displacement yaw table as shown in Fig. 2.

Since prior publication [Ber2] provided a description of the GM simulator (with the exception of the motion system), the following will only provide an explanation of the motion system.

Two important reasons for adding motion capability in the simulator were to:

- Reduce incidence of simulator discomfort for large amplitude directional maneuvers by providing realistic cab yawing motions to complement visual cues

- Enhance "realism" for the driver by providing higher bandwidth onset cueing motions related to the vehicle's response to driver control inputs

Fig. 2. Hexapod and yaw table.

Maneuvers that may be enhanced by the addition of yaw motion include those with lower speeds and higher yaw rates such as maneuvering at intersections. The addition of a yaw table makes possible large scale rotations that will allow 1 to 1 scaling of the yaw motion for almost all practical maneuvers. The selected yaw table provides ±175 degrees of yaw motion at rates up to 60 degrees/second. A bearing ring mounts directly to the facility foundation, and carries the load of the hexapod and cab.

For a typical turn or maneuver, the graphic image remains stationary (in yaw) on the screen while the cab and the yaw table rotate. If, at the end of the turn or maneuver, the yaw table position is too close to exceeding its excursion limit, the graphics and yaw table can be gradually rotated back to center position. Knowledge of the roadway and maneuvers to come are used to modify and optimize the washout process and reduce unnecessary re-centering motions.

The hexapod subsystem is used to provide only onset acceleration cues and ride feel to the driver. This makes it particularly suitable for on-center lane regulation. Since the hexapod only supports the cab and driver, and not a yaw table, projectors and screens, it can be substantially smaller and/or higher frequency response per unit of energy. The actuators have a 190 mm stroke and, based on the geometry of the upper and lower attachment triangles, the achieved 6 DOF motion is about ±200 mm in translation, and approximately ± 6 degrees in rotation. Yaw motion can be provided either through the yaw table or hexapod, separately and independently. For purposes of this study, hexapod yaw was turned off and all the yaw motion was provided by the yaw table.

4. Methodology

There were two independent factors; motion and driving session. The three conditions of motion were No-motion, Hexapod/No-Yaw (consisting of 0.5 scale for pitch & roll accelerations but no-yaw, and 0.5 scale for surge & lateral translation accelerations with traditional washout within the motion envelope), Hexapod with Yaw table (same translational and rotational settings as in the prior condition but with ±180 degrees of yaw).

Twelve subjects with equal gender distribution, drove 3 times in a factorial design with random order for conditions as shown in Table 1. To reduce carryover effects from prior motion condition, subjects received 24 hours of rest between unique condition drives. This was done for all but two subjects who for convenience, waited only 4-6 hours between two of the conditions.

The drive task consisted of two road segments, one segment had two intersection turning maneuvers, a left turn followed by a right turn; the other segment had two traffic circle maneuvers, a straight and a 45 degree diagonal turn (The measured total transport delay for these scenarios was 67±5ms). There was a 5 minute rest between segments.

The drive task was balanced for order such that for half the drives, subjects experienced the intersection segment first and the other half received the traffic circle segment first. The route was selected from a prior and convenient drive scenario and thus not particularly created for this study as shown in Fig. 3a-b.

Lateral and longitudinal motion was present during the Hexapod motion conditions with classical washout filters, but no tilt coordination. High frequency vibration generated by the sound system subwoofer and shaker drivers (mounted on structure under seat and engine compartment) was present in the driving compartment for all conditions relating to engine r.p.m.

Table 1. Study condition order.

Subject# and Gender	Motion Condition Day 1	Motion Condition Day 2	Motion Condition Day 3
S1 male	No-motion	Hexapod/ No-Yaw	Hexapod/ 1:1 Yaw
S2 female	Hexapod/ No-Yaw	Hexapod/ 1:1 Yaw	No-motion
S3 male	Hexapod/ 1:1 Yaw	No-motion	Hexapod/ No-Yaw
S4 female	No-motion	Hexapod/ 1:1 Yaw	Hexapod/ No-Yaw
S5 male	Hexapod/ No-Yaw	No-motion	Hexapod/ 1:1 Yaw
S6 female	Hexapod/ 1:1 Yaw	Hexapod/ No-Yaw	No-motion
S7 female	No-motion	Hexapod/ No-Yaw	Hexapod/ 1:1 Yaw
S8 male	Hexapod/ No-Yaw	Hexapod/ 1:1 Yaw	No-motion
S9 female	Hexapod/ 1:1 Yaw	No-motion	Hexapod/ No-Yaw
S10 male	No-motion	Hexapod/ 1:1 Yaw	Hexapod/ No-Yaw
S11 female	Hexapod/ No-Yaw	No-motion	Hexapod/ 1:1 Yaw
S12 male	Hexapod/ 1:1 Yaw	Hexapod/ No-Yaw	No-motion

Dependent measures were position and velocities for steering, accelerator and brake pedal control; lane deviation, speed, yaw rate, and subjective ratings for realism and discomfort. Summary statistics for the performance measures were calculated for the road segments 50 feet before and after the apex of the turn maneuvers.

Fig. 3a. Intersection.

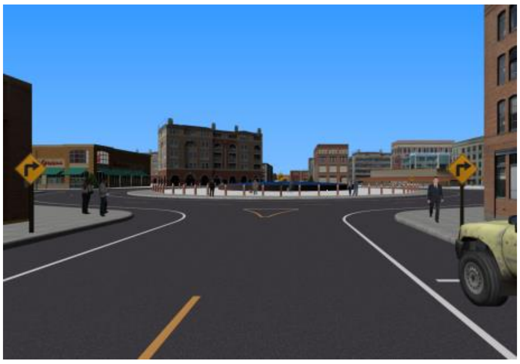

Fig. 3b. Traffic circle.

Participants filled out a baseline SSQ and then received 1 minute of drive training in the simulator driving a two block straight road to familiarize themselves with the simulator speed and steering control tasks. They received the same motion condition they would experience in the test for the up-coming run.

After the familiarization drive participants were then taken outside to drive a real vehicle (compact car). They pulled out of a roadside parking space and drove 15-25 mph to a stop sign, continued for a short distance (1/4-1/2 mile) and turned into a parking lot, turned around and returned to the starting location. This drive lasted about 5 minutes. The real vehicle was identical to the driving compartment used in the simulator.

The simulated vehicle's dynamic response did not correspond to the actual physical vehicle, but represented a crossover type vehicle used in a prior study. Other than the driver eye point difference (a crossover vehicle is higher), it was thought that at the low driving speed there was no practical difference. There was no attempt to replicate maneuvers represented in the simulator test for the real track driven during the real drive (anchoring) period.

After the real car drive, participants were shown the study route using a prerecorded video and instructed where to expect turn locations and the type of directional signs they were to look for and follow. Participants then drove the assigned test segment drives resting between each drive. Participants completed the Kennedy SSQ and simulator realism questionnaire after each drive segment.

4.1. Participants

Twelve employees at General Motors Research were recruited. None had driven the simulator before and all were screened for prior history of motion sickness.

4.2. Kennedy SSQ

The Kennedy enhanced SSQ [Ken1] and the prescribed scoring procedure was used to evaluate simulator comfort levels before and during the course of trial drives.

4.3. Realism survey

A survey was created to assess realism of motion, controller feel, environment and vehicle control in the simulator.
Participants were asked to check a box for each subcategory indicating their opinion using the five point scale corresponding to:

1. Not at all like a real car and the difference is disturbing or bad
2. Different and the difference is weird or odd, not that good
3. Different but the difference is OK, or does not detract in a negative way
4. I'm not sure. I cannot tell a difference from the simulator and a real car
5. This experience is what I think a real car feels like

Realism score for each category was calculated by assigning a number corresponding to the checked box rating for the following categories: Overall sense of Real Driving, Sense of Motion, Road Feel Realism, Car Braking Response, Car Acceleration Response, Forces Felt Turning the Steering Wheel, Brake Pedal Forces, Accelerator Pedal Forces, Controlling the Car in the Lane, Controlling Speed, Visual Scene of Road and Environment, Quality of Sounds Experienced, Seating Comfort, and Air Temperature and Humidity. There was also a comment section for each category for participants to qualify their rating in each category.

5. Analyses and results

5.1. Sickness Questionnaire (SSQ)

Five participants reported at least one symptom in the baseline questionnaire. They were not included in the SSQ data analyses. Composite scores of Nausea (nausea, stomach awareness, increased salivation, burping); Oculomotor (eyestrain, difficulty focusing, blurred vision, headache); Disorientation (dizziness, vertigo) and a total SSQ score were calculated according to formulas developed by Kennedy and Lane (1993). These scores were then transformed to percentiles [Ken1].

All analyses on SSQ data were conducted on the percentile scores. Friedman tests were performed to compare between motion base conditions on each composite score for each segment. None of the tests were significant, *ps* < .20 (see Figure 4 for counts of the percentile scores). However, there is a consistent trend of higher values associated with the traffic circle segment for all composite scores. In contrast, the trend of difference between conditions was less clear.

In general, the two conditions with motion seemed to lead to more severe discomfort.

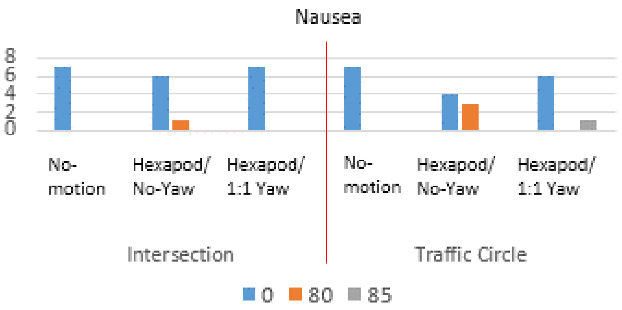

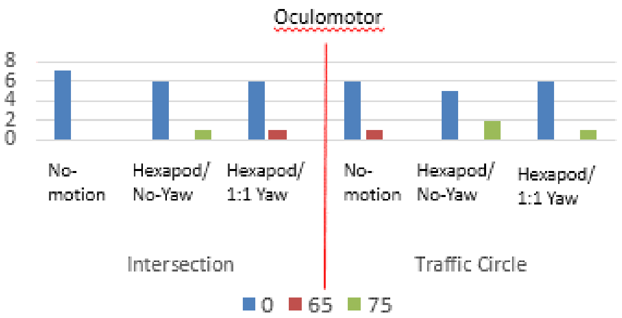

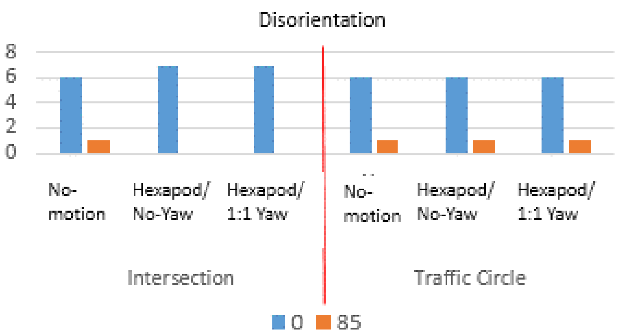

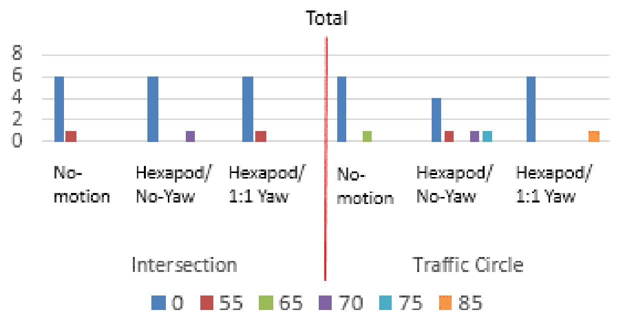

Fig. 4. Counts of percentile scores of SSQ by condition and segment.

For the Nausea and Oculomotor scores, there was a slight trend that the Hexapod/No-Yaw condition resulted in more severe discomfort compared to the Hexapod/1:1 Yaw condition.

In addition, we found a trend of fewer symptoms being reported in the later sessions compared to the first session (see Figure 5), although no statistical analysis was conducted.

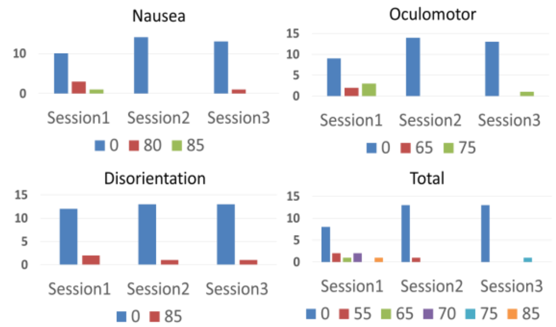

Fig. 5. Counts of percentile scores of SSQ by session.

5.2. Realism questionnaire

Friedman tests were conducted on each item to compare between motion conditions for each segment. Due to missing data, Overall Sense of Real Driving and Quality of Sounds Experienced for the intersection segment and Sense of Motion, Road Feel Realism and Quality of Sounds Experienced for the traffic circle segment had only 11 participants' data included in the analyses. None of these tests reached significance. Two tests were marginally significant, including for Controlling Speed, $S(12)=4.57$, $p=.10$ and Car Acceleration, $S(12)=5.21$, $p=.07$. Participants rated the two motion conditions higher than the No-motion condition for Car Acceleration, indicating they experienced a higher sense of acceleration in these motion conditions. Controlling Speed was rated lower in the motion conditions, indicating they felt less velocity control in the motion condition (see discussion).

Participants were asked to also provide comments while rating realism categories. An assignment of positive or negative tendency was made (i.e. if words like "too sensitive", "not good" or "bad" were mentioned the comment tendency was labeled negative, if positive words like "good" or "better" were used, the comment was labeled positive).

The No-motion, Hexapod/No-Yaw, and Hexapod/1:1 Yaw conditions generated 81, 74, 66 individual comments, respectively. A contingency analysis on the assigned tendency was performed using Pearson Chi Square test which showed a significant difference for condition p< .0001, a post hoc test was not performed. The corresponding mosaic plot is shown in Fig. 6 and indicates a proportionally higher number of negative comments were associated with the No-motion condition compared to the others.

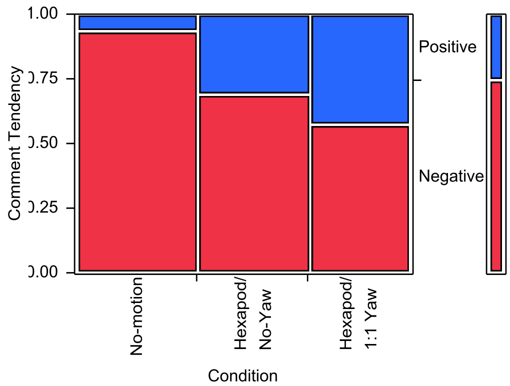

Fig. 6. Percentage of negative or positive comments received for condition.

5.3. Driver performance

Nine driver performance variables were examined, including mean lane center position difference (LCPD), standard deviation of LCPD, maximal LCPD, mean speed, minimal speed, mean brake position, standard deviation of brake position, maximal brake position, brake time, mean steering wheel angle, maximal steering wheel angle, and standard deviation of steering wheel position.

One participant had missing data on all dependent variables. Repeated measures ANOVAs were conducted on each of these variables. Here we only report analyses in the intersection segment. Analyses in the traffic circle segment has not been completed. Independent variables included intersection type (right vs. left turn) and motion condition.

First, the main effect of intersection type was significant on some of these measures. The maximal lane deviation and the mean lane deviation was larger for the left turn than the right turn, $F(1,53) = 64.89$, $p < .001$; $F(1,53) = 16.02$, $p < .001$, respectively.

The maximal, mean and standard deviation of steering wheel position is also larger for the right turn than the left turn, $F(1,53) = 291.82$, $p < .001$; $F(1,53) = 289.71$, $p < .001$; $F(1,53) = 206.11$, $p < .001$.

The mean brake position was larger for the right turn than the left turn, $F(1,53) = 4.04$, $p = .049$. The minimal and mean speed was larger for the left turn than the right turn, $F(1,53) = 20.16$, $p < .001$, $F(1,53) = 66.34$, $p < .001$ respectively.

The main effect of condition was significant on maximal brake position, $F(2,53) = 8.22$, $p = .001$ and marginally significant on the mean speed, $F(2,53) = 3.01$, $p = .06$. Simple effect analyses showed that participants brake harder in the No-motion condition compared to the two motion conditions, and there was no significant difference between the two motion conditions.

None of the interaction effects were significant. See Table 2 for the means of the variables that showed at least a marginal significant main effect of motion condition.

Table 2. Condition means of variables with marginally significant effect of motion.

Motion condition	Mean speed (mph)	Maximal brake position (degrees)
No-motion	11.91	3.23
Hexapod/ No-Yaw	11.86	2.76
Hexapod/ 1:1Yaw	11.25	2.81

6. Discussion

6.1. Driver performance

An effect of motion cueing was found on maximal brake position. Participants braked less in the two motion conditions compared to the No-motion condition, consistent with Siegler et. al. [Sie1]. Adding yaw to hexapod did not affect this measure. This is understandable because peak braking occurred prior to the turn and not during the turn where yaw cueing would be present. In addition, we found a trend of lower mean speed during turns in the hexapod with yaw condition than the other two conditions. This replicated the finding of Hogema [Hog1] that yaw cueing resulted in lower mean speed. Hogema concluded this was because drivers drove more cautiously in anticipation of the turn as a result of experiencing rotational motion of the vehicle. However, no effect of motion cueing was found on any other measure. It is possible that maximal braking behavior during turning maneuvers is the most sensitive measure in a short driving route. The effect of motion cueing during intersection maneuvering on other driver performance measures may require a higher numbers of participants.

6.2. Realism questionnaire

Although no statistical difference was present between motion cueing conditions, we found a trend of higher ratings on Car Acceleration and lower ratings on Controlling Speed for the two motion conditions compared to the No-motion condition. Motion cueing increased the realism of Car Acceleration, consistent with previous studies [Col1; Dam1]. Results on Controlling Speed, however, was in the opposite direction as predicted. A clue to this discrepancy is indicated in the verbatim responses associated with Controlling Speed. Many drivers indicated they were not satisfied with the coasting response of the vehicle and characteristics of the brake pedal response during braking. They felt the vehicle did not allow them to coast to a stop as in the real car, the braking response was too fast, the pedal displacement was too short, and the pedal forces too high.

After investigation it was discovered these dynamics were the result of an earlier study's automated braking system model which was active during this study. It is interesting that the motion conditions exaggerated the perception of this vehicle model characteristic as noted in the subjective ratings.

6.3. SSQ

We did not find statistically significant or even a trend of difference between motion conditions in SSQ scores. However, there was a trend of worse discomfort symptoms in the traffic circle segment than the intersection segment. In addition, we found a trend of less discomfort symptoms reported in later sessions than earlier sessions regardless of motion cueing conditions, indicating a positive practice effect of reducing simulator discomfort. However, with limited number of participants it was difficult to detect these effects or motion cueing effect statistically.

Further studies will be needed to reexamine these effects with a higher number~~s~~ of participants. Moreover, in this study several participants reported symptoms in the baseline questionnaire. These pre-drive symptoms made it difficult to infer whether the post-drive symptoms were indeed caused by simulator driving. These participants, therefore, were not included in the analyses. Future studies will excuse participants with baseline symptoms.

7. Conclusion

In this study, we replicated the findings of prior studies that motion cueing had a positive effect on driver performance. This result indicates that the configuration of the current GMRDS is effective in using motion cueing to improve driver performance.

For simulator sickness and realism, however, we did not find any statistical effect of motion cueing. Further studies with a larger number of participants, improved questionnaire tools, and adjusted methodology are needed to better evaluate functions of the simulator in reducing simulator sickness and increasing realism.

8. Acknowledgments

Authors gratefully thank Chris Kumle, Aashwita Shah, Michael Graham for their support in configuring and operating the driving simulator for this study. We also thank Kevin Chao and Peter Broen of Dynamic Research Inc. (DRI) and Philip van der Borch of Moog for motion system support and design consultation.

9. References

[Asa1] Asano Y., Uchida N., Improvement of driver's feeling by turning cabin driving simulator. DSC, Orlando, 2005.

[Ber1] Berthoz, A., The sense of movement. Odile Jacob (Ed.), Paris. 1997.

[Ber2] Bertollini G., Brainer L., Chestnut J., Oja S., Szczerba J., General Motors driving simulator and applications to human machine interface (HMI) development. SAE 2010-01-1037, 2010.

[Bos1] Bos J., Bles W., Groen E., A theory on visually induced motion sickness. TNO Human Factors, Displays 29: 47–57, 2008.

[Cas1] Casali, J., Frank, L., Perceptual distortion and its consequences in vehicular simulation: Basic theory and incidence of simulator sickness. Transportation Research Record, 1059: 57-65, 1986.

[Col1] Colombet F., Dagdelen M., Reymond G., Pere C., Merienne F., Kemeny A., Motion cueing: what's the impact on the driver's behavior. DSC, Monoco, 2008.

[Cur1] Curry R., Artz B., Cathey L., Grant P., Greenburg J., Kennedy SSQ results: fixed vs. motion-based ford simulators. DSC, Paris, 2002.

[Dam1] Damveld H., Wentink M., van Leeuwen P., Happee R., Effects of motion cueing on curve driving. DSC, Paris, 2012.

[Gre1] Greenberg J., Artz B., Cathey L., The effect of lateral motion cues during simulated driving. DSC, North America, 2003.

[Hog1] Hogema J., Ledegang W., Wentink M., Yaw motion effects in driving simulation: a pilot study in desdemona. TNO Report; TNO-DV 2010 C396, 2011.

[Hog2] Hogema J., Wentink M., Bertollini G., Effects of yaw motion on driving behavior, comfort and realism.

DSC, Paris, 2012.

[Ken1] Kennedy R., Lane N., Simulator sickness questionnaire: an enhanced method for quantifying simulator sickness. International Journal of Aviation Psychology, 3(3): 203-220, 1993.

[McC1] McCauley, M. E. (Ed.) Research issues in simulator sickness: proceedings of a workshop. Washington, DC, National Academy Press, 1984.

[Mou1] Mourant R., Yin Z., A turning cabin simulator to reduce simulator sickness. Proceedings of SPIE, ISSN 0277-786X, 2010.

[Nes1] Nesti A., Masone C., Barnett-Cowan M., Giordano P., Bulthoff H., Pretto P., Roll rate thresholds and perceived realism in driving simulation. DSC, Paris, 2012.

[Rea1] Reason J., Motion sickness adaptation: A neural mismatch model. Journal of the Royal Society of Medicine, 71:819-829, 1978.

[Sie1] Siegler I., Reymond G., Kemeny A., Berthoz A., Sensorimotor integration in a driving simulator: contributions of motion cueing in elementary driving tasks. DSC, Sophia Antipolis, 2001.

[Sto1] Stoffregen, T. A., & Bardy, B. G. On specification and the senses. Behavioral and Brain Sciences, 24: 195-261, 2001.

[Wen1] Wentink M., Valente Pais R., Mayrhofer M., Feenstra P., Bles W., First curve driving experiments in the Desdemona simulator. DSC, Monoco, 2008.

[Yam1] Yamaguchi, D., Suda, Y., Onuki, M., Shimoyama, O., Approach to improvement of realistic sensation on universal driving simulator. Proceedings of the Driving Simulation - Conference Europe, 2010.

[Yoi1] Yoichi, A., Nobuyuki, U., Improvement of driver's feeling by turning cabin driving simulator. DSC North America, Orlando, FL, 2005.

AN MPC APPROACH TO THE DESIGN OF MOTION CUEING ALGORITHMS FOR A HIGH PERFORMANCE 9 DOFS DRIVING SIMULATOR

Mattia Bruschetta [1], Fabio Maran [1], Alessandro Beghi [1], Diego Minen [2]

(1) : Department of Information Engineering
University of Padova, Italy
{name.surname}@dei.unipd.it

(2) : Vi-Grade s.r.l.
Tavagnacco, Udine, Italy
diego.minen@vi-grade.com

Abstract – Driving simulators (DS) of innovative mechanical structures tailored to specific market needs have been recently designed, due to the increasing diffusion of such devices in many different application fields. The effectiveness of DSs is related to the capability of the motion control strategies of faithfully reproducing the driving feelings, while staying within the operation space. Such strategies are called Motion Cueing Algorithms (MCAs). Their implementation strongly depends on the particular mechanical structure. In this paper, a MCA based on *non-linear* Model Predictive Control (MPC) is considered for a new-concept simulator, which is based on a combination of a hexapod over a flat base moved by a tripod, exhibiting a highly non-linear behaviour. In particular, the main goal is that of increasing performance in terms of yaw DOF exploitation, a crucial one to well reproduce driver feelings that is limited by the architecture of classical platforms. Preliminary results show a full exploitation of the working area, while managing all the limitations given by the structure.

Key words: Motion Cueing, Yaw angle, Hexapodal Simulator, Non-linear Control, Model Predictive Control.

1. Introduction

In the framework of dynamical motion simulation platforms, Motion Cueing Algorithms (MCAs) play a central role. The effectiveness of those devices is strongly related to their capabilities of faithfully reproducing the motion feeling the driver would have inside a real vehicle: a well designed MCA can exploit at best the capabilities of the platform on which they have been implemented, whatever the final aim is (e.g., virtual vehicle prototyping, racing setup and development, rehab.) At the same time, MCAs have to deal with the physical constraints of the specific platform, preventing discontinuities in motion due to the limitations of the actuators that can lead to unfeasible positions, unphysical accelerations and possible damage of the platform. This is commonly known as Washout Action (WA).

Achieving good results is not an easy task, due to the complex nature of the human perception systems: It is not clear yet, from a physiological point of view, the roles and priorities of stimuli of different nature to the overall perception of accelerations and forces. Moreover, human reactions are subjective and experience dependent (e.g. professional pilots are more sensible to some aspects of motion than non professional drivers).

From these considerations, a model-based approach appears to be better suited for this kind of application than the "classical" one based on a simple combination of high-pass/low-pass filters. To this aim, the Model Predictive Control (MPC) paradigm can be used, where model-based, optimal control techniques are employed that make explicit use of constraints, which can include both the physical limitations of the actuators and the human perception system [Wan1]. The use of an appropriate model and cost function makes this approach an efficient, viable solution [Aug1], [Dag1].

In [Bru1, Bru2, Mar1] a MCA based on a MPC technique for a 6 DOFs dynamic platform has been proposed. In that particular setup, given that the degrees of freedom are partially decoupled, the system has been split into four sub-systems to "parallelize" the computation of the optimal solution, thus improving real-time performance. The algorithm has been implemented and widely tested on the testbed machine before been released for use on other platforms. A further improvement has been presented in [Mar2] by introducing a more accurate prediction step, with the exploitation of the repetitive pattern typical of the racing context, together with a decimation strategy to improve the real time performance. Concerning more traditional and complex platform structures, a recent work deals with the problem of exploiting the inverse kinematic model of a classical hexapod, still adopting linear models [Gar1].

One of the main limitations of commercial simulators, for what concerns the automotive field, is the yaw degree of freedom. Satisfactory platform movements along this DOF are crucial but very difficult to achieve. A new concept structure, from now on referred to as DiM (Driver in Motion, see Fig. 1), has been introduced to overcome these difficulties, besides bringing other advantages. From a mechanical point of view, it is composed by a hexapodal structure installed upon a tripodal-actuated plane, able to perform longitudinal, lateral, and yaw displacements: hence the yaw angle is contributed both my the hexapod and the tripod. To develop a motion cueing capable of exploiting at the best all the degrees of freedom of the DiM architecture, a nonlinear, MPC based algorithm is proposed that can be considered a substantial evolution of the algorithm described in [Bru2, Mar1]. In this previous work, in fact, a small platform with decoupled degrees of freedom was considered, whereas the DiM has a relevant coupling between the different degrees of freedom. The two main coupling factors are:

- the continuous, non-linear map between general coordinates and actuators displacement, typical of hexapodal structure.
- the interaction between actuators which is related to the relative position of the tripod over the hexapod. This is a peculiar feature of the DiM.

Starting from an analytical study of the platform motion envelope, this latter factor, specifically along the yaw direction, has been identified as the main obstacle to a wide exploitation of the platform working area. The proposed approach consists in a combination of linear and non-linear real time MPC based motion cueing, capable of avoiding actuators interaction, exploiting a full inverse kinematic model of the platform. Furthermore, the algorithm allows handling in an optimal way the separation of the global yaw displacement between the hexapod and the tripod.

2. Problem statement

The mechanical structure of the simulator consists of a hexapodal structure mounted on a tripod frame, which slides on special air/mag pads on an extremely even and stiff steel surface. In this way, it is possible to achieve satisfactory results in physical simulation with a relatively small size assembly, whereas an equivalent-net-workspace traditional hexapodal platform would require a dedicated hangar. The planar tripod is responsible for longitudinal, lateral, and yaw sliding movements and the hexapod for pitch, roll and vertical ones, while being also used for small longitudinal, lateral, and yaw movements. The redundant DOFs allow to increase the overall bandwidth and to have a large motion envelope while maintaining a limited occupied volume. The simulator kernel, i.e. the vehicle dynamics physical engine, has been developed and extensively tested on the field and provides a highly reliable representation of the real vehicle behaviour [Fre1]. The screen covers over 220deg angle and the projected image moves in proper coordination with the platform to guarantee full immersion of the driver in the virtual environment. Force feedback on the steering wheel and the braking system implements the driver’s feeling of the vehicle behaviour. The platform dynamic performance reported in Table 1 highlight the limitations of the operational space.

The overall system is clearly nonlinear, both in the operational space and the actuators space. When calculating the motion displacements the need for avoiding interference between the actuators must be taken into account, that can result in a dangerous situation for the driver and damage of the device.

The MC strategy has to provide the displacement references to the control system of the platform, which is assumed to be able to perfectly track the reference signals, with a fixed time delay. The conceptual scheme of the MC procedure comprises the following steps:

1. obtain the current vehicle states, i.e. translational acceleration and angular velocities calculated on the driver eye-point, from the simulation software;
2. obtain the “perceived acceleration” by filtering vehicle states via the vestibular system model, thus generating the reference signal for the NMPC algorithm;

3. compute via NMPC the displacement signal to be passed to the platform motion control system in order to achieve the desired behaviour on the eye-point.

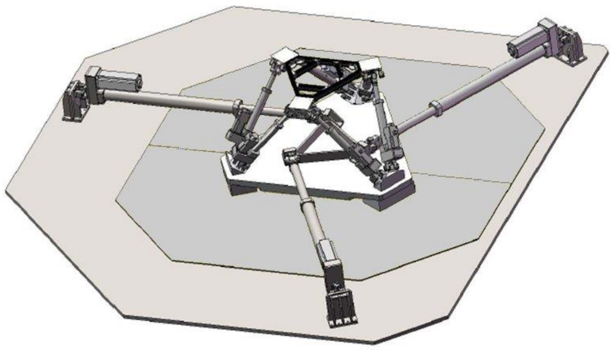

Fig. 1. DiM outline

Table 1. Platform Tripod (t) and Hexapod (h) performance

DOF	Position	Velocity	Acceleration
x_t	±0.8m	1.7m/s	12m/s^2
y_t	±0.75m	1.5m/s	10m/s^2
Yaw, ϕ_t	±25deg	165deg/s	900deg/s^2
x_h	±0.28m	2m/s	25m/s^2
y_h	±0.25m	1.7m/s	25m/s^2
z_h	±0.22m	1.6m/s	35m/s^2
Roll, ψ_h	±20deg	135deg/s	2500deg/s^2
Pitch, θ_h	±20deg	130deg/s	2000deg/s^2
Yaw, ϕ_h	±20deg	135deg/s	3000deg/s^2

3. Non-linear MPC for Motion Cueing

The proposed Motion Cueing Algorithm is based on Model Predictive Control (MPC), and it is the development of the one described in [Bru2, Mar1]. The advantages of MPC paradigm are well known: the procedure solves at each step a constrained, optimal control problem over a prediction window, applies the first element of the computed solution and iterates again, so that the effect of uncertainties in the model and of disturbances can be countereacted. Availability of a satisfactory model of the system under control plays a fundamental role in this approach. The effectiveness of the model is strictly related to the presence of constraints. In fact, limitations on the different parameters of the system can be imposed, that are taken into account when solving the minimization step. In this way, the system behaviour can be defined by acting on quantities that have a physical meaning, leading to a more practical setup with respect to more traditional approaches. Analogously, the presence of a weighted cost function [Wan1] defines the tuning procedure, making possible the regulation of performance by acting on the weights themselves.

From the implementation point of view, the optimization procedure is the core of the MPC procedure, in particular when dealing with non-linear MPC (NMPC). In the specific framework, there are strict real-time requirements, involving fast dynamics (the requested control frequency is 100 Hz), hence fast computation is crucial. From these considerations, for our application the choice has to be done among fast NMPC tools.

3.1. Model

One of the distinctive elements of adopted approach is the modelling of the human perceptive system, i.e. the dynamics of the set of organs that are responsible for the perception of linear acceleration and angular velocities [Bru1, Bru2, Mar1]. Each perceptive degree of freedom is represented by a linear, continuous-time, second order system, derived from the aerospace literature [Hou1] with parameters adapted to the automotive contest. The state-space representations of each organ are then combined to get the complete otoliths and semicircular channels systems, named Σ_O and Σ_S, respectively. The former takes as input the vehicle linear accelerations to produce the perceived ones, the latter acts in the same way with the rotational velocities.

The otoliths system Σ_O must then be modified to introduce the *tilt-coordination* effect. The low-frequency components of accelerations cannot be reproduced within the limited space of a simulation platform, by only using linear displacements: the state-of-the-art workaround is known as tilt-coordination, according to which, the gravitational force is used to reproduce the low frequency components of accelerations, by appropriately tilting the device. To achieve a correct perception the driver's frame rotation has also to be taken into consideration. When using large yaw values, that frame is rotated by a non-negligible angular displacement with respect to the inertial one, hence the inertial frame accelerations would be incorrectly reproduced on the driver if they are not projected in the correct way. Let a be the acceleration the driver is subject to, and a_x, a_y, a_z its components along the inertial reference system. If θ and ψ are the pitch and roll angles, respectively, we have that the gravity vector g_{TILT} of the non-inertial system moving together with the eye-point of the driver is obtained by rotating the inertial gravity vector as

$$g_{TILT} = R(\theta) \cdot R(\psi) \cdot \begin{bmatrix} 0 \\ 0 \\ g \end{bmatrix} = \begin{bmatrix} -g \sin\theta \\ g\cos\theta \sin\psi \\ g \cos\theta \cos\psi \end{bmatrix} \quad (1)$$

On the other hand the driver's reference frame transformation can be characterized by

$$a_d = \begin{bmatrix} a_x \cos\phi - a_y \sin\phi \\ a_x \sin\phi + a_y \cos\phi \\ a_z \end{bmatrix} \quad (2)$$

where a_d is the acceleration on the driver's frame. By combining a_d with Eq. 1, we obtain that with the use of tilt coordination, if suffices to provide the driver with the specific acceleration $\tilde{a} = a_d - g_{TILT}$,

$$\tilde{a} = \begin{bmatrix} a_x \cos\phi - a_y \sin\phi + g\sin(\theta) \\ a_x \sin\phi + a_y \cos\phi - g\cos\theta \sin\psi \\ a_z - g\cos\theta\cos\psi \end{bmatrix} \approx \begin{bmatrix} a_x + g\,\theta \\ a_y - g\psi \\ a_z - g \end{bmatrix} \quad (3)$$

where a linear approximation is used. The small-angles approximation in Eq. 3 is acceptable in the situation at hand. Tilt coordination provides an essential contribution to the effectiveness of a dynamical platform, and must be well managed. In this sense, it has to be combined with visual and audio clues to foul the driver perceptive system, and, at the same time, the simulator has to rotate slowly enough not to trigger the semicircular channels reaction. This is a constraint that has to be taken care of in the problem formulation. Following the approach in [Bru2, Mar1], this is achieved by augmenting the state of the otolithic system to include the effect of the platform inclinations, obtaining the "augmented" systems $\Sigma_{\bar{O}}$.

Σ_S and $\Sigma_{\bar{O}}$ are then combined to get the complete vestibular model. Model inputs are the actual vehicle accelerations and rotational velocities, and its outputs are the corresponding perceived quantities. The motion control systems of most devices require to specify the positions of the eye-point, and not accelerations and rotations, therefore linear velocities v_i and positions p_i, $i = x,y,z$ are obtained by using a simple integral subsystem $\dot{x}_I = Ax_I + Ba$, where

$$x_I = \begin{bmatrix} p_x & v_x & p_y & v_y & p_z & v_z \end{bmatrix}^T, \; a = \begin{bmatrix} a_x & a_y & a_z \end{bmatrix}^T \quad (4)$$

the same is applied to calculate the yaw position ϕ from $\dot{\phi}$.

The complete model has the following state, input and output vectors

$$x_V = \begin{bmatrix} x_S^T & x_{\bar{O}}^T & x_I^T \end{bmatrix}^T \in \mathbb{R}^{21} \quad (5)$$

$$u_V = [a^T \;\; \beta^T]^T \in \mathbb{R}^6 \quad (6)$$

$$y_V = \begin{bmatrix} y_S^T & y_{\bar{O}}^T & \beta^T & x_I^T & \dot{\beta}^T \end{bmatrix}^T \in \mathbb{R}^{18} \quad (7)$$

where $\beta = [\psi \;\; \theta \;\; \phi]^T$.

With respect to the implementation described in [Bru2, Mar1, Mar2], the mechanical structure of DiM introduces an increase in the complexity, due to some non-linear aspects and the increase in the model dimension. As seen in Fig. 1, the platform can be thought as the combination of two dynamical subsystems, the hexapod and the tripod. This specific constructive choice introduces a "redundancy" in three DOFs, i.e. longitudinal, lateral and yaw displacements. Both the tripod and the hexapod contribute to all of those displacements, but in a different way depending on the tuning of the algorithm, as will be explored in the next section. For instance, one could set the parameters so that the low frequency components of the yaw displacement are reproduced by the tripod (which has a larger operational space) while the high frequency ones are managed by the hexapod. Longitudinal, lateral accelerations a_x, a_y, and yaw velocity $\dot{\phi}$ can then decomposed as

$$a_x = a_{x,t} + a_{x,h}, \quad a_y = a_{y,t} + a_{y,h}, \quad \dot{\phi} = \dot{\phi}_t + \dot{\phi}_h \quad (8)$$

were indexes t and h denote tripod and hexapod components, respectively. The input vector is now of size 9. As a consequence, the integrated velocities and positions in the model are split as well, yielding to 5 additional states (linear positions and velocities, yaw position). The complete system is now of size 26 with 9 inputs, posing quite a challenge from a computational point of view. A further, relevant modification with respect to the linear case is the reformulation of Eq. 3. Given the extended yaw range available with the DiM platform compared to the one described in [Bru2], $\tilde{a}$ must be rewritten as

$$\tilde{a} = \begin{bmatrix} a_x \cos\phi - a_y \sin\phi + g\,\theta \\ a_x \sin\phi + a_y \cos\phi - g\psi \\ a_z - g \end{bmatrix} \quad (9)$$

With this modification the longitudinal and lateral subsystems cannot be considered linear anymore.

Note that the model derived in this way does not take into account any dynamic information about the platform's actuators. This is due to the high complexity of the device. A closed form expression for the hexapod dynamics can be derived only in few, specific situations [Yan1] that do not include the one at hand, that is further complicated by the integration with the tripod. The non-linearities due to the actuators behaviour and their reciprocal interferences are managed through the introduction of specific constraints, derived from the inverse kinematics as specified in the next section.

3.2. Constraints

The constraints the system is subject to, and that have to be considered when solving the optimization problem, are basically two, due to:

- Maximum and minimum length admissible for each of the nine actuators (six on the hexapod, three on the tripod);
- Interference avoidance between hexapod and tripod actuators.

By only providing the limitations on the actuators length to the solver, feasibility of the problem it is not yet guaranteed. Actuator physical dimensions and reciprocal positions also impose the fulfilment of a non-interference constraint to avoid configurations not reachable by the actuators, due to their not negligible size.

This second point is more critical, affecting the integrity of the platform instead of dealing with driver comfort. Due to the necessity of maintaining a feasible real time procedure only this latter constraint is taken into account.

To obtain an analytical solution one should derive a closed form expression of the admissible space. Such a task is a challenging one, therefore it is proposed to use instead an approximated analytical surface.

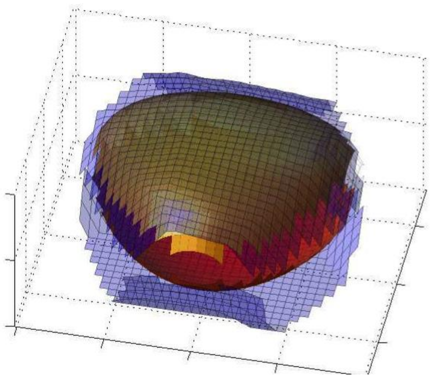

Fig. 2. Closed form surface fitting

First, a (dense) set of measurements is collected by mapping the maximum tripod yaw ϕ_t for each possible couple x_t, y_t (Fig. 2). This $\mathbb{R}^2 \to \mathbb{R}$ map is then approximated with an implicit function of the form

$$ax_t^2 + by_t^2 + cx_t^2 y_t + dx_t y_t^2 + ex_t y_t + f\phi_t + g = 0 \quad (14)$$

and the parameters *a,…,d* computed with a standard curve-fitting procedure. The resulting non-linear function can be directly used as constraint during optimization.

3.3. Optimization

Among the several fast NMPC toolboxes, `ACADO toolkit` [Hou2] has been chosen for the following reasons:

- it is intuitive and easy to use;
- it is open-source;
- it supplies an automatic code generator for fast implementations;
- it deals with mixed linear/non-linear models.

The optimization function is

$$\min_{\substack{x_0,\dots,x_N \\ u_0,\dots,u_{N-1}}} \sum_{k=0}^{N-1} \|h(x_k,u_k) - \tilde{y}_k\|_{W_k}^2 + \|h_N(x_N) - \tilde{y}_N\|_{W_N}^2 \quad (15)$$

$$\begin{aligned} \text{s.t.}\quad & x_0 = \hat{x}_0 \\ & x_{k+1} = F(x_k,u_k,z_k), && \text{for } k = 0,\dots,N-1 \\ & x_k^{lo} \le x_k \le x_k^{up}, && \text{for } k = 0,\dots,N \\ & u_k^{lo} \le u_k \le u_k^{up}, && \text{for } k = 0,\dots,N-1 \\ & r_k^{lo} \le r_k(x_k,u_k) \le r_k^{up}, && \text{for } k = 0,\dots,N-1 \\ & r_N^{lo} \le r_N(x_N) \le r_N^{up} \end{aligned}$$

where $x \in \mathbb{R}^{26}$ denotes the differential state, $u \in \mathbb{R}^9$ the control input, $z \in \mathbb{R}^9$ the algebraic variables, and value 0 for the time index k denotes the current time. h and h_n are the reference functions and $W_k, W_N \in \mathbb{R}^{35}$ are the weighting matrices. $\tilde{y}_k$ and $\tilde{y}_N$ denote the time varying reference. $(\cdot)^{lo}$ and $(\cdot)^{up}$ denote the lower and upper bound of the relative variable and r_k, r_N are the constraint function applied along the horizon window and on the final term, respectively. Finally, F defines an ordinary differential equation.

A useful feature of `ACADO` is that it allows mixing linear and non-linear models exploiting the linearity to improve performance [Qui1]. A convenient reformulation of the problem requires writing the model in two parts:

- Vertical and yaw DOFs compose a linear submodel
- Longitudinal and lateral DOFs has a (partial) non-linear description.

As can be seen from Eq. 15, reference trajectories have to be provided to each of the output variables. This can be done by using the simulation environment, where perceived transactional accelerations and angular rates are generated, and then scaled prior to be used in the MPC algorithm. To keep the platform within its operational limits, differently from the classical washout approach, constant zero references for the position of the all the six DOFs and for the velocities of the longitudinal ones are used. The tuning of the algorithm consists in choosing the weights, the length of prediction and control window, and the scaling factors to obtain satisfactory performance of the overall system, in terms of realistic sensations and effective usage of the platform working area.

The integration of gravity effect into the model as described in Subsection 3.1 automatically introduces tilt coordination as an effect of the optimal control procedure. Performance can also be increased by using long prediction/control windows. However, this is hard to accomplish due to the difficulty in getting reliable information on the future driver's behaviour, and to the hard real-time computational constraints. Hence, in this first implementation a short, constant-valued prediction window is used.

Compared to linear case described in [Bru2, Mar1] the use of non-linear MPC introduces other advantages, such as:

- When using large values of yaw angle, it is possible to precisely take into account the lateral/longitudinal component needed to correctly reproduce acceleration on the driver's frame, while fulfilling the constraints;
- It is straightforward to combine the tripod and hexapod using weight of the cost function;
- Avoiding interference can be obtained by simply imposing a proper constraint;

4. Results

In this Section, some simulation results are presented. The simulated vehicle is a GT class car, and the virtual test track is a digital version of the Calabogie track. In order to better explain the advantages of the proposed procedure the longitudinal, lateral and yaw interaction during big tripod movements is reported. Also, due to space constraints, values of the tuning parameters are omitted. The MCA is set-up so that platform working area is exploited at best.

Fig. 5 illustrates the value of the non-interference constraint (Eq. 14) during the simulation. After 10 and 20 seconds its limit is reached, and consequently the yaw action is transferred from the tripod to the hexapod (Fig. 4), in order to keep the platform within its operational space. The cost of this manoeuver is a negligible decrease of the perceived yaw velocity tracking performance (Fig. 3), which is almost imperceptible to the driver. The advantage in terms of device exploitation, safety management and motion reliability is clear.

From the computational point of view, the simulations have been performed on a standard Intel i5 2.4 GHz, OSX 10.9, with an average computation time of about 1x the required one (control frequency of 100 Hz). Further study is required to test the proposed solution with dedicated hardware in order to guarantee real time in any possible situation.

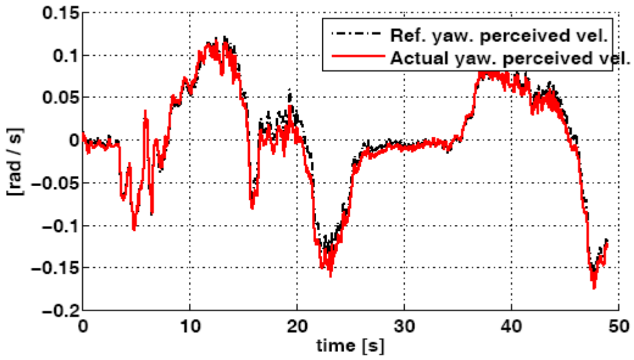

Fig. 3. Perceived Yaw velocity tracking

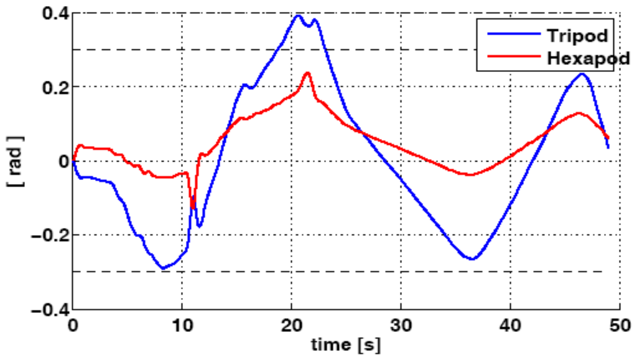

Fig. 4. Yaw displacement

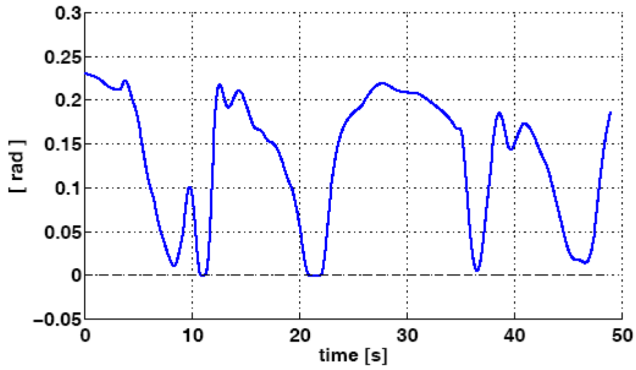

Fig. 5. Non-interference constraint value

5. Conclusions

In this paper a MC algorithm for a high performance, 9 DOFs dynamic simulator has been described, which is based on non-linear MPC techniques. The algorithm represents an important improvement w.r.t. the linear algorithm described in [Bru2], and it allows handling the complex platform mechanical structure in a natural way. The present algorithm is based on a perception model, and it exploits a partial correct inverse kinematic characterization of the platform. Simulation results show that satisfactory performance can be achieved in terms of reproducing accurate perception even if in particularly critical operating conditions.

6. References

[Wan1] L. Wang. Model predictive control system design and implementation using MATLAB. Springer Verlag, 2009.

[Aug1] B. Augusto, R. Loureiro. Motion cueing in the Chalmers driving simulator: A model predictive control approach. Master’s thesis, Chalmers University of Technology, 2009.

[Dag1] M. Dagdelen, G. Reymond, A. Kemeny, M. Bordier, N. Ma zi. Model-based predictive motion cueing strategy for vehicle driving simulators. Control Engineering Practice, vol. 17, no. 9, pp. 995–1003, 2009.

[Bru1] M. Bruschetta, F. Maran, M. Baseggio, A. Beghi, D. Minen. An mpc approach to the design of motion cueing algorithms for driving simulators. Intelligent Transportation Systems (ITSC), 2011 14th International IEEE Conference on, pp. 692 –697.

[Bru2] M. Bruschetta, F. Maran, A. Beghi. A real time implementation of mpc based motion cueing strategy for driving simulators. Decision and Control (CDC), 2012 51st International IEEE Conference on, dec. 2012.

[Mar1] F. Maran. Model based control techniques for automotive applications. Ph.D. dissertation, University of Padova, February 2013.

[Mar2] F. Maran, M. Bruschetta, A. Beghi. A real-time implementation of an mpc-based motion cueing strategy with time-varying prediction. Systems, Man, and Cybernetics (SMC), 2013 IEEE International Conference on. IEEE, 2013, pp. 4149–4154.

[Gar1] N. J. Garrett, M. C. Best. Model predictive driving simulator motion cueing algorithm with actuator-based constraints. Vehicle System Dynamics, vol. 51, no. 8, pp. 1151–1172, 2013.

[Fre1] R. Frezza, A. Saccon, D. Bacchet. Smartdriver: a sensor based model of a car driver for virtual product development. Advanced Intelligent Mechatronics, 2003. AIM 2003. Proceedings. 2003 IEEE/ASME International Conference on, vol. 1, july 2003, pp. 366 – 370.

[Hou1] J. A. Houck, R. J. Telban, F. M. Cardullo. Motion cueing algorithm development: Human-centered linear and nonlinear approaches. NASACR, vol. 213747, May 2005.

[Yan1] J. Yang, Z. Geng. Closed form forward kinematics solution to a class of hexapod robots. Robotics and Automation, IEEE Transactions on, vol. 14, no. 3, pp. 503–508, Jun 1998.

[Hou2] B. Houska, H. J. Ferreau, M. Diehl. Acado toolkitan open-source framework for automatic control and dynamic optimization. Optimal Control Applications and Methods, vol. 32, no. 3, pp. 298–312, 2011.

[Qui1] R. Quirynen, S. Gros, M. Diehl. Efficient nmpc for nonlinear models with linear subsystems. Decision and Control (CDC), 2013 IEEE 52nd Annual Conference on, Dec 2013, pp. 5101–5106.

REVIEW AND PROSPECTS OF RENAULT'S MPC BASED MOTION CUEING ALGORITHM FOR DRIVING SIMULATOR

Zhou FANG[1], Andras KEMENY[1]

(1): RENAULT, Virtual Reality and Immersive Simulation Center
TCR AVA 0 13, 1 avenue du Golf,
78288 Guyancourt, France
zhou.fang@renault.com, andras.kemeny@renault.com

Abstract – In recent years, MPC algorithm as a new method has been successfully applied for the design of motion cueing algorithm. By using an adequate formulation of MPC model and an efficient QP solver, the MPC algorithm can provide better motion restitution results than the more conventional algorithms. However, few papers give a description in detail of the used MPC technique together with the right tuning parameters. Furthermore, the algorithm's stability condition is hardly addressed in motion cueing algorithm design, except a small number of studies where generally a quasi-zero terminal set condition was applied. It is probably less critical for driving simulators without large motion platform, but it can be a crucial safety factor to consider for high performance driving simulators where the motion velocity and acceleration can be high. In this paper, we summarize the most important works on the MPC based motion cueing algorithm, including the tuning experiences.

Key words: MPC, motion cueing algorithm, driving simulation, driver perception, washout.

1. Introduction

MPC algorithm, as an important advanced control technique was proposed by the end of 70s by Richalet et al., Cutler and Ramaker respectively. Thereafter, during about ten years, it was the most important control research topic. Nowadays, it becomes one of the most popular modern control methods both in academy and industry, with an exponential increase of publications from 1995 [Sor1]. In the driving simulation field, Dagdelen et al. [Dag1](2004) proposed a first MPC based motion cueing algorithm to optimize 1DOF motion cues with acceleration threshold control in washout process. Then we proposed an explicit MPC algorithm [Fan1] where an efficient stability condition was proposed. Augusto [Aug1], Beghi et al. [Beg1] and Al Qaisi et al. [Alq1] published the MPC algorithm using human vestibular model. Garrett et al. [Gar1](2013) published their MPC work taking into account vestibular model and hexapod constraints. Compared with that of more conventional motion cueing algorithms, such as classical, LQR optimal filters, the MPC technique reveals several potential advantages. However, by authors' experiences, different conclusions could be reached according to the cost function expression, the adopted stability condition, the weighting matrices and the predictive step length. It is worth to make some investigations to these sensible factors. This is the main motivation for the current paper.

In this paper, we have reviewed our MPC algorithm experiences and presented its prospects for future developments. A robust stability condition which can influence significantly the motion cueing results is addressed. The potential benefits to use vestibular model, the algorithm's tuning technique and in-line pre-position strategy are also investigated. Finally, diverse simulators performances are evaluated by using the proposed MPC-MCA (motion cueing algorithm).

2. MPC's formulation and stability condition

A complete formulation of MPC-MCA is given in reference [Fan3]. In MPC algorithm, the cost function can be written by means of following basic formulation:

$$J_N(X_k) = \min_{u_0,u_1,\ldots u_{N-1}} \sum_{i=0}^{N-1} \|\phi.\hat{x}_i - r_i\|_{q_Y}^2 + \sum_{i=0}^{N-1} \|\Delta u_i\|_{Ru}^2 + \sum_{i=0}^{N-1} \|\hat{x}_i\|_{Qx}^2 + \|\hat{x}_N\|_{Q_N}^2 \qquad (1)$$

subject to:

$$\begin{gathered} \hat{x}_k = A.\hat{x}_{k-1} + B.u_{k-1} \\ constraints: H_x.\hat{x}_k + H_u u_k \le K \qquad (2) \\ stability \ \ constraints: \hat{x}_N \in \Omega \end{gathered}$$

where $\hat{x}_k$ is an augmented state vector including motion perceived variables and simulated vehicle's acceleration. The vector, ϕ, is for extracting the corresponding motion feeling variable from $\hat{x}_k$. Δu is the linear or tilt acceleration input vector in differential form given by: $\Delta u_{k-1} = u_k - u_{k-1}$. $\hat{x}_N$ is the last terminal state, introduced for algorithm's stability consideration. Ω is a positively invariant set. The weighting coefficient or matrices, q_y, R_u, Q_x, Q_N are used to balance the trade-off between reproducing the vehicle's dynamic motion and using simulator's workspace, velocity and acceleration within its bounds.

In MPC-MCA, the cost function minimisation is generally subject to a linear system with input, output and state constraints. The system can be an ideal driving simulator, i.e. a double integrator, a simulator's transfer function, or a simulator model incorporated with human vestibular one. The macroscopic algorithm's scheme is very similar to that of LQR optimal filter, as illustrated by figure 1.

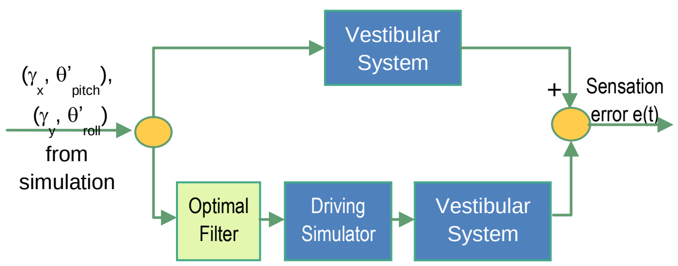

Fig. 1: LQR based motion cueing algorithm [Siv1, Tel1]

For the MPC approach, the optimal filter is replaced by MPC optimizer which minimizes the error of sensation produced from between vehicle and simulator at each time step. Generally, in motion cueing algorithm design, the actuator's motion control system provided by manufacturer is assumed perfect and without delay. Based on this hypothesis, the system model is actually an accurate numerical model. The offset problem encountered in a real plant control due to model-plant mismatch or disturbances will disappear. Thus, the algorithm's formulation can be reduced to its simplest expression. If the simulator's actuator delay is important, the induced mismatch between visual, acoustic and motion sensor cues can generate the occurrence of motion sickness [Oma1]. In this case, it is necessary to compensate the delay in motion cueing algorithm design. As we reported [Fan4], it is possible to reduce this delay by using only the identified simulator transfer function. In our approach, the plant model is always a pure numerical model for the reasons of simplicity and the cost for extensive hardware modifications. Actually, we have developed a MPC algorithm to correct this delay. The feedback from the professional drivers who are very sensitive to the phase lag confirms the significant improvement of driving perception, even with a low frequency 0.2Hz slalom scenario. Later, we will present this work.
The vestibular system, situated in inner ear, consists of two important parts. One contains the semicircular canals that sense rotational motion and the other, the otoliths that sense linear motion. Numerous vestibular transfer functions are presented in detail by Zacharias, Telban et al. [Tel1]. One of the typical transfer functions proposed by Young and Meiry(1968) describing the relationship between the specific force, f, and the perceived force, $\hat{f}$, is:

$$G_{oto}(s) = \frac{\hat{f}}{f} = \frac{k(\tau_a.s+1)}{(\tau_L.s+1)(\tau_S.s+1)}$$

The semicircular canal sensation model is given as (Young & Oman 1969):

$$G_{scc}(s) = \frac{\hat{\omega}}{\omega} = \frac{k_{scc}T_L.T_a.s^2}{(T_L.s+1)(T_s.s+1)(T_a.s+1)}$$

The corresponding state-space model can be written in different forms according to the tilt variable to consider in input of system, e.g. θ for Siven et al. [Siv1], ω for Telban et al. [Tel1] and Chen et al. [Che1]. We give below the formulation of tilt acceleration as input in order to be able to control the acceleration threshold in MPC based motion cueing algorithm:

a) otholith's model:

$$\dot{x}_{oto} = A_{oto}.x_{oto} + B_{oto}.u$$
$$x_{oto} = \begin{bmatrix} x_{oto1} & x_{oto2} & x_{oto3} & x_{oto4} \end{bmatrix}^T \hat{f} = x_{oto1}, \quad u = \begin{bmatrix} \ddot{\theta} & u_{acc} \end{bmatrix}$$
$$where:$$
$$A_{oto} = \begin{bmatrix} -\frac{\tau_L + \tau_S}{\tau_L \tau_S} & 1 & 0 & 0 \\ -\frac{1}{\tau_L \tau_S} & 0 & 1 & 0 \\ 0 & 0 & 0 & 1 \\ 0 & 0 & 0 & 0 \end{bmatrix} \quad B_{oto} = \begin{bmatrix} 0 & \frac{k.\tau_a}{\tau_L \tau_S} \\ 0 & \frac{k}{\tau_L \tau_S} \\ \frac{k.\tau_a.g}{\tau_L \tau_S} & 0 \\ \frac{k.g}{\tau_L \tau_S} & 0 \end{bmatrix} \qquad (3)$$

b) semicircular canals' model:

$$\dot{x}_{scc} = A_{scc}.x_{scc} + B_{scc}.u$$
$$x_{scc} = \begin{bmatrix} x_{scc1} & x_{scc2} & x_{scc3} & x_{scc4} \end{bmatrix}^T \hat{\omega} = x_{scc1}, \quad u = \begin{bmatrix} \ddot{\theta} & u_{acc} \end{bmatrix} \qquad (4)$$
$$where:$$
$$A_{scc} = \begin{bmatrix} 0 & 1 & 0 & 0 \\ 0 & -T_2 & 1 & 0 \\ 0 & -T_1 & 0 & 1 \\ 0 & -T_0 & 0 & 0 \end{bmatrix}, \quad B_{scc} = \begin{bmatrix} 0 & 0 \\ T_3 & 0 \\ 0 & 0 \\ 0 & 0 \end{bmatrix}, \quad T_0 = \frac{1}{T_L T_s T_a}$$
$$T_1 = \frac{T_L + T_s + T_a}{T_L T_s T_a}, \quad T_2 = \frac{T_L.T_s + T_L.T_a + T_s T_a}{T_L T_s T_a}, \quad T_3 = \frac{1}{T_s}$$

By using equations (3) and (4), we can define the system state, $\hat{x}_k$, as:

$$\hat{x} = \begin{bmatrix} x_{oto} & x_{scc} & x_{simu} \end{bmatrix}^T$$
$$with \quad x_{simu} = \begin{bmatrix} \theta & \omega & p & v & \dot{\omega} & \dot{v} \end{bmatrix}^T$$

where θ represents the tilt angle and p, x or y position, ω, v the corresponding velocity.

The state-space model is given:

$$\hat{x}_k = \begin{bmatrix} A_{oto} & 0 & 0 \\ 0 & A_{scc} & 0 \\ 0 & 0 & A_{simu} \end{bmatrix} .\hat{x}_{k-1} + \begin{bmatrix} B_{oto} & 0 & 0 \\ 0 & B_{scc} & 0 \\ 0 & 0 & B_{simu} \end{bmatrix} .\Delta u_{k-1} \qquad (5)$$

$$subject \quad to \quad H_m.\hat{x}_k + H_u.\Delta u \le K$$

where A_{simu} is the simulator's double integrator matrix. For N step states prediction, using equation (5) as recurrent formulation, we can finally express the quadratic cost function in standard form [Fan3]:

$$J_N(X_k) - J_0(x_m, R(k)) = \frac{1}{2} U^T Q_{U2} U + Q_{U1}.U$$
$$A_u.U \le b$$
$$U = \Big[\underbrace{\Delta u_1, \Delta u_2, .. \Delta u_M}_{matrixmxM}, \underbrace{\Delta u_M, .. \Delta u_M}_{matrix(mx(N-M))} \Big]^T \qquad (6)$$

Based on an efficient QP solver [Kyv1, Fer1], if the system has feasible solution, the input command U can be solved out. In MPC process, only the first term of optimal solution U is used. After updating the system with the input command Δu_1 and using the next reference signal r_{k+1}, the calculation process is repeated. This is the basic principle of MPC based motion cueing algorithm. In a real plant system control, the noise disturbances could be important and the model may not be enough accurate to describe the plant physical phenomenon. MPC algorithm can take into account the plant's measurement to correct the model predictive state and perform an offset-free reference tracking by using an integrating disturbance model. The variables in cost function should be shifted by using the steady-state reference values [Pan1]. The principle of MPC algorithm remains the same.

It is found that without any additional restriction, the standard MPC algorithm can lead to some unexpected solutions for slalom test, as illustrated in figure 2:

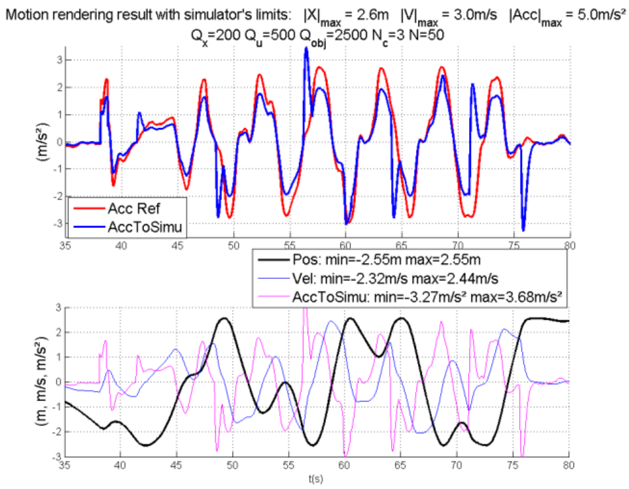

Fig. 2 Illustration of unexpected solution given by standard MPC algorithm

In fact, when the motion platform approaches its workspace limit, the simulator must slow down, called also washout process, in order to restrict its motion trajectory within bounds.

Without any additional constraint in motion cueing algorithm, the simulator acceleration could change abruptly or be in opposite direction to the vehicle acceleration with high discrepancy which can provoke a conflicted motion feeling between driver's expectancy, visual and inertial perceptions. By several off-line tuning tests for the scenario, it is possible to find a rather satisfying solution (with N=150 and Δt=8ms e.g.). But for other scenarios, the tuning parameters are not applicable, not to mention the stability problem. Thus, it is important to develop new MPC-MCA which can ensure a smooth and low discrepancy motion cues during washout process. For this purpose, we have introduced a new system constraint (see below proposed "adaptive" filter) and investigated implicit and explicit MPC algorithms to analyse the performances of existent MPC-MCA.

Another important and difficult issue is how to guarantee the stability of MPC algorithm in all cases. By using the Lyapunov function approach, the stability condition can be described by some explicit terminal set constraints, i.e. that the last predictive state must be steered into the original point or a positively invariant set. Generally, two well-known explicit terminal set conditions are adopted: the first is a zero terminal set stability condition, the second, with more large feasible solution domain is the LQR terminal set condition in which the LQR control law is completely available [Bem1]. Authors' study showed that in real-time system, the MPC algorithm using these standard conditions is efficient only if the system is 1DOF motion rendering problem. For a 2, 3DOF motions cueing problem, a limited area of feasible solutions was found [Fan2], otherwise, as used by Dagdelen et al., Augusto and Garrett et al., the stability condition must be relaxed. To improve the efficiency of MPC-MCA with perceived motion threshold control in washout process, a new system's constraint is proposed by authors, which can not only guarantee the system's stability but also keep a smoothing washout transition. This condition is expressed by the following equation:

$$x_i(t) + c_v.v_i(t).T + c_u.u_i(t).T^2/2 = x_{max} \qquad (7)$$

where x, v, u are respectively the simulator's position, velocity and acceleration and x_{max}, the simulator's excursion limit.

If the equality condition is detected in-line with current state value, the system must be slowed down.

The equation (7) can be written in Laplace-transform space as follows [Fan3]:

$$\mathrm{x_i(s)} = \frac{x_0}{s} + \frac{\mathrm{v}_0 + \omega_n{}^2(x_{\max} - x_0)/s}{\left(\mathrm{s}^2 + 2\xi.\omega_\mathrm{n}.s + \omega_n{}^2\right)} \qquad (8)$$

where the natural frequency $\omega_n = [2/(c_u.T^2)]^{0.5}$ and the damping ratio: $\xi = c_v/(2.c_u)^{0.5}$, x_0 and v_0 are the last simulator state from which the braking process or washout process is engaged. From (8), we can find that the position, $x_i(s)$, is composed of an offset, x_0, a second order system homogenous response and a step response with amplitude $(u_0+2\xi.\omega_n.v_0)$. The characteristics of second order system [Row1] show that the response feature of $x_i(s)$ is determined by the system's natural frequency and damping coefficient. Assuming that the damping ratio is superior to 1, the maximum value of $x_i(t)$ is equal to x_{max}. As a consequence, the workspace constraint condition is fulfilled at all times and the washout motion's acceleration is completely controlled by the system parameters. Recall that if the system (8) is underdamped, it can produce an overshot value which can, in some cases, be benefit to motion rendering results. If the underdamped strategy is used, the overshot value should be taken into account in the limitation of workspace consequently.

Note that in the classical filter approach, a 2e order HP filter is applied to limit the simulator excursion:

$$G_{HP}(s) = \frac{u_s(s)}{u_{veh}(s)} = \frac{\mathrm{k.s}^2}{\left(\mathrm{s}^2 + 2\xi.\omega_{\mathrm{n}1}.s + \omega_{n1}{}^2\right)} \qquad (9)$$

where $k/\omega_{n1}{}^2 < x_{\max}/u_{step}$ and:

$$for.small.simulator.stroke: \omega_{n1} = 2.5 - 4, \xi = 1 - 1.4$$

$$for.big.simulator.stroke(\mathrm{Renault}, PSA.etc.): \omega_{n1} = 0.7 - 1, \xi = 0.7 - 1.4$$

The HP filter's parameters must be designed at worst case, i.e. the step signal for which the maximum stroke is required. Another disadvantage of classical filter is the backlash effect produced at the end of acceleration or braking signal (cf. fig. 3) which is very difficult to be fully compensated by the tilt motion and causes often the artifacts effect or simulator sickness [Rey1]. Compared with relation (9), the corresponding acceleration HP filter of relation (8) can be rewritten as [Fan3]:

$$G_{HP2}(s) = \frac{u_s(s)}{u_0/s} = \frac{\left[1 - \frac{\omega_n^{\ 2}(v_0/u_0)}{s}\right]s^2}{\left(s^2 + 2\xi.\omega_n.s + \omega_n^{\ 2}\right)} \qquad (10)$$

which can be considered as a special explicit adaptive filter with filter's gain taking into account the evolution of simulator state. If we fixed c_v = 1, and c_u = 0.45, we have only one parameter T to consider. In this case, the reasonable value of T deduced by simulation experiences is between 0.8 to 3, and thus leads to ω_n = 0.7 to 3.0. The figure 3 illustrates the classical filter and proposed "adaptive" filter's results for the rectangular pulse reference signal.

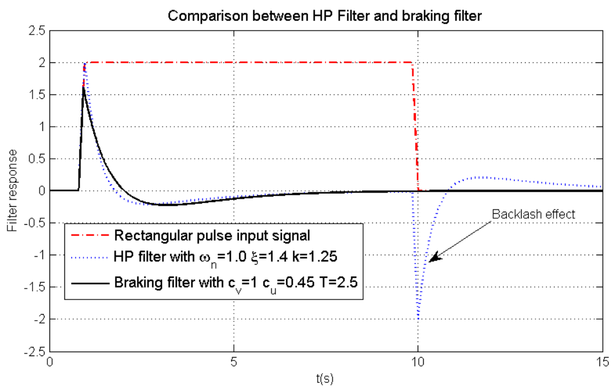

Fig. 3 Comparison of filters results between classical HP filter and proposed filter

According to the filters results presented in figure 3, we can find that the backlash effect is completely removed by using the proposed filter (10). The relation (7) is a linear combined expression of state variables. It is easy to integrate, as system constraint, in MPC model.

3. Influence of vestibular system and tuning process description

3.1. Tuning process description

Before addressing the topic of vestibular model's influence in the MPC algorithm, we describe at first the tuning method and the used tuning signal, a rectangular pulse. Not only it is simple, but also it is very close to the braking deceleration measurement. Compared with the acceleration or deceleration signal in full throttle or gas pedal releasing manoeuvers, both accelerations are similar too, but not for deceleration caused by the natural vehicle resistance forces (aerodynamic force, rolling resistant force, powertrain force). The slope of deceleration at the end of the rectangular pulse is steeper than that of vehicle's natural deceleration. So it is a severe motion rendering signal. Hence, if we can get a satisfactory tuning result for this basic signal, the tuning task for a general purpose driving test is almost achieved.

By choosing the different weighting coefficient or matrices, 8 coefficients in total with 2 additional constants T_x and T_θ, a rather good trade-off result is obtained within the required system constraints (cf. fig. 4). Once the step signal tuning is realized, the position weighting parameter can afterwards be adjusted to enhance the washout occurrence for the general driving tests. The motion cueing algorithm is then tested in Renault's 8DOF driving simulator. A satisfactory driving simulator feeling is obtained from normal drivers as well as internal professional drivers.

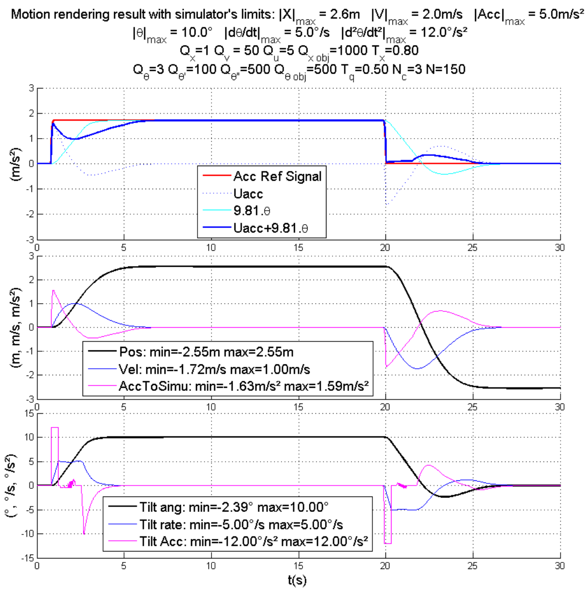

Fig. 4: 2DOF motion rendering result using MPC ideal simulator's model for rectangular pulse

In practice, the tilt threshold control is a more complex issue. As reported by [Cha1], the threshold can be raised if a linear motion occurs simultaneously. In addition, vehicle's pitch rate or pitch acceleration can be higher than the conventional tilt thresholds in some short lapse of time. These two factors are also considered in our MPC algorithm to have an optimal tilt motion. The accurate dynamic thresholds will be quantified in our future experiences for the restitution of longitudinal motion.

3.2. Using vestibular model or not

The integration of vestibular system in the MPC state-space model aims at approaching as close as possible the perceived inertial force and rotational rate between a real car and the simulator virtual environment. From a scientific standpoint, it could improve the efficiency of motion cueing algorithm if the models are representative of the human vestibular system. In fact, we have used the model's dynamic and dead-detection features to optimize the washout process or the motion cues. As reported by Chen et al. [Che1], when the reference signal is below some threshold, a washout process is automatically started. This simple strategy can improve motion cueing efficiency due to more exploitable simulator excursions. But the use of such threshold can unfortunately increase the system's delay and disturb more or less the delay compensation function if it is implemented. It is a method suitable for relatively calm motion situation. The washout algorithm based on the vestibular dynamic feature, as studied in a fight simulator [Tel1] firstly, reveals its potential advantages for general purposes. However, the evaluation of benefice using vestibular model is not so obvious without experimental tests. In fact, the motion cueing result depends on in some ways the used parameters of vestibular model. We report in table 1, some typical transfer functions of vestibular system. The convolution results between the transfer functions and the rectangular pulse signal demonstrate that not all the dynamic features given by various vestibular models are similar. The perceived specific force evaluated by using Telban's otoliths model is similar to that of Glasauer & Israël. These two models have more large frequency bandwidth than others. Young and Ormsby's otoliths models have more LP filer feature and give smoother response signal than the two previous ones. Figure 5 shows that the high frequency bandwidth otoliths' models give a filter result close to the ideal simulator's one for a fast change signal. But for the final response of a steady specific force, the perceived value is about twice lower than the beginning for the rectangular pulse signal. It is probably the area that we can exploit to optimize the washout process with some allowed tracking error. So it would be a useful work to compare the motion rendering results given by incorporating or not the vestibular model in motion cueing algorithm.

Table 1. Human vestibular model parameters [Tel1]

$\frac{\hat{f}}{f}=\frac{k(\tau_a.s+1)}{(\tau_L.s+1)(\tau_S.s+1)}$				
Parameter	Young & Meiry (1968)	Ormsby (1974)	Glasauer & Israël (1995)	Telban et al. [7]
τ_a	5.3	7.5	7.5	5.0
τ_L	0.66	0.51	0.0	0.016
τ_S	13.2	10.1	20.0	10
k	0.4	0.4	0.4	0.4
Threshold, d_{TH} (m/s²)	Sway = 0.17 Surge = 0.17 Heavy = 0.28 [16]			
$\frac{\hat{\omega}}{\omega}=\frac{k_{scc}T_L.T_a.s^2(1+T_b.s)}{(T_L.s+1)(T_s.s+1)(T_a.s+1)}$				
Parameter	Ormsby & Young (1977)	Reid & Nahon [16]	Reid & Nahon [16]	Telban et al. [7]
T_L	18	6.1 (Roll)	5.3 (Pitch) 10.2 (Yaw)	5.73
T_S	0	0.1	0.1	0.005
T_a	30	30	30	80
T_b	0	0	0	0.06
k_{scc}	1.0	1.0	1.0	28.65
Threshold	Pitch=2.0°/s Roll = 2.0°/s Yaw = 1.6°/s [16]			

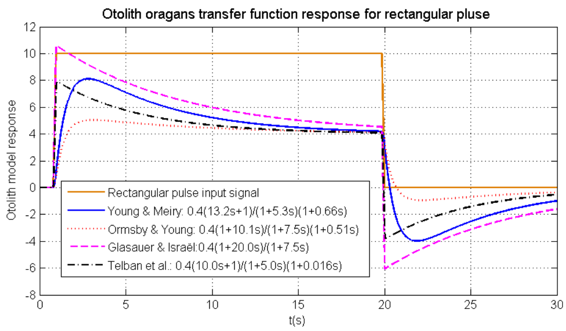

Fig. 5: Comparison of dynamic features given by various otoliths' models

Figure 6 illustrates that a motion rendering result obtained from Young & Meiry otoliths model can give high frequency false cues. It is consistent with the result presented in figure 5. Naturally, using Δu as input MPC control, the corresponding state variable u can be regulated more smoothly in MPC algorithm.

Figure 7 illustrates an experience's test result. A good feedback is obtained from normal and professional drivers. Note that, in this test, the vertical acceleration plays also a non negligible role for the fidelity of driving simulation.

The professional drivers remarked also the benefice of hexapod linear motion to enhance the longitudinal acceleration feeling. One of the developed MPC 3DOF motion cueing algorithm structures not detailed here is very similar to that in classical filter [Fis1].

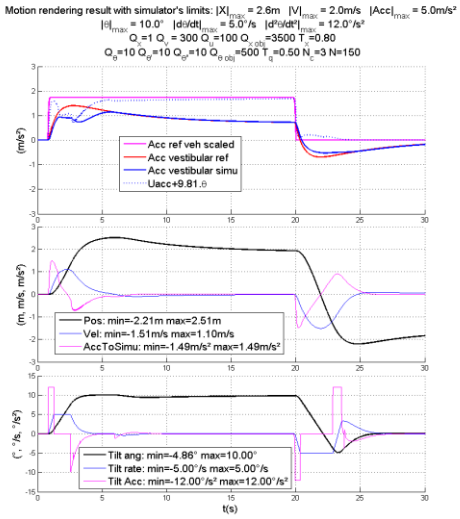

Fig. 6: 2DOF motion rendering result using vestibular models for rectangular pulse

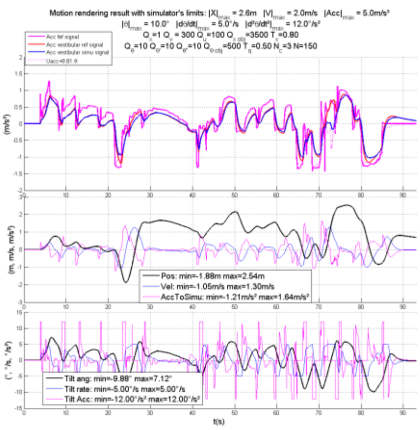

Fig. 7: 2DOF motion rendering result using vestibular models for longitudinal acceleration

4. Pre-position technique and vehicle motion prediction

The figure 4 shows that a good agreement is generally obtained by using MPC based motion cueing algorithm. However, if we focus on the first fraction of motion rendering result, we can observe that there is a lack of linear acceleration level in specific force 2 seconds after tracking the reference signal. We can also observe that the falling signal tracking at the end of rectangular pulse is well achieved. In fact, the different motion rendering results of these two similar reference signals can be explained by the available rail length. In the beginning, the simulator is in its neutral position. We have 2.6m rail stroke, at the end, double available distance. If a pre-position technique is carried out just before the desired event, the motion rendering result will be better. By using the pre-position technique, a simulated result presented in fig. 8 confirms the preceding analysis. Compared with the motion rendering result reported in fig. 4, we can find the crucial role played by this technique. For this purpose, a bang-bang motion control algorithm (time minimization algorithm) which can be activated in-line by scenario is developed in Renault's driving simulator. Once the optimal position is reached, by means of detecting some trigger signal, e.g. a fast velocity change from pedal, the MPC algorithm takes the motion cueing task immediately. Note that the senseless pre-position motion must be controlled under the perceived threshold. It takes about 7-15s to reach the optimal position for the ULTIMATE. The benefice given by pre-position technique leads us to think naturally our future development to incorporate a driver's model in order to predict oncoming trajectory. For MPC based driver model, using road information, imposed velocity range, acceleration limit and vehicle's dynamic model, a vehicle motion prediction is possible. As presented by LMS and VI-Grade, the MPC algorithm can already forecast a right vehicle trajectory using 40-50m of forward road information. Using this technique to predict the vehicle's acceleration or deceleration could be helpful to accomplish the pre-position task. However, the driver's small random action on vehicle's command (steering-wheel, gas pedal or brake) can completely change the simulator's trajectory. It is important to set appropriated threshold to filter any undesired manoeuvre.

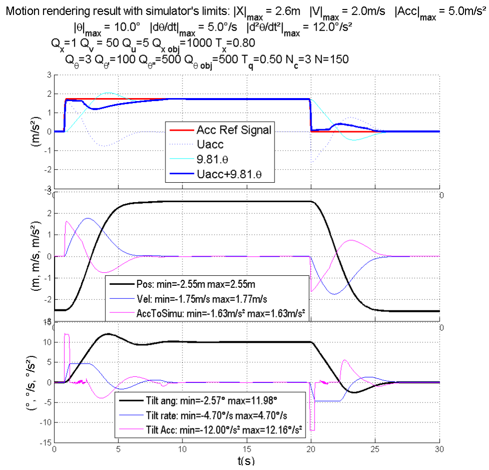

Fig. 8: 2DOF motion rendering result with help of pre-position technique

5. Evaluation of simulators potential performances based on motion cueing algorithm

One of important questions to build X, Y rails based simulator is that what is the optimal rail stroke to achieve a desired specific force or acceleration tracking task? Based on ULTIMATE actuators' performances and others, we have compared here simulators performances using three scenarios. The first is the 0.2Hz slalom manoeuvre in scale 1:1 or an artificially amplified acceleration signal, the second, a scaled emergency braking signal limited to 5m/s², and the last, a general starting braking scenario. The reason to limit the deceleration level to 5m/s² for the emergency braking is given as below:

- the tilt angle can't exceed 30° without perceived tilt cockpit position (Aubert effect[Rey1]).
- the limitation on rail stroke and tilt rate makes the full specific force signal tracking difficult, even impossible in the case of tracking a sustained acceleration signal superior to 5m/s².

Note that, for the slalom test, the higher the slalom frequency, the higher the lateral acceleration which can be reproduced by linear motion if the simulator's frequency bandwidth allows to. For the 0.2Hz slalom test, only 1DOF motion cueing results are compared.

The table 3 summarizes the simulated potential performances.

Table 3: Simulators performances evaluated by 1DOF and 2DOF MPC based motion cueing algorithm

Scenario Simulator	*0.2Hz slalom / 1DOF*	*emergency braking for 5s(>5m/s²) / 2DOF*	*starting & braking longitudinal cues[(b)] /2DOF*
ULTIMATE	2.8m/s²	1.7m/s²	1.8m/s²
DAIMLER	7.5m/s²	2.5m/s²	3m/s²
TOYOTA*	6m/s²	5m/s² [(a)]	5m/s²

*Assumption: available stroke X=35m, Y=20m, V≤6m/s, Acc≤6.5m/s²; (a): in limited acceptance (b) 2-3s events

It can be found from table 3 that the simulators lateral performances could be high for slalom test, while the longitudinal performances, rather limited to 5m/s² for sustained acceleration or deceleration. Note that, if the event takes place in short duration, the combined rail and hexapod linear acceleration can reach very high performance. This situation is not compared here.

6. Conclusion

In this paper, the Renault's latest MPC based motion cueing algorithm theory and practices have been reviewed. The proposed system stable condition is emphasized by a comprehensive physical mean and can be considered as a special adaptive filter. It doesn't need to steer again the last predictive step into a positively invariant set, because it is [Fan2]. Beside of its important role played in the algorithm's stability, another one is its capability to reduce the predictive step length's influence on the motion cueing results. It thus enhances significantly the efficiency of MPC-MCA with motion threshold control in washout process. Using this condition, we have developed both explicit and implicit MPC-MCA. The former is more robust for algorithm implementation and the later, more flexible and more powerful is suitable for handling high complex-system and also for performing off-line simulation, tuning task. However, the iteration-limit set in the QP solver due to the on-line requirement could make the implicit MPC algorithm unstable [Mor1]. Even if it is a very low probability event, specific safety algorithm needs to be implemented to prevent from motion cueing algorithm's crash in high performance simulators.

7. References

[Alq1] Al Qaisi I., A. Traechtler, "Constrained Linear Quadratic Optimal Controller for Motion Control of ATMOS Driving Simulator", DSC Europe 2012 proceedings, Paris, France

[Aug1] Augusto B.D.C., "Motion Cueing in the Chalmers Driving Simulator: An Optimization-Based Control Approach", Master of Science Thesis, 2009

[Beg1] Beghi A., M. Bruschetta, F. Maran, D. Minen "A Model-based Motion Cueing strategy for compact driving simulation platforms", DSC Europe 2012 proceedings, Paris, France

[Bem1] Bemporad A. and M. Morari, "Robust Predictive Control: A Survey", Robustness in Identification and Control, vol. 245, pp. 207-226, 1999

[Cha1] Chapron T., Colinot J.P., "The new PSA Peugeot-Citroën Advanced Driving Simulator – Overall design and motion cue algorithm", DSC North America 2007 proceedings, Iowa City

[Che1] Chen S.H., and Li-Chen Fu, "An Optimal Washout Filter Design for a Motion Platform with Senseless and Angular Scaling Maneuvers", American Control Conference (ACC), 2010: Baltimore, Maryland, USA, 30 June - 2 July 2010

[Dag1] Dagdelen M., G. Reymond, A. Kemeny, M. Bordier, and N. Maýzi (2004). "MPC based motion cueing algorithm : Development and application to the ULTIMATE driving simulator", DSC Europe 2004 proceedings, pp. 221-233, Paris, France

[Fan1] Fang Z., A. Kemeny. "Motion cueing algorithms for a real-time automobile driving simulator", DSC Europe 2012 proceedings, pp. 159-174, Paris, France

[Fan2] Fang Z., A. Kemeny. "Explicit MPC motion cueing algorithm for real-time driving simulator", IPEMC 2012 (June-2-5 2012) Harbin, China Vol. 2 (2012) 874-878

[Fan3] Fang Z., A. Kemeny. "An efficient MPC based motion cueing algorithm to driving simulator", Internal report, Renault, May 2014

[Fan4] Fang Z., G. Reymond, A. Kemeny, "Performance identification and compensation of simulator motion cueing delays", DSC Europe 2010 proceedings, Paris, France

[Fer1] H.J. Ferreau and H.G. Bock and M. Diehl, "An online active set strategy to overcome the limitations of explicit MPC", International Journal of Robust and Nonlinear Control, 2008, vol. 18, N°8, pp.816—830

[Fis1] Fischer M., Sehammer H. and Palmkvist G., "Motion cueing for 3-, 6- and 8-degrees-of-freedom motion systems", DSC Europe 2010 proceedings, Paris, France

[GAR1] Garrett N.J.I., M. C. Best, "Model predictive driving simulator motion cueing algorithm with actuator-based constraints", Vehicle System Dynamics: International Journal of Vehicle Mechanics and Mobility Vol.51, Issue8, (2013) 1151-1172

[Kva1] M. Kvanisca, "Real-Time Model Predictive Control via Multi-Parametric Programming: Theory and Tools, VDM Verlag, 2009

[Mor1] Morari M. & Jones C. et al., "Real-time optimization for distributed model predictive control", 2010, Automatic control Laboratory, ETH Zürich

[Oma1] Oman C.M., 1990, "Motion sickness: a synthesis and evaluation of the sensory conflict theory", Can J Physiol Pharmacol 68(2), 294-303

[Pan1] Gabriele Pannocchia, "Course on Model Predictive Control Part II – Linear MPC design", University of Pisa, Italy, July 2012

[Row1] Rowell D., "Review of First- and Second-Order System Response", (2004), MIT, web.mit.edu/2.151/www/Handouts/FirstSecondOrder.pdf

[Siv1] Sivan R., Ish-Shalom J., and Huang J. K., "An Optimal Control Approach to the Design of Moving Flight Simulators", IEEE Transactions on Systems, Man, and Cybernetics, 1982. 12(6): p. 818-827

[Sor1] Olof Sörnmo and Anna Lindholm, "An Evaluation of the Development of Different Areas within Automatic Control over the Years", May, 2012 http://www.control.lth.se/media/Education/DoctorateProgram/2012/HistoryOfControl/Anna_Olof-SomeFields-rep.pdf

[Tel1] Telban Robert J. and Frank M. Cardullo, "Motion Cueing Algorithm Development: Human-Centered Linear and Nonlinear Approaches", NASA /CR-2005-213747

SUBJECTIVE EVALUATION OF DIFFERENT MOTION CUEING ALGORITHMS IMPLEMENTED ON ATMOS DRIVING SIMULATOR

Imad Al Qaisi [1], Daniel Zimmermann [1], Andreas Kohlstedt [1], Sandra Gausemeier [1], Ansgar Trächtler [1]

(1) : Heinz Nixdorf Institute, University of Paderborn, Fürstenallee 11, 33102 Paderborn, Germany
Tel : +49 5251 60-6276 Fax : +49(0) 5251 60-6297
E-mail : {alqaisi, Daniel.Zimmermann, Andreas.Kohlstedt, Sandra.Gausemeier, Ansgar.Traechtler}@hni.uni-paderborn.de

Abstract – The objective of this work is to compare a novel motion cueing algorithm based on the constrained linear optimal controller (CLOC) as introduced in [Alq1] to two established algorithms, namely the classical and adaptive algorithms [Neh11, Neh12]. A subjective motion cueing quality criterion was used to evaluate the fidelity of the ATMOS driving simulator and to assess the quality of the motion cueing algorithms. A group of test subjects attended three pre-simulated rides on the same track, each controlled by one of the different control strategies. The analysis of the subjective evaluation shows that the adaptive motion cueing algorithm provides the best impression in longitudinal direction. However, the subjects perceive that the CLOC strategy provides the most realistic impression in the lateral direction as well as the most comfortable and realistic feeling. None of the subjects experienced simulation sickness. All of them easily and quickly overcame any kind of discomforts.

Key words: Driving simulators**,** Motion cueing, CLOC, Subjective quality criterion, Real-time implementation.

1. Introduction

Any driving simulator aims to give a realistic impression of the vehicle motion to the driver. Typically, driving simulators are constructed from several subsystems that contribute to the overall replication of the senses felt in a vehicle. Driving simulators are mainly constructed from mechanical moving parts to provide inertial cues as well as a virtual reality system to provide the visual cues corresponding to the actual driving situation. Ideally, the driver perceives the same accelerations and rotational movements as he anticipates from the visual environment in order to give him a more realistic impression of the simulated driving maneuver. Due to the limitations of the workspace and the simulator motion systems' technological constraints, the vehicle's translational accelerations and angular velocities as generated by the vehicle dynamic model cannot be reproduced unaltered by the motion system. Therefore, the simulated vehicle's motion must be rendered in a specific manner in order to provide the simulator with admissible signals. Those signals should provide the driver with a feeling close to reality while keeping the simulator within its technological constraints and capabilities. Any kind of contradiction between the motion trajectories of the simulator and the trajectories generated by vehicle dynamic virtual reality models will have significant detrimental effects on the driving simulation and could provoke simulator sickness which is more likely to cause dizziness, headaches and nausea to the simulator driver. Therefore, the use of motion in simulators is still subject to debate and the implementation of motion control/cueing strategies is vital.

The motion control strategy that is used to render the vehicle accelerations and velocities is commonly called motion cueing algorithm. Several motion cueing algorithms which use frequency domain techniques to calculate the simulator's motion from the simulated vehicle's accelerations have been proposed for flight and driving simulators, such as classical motion cueing algorithms [Sch16, Gra9, Neh11, Neh12], adaptive motion cueing algorithms

[Par13, Rei14, Rei15], and optimal algorithms [Rei14, Rei15, Tel18, Siv17]. Furthermore, a few model predictive approaches have been developed for motion control of driving simulators [Dag6, Aug4].

Subjective and objective motion cueing quality criteria may be used out to evaluate the fidelity of driving simulators and to rate the quality of motion cueing algorithms to transfer vehicle accelerations and velocities to those in the actual simulator.

This work focuses on a subjective quality criterion to compare three different motion cueing approaches, namely the classical motion cueing algorithm, the adaptive motion cueing algorithm and the model based constrained linear optimal control (CLOC) strategy [Alq1], implemented on the ATMOS driving simulator. Several test persons were asked to participate in three simulated driving maneuvers and to rate their experiences afterwards.

2. ATMOS Driving Simulator

The driving simulator of the University of Paderborn (ATMOS driving simulator) serves a wide range of applications. Primarily, it is used as a virtual prototyping tool in the development of advanced driver assistance systems (ADAS). The simulator enables developers to test these systems under safe and reproducible conditions. Furthermore, it may be used to study the driver's behavior and to systematically train the driver for specific situations or in the handling of various driver assistance systems.

Fig. 1. ATMOS Driving Simulator.

The ATMOS driving simulator (Fig. 1) is a modular system. It grants high flexibility by offering the ability to replace the driving cabins not only as a hardware component, but also with fully parametrisable software [Has10]. The simulator consists of two main components: a visualization system and a motion system.

The visualization system includes a 240° circular projection wall with eight identical projectors. Each projector has a resolution of 1400 x 1050 pixels, covers 30° and a 128 pixel edge-blending zone with neighboring projectors.

The motion system provides five independent degrees of freedom (DOF). This is accomplished by two dynamical components. The first one is the motion platform which can be tilted around the lateral as well as the longitudinal axis with maximum angles of 13.5° and 10.0° respectively. Two belt drives in each direction perform these movements in arbitrary combination. The platform is used to simulate the vehicle's longitudinal and lateral acceleration. The other three DOF are provided by the second dynamical component: the shaker platform. It is actuated by crank drives and is used to simulate the vehicle's roll velocity, pitch velocity and vertical acceleration.

The computations of the underlying vehicle model and the motion cueing algorithms are carried out by a dSPACE real-time simulator. It has several IO-ports which are connected to the simulator's vehicle mock-up interface, an inertial measurement unit (IMU) and the inverters controlling the electrical drives of the motion system (Fig. 2). A controller area network (CAN) interface is used for transmitting the appropriate signals such as the desired actuator actions.

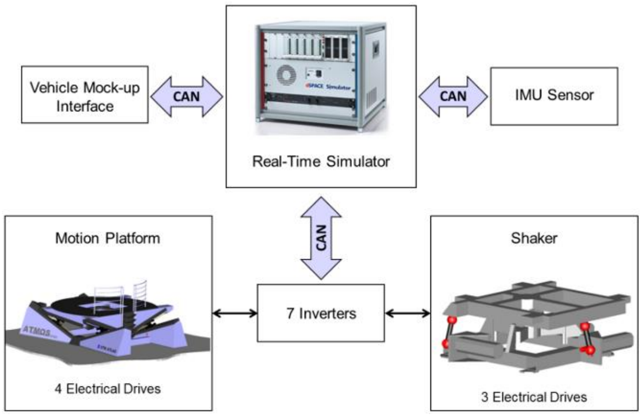

Fig. 2. Hardware components of the motion system.

The vehicle mock-up provides the driver's inputs such as the steering angle, accelerator and brake pedal position and current gear. It receives the calculated vehicle velocity and the engine speed from the real-time simulator and displays these values on the vehicle's dashboard. The IMU is located near the vehicle's center of gravity to compare the measured and desired vehicle accelerations and angular velocities.

3. Motion Cueing Algorithms

Traditionally, motion cueing algorithms were derived experimentally. However, the most common fundamentals of these algorithms are scaling, tilt coordination and filtering. Combinations of these techniques are necessary to meet the performance and fidelity requirements of motion simulators.

One of the oldest and most commonly used in driving simulators is the classical motion cueing algorithm. It renders the translational vehicle accelerations using a combination of linear high-pass and low-pass filters. However, only high pass filters are used to render the vertical vehicle acceleration since the tilt coordination can only be used to render the sustained longitudinal and lateral accelerations. The outputs of the tilt coordination are then fed into the channel of the rendered angular velocities. Afterwards, the combined generated angles are used to drive the simulator in pitch and roll cues. The classical algorithm implemented in this work is shown in Fig. 3(a).

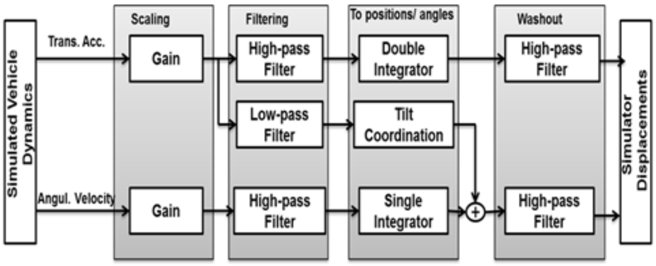

(a) Classical motion cueing algorithm.

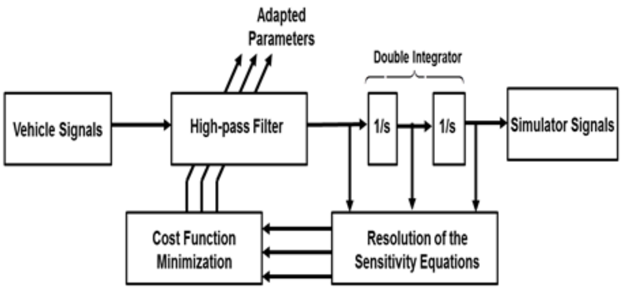

(b) Scheme of the adaptive washout filter.

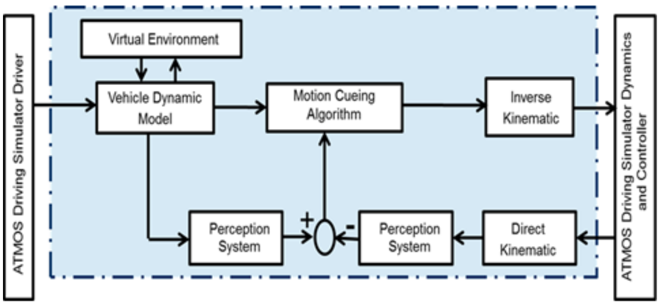

(c) Model based motion control strategy (CLOC).

Fig. 3. Implemented washout algorithms.

Unlike the classical approach, adaptive motion cueing algorithms use the steepest descent technique to carry out a minimization of a cost function consisting of the acceleration errors subject to the constraints regarding the velocities and displacements of the simulator. For that reason, the resulting filter parameters are variable in real-time and are computed at each time step of the simulation. Fig. 3(b) shows the general scheme of the adaptive high-pass washout filter.

In the constrained linear quadratic optimal controller (CLOC) strategy as introduced in [Alq1], an optimization problem is solved online over a finite time horizon. This approach minimizes the difference between the accelerations anticipated by the driver and the actual perceived motions generated by the motion system while keeping the simulator within its technological constraints. The parameters of the model based approach are chosen by trial and error to guarantee the best tracking of the perceived movements in the vehicle and to ensure the stability of the constrained linear quadratic optimal controller implementation. Fig. 3(c) shows the block diagram of the model based motion control strategy in the ATMOS driving simulator.

To implement the CLOC strategy, it is necessary to solve a quadratic programming problem [Alq1]. There are many software tools with integrated solvers available [And3, Cga5, Ger8]. However, these tools use operating system specific precompiled files and, thus, cannot be used to generate code for the employed dSPACE real-time simulator. One possibility to use the CLOC algorithm for the generation of motion signals in real-time (for so-called active driving scenarios) is to reimplement it using the Model Predictive Control Toolbox by The MathWorks. The toolbox supports C-code generation for embedded systems such as dSPACE real-time hardware.

4. Motion Cueing Quality Criterion

The main goal of motion cueing algorithms is to produce admissible motions within the driving simulator's physical boundaries. The simulated vehicle's motion is reproduced in order to provide a high degree of realism in a computer generated virtual environment. Subjective and objective motion cueing quality criteria may be used to evaluate the fidelity of driving simulators and to measure the quality of motion cueing algorithms.

The objective motion quality criterion is used to evaluate different motion cueing algorithms offline and without time consumption [Alq2].

However, subjective motion cueing quality criteria offer various advantages such as the possibility to get a subjective evaluation of experienced and inexperienced drivers. The driving impressions of the test drivers can be collected by a questionnaire, which includes technical questions as well as questions about the perception of motions or realism of the simulator in particular. This human-in-the-loop evaluation method is considered as a straightforward and consistent method to assess the fidelity of a driving simulator. Furthermore, different motion cueing algorithms are evaluated and compared to each other based on subjective ratings of realism regarding the rendered vehicle motions. The questionnaire focuses on different aspects and situations including the feelings during braking, acceleration and cornering maneuvers, simulator sickness, opinion of realism, visual environment and hardware evaluation.

Moreover, these evaluation tests can be conducted to study the fidelity of the simulator response to specific driver inputs (active mode) or by applying the simulator with pre-specified trajectories generated by different motion cueing algorithms (passive mode).

After the experiments, subjective reactions are collected to evaluate the behavior validity, quality of various motion cueing techniques and the driving simulator behavioral fidelity in general.

5. Implementation and Results Analysis

The driver's perception of motions depends on several factors such as the virtual environment, the acoustic system as well as the vehicle motion. Hence, to attribute the subject's perception of motions solely to the underlying motion cueing variant, a precalculated driving scenario was used during the experiments (passive driving). All test persons took part in the same ride three times except for the fact that the simulator's motion was computed by different motion cueing algorithms.

In the present case an actual track in a non-urban area of Northrhine-Westphalia with a length of 3 km, several curves and various velocities was used as testing scenario. Thereby, a wide range of lateral and longitudinal accelerations is included in the ride. The simulated vehicle's accelerations were calculated by an ASM-dSPACE [dSP7] vehicle model. The results have been used as reference inputs for the three motion cueing algorithms. Afterwards, the three different control strategies for the driving simulator were computed.

The test subjects attended these three precalculated rides on the same track. Altogether, 23 subjects took part in the evaluation. The participants, aged from 25 to 56 years, owned a valid driver's license and were of varying driving experience. The experience criterion is based on the test subject's driving experience concerning simulators and real vehicles. The evaluations of each group are multiplied by a suitable weighting factor. The subjects were asked to evaluate the driving simulator while being passive drivers in the cabin, i.e., they did not control the motion of the car.

At the end of the experiments, each subject was asked to fill out a survey on the realism and quality of the rides. This questionnaire served as the subjective evaluation of the ATMOS driving simulator performance based on the participant's experience. The participants were asked to evaluate the three algorithms based on the following criteria: i) perceived motion in the simulator compared to the reality, ii) simulator sickness, iii) comfort and iv) realism of the whole driving test. Each subject had to evaluate his/her driving experience on a scale of 1 to 5, where 1 denoted the worst performance and 5 denoted the best performance. Fig. 4 shows the results of this evaluation.

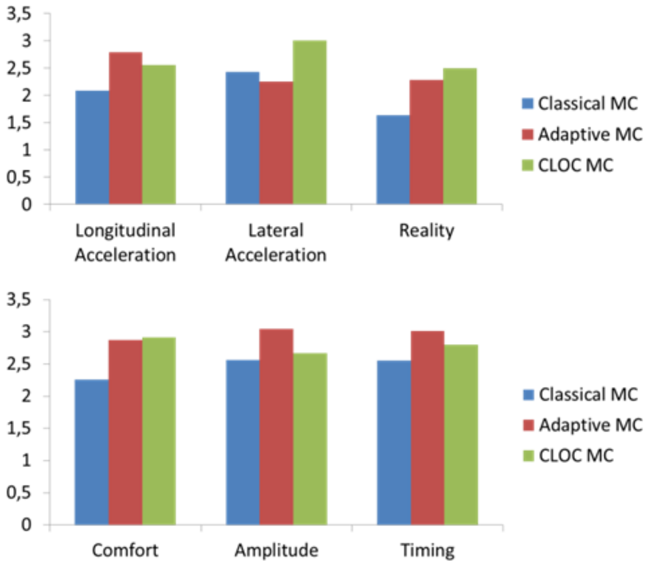

Fig. 4. Subjectives' performance evaluation of ATMOS Driving Simulator.

The analysis of the evaluation results shows that the adaptive motion cueing algorithm provides the best impression in longitudinal direction. Obviously, many subjects prefer low acceleration gain scaling compared to high scaling. However, the subjects perceive that the CLOC strategy provides the most realistic impression in the lateral direction as well as the most comfortable and realistic feeling. None of the subjects experienced simulation sickness. All of them easily and quickly overcame any kind of discomforts.

Jerky movements were observed in each of the three rides, but most significantly, they appeared within the ride based on the classical motion cueing algorithm.

Fig. 5 shows a physical trajectory comparison between the perceived signals in the simulator and the perceived signals in the vehicle. The perceived signals in the simulator are the simulator translational acceleration and angular velocity measurements filtered by a model of the human perception system. The comparison shows that there is a noticeable difference between the signals rendered by the classical or adaptive algorithms and those rendered by the CLOC strategy.

The results show a very good matching between the two perceived signals in the driving simulator generated by CLOC approach and the simulated vehicle. This good matching is a result of integrating human perception models in the optimization problem and considering the constraints of the simulator in the optimization problem instead of using gains scaling and limiters. Moreover, using the adaptive motion cueing algorithm provides a slightly better performance compared to the classical motion cueing algorithm. Nevertheless, the classical algorithm has an advantage of simple parameter tuning compared to the adaptive algorithm.

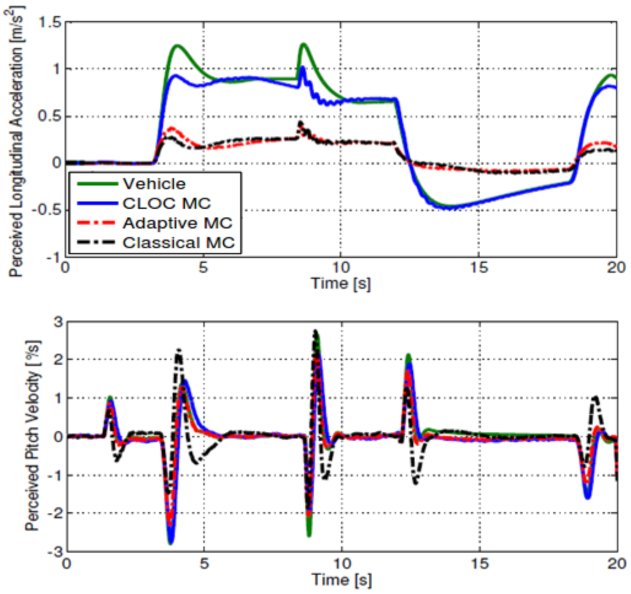

Fig. 5. Physical trajectory comparison.

6. Conclusion

In this work, three different motion cueing algorithms were investigated, designed, implemented and tested in the simulation environment of the ATMOS driving simulator. The performance of the model based strategy was compared against the classical and adaptive algorithms. The classical and adaptive motion cueing algorithms represent conventional approaches commonly used in driving simulators. The performance and quality of the three control strategies were subjectively evaluated.

The subjective quality evaluation was based on subjective impressions of a group of experienced and inexperienced drivers. The subjects rated the driving simulation while being passive drivers in the cabin, i.e., they did not control the motion of the car. Then, each subject was asked to fill out a survey on the realism and quality of the ATMOS driving simulator. The subjective evaluation results show that the model based strategy (CLOC) provides significantly the most realistic impression in the lateral direction. However, the subjects preferred the adaptive motion cueing algorithm in the longitudinal direction due to its low gain scaling. Moreover, the CLOC approach provides the most comfortable and realistic driving feeling without any simulator sickness.

7. Acknowledgement

This work, as part of the project TRAFFIS (German acronym for "Test and Training Environment for Advanced Driver Assistance Systems"), is funded by European Union and the Department for Economy, Energy, Industry, Trade and Craft of North Rhine-Westphalia, Germany.

8. References

[Alq1] Al Qaisi I., Trächtler A. Constrained Linear Quadratic Optimal Controller for Motion Control of ATMOS Driving Simulator. In Driving Simulation Conference. 2012.

[Alq2] Al Qaisi I., Trächtler A. Human in the Loop: Optimal Control of Driving Simulators and New Motion Quality Criterion. In IEEE International Conference on Systems, Man and Cybernetics (SMC). 2235-2240, 2012.

[And3] Andersen E. D., Jensen B., Jensen J., Sandvik R., Worsoe U. MOSEK version 6 Technical report TR-2009-3. 2009.

[Aug4] Augusto B., Loureiro R. Motion Cueing in the Chalmers Driving Simulator: A Model Predictive Control Approach. Master thesis, Chalmers University of Technology, Goeteborg. 2009.

[Cga5] The CGAL Project. CGAL User and Reference Manual. CGAL Editorial Board, 4.4 edition. 2013.

[Dag6] Dagdelen M., Reymond G., Kemeny A., Bordier M., Maïzi N. Model-based predictive motion cueing strategy for vehicle driving simulators. In Control Engineering Practice. 17(9): 995-1003, 2009.

[dSP7] dSPACE GmbH: ASM Vehicle Dynamics Simulation Package. Product Information, Paderborn, Germany, 2000.

[Ger8] Gertz E. M., Wright S. J. Object-Oriented Software for Quadratic Programming. In ACM Transactions on Mathematical Software (TOMS). 29(1): 58-81, 2003.

[Gra9] Grant P. R., Reid, L. D. Motion washout filter tuning: Rules and requirements. In Journal of Aircraft. 34(2): 145-151, 1997.

[Has10] Hassan B., Berssenbrügge J., Al Qaisi I., Stöcklein J. Reconfigurable Driving Simulator for Testing and Training of Ad-vanced Driver Assistance Systems. In IEEE International Symposium on Assembly and Manufacturing (ISAM). 337-339, 2013.

[Neh11] Nehaoua L., Arioui H., Espie S., Mohellebi H. Motion cueing algorithms for small driving simulator. In IEEE International Conference on Robotics and Automation (ICRA). 3189-3194, 2006.

[Neh12] Nehaoua L., Mohellebi H., Amouri A., Arioui H., Espié S., Kheddar A. Design and control of a small-clearance driving simulator. In IEEE Transactions on Vehicular Technology. 57(2): 736-746, 2008.

[Par13] Parrish R. V., Dieudonne J. E., Bowles R. L., Martin D. J. Coordinated Adaptive Washout for Motion Simulators. In Journal of Aircraft. 12(1): 44-50, 1975.

[Rei14] Reid L. D., Nahon M. A. Flight Simulation Motion-base Drive Algorithms: Part 1 - Developing and Testing the Equations. In UTIAS Report No. 296, 1985.

[Rei15] Reid L. D., Nahon M. A. Flight Simulation Motion-base Drive Algorithms: Part 2 - Selecting the System Parameters. In UTIAS Report No. 307. 1986.

[Sch16] Schmidt S.F., Conrad B. Motion drive signals for piloted flight simulators. Technical Report CR-1601. 1970.

[Siv17] Sivan R., Ish-shalom J., Huang J. K. An optimal control approach to the design of moving flight simulators. In IEEE Transactions on Systems, Man and Cybernetics (SMC). 12(6): 818-827, 1982.

[Tel18] Telban R. J., Cardullo F. M. Motion Cueing Algorithm Development: Human-Centered Linear and Nonlinear Algorithms. In NASA CR-2005-213747. 2005.

SIMULATION DESIGN AND ARCHITECTURE

REAL VS. SIMULATED SURROUNDING TRAFFIC – DOES IT MATTER?

Dominik Muehlbacher [1], Lena Rittger [2] & Christian Maag [3]

(1) : Center for Traffic Sciences
University of Wuerzburg
Roentgenring 11
97070 Wuerzburg
Germany
+49-931-3819051
muehlbacher@psychologie.uni-wuerzburg.de

(2) : Adam Opel AG
65422 Ruesselsheim
Germany
+49-6142-7-69912
lena.rittger@de.opel.com

(3): WIVW GmbH
Robert-Bosch-Straße 4
97072 Veitshoechheim
Germany
+49-931-78009114
maag@wivw.de

Abstract – Multi-driver simulators include several human participants who are able to interact in the same situation at the same time. The present study demonstrates the benefit of this simulation via a comparison to single-driver simulations, which contain one participant and simulated surrounded traffic.

In total, N=20 drivers participated. Each participant completed a run in both driving simulations. Half of the drivers were assisted by a traffic light assistant. This system informs the driver about economic driving behaviour when approaching traffic lights. In some cases the system recommends to drive slowly or to brake at large distances in front of the traffic light.

In the multi-driver simulation, the participants follow the system's recommendations to a lesser extent compared to driving in the single-driver simulation. Additionally, driving in the multi-driver simulation is rated as more realistic compared to the single-driver simulation.

These results show the importance and the benefit of the multi-driver simulation. The multi-driver simulation is an appropriate tool for questions regarding interactions between several drivers.

Key words: connected driving simulation, methodology, driver assistance systems.

1. Introduction

For a long time, driving simulators have been used successfully for research in traffic sciences. By means of this method, a participant steers a virtual vehicle in a simulated environment. The surrounding traffic is realized via simulated driver models. Recently, advancements in driver simulators have allowed for a multi-driver simulation, which is an enhancement of the traditional single driving simulator [Han1; Hee1; Maa1; Mue1; Mue2]. Using this linked driving simulation, several human participants can drive in the same situation at the same time under controlled conditions.

The use of several human drivers contributes to a higher external validity: Driving behaviour of human participants is more realistic compared to the behaviour of the simulated traffic generated by the driver models. Additionally, the participants know that the surrounding traffic consists of real drivers with human behaviour and cognitions and not of simulated computer models. [Fri1] showed that the presence of human-controlled surrounding traffic in driving simulators is important for participants' behaviour: Participants who thought that another vehicle was controlled by another participant behaved more cooperatively than participants who thought it was controlled by a computer (e.g. allowed another vehicle to merge into their lane).

Human-controlled and computer-controlled agents were also compared in other kinds of virtual environments. Several studies on human behaviour in video games demonstrate higher presence (i.e. the illusion to be physically in a mediated environment [Min1]) when participants are playing against human-controlled opponents compared to playing against computer-controlled opponents [e.g. Wei1; Rav1].

However, the participation of several human drivers at the same time has a disadvantage: Compared to a single-driver simulation with standardized surrounding traffic, several human drivers reduce the controllability of the experimental situation. Hence, it is important to examine for which research purposes each driving simulation is more applicable.

One application of driving simulators is the evaluation of driver assistant systems. A system which has been the focus of much research in driving simulators in recent years is the traffic light assistant [Dui1; Kra1]. This system informs the driver about economic driving behaviour when approaching traffic lights. In some cases the system recommends to drive slowly or to brake at large distances in front of the traffic light. A previous study by [Mue2] showed that following drivers without traffic light assistant could be annoyed by this driving behaviour. Therefore, assisted drivers might worry about hindering the drivers following behind them. This could result in a weak compliance to the system recommendations. In the present study it was analysed if compliance to the recommendations of the traffic light assistant depends on the presence of surrounding traffic. This was investigated by means of a multi- and a single-driver simulation. It was expected that compliance was independent of surrounding traffic in the single-driver simulation setting, because here the driver is surrounded by simulated driver models which cannot be annoyed. If the effect does not occur in the single-driver simulation but does occur in multi-driver simulation, a benefit of the latter is demonstrated.

2. Methods

2.1. Driving simulation laboratory

The driving simulation laboratory consists of four driving stations with one subject at each driving station (see Figure1).

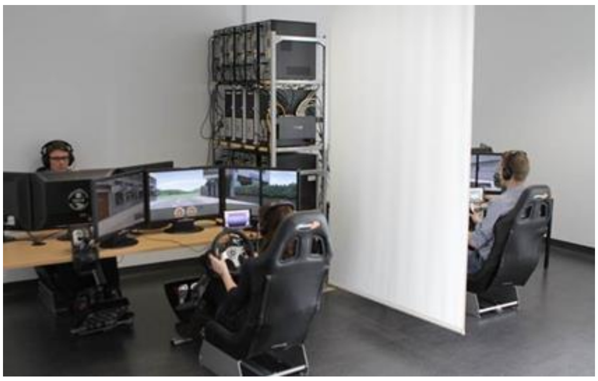

Figure 1: driving stations of the driving simulation laboratory.

The driving simulation laboratory can be used either as a single-driver simulation or as a multi-driver simulation: (1) In the single-driver simulation each participant drives through a separate but identical virtual environment. Only simulated driver models generate the surrounding traffic. (2) In the multi-driver simulation the four participants drive through the same virtual environment. In this virtual environment, the drivers are able to see the vehicles of the other study participants and can react to their behaviour. Only the vehicles of the study participants make up the surrounding traffic.

The visual system of each driving station provides a horizontal field of view of 150 degrees which is shown on three 22″ size LCD-displays with a pixel resolution of 1680x1050. The left, right and rear mirrors are shown in the front view. The drivers control their vehicle via a high-quality PC-game steering wheel with force feedback and accelerate and brake with pedals on the ground. In addition, a 10″ LCD-display with a pixel resolution of 800x480 can be used for visual secondary tasks, HMI-studies or touchpad-based questionnaires. The drivers wear a headset that enables them to hear the sounds of the simulated vehicle and its environment. Furthermore, the operator is able to communicate to the driver(s) in two possible modes: (1) The operator can communicate with one driver or with all drivers simultaneously. (2) The drivers can communicate with the operator. The simulator is run by the software SILAB developed by the Wuerzburg Institute for Traffic Sciences (WIVW GmbH).

2.2. Traffic light assistant

The traffic light assistant aims at increasing traffic efficiency and enhancing traffic flow. While approaching a traffic light, this system informs the driver via a HMI about the optimal driving behaviour (e.g. "drive 20 km/h", "slow down to 30 km/h"; see Figure 2) to reach a green traffic light. To generate these recommendations, the algorithm of the traffic light assistant considered the current and next traffic light phase, participants' driving speed and distance to traffic light. In the HMI, the driving recommendations contained a combination of action and speed recommendations, which were presented as text with distinctive colors. The minimum speed recommendation for approaching the traffic light was 20 km/h. The HMI was presented on the 10″ LCD-display.

The participants were instructed that following the system recommendations is voluntary and not obligatory.

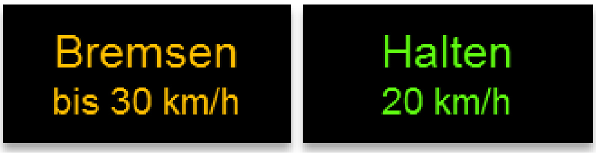

Figure 2: examples for recommendations of the traffic light assistant in the HMI (on the left: slow down to 30 km/h ; on the right: drive 20 km/h).

2.3. Penetration rate

In the multi-driver simulation condition, the penetration rate of the traffic light assistant was 50%. While two drivers were assisted by the system, the other two drivers had no assistance.

In the single-driver simulation, the platoon consisted of one participant and three driver models. While two driver models followed the recommendations of the traffic light assistant, the third driver model was unequipped. It had target velocity of 55 km/h while approaching the traffic light. Therefore, the penetration rate was either 50% or 75%, depending on the equipment of the individual driver.

In both runs, the participants were not informed if the other drivers/models were equipped with the traffic light assistant or not.

2.4. Test scenario

The course was a one-lane urban road. It consisted of eight identical segments: At the beginning of each segment the four vehicles approached an intersection with a traffic light in platoon formation (i.e. in line). The traffic light was timed so that if the drivers travelled at the recommended speed they arrived at the intersection when the light turned green and avoided a stop. If the participant drove faster than recommended they arrived at a red light and had to stop. After crossing the intersection the drivers had to stop at a 'positioning sign' (see Figure 3).

The positioning sign pictured all four vehicles of the platoon (with their different colours). Below each displayed vehicle was a parking space on the road. Each driver had to stop at the designated parking space. After all four drivers had stopped, the driver on the left parking space started to drive towards the next traffic light. The other drivers followed him/her in the prescribed sequence from left to right. In each element, the vehicle order on the positioning sign was different. By means of this method the order within the platoon was controlled and balanced such that each driver experienced each position for an equal number of times.

Figure 3: positioning sign.

2.5. Study design

The main independent variable was the type of driving simulation: single-driver or multi-driver simulation. Each participant completed a session in both driving simulations (within-subjects factor). In the single-driver simulation, each platoon consisted of one human driver and three driver models. In the multi-driver simulation, each platoon consisted of four human drivers. Before each run, the experimenter informed the participants whether they would be using the single-driver or the multi-driver simulation, respectively.

In both runs, the drivers were either assisted by the traffic light assistant or not assisted (between-subjects-factor).

Each run consisted of eight elements - each element included one traffic light at an intersection. The drivers had to approach the traffic light in platoon formation. After each element, the drivers changed positions within the platoon and approached to the next traffic light in another sequence of drivers. By means of this method, each driver was in 2 of 8 approaches each on first, second, third or fourth position in the platoon (within-subjects factors).

2.6. Dependent variables

After each run, the drivers rated different aspects of the run (e.g. "In the virtual world, I felt surrounded by real drivers") on a 7-point scale from 1="disagree" to 7="agree". In a final inquiry at the end of the session, the drivers had to compare both runs in an open-question format.

To assess compliance to the traffic light assistant, the percentage of stops at intersections was calculated. A stop was defined as reaching a driving speed of <1 km/h. Only if the assisted drivers followed the system recommendations, they could avoid a stop at the traffic light. Therefore, the percentage of segments without a stop at the traffic light is an indicator for the system compliance (so-called compliance rate).

2.7. Sample

Four test drivers participated in each session. In total, there were N=20 participants (10 women and 10 men) between 20 and 65 years of age (M= 36.8; SD= 15.6). The participants were recruited via the test driver panel of the WIVW. Prior to the study, all participants were trained with the multi-driver simulation (the training based on [Hof1]) in order to introduce them to the simulator and reduce the probability of simulator sickness. The participants were paid for taking part in the study.

3. Results

3.1. Drivers' judgments

After each run, all drivers rated different aspects of the run in a questionnaire. Several differences between driving in a single-driver simulation and a multi-driver simulation are noticed both from drivers with and without system: According to the participants, the virtual world of the multi-driver simulation is more realistic compared to the single-driver simulation (t(19)=2.27; p=.035; see Figure 4). Additionally, the driving behaviour of the surrounding traffic is rated as more realistic in the multi-driver simulation (t(19)=4.24; p<.001). Furthermore, the participants state that they feel observed by the other drivers in a higher degree in the multi-driver simulation (t(19)=4.53; p<.001).

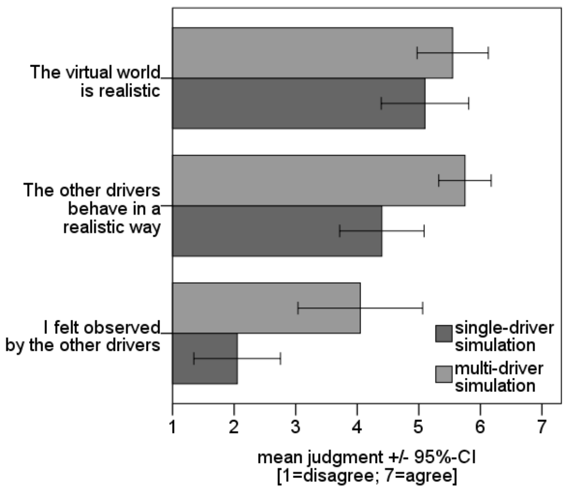

Figure 4: mean subjective judgments for various items in the questionnaire for multi-driver and single-driver simulation.

3.2. System compliance

In the single-driver simulation the compliance rate lies between 80% and 90% on average and is independent from the position (F(3, 27)=1.00; p=.864; see Figure 5). However, the position has an effect (F(3, 27)=5.21; p=.006) in the multi-driver simulation: While the compliance rate is approx. 20% on position 1, it increases gradually to 80% at position 4.

In the direct comparison between single-driver simulation and multi-driver simulation drivers in the multi-driver simulation have a lower compliance rate on position 1 (t(9)=3.97; p=.003) and position 2 (t(9)=2.86; p=.019). In position 3 (t(9)=1.50; p=.168) and position 4 (t(9)=1.00; p=.343) are no significant differences.

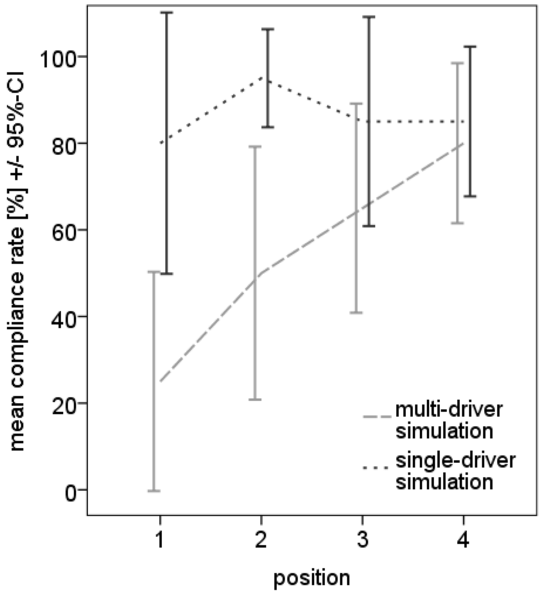

Figure 5: mean compliance rate for each position in the platoon in multi-driver and single-driver simulation.

4. Discussion

The present study analyses if compliance to the recommendations of a traffic light assistant depends on the presence and type (real vs. simulated) of surrounding traffic. For this purpose, drivers performed one run in the multi-driver simulation and one run in the single-driver simulation. The runs occurred in platoon formation, four vehicles drive in line.

First, the participants notice several differences between both runs. In total, the run in the multi-driver simulation with human surrounding traffic is rated as more realistic compared to the run in the single-driver simulation with simulated surrounding traffic. This result underlines the external validity of the multi-driver simulation.

Additionally, the type of surrounding traffic effects the participants' compliance to the traffic light assistant. When driving in front of two or three human drivers, the participants do follow the system's recommendations to a lesser extent compared to driving in front of one or no human drivers. In contrast, when driving in front of simulated drivers there is no effect of the number of vehicles driving behind. The reason for this behaviour could be that assisted drivers might worry about hindering the drivers following behind them.

These results show the importance and the benefit of the multi-driver simulation. Compared to a single-driver simulation, the external validity is enhanced and driving is more realistic. In particular, the multi-driver simulation is an appropriate tool for research questions regarding interactions between several drivers.

5. Acknowledgements

This study was performed in the scope of the German project UR:BAN (Urban Space: User oriented assistance systems and network management), funded by the Federal Ministry of Economics and Energy, due to a decision of the German Bundestag.

6. References

[Dui1] Duivenvoorden K. Roadside versus in-car speed support for a green wave: a driving simulator study, Master's Thesis, University of Twente. 2007.

[Fri1] Friedrich M., Nause D., Heesen M., Keich A., Kelsch J., Baumann M., Vollrath M. Evaluation und Validierung des MoSAIC-Fahrsimulators. Presentation at the 55. Tagung experimentell arbeitender Psychologen, Vienna. 2013.

[Han1] Hancock P. A., De Ridder S. N. Behavioural accident avoidance science: understanding response in collision incipient conditions. In Ergonomics. 46(12): 1111-1135, 2003.

[Hee1] Heesen M., Baumann M., Kelsch J., Nause D., Friedrich, M. Investigation of Cooperative Driving Behaviour during Lane Change in a Multi-Driver Simulation Environment. In D. De Waard, K. A. Brookhuis, F. Dehais, C. Weikert, S. Röttger, D. Manzey, S. Biede, F. Reuzeau, P. Terrier (Eds.), Human Factors of Systems and Technology. Toulouse. Available under http://hfes-europe.org. 2012.

[Hof1] Hoffmann S., Buld S. Darstellung und Evaluation eines Trainings zum Fahren in der Fahrsimulation. In VDI-Gesellschaft Fahrzeug- und Verkehrstechnik (Ed.), Integrierte Sicherheit und Fahrerassistenzsysteme (pp. 113-132). Düsseldorf: VDI Verlag. 2006.

[Kra1] Krause M., Bengler K. Traffic Light Assistant – Driven in a Simulator. In R. Toledo-Moreo, L. M. Bergasa, M. Á. Sotelo (Eds.), Proceedings of the 2012 International IEEE Intelligent Vehicles Symposium Workshops. 2012.

[Min1] Minsky M. Telepresence. In Omni. 2(9): 45-51, 1980.

[Maa1] Maag C. Emerging Phenomena During Driving Interactions. In E. Mitleton-Kelly (Ed.), Co-evolution of Intelligent Socio-technical Systems (pp. 185-217). Berlin: Springer. 2012.

[Mue1] Muehlbacher D., Zimmer J., Fischer F., Krueger H.-P. The multi-driver simulator – a new concept of driving simulation for the analysis of interactions between several drivers. In D. de Waard, N. Gérard, L. Onnasch, R. Wiczorek, D. Manzey (Eds.), Human Centred Automation (pp. 147-158). Maastricht, the Netherlands: Shaker Publishing. 2011.

[Mue2] Muehlbacher D., Fischer F. The multi-driver simulation as a new method for researching driver behavior and traffic. Presentation at the Driving Simulation Conference, Paris. 2012.

[Mue3] Muehlbacher D., Fischer F., Buld S., Totzke I., Krueger H.-P. The multi-driver simulation as a tool for the evaluation of traffic efficiency-orientated driver-assistance systems. Presentation at the 5th International Conference on Traffic and Transport Psychology, Groningen. 2012.

[Rav1] Ravaja N., Saari T., Turpeinen M., Laarni J., Salminen M., Kivikangas M. Spatial Presence and Emotions during Video Game Playing: Does It Matter with Whom You Play? In Presence: Teleoperators and Virtual Environments. 15(4): 381-392, 2006.

[Wei1] Weibel D., Wissmath B., Habegger S., Steiner Y., Groner R. Playing online games against computer- vs. human-controlled opponents: Effects on presence, flow, and enjoyment. In Computers in Human Behavior. 24(5): 2274-2291, 2008.

A NETWORKED MULTI-DRIVERS SIMULATION PLATFORM FOR INTERACTIVE DRIVING BEHAVIOR STUDY

Jing Xu[1], Yingzi Lin[1*]

(1): Intelligent Human-Machine Systems Lab
Department of Mechanical and Industrial Engineering, Northeastern University
360 Huntington Ave, Boston, MA 02115, USA
xu.jing1@husky.neu.edu, yi.lin@neu.edu
* The Corresponding Author

Abstract – Traffic simulations are becoming increasingly important to acquire dynamic interaction behavior of drivers. To improve the fidelity and realistic experience of driving behavior studies, research as advanced from single- to multi-driver simulations. In this paper, several existing models were discussed in the context of interactive driving behavior. Recent studies and their applications relevant to multi-driving simulation were also reviewed. A concept framework of interactive behavior model was postulated in which all the influence factors were comprehensively considered during the interactive process between two vehicles. Based on this framework, we have established a Networked Multi-Drivers Simulation Platform. This new simulation platform engaged multiple drivers interacting on in common virtual environment. Performance data and psycho-physiological measures of individual drivers can be collected by the system and transmitted among subjects in real-time. Using this configuration, a virtual traffic simulation was established by including multiple participating drivers for a real-life scenario. Therefore, we propose that conclusions drawn from behavior studies under such simulation and thus based on comparable performance data is more realistic and meaningful than before.

Key words: driving simulator, driver interactive behavior, cognitive state, psychophysiological measures, multiple driver simulation.

1. Introduction

A driver on the road shares the same traffic environment and thereby has to interact with other drivers. Several studies have indicated that the perception of other ambient traffic subjects would likely change a driver's performance or behavior; meanwhile, each driver also influences the behavior of other drivers. Current research focuses on representative behavior of drivers but overlook the individual differences, and the interactive behavior among other drivers and road users and their impact on each other are less discussed. But the probability and severity of traffic accident depends on the driving variations between different drivers [Yas1].

Driving simulators have been widely used in traffic simulation and driving behavior study. Despite the many advantages that driving simulators can provide better than field study, such as safer, more controllable, repeatable and low cost. An important question, however, is whether driving simulators can provide a realistic impression like driving in real life with high validity. Furthermore, it is difficult to account for human feelings invoked on a simulator, such as stress, haste, anxiety and anger and mimic the complex of real-life traffic situations. Unlike an experiment that runs with real drivers on the road, relying on a single-user driving simulator or standalone systems only devote limited contribution on the analysis of interaction processes between multiple drivers. Meanwhile, with the rapid development of computer graphics and human-computer interaction technologies recent years, it becomes apparent that the emulated "human-like" behavior for more complex phenomena such like dynamic human-will-motivated interaction are open to more possibilities than in the past. Compared with the vehicles operated by real drivers, simplified autonomous vehicles (e.g. preprogrammed and randomly triggered) lack human judgment, intention, adaptability, flexibility, and logic, even though they may have realistic 3D representation in virtual environment [Cai2].

In this paper, we present how a better understanding of the interaction process among individual road users can be achieved. To further study the complex interaction behavior between each driver, we developed a high fidelity driver-to-driver interaction platform by replacing driver models with real human drivers to conduct the interactive behavior studies. A new driving simulation platform was built up for the interactive driving behavior studies based on a networked multi-users virtual environment. It provides a laboratory environment to investigate driver behavior in case of different traffic events.

2. Interactive drivers' behavior framework

Traffic danger can be effectively reduced starting from the perspective of individual roadusers. It is convinced that two points overwhelmingly determine an individual's risk in traffic: the individual's behavior and the behavior of other road users [Eva3]. The individual's behavior has been widely discussed before. On the scope of the interactive behavior between individual vehicles, the knowledge of drivers' behavior in such situations was gathered. Our current study focuses on the microscopic Psycho-Physical modeling approaches. This modelling idea establishes on perception-reaction characteristics or psycho-physiological indicators of human beings. Such ideas include Weidemann's Psycho-Physical Car-Following Model [Wie4], Van Winsum's psychological knowledge-based math model about car following behavior [Van5], Andersen's visual angle (DVA) model [And6], and "ARCHISIM" from the French National Institute for Research in Transportation and Safety (INRETS) [Mor7]. These models are centered on single-driver and widely used in the traffic flow simulation software. They take the human factors into consideration and can describe the interaction between adjacent vehicles. Meanwhile, there are few theoretical frameworks focused on driver-driver interaction. Houtenbos et al. [Hou8] proposed an interactive behavior model on a cognitive level to describe the interaction process between drivers with a central role for the concept of expectancy. The main idea of the model is that all road users involved in the interaction perceive the environment through a "window", which is a filtering process that takes place outside the road user, physically selecting what information from the environment can be processed. Ba and Zhang [Ba9] proposed a perception-cognitionemotion behavior framework, which contains attributes and influence factors to interaction process between drivers. These works, together with previous research from our lab [Cai10, Cai11, Lin12, Lin13], form a basis for multi-driver studies.

We have in the past proposed an interaction framework for drivers, which focused on the interrelationship between two single "driver-vehicle" units. It combined physiological measures to provide a comprehensive representation of behavioural performance with the interactive process (Fig.1). The factors that influence the behavior of a driver can be categorized into two parts: individual factors and external factors. Individual factors include personality, further divided into age, experience, gender and education, and driving style, which can be achieved from Driving Behavior Questionnaire (DBQ). The external factors include traffic environment, social norms, public policy, traffic rules, culture, target context and car conditions [Ba9, Zai14, Bjö15]. All of these factors can provide a comprehensively context of the driver as well as affect a driver's decision and manipulation. Drivers' state measures (e.g. eye movement, facial expression and psycho-physiological factors) and performance indicators will reflect the interaction process over all the interactive behaviors. Each couple of interacted vehicles can be regarded as a basic unit on the road and numerous units form a whole traffic platoon.

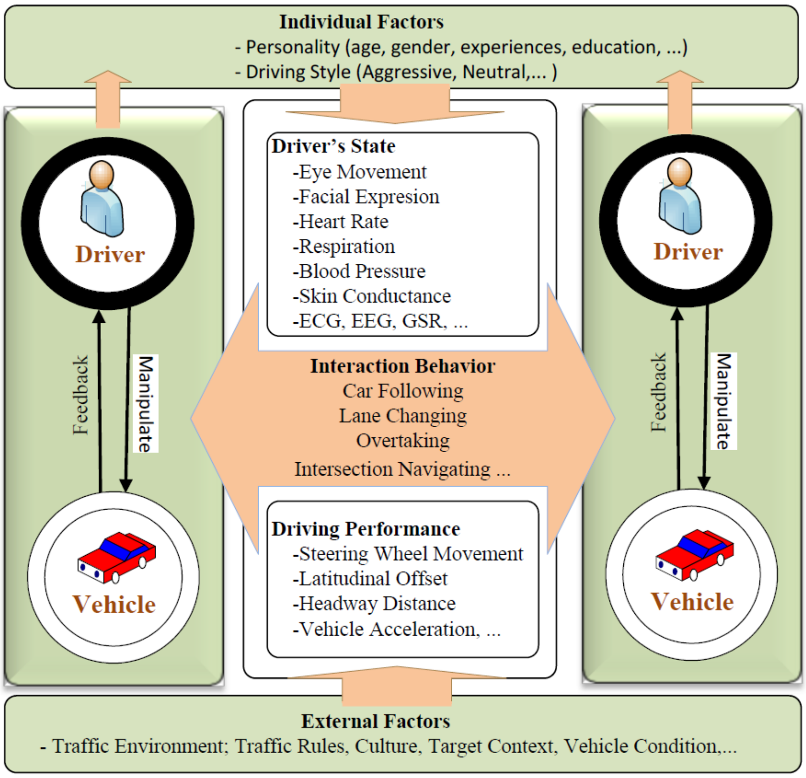

Fig.1 The Framework of Drivers' Interaction Mod

3. Approaches to study interactive driving behavior

There are two approaches to study the individual drivers' behavior. The first one is driving on the real road with infrastructures and real people. This method can enable studying authentic driving behavior on real life. However, uncontrollable conditions make the realization of test situations in real-life traffic very challenging and limited. This becomes especially difficult in safety-critical situations that will lead to seriously ethical problems and might endanger test drivers [Maa16].

A second approach is driving on a simulator with driving models. The movementbased simulators are more precise than other fixed simulators that can give drivers feedback from the steering wheel and chair about how virtual car moved in the environment [Ree17]. However, whichever type of driving simulator is, low fidelity may lead to imperfect replication of real driver behavior and real driving performance. It is relatively easy to use real steering wheels, cabin, moving feedback seat and high quality virtual environment to improve the fidelity of interactive interface and drivers' perception.

Such type of simplified machine driver may lead to some drawbacks as we summarized in our previous work [Cai2]. For example, the weird movement can't convince test drivers that they are driving with real driver; too perfect (or ideal) to produce 'human-like' errors or turbulence that make test drivers feel easily predictable; no active motivation to interact with the neighboring vehicles. Commonly, all the drivers' interaction is either pre-programmed or randomly triggered which are seem not natural.

The majority of currently available simulators are single-user stand-alone systems; traffic engineers cannot easily analyze more complex phenomena, such as the interaction between multiple human drivers or pedestrians [Nak18]. Therefore, we combine the feature of both simulations to establish a novel approach involving multiple real drivers on interconnected simulators under the same virtual environment.

3.1. Multiple-user driving simulation

In recent years, there is an increasing demand for test methods in traffic engineering and drivers' behavior research that involve the dynamic interactions between vehicles. The topic of driver-driver interaction and multipleuser driving simulation has therefore attracted great attention from the US, Germany, China, Japan and Sweden. Examples of these studies show the possibilities and applications by using multi-driver simulation systems to improve driving safety as shown on Table 1.

Table 1. The Recent Studies on Multi-driver Simulation

Country	Literature	Software Platform	Hardware	Parameters	Application
US	[Cai2, Cai19]	OpenGL, VC++	Logitech MOMO game wheel/pedal	-	Drivers' emotion; Traffic flow simulation
Japan	[Nag20]	Java 3D VC++	FBBW and $^{SC}ha_ir^e$; Rotary motion platform; 2 stations	-	Double-driver fire-truck simulation.
Sweden	[Yas1]	-	Game wheel/ pedal 4 stations	Conflict Indicating Variables: TTC, PET.	Voice based command GPS; traffic lights influences
China	[Wan21]	UC-windroad	UC-windroad; 2 stations	Velocity, acceleration, steering angel, brake.	Driving tendency recognition
Germany	[Maa16, Müh22]	SILAB multi-driver simulation system	FBB steering wheel; 5 stations	Data of longitudinal control, lateral control, …	Driving Assistant System: Emerging Assistant, intersection, traffic light assistant, …
Japan	[Ban23]	SIGVerse	Game wheel/pedals	E.g. inter-vehicle distance; acceleration, steering angel, brake.	Lane changing Training
Germany	[Hee24]	DLR Multi-driver simulation MoSAIC	G27 game wheel/pedal; 2 stations	Lane change, acceleration, brakes.	Cooperative lane change assistant

Most of simulations in Table 1 use commercial 3D software or traffic simulation software to build up the system (SILAB, Java3D/VC++, UC-windroad, SIGVerse, etc). Four or five driving simulators were connected to form a whole driver group that describes the behavior of the entire traffic platoon. The remaining simulations use two networked simulators to evaluate the interactive affects between two vehicles. In terms of the application, they use multiple-driver system to form a platform. This platform can study the effects of ADAS, IVS, AmI, C2X, ICT systems on different interactive traffic situations. Such representative situations include merging assistant, hazard warning and traffic light assistant in intersection, rubbernecking and even collision. Other than the driving performance data (acceleration, steering angel, brake, lateral control, etc.), the indicating variables such as inter-vehicle distance, TTC (time to collision), PET (Post Encroachment Time), variation, coherence are also introduced to quantitative describe the interactive behavior between two cars or whole platoon.

Similarly, current research that induces a drivers' individual differences and physiological and psychological characteristics into the interactive driving behavior study is limited. One study obtains driving data of different drivers through the interactive parallel driving simulated experiment, and using this data to testify their driver tendency recognition model [Zha25]. The headway distance on car following process is the only recognition indicator in this project. In our previous study [Cai2], we suggest the virtual traffic flow of driving simulators be realistic rather than perfect. Therefore we updated our standalone simulator and presented an extended human-in-loop simulation framework. It supports multiple driving terminals that can be used to improve the fidelity of driving simulators. Realistic driver-driver interaction is also essential to investigate the emotional behavior of certain drivers. Provoking the emotion by traditional ways (e.g. watching movies, hearing stories or recalling personal experiences) is inefficient in driving experiments, as it is only a short-term state. In order to investigate the influence of a driver's emotion on performance, we also induced two kinds of emotional states (anger and excitation) through realistic driver-driver interaction by using networked driving simulators [Cai19]. The result indicates that multiple networked driving simulators are feasible for inducing the psychophysiological parameters changes, which can be used as the indicators of emotions.

4. Multi-drivers simulation platform

According to our theoretical framework of drivers interaction model shown as Figure 1, the prototype of the multi-user driving simulation system satisfies three features. First, at least two human drivers participate the simulation by which one driver controlling one driving simulator. Second, all drivers simultaneously in one simulated environment in which they can share same scenarios, follow same task rules, as well as can see and react to each other. Three, drivers' performance information can be transmitted between vehicles synchronously via network; drivers' state can be measured on real-time.

4.1. System Implementation

Our networked multiple-drivers simulation system (Fig.2) is located in the Intelligent Human-Machine Systems Laboratory at Northeastern University. Each simulation terminal contains separate input and output devices. They appear as autonomous vehicles in each other's virtual scenarios and can behave like exposing human drivers to specific traffic situations. For simulator 1, a racing seat is mounted on an AC servo actuator at the center of the cylindrical screen. The projector was connected to the computer, projected the scenarios on the cylindrical screen. Simulator 2 comprised a workstation, a high-fidelity steering system (ECCI TracStar 6000), and three LCD screen. Two Macintosh Computers with NVidia GeForce 8800 GT graphics cards are used here.

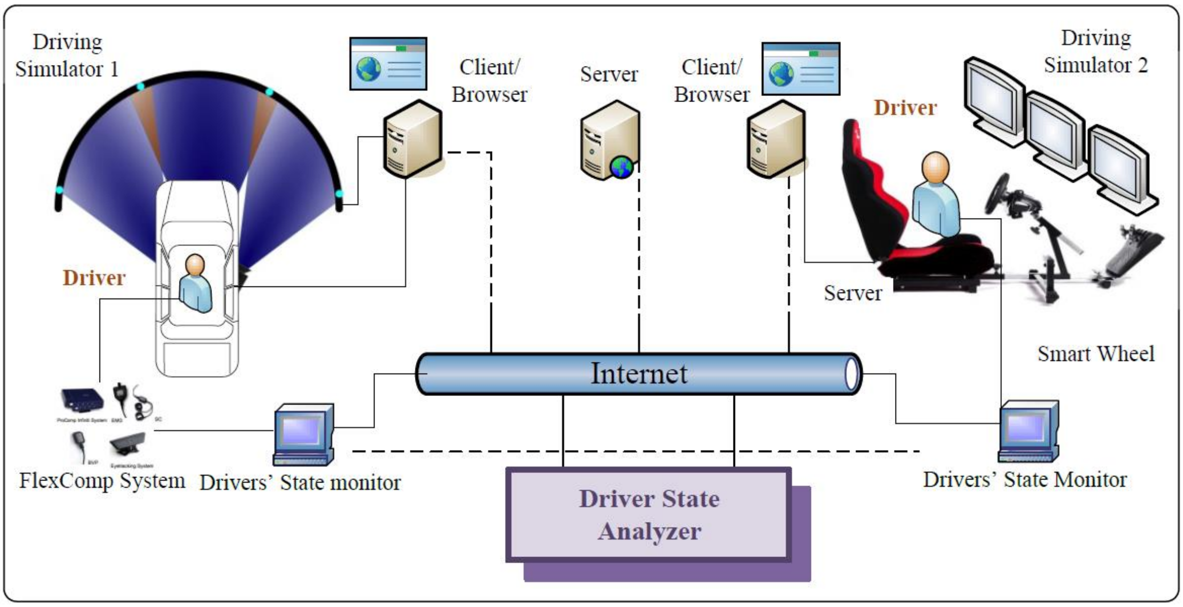

Fig.2. The Prototype of Networked Driving Simulation System

4.2. Network communication module

Because of the concern that data exchange in our multiple driving simulation applications, the simplicity and efficient need to be considered for real time effect satisfactory. Here we implemented the server-client protocol by Java Script and Unity 3D Network Manager Component. A separate network server was set up in a single computer. It calculates computer and clients' state based on the signals received from clients. The clients provide interfaces for driving, which obtain operation signals from drivers and create the real-time updates of virtual scenario. The Driving performance data (position, heading direction and speed) can be recorded by any terminals, which will benefit for the different locations among different driving terminals.

4.3. Data Acquisition Module

As we mentioned above, the following performance data can be calculated and transmitted among any simulation terminals: speed (S), headway distance between two cars (HD), steering wheel angel (SA), gas throttle (GT), operational reaction time (RT), and lane position deviation (LD).

To achieve drivers' psychophysiological response on interactive process, we employed two psychophysiological data acquisition system for both driving simulators. A FlexComp Infinity Biofeedback system is implemented for Simulator 1. We also adapted our previous work -"smart wheel", which has been validated in the laboratory environment for Simulator2 [Len26]. Four types of sensors were embedded into the steering wheel to perform real-time non-intrusive measurements of the physiological states. The parameters including: heart rate (HR), respiration (RR), skin conductance (SC) and the Heart rate variability (HRV) were then derived. In addition, a Tobii X50 Eye-tracker and a low-cost commercial eye tracker were planned to detect the drivers' eye movements and to collect eye fixation positions and durations for interactive cognitive engagement estimation. These subjects' cues can help to understand drivers' mental workload, attention and emotion during the interactive process. Moreover, combined with the individual/external contextual factors shown in Fig. 1, we can input all these information into the Data Analyzer as the context of inference or prediction, or provide the information or suggestion to drivers.

4.4. Virtual Environment Module

A low-cost but high efficiency, flexible and practical graphical interface (3D physics engine powered by Unity3D) was introduced to create simulation systems. The Unity3D is well suited for building environments, external data exchange, and controlling target objects, as well as Graphic User Interface as well as human-machine interaction with scripting [Hig27]. Other than the basic city infrastructures such as buildings, city and rural roads, intersections, traffic lights, pedestrians and cyclists with movement as important road users were also simulated in our traffic environment. They can help to create some hazard traffic situations on the road. Each driving terminal appears as an autonomous vehicle in each other's virtual scenarios and can behave like exposing human drivers to specific traffic situations (Fig.3). Three driving interaction conditions are considered: car following, lane changing and overtaking. With this configuration, multiple subjects' simulator experiments can be conducted and thus comparable performance data can be obtained to draw meaningful conclusions for interactive driving behavior study.

Fig.3. The virtual scenes of Networked Multi-drivers Simulation System

5. Discussions and Future Study

A main objective of this project is to achieve a better understanding of the interaction process between road users and interrelationship between individual behaviors. This paper provides an overview of the interactive driving behaviors' study. It has also expanded the development of recent research based on of multiple-drivers simulations. Based on our knowledge from the literature, we proposed a driver's theoretical interaction framework and built a new networked multiple drivers' simulator system. High fidelity driverdriver interactions were achieved by replacing driver models with real human drivers. Our simulation can provide detailed information about the behavior of the driven vehicle, in relation to the environment and to other vehicles. Other than the driving performance data, it combined with specific physiological measures to each driver that can provide a detailed and comprehensive representation of interactive behavioral performance. In future research, experiment should be conducted to examine the validation of our simulation system. The validation work will focus on ensuring that the drivers can expose their behaviors naturally, and co-drivers can evoke each other's emotion and performance changes in a valid way. Also, future studies on this platform should be demonstrating more feasibility of using multiple driving simulators to investigate driver's performance and cognitive states.

In this work, we take into account the need for different user requirements, as well as for flexibility and extensibility in configuring the networked driving simulation system. In future, with the support of software platform, our simulation software can be easily published to be an application on Windows, Mac OS, Linux, Android, and IOS etc. Different level of end-users from the public such as researchers, innovators, and game players, can enter to the system via internet/intranet and cloud collaboratively. The interface of input devices can be easily extensible to different ways, such as driving simulators, commercial game joysticks, keyboard and mouse, and strokes on a Smartphone (currently named WebDriver). It is easier to extend this platform from traditional client/server (C/S) model to Browser/Server (B/C) model that end-users can use to access the platform online and exchange information. In addition, different levels of driving participants can be recruited into the framework: the autonomous vehicles, the WebDriver, the low-cost game joystick and the high fidelity simulator (Fig.4). The autonomous car models can be used to build up the basic traffic flow; the random web drivers and low-cost simulators can be anyone or located in other places, join the platoon under certain rules to enhance the realistic effect of the traffic. The features of crossplatforms can make the cross-regions become easier. Users could come from different locations, different environment and different interfaces, which even can provide a way to study the differences of the drivers' behaviour across countries, cultures, driving habits, etc.

AIDE's report [AID28] mentioned the future effort on a more personalized behaviour and dynamic adaption is needed to make the ADAS more intelligent. This approach can allow studying the individual driving behavior, which might make improvement in prediction or inference of human state and behavior. It can expand the possibilities to able to represent individual differences in cognitive state and behavior as well as the personalized drivers' behavior study for ADAS. Recently, American Feds also plans to mandate that newly manufactured cars include "vehicle-to-vehicle" communication technology. The V2V communication is an expanding technology that has great potential of becoming the mainstream equipment on car. The car and driver can talk to each other will not only about the information of ambient car or public infrastructures. Imaging if the concise, effective but necessary ambient driver's state can be conveyed to others as the reminder of potential danger, this would benefit from the use of networked multi-driver simulators.

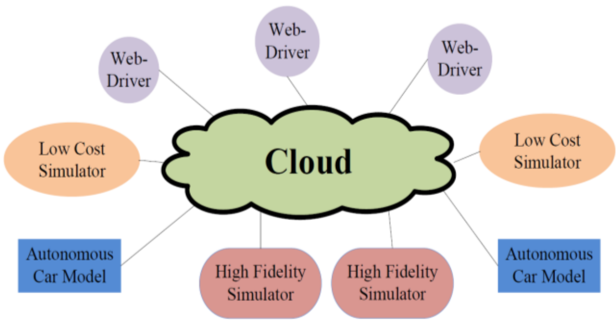

Fig.4. The Extended Networked Multi-drivers Simulation System

6. Acknowledgement

This work has been financially supported by the National Science Foundation (award #1333524).

7. References

[Yas1] Yasar, A.-U.-H., Y. Berbers, and D. Preuveneers. "A computational analysis of driving variations on distributed multiuser driving simulators". in *IASTED International Conference on Modelling and Simulation*. 2008.

[Cai2] Cai, H., Y. Lin, and B. Cheng, "Mimicking human driving behaviour for realistic simulation of traffic flow". *International Journal of Simulation and Process Modelling*, 2010. 6(2): p. 126-136.

[Eva3] Evans, L., "Vision for a safer tomorrow". *Traffic Safety*, Bloomfield Hills. Science Serving Society, 2004.

[Wie4] Wiedemann, R., "SIMULATION DES STRASSENVERKEHRSFLUSSES". 1974.

[Van5] Van Winsum, W., "The human element in car following models". *Transportation research part F: traffic psychology and behaviour*, 1999. 2(4): p. 207-211.

[And6] Andersen, G.J. and C.W. Sauer, "Optical information for car following: The driving by visual angle (DVA) model". *Human factors: The journal of the human factors and ergonomics society*, 2007. 49(5): p. 878-896.

[Mor7] Moridpour, S., M. Sarvi, and G. Rose, "Lane changing models: a critical review". *Transportation Letters-the International Journal of Transportation Research*, 2010. 2(3): p. 157-173.

[Hou8] Houtenbos, M., et al., "The role of expectations in interaction behaviour between car drivers". *Traffic and transport psychology: Theory and application*, 2005. 1: p. 303-314.

[Ba9] Ba, Y. and W. Zhang, "An Empirical Approach for Driver-Driver Interaction Study: Attributes, Influence Factors and Framework". *Advances in Usability Evaluation*, 2012: p. 404.

[Cai10] Cai, H., Lin, Y., 2011. "Modeling of Operators' Emotions and Task Performance in a virtual driving environment", *International Journal of Human Computer Studies*, Vol. 69, Issue 9, August 2011, p. 571-586.

[Cai11] Cai, H., Lin, Y., Cheng, B., 2012. "Coordinating Multi-level Cognitive Assistance and Incorporating Dynamic Confidence Information in Driver-Vehicle Interfaces", *Journal of Human Factors and Ergonomics in Manufacturing & Service Industries (HFEM&SI)*, Special Issue on "Cognitive Engineering for Next Generation Transportation Systems", Vol. 22, No. 5, pp. 437-449.

[Lin12] Lin, Y. 2008b. "Detecting driver states on the road: state of the arts and future". *The 11th Automotive Safety Technology Annual*

Conference of the Society of Automotive Engineering of China (SAEChina), June 10-12, 2008, Shanghai, China, pp. 73-77.

[Lin13] 100. Lin, Y., Leng, H., and Cai, H., 2006b. "A study on driver's physiological nonintrusive monitoring in a virtual environment", *The 50th Human Factors and Ergonomics Annual Meeting*, San Francisco, Oct. 16-20, 2006, pp. 2707-2711.

[Zai14] Zaidel, D.M., "A modeling perspective on the culture of driving". *Accident Analysis & Prevention*, 1992. 24(6): p. 585-597.

[Bjö15] Björklund, G., "Driver interaction: informal rules, irritation and aggressive behavior". 2005, Uppsala University.

[Maa16] Maag, C., et al., "Studying effects of Advanced Driver Assistance Systems (ADAS) on individual and group level using multidriver simulation". *Intelligent Transportation Systems Magazine*, IEEE, 2012. 4(3): p. 45-54.

[Ree17] Reed, M.P. and P.A. Green, "Comparison of driving performance on-road and in a low-cost simulator using a concurrent telephone dialling task". *Ergonomics*, 1999. 42(8): p. 1015-1037.

[Nak18] Nakasone, A., et al. "Openenergysim: A 3d internet based experimental framework for integrating traffic simulation and multiuser immersive driving". in Proceedings of the *4th International ICST Conference on Simulation Tools and Techniques*. 2011. ICST (Institute for Computer Sciences, Social-Informatics and Telecommunications Engineering).

[Cai19] Cai, H., Y. Lin, and R.R. Mourant. "Study on driver emotion in driver-vehicle environment systems using multiple networked driving simulators". in Proceedings of the *Driving Simulation Conference North America (DSC'07)*. 2007.

[Nag20] Nagai, T., et al. "Dual-driver networked fire truck simulator with multimodal display including force feedback steering and rotating motion platform". in *Enabling Technologies: Infrastructure for Collaborative Enterprises*, 2007. WETICE 2007. 16th IEEE International Workshops on. 2007. IEEE.

[Wan21] Wang, X. and J. Zhang, "Extraction and recognition methods of vehicle driving tendency feature based on driver-vehicleenvironment dynamic data under car following". *International Journal of Computational Intelligence Systems*, 2011. 4(6): p. 1269-1281.

[Müh22] Mühlbacher, D., et al., "The multidriver simulator–a new concept of driving simulation for the analysis of interactions between several drivers". *Human Centred Automation*, 2011: p. 147-1 58.

[Ban23] Bando, T. and T. Shibata. "Networked driving simulator based on SIGVerse and lane-change analysis according to frequency of driving". in *Intelligent Transportation Systems* (ITSC), 2012 15th International IEEE Conference on. 2012. IEEE.

[Hee24] Heesen, M., et al., "Investigation of Cooperative Driving Behaviour during Lane Change in a Multi-Driver Simulation Environment". *Human Factors: a view from an integrative perspective*, 2012.

[Zha25] Zhang, Y., X. Wang, and J. Zhang, "The verification method of vehicle driving tendency recognition model based on driving simulated experiments under free flow". Wuhan Ligong Daxue Xuebao(Journal of Wuhan University of Technology), 2011. 33(9): p. 82-86.

[Len26] Leng, H. and Lin, Y., 2005. "Design and application of a novel driver condition monitoring device – smart wheel", Tech Report, Northeastern University (Boston), USA.

[Hig27] Higgins, T., *Unity-3D game engine*. 2010.

[AID28] AIDE project, 2007. *Behavioural effects and DVE modeling*.

Scalable and Detail-Preserving Ground Surface Reconstruction from Mobile Laser Systems for Driving Simulators Engines

Daniela Craciun[1], Jean-Emmanuel Deschaud[1] and François Goulette[1]

(1) : Ecole des Mines de Paris, Centre de Robotique, 60 Bd. Saint Michel, 75272 Paris Cedex 6
0033(0)1 40 51 94 54, Fax 0033 (0)1 43 26 10 51
E-mail : {daniela.craciun,jean-emmanuel.deschaud, francois.goulette}@mines-paristech.fr

Abstract – Driving simulation engines represent a cost effective solution for vehicle development, being employed for performing feasibility studies, tests failure and for assessing new functionalities. Nevertheless, they require geometrically accurate and realistic 3D models in order to allow driver's training. This paper presents the **A**utomatic **G**round **S**urface **R**econstruction (**AGSR**) method, a framework which exploits 3D data acquired by mobile laser systems. They are particularly attractive due to their fast acquisition at terrestrial level. Nevertheless, such a mobile acquisition introduces several constraints for the existing 3D surface reconstruction algorithms. The proposed surface modeling framework produces a regular surface and recovers sharp depth features within a scalable and detail-preserving framework. Experimental results on real data acquired in urban environments allow us to conclude on the effectiveness of the proposed method.

Key words: surface reconstruction, LiDAR, driving simulator engines, road network, mobile laser systems.

1. Introduction and Motivation

Driving simulation engines require geometrically accurate and realistic 3D models of urban environments. Nowadays, such 3D models are computed manually by graphic designers who combine a wide variety of data ranging from GPS car maps to aerial images, passing through GIS data [Des7]. However, the resulted 3D models lack geometrical accuracy and photorealism, limiting therefore driver's training in real conditions. A more difficult task is represented by the road modeling process as it requires very accurate geometrical information in order to supply driver's perception for car's maneuverability.

In order to overcome the limitations of the existing 3D road modeling methods, several research projects [SIM21] are directed towards the use of Mobile Laser Systems (MLS) which allow sensing the environment of their surroundings with high sampling rates at high vehicle velocities. Such systems provide geometrically accurate 3D measurements at terrestrial level over large scale distances. Nevertheless, such mobile acquisition results in a high amount of data which requires a fully automatic road surface reconstruction framework. When dealing with the surface reconstruction problem using 3D point clouds acquired by MLS, several key issues must be addressed. Noise sources coming from the laser sensing device, external calibration and mobile acquisition (distance to the scanned surface, incidence angle, surface geometry and material type) must be carefully identified and modelled correspondingly. In addition, in structured environments such as urban scenes, sharp depth features and geometrical details must be preserved. This is a key aspect for driving simulator engines which require a very accurate surface modeling of road borders, accessibility ramps and other geometric details. Smoothing the noise in MLS data while preserving sharpness is still a difficult task for the existing surface reconstruction algorithms. Furthermore, in order to perform surface reconstruction automatically over large distances, memory constraints and scalability issues must be addressed.

The research work reported in this paper aims at exploiting 3D data acquired by a MLS for generating automatically geometrically accurate surface reconstruction of urban environments for driving simulation engines. In this paper we propose a fully automatic surface reconstruction framework for roads and sidewalks which copes with the aforementioned constraints imposed by MLS, while fulfilling the requirements of driving simulation engines. The paper is organized as following. Section 2 introduces our method for improving perceptive realism from MLS data and the implementation of ground 3D models within the simulator software. The next section presents the overview of the proposed ground surface framework. Sections 4 and 5 are dedicated to a description of the two main phases of our ground surface reconstruction algorithm. Sections 6 and 7 present the performance evaluation, including scalability, followed by Section 8 which resumes the proposed method.

2. Perceptive Realism from MLS Data

Driving simulation engines represent a cost effective alternative for improving vehicle development with minimum costs. Such systems allow the simulation of a wide variety of traffic scenarios with visually enriched environments for developing vehicle dynamics, driving assistance systems and car lighting.

2.1. Perceptive realism from scanned reality

Driving simulation engines fuse visual, audio and motion senses within a global architecture composed by several modules. A detailed description of the functional structure of a simulator engine can be found in [Bou1]. The spatio-temporal coherence in a driving simulation engine is a major concern. It is related to the proprioceptive integration, i. e.: human's sensibility to delay and perception incoherence (depth, motion) [Pet15, Bre2]. If they are not treated accordingly, they can lead to severe misperception, headaches and accidents. A major concern in car manufacturing is represented by the use of realistic data and driving scenarios for designing adapted functional units. This requires consistent resources for collecting real-time traffic information such as vibrations, visual data bases, sounds and traffic incidents. As presented in [Cha4], realistic restitution of longitudinal and lateral acceleration improves realism during driving simulation. A critical component in generating a suitable visual layer for driving simulation engines is represented by the realism of the 3D model which must be correlated to both, car's vibrations [Bol3, Seh19] and sound component.

2.2. Visual layer from MLS data.

The use of GIS data within driving simulator engines provides an effective testbed for vehicle developing. The visual layer is composed by two main ingredients: 3D environment models and the road network supplied by GIS datasets. Nowadays, such 3D models are created by graphic designers using manual frameworks. In presence of occlusions, missing data is filled with synthetic information extracted from similar non-occluded areas. Such workflows do not provide a real model, producing drivers' misperception. In addition, continuous changing in urban planning requires up-to-date 3D models and GIS datasets. This calls for automatic procedures capable to survey and generate 3D models over large distances in a relatively short time. Furthermore, the cost for generating manually 3D models represents in average a third of the overall expenses required by a driving simulation engine.

2.3. From MLS data to scalable road networks via logical description

In order to overcome the fastidious processing of manual methods, the design of automated 3D modeling frameworks becomes a must. In addition, with the new advancements in mobile mapping systems, it is now possible to acquire real data, at terrestrial level while driving in normal traffic conditions. This allows acquiring real data and generating 3D models over large distances within a cost effective methodology. Nevertheless, such a mobile acquisition results in a high amount of data which requires automated 3D modeling frameworks.

The workflow presented is paper was developed within an ongoing research project, [SIM21] which is focusing on the generation of geo-specific 3D models for driving simulation engines in order to allow vehicle design and drivers' training with minimal costs. The project is mainly concerned with the design of an automatic framework capable to generate geometrically accurate 3D models from MLS data over large distances. The reconstructed ground surfaces generated by our algorithm are further exploited via a logical description for road networks encoded in different file formats, such as CityGML [Cit6] or RoadXML [Roa16], accepted by driving simulation engines. They are usually widely employed to supply the software of driving simulation engines. A good example is SCANeR™ [Okt13] which provides a complete description of roads network for a variety of driving simulation engines.

3. Automatic Ground Surface Reconstruction (AGSR)

The overall processing workflow of the proposed surface reconstruction method comes together with the global framework illustrated in Fig. 1 which has as input a massive 3D point cloud acquired by a MLS. The dataset is first sliced into 3D chunks of N Mpts (Million points) each, where N denotes the number of 3D measurements recorded per chunk. According to the vehicle speed, the length of the surveyed area may vary. Fig. 2 (a) illustrates an example of a 3D chunk acquired over a dense urban area situated in Paris, France. We do not make any assumption about the acquisition setup, so the input data can be supplied by different platforms. When choosing a surface reconstruction method, the geometric properties of the underlying surface must be taken into account in order to design an adaptive framework, geometrically consistent with each object.

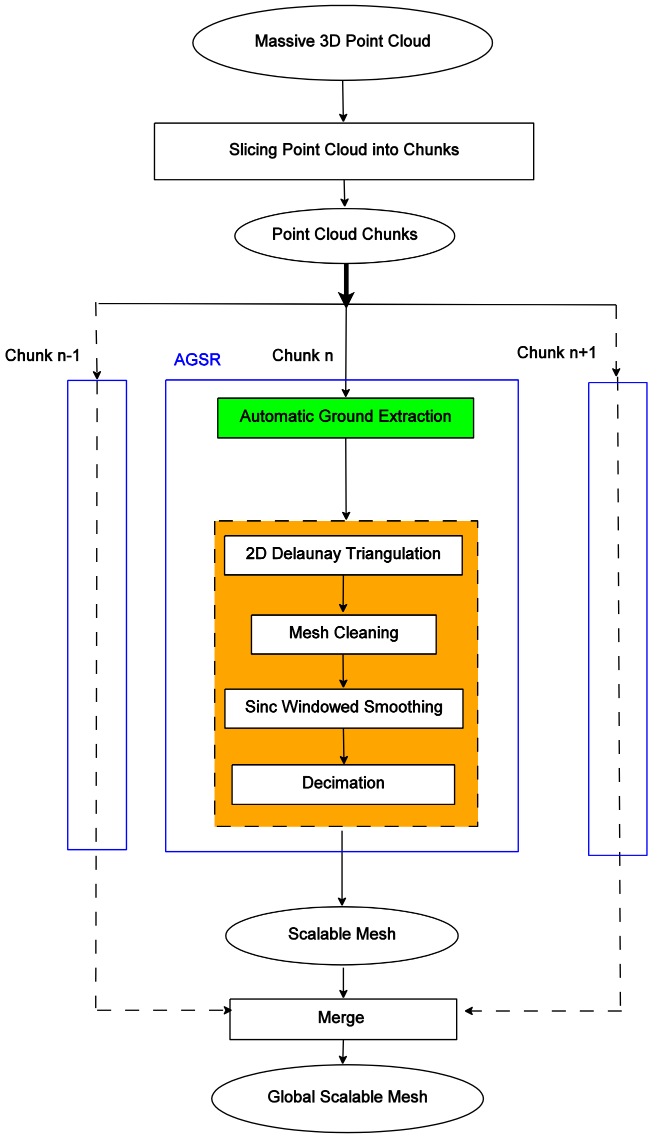

Fig. 1. The workflow of the proposed Automatic Ground Surface Reconstruction (AGSR) framework designed to be integrated within a global parallel computation scheme dedicated to massive 3D point cloud processing.

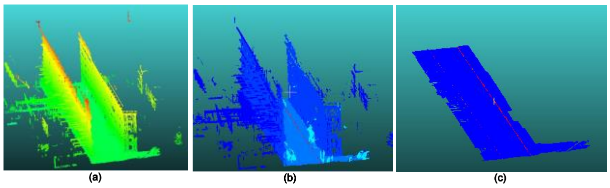

Fig. 2. Ground extraction results: (a) example of a 3D chunk acquired over Assas street located in Paris (France): approximative length of 82 m, N=3 Mpts. For visualization purposes, the original point cloud is colored with respect to elevation values; (b) 3D object segmentation results; façade – dark blue, road and sidewalks – blue, non-ground objects – light blue, sidewalk borders and ramp access – red; (c) the extracted ground corresponding to road, sidewalk and ramp access: 1.27 Mpts.

To this end, the proposed surface reconstruction framework starts with an automatic ground extraction phase performed through the use of a 3D point cloud segmentation and classification algorithm [Ser19] which assigns semantic labels with respect to different classes: ground, buildings, urban furniture and cars. Such a semantic labeling scheme provides two advantages: (i) it gives the possibility to parallelize the surface reconstruction at class level, while adapting the surface reconstruction method with respect to its geometric properties; (ii) in dynamic environments, when similar objects are detected, the already computed model can be inserted within a global reference scene.

In a second step, the 3D points corresponding to the ground are injected into the surface reconstruction procedure which combines a planar Delaunay triangulation method with smoothing and decimation techniques to generate automatically a regular and scalable mesh representation of the ground. Each decimated mesh resulted from the surface reconstruction method is further merged within a global reference scene. Note that the entire workflow can be applied in parallel to each chunk, while merging each current ground surface with a global scene, on the fly, as they are computed.

This paper is concerned with the automatic ground surface reconstruction (AGSR) phases, mainly its extraction and surface reconstruction procedures which are described in the following two sections.

4. Point Cloud Segmentation and Classification

The focus here is the accurate and automatic segmentation of 3D point clouds from MLS data, applying the method proposed in [Her9, Ser19]. It is based on elevation images and it relies on image processing techniques, especially Mathematical Morphology [Mat11, Mer12]. The general workflow is composed by several steps: first, the 3D point cloud is projected to an elevation image. After images creation, a morphological interpolation is performed in order to fill holes caused by occlusions and missing scan lines. An interpolation technique based on the morphological fill holes procedure $Fill(f)$ is used since this transformation does not create new regional maxima in the image. At that point, ground is segmented and object hypotheses are generated as discontinuities on the model. Then, small and isolated regions are eliminated. Facades are segmented as the highest vertical structures. Finally, the segmented image is reprojected to the 3D point cloud in order to get the final result. This section resumes the ground segmentation and classification steps. For further details and complete analysis in each step, the reader is encouraged to review [Ser19].

4.1. Ground extraction

Ground segmentation is a critical step since urban objects are assumed to be located on it. When objects are filtered out it is possible to define the digital terrain model. With the aim of segmenting the ground, we use the approach proposed in [Her9]. It is based on the λ-flat zones labeling algorithm defined in [Mey12]. The parameter λ is set to 20 cm because it is usually high enough to join road and sidewalk without merging other objects, even if there are not ramp access for the sidewalk. Fig.2 (b) presents the segmentation and classification result corresponding to the input point cloud illustrated in Fig. 2 (a). Fig.2 (c) depicts the 3D point cloud representing the ground composed by roads, sidewalks and accessibility ramps. The 3D points belonging to the ground are further injected into the surface reconstruction process which is described in the following section.

5. Ground Surface Reconstruction

The ground surface reconstruction module transforms a 3D point cloud previously labelled as ground (illustrated in Fig. 2 (c)), into a continuous and scalable surface representation. The proposed framework is composed by several steps which are illustrated in Fig. 1 and described through the following sections. First, the 3D point cloud representing the ground is triangulated in the (x, y) plane using a constraint Delaunay algorithm which provides points connectivity. Then, we apply a mesh cleaning process to eliminate long triangles. In order to provide a continuous and regular surface model of the road, we apply the Sinc Windowed [Tau22] smoothing algorithm which eliminates high frequencies, while preserving sharp depth features and avoiding surface shrinkage. In a final step, a progressive decimator [Hop10] is applied to the smoothed mesh in order to cope with scalability constraints when performing surface reconstruction over large distances. It provides surface representation with low memory usage, enabling efficient data transmission and visualization. In addition, the decimation procedure enables progressive rendering in order to deal with real-time constraints imposed by driving simulation engines.

5.1. Point Cloud Triangulation

Let us note with $\mathbf{P} = \{x_i, y_i, z_i | i = 1,..., N_p\}$ the 3D point cloud corresponding to the ground, where N_p denotes the number of points. We apply the Triangle algorithm [She20] to the 3D point cloud **P** to generate a planar constraint Delaunay triangulation which provides the connectivity between points. Let us note with M_{DT} the resulting ground mesh, which has $N_t \approx 2N_p$ triangles.

5.2. Long Triangles Elimination

In order to eliminate long triangles from non-uniform boundary points, we perform statistics on the edge lengths and identify those with maximum length, noted $e_{\max}$. We identified that long edges correspond to $e_{\max} \approx \delta \bar{e}$ where $\bar{e}$ denotes the mean length computed over all edges $e_i^j \in M_{DT}$, i.e. over all triangles $t^j \in M_{DT}, j = 1,.., N_t$ and for its corresponding edges $e_i^j, i = \{1,2,3\}$. The term δ denotes a proportionality factor. A triangle t^j is eliminated if any of its edges $e_i^j > e_{\max}, i = \{1,2,3\}$. In practice, for several datasets acquired by different MLS systems, we found that a coefficient $\delta = 20$ results in a mesh without long triangles, which we note M_C.

5.3. Building a Regular Surface

As illustrated in Figures 3 (a) and (b), the triangulation of noisy 3D measurements results in high frequency peaks. Since we want to inject the ground surface model in driving simulator engines, an important issue which needs to be addressed is the geometrical accuracy. The 3D model must be distortion-free and regular. In order to obtain a regular surface, the Sinc windowed smoothing procedure [Tau22] is applied which approximates low-pass filters by polyhedrons in order to eliminate high frequency peaks. Figures 3 (c) and (d) illustrate the smoothed mesh, noted M_S; it can be observed that the Sinc Windowed smoothing technique provides a regular surface, while preserving roads and sidewalk borders sharpness.

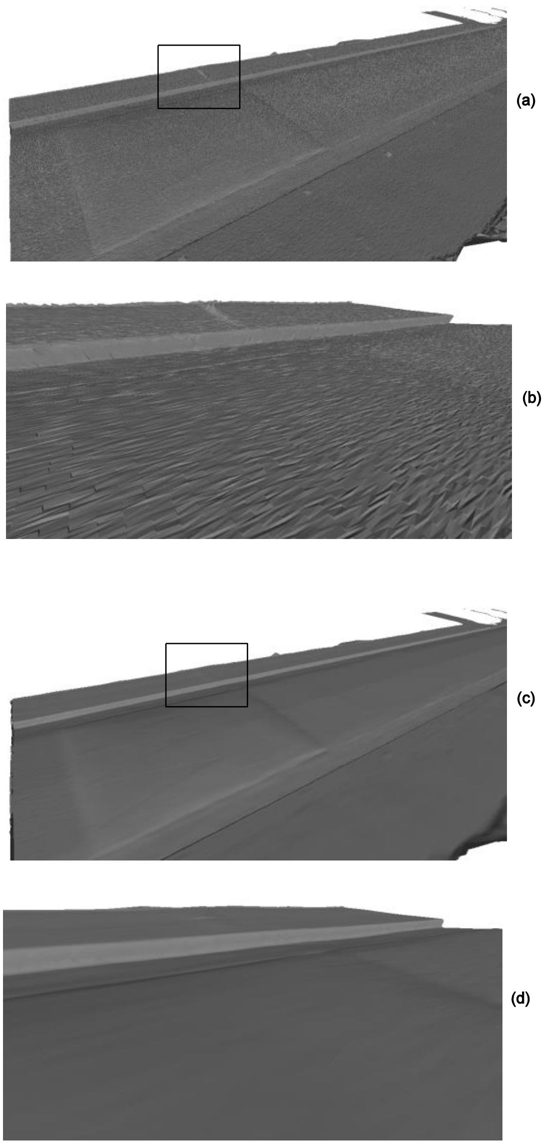

Fig. 3. Mesh smoothing results on dataset Cassette acquired over Cassette street situated in Paris, (France) by the STEREOPOLIS MMS [Pap14] equipped with a Riegl sensing device. (a) planar Delaunay triangulation, (b) zoom-in view on the sidewalk border corresponding to the black rectangle area illustrated in Fig. (a); (c) the result of the Sinc windowed smoothing procedure; (d) zoom-in view on the sidewalk border corresponding to the black rectangle area illustrated in Fig. (c).

5.4. Scalability

The smoothed mesh has a high number of triangles, being redundant and causing a high memory usage. Moreover, in order to merge several mesh segments into a global scene, the mesh resolution must be drastically reduced. To this end, we apply the progressive decimation method described in [Zar24, Hop10]. The resolution of the decimated mesh M_D given by $r(M_D)$ is controlled by the reduction factor, noted $f_D(\%)$. A second advantage of the progressive decimation algorithm is that it can generate progressive meshes in an incremental fashion for efficient visual rendering. The algorithm proceeds as follows: first, each vertex is classified and inserted in a priority queue for further processing. The priority is set following the error caused by the vertex elimination and by the re-triangulation of the resulting hole. Let us note with N_t^D the number of triangles of the decimated mesh. Fig. 4 illustrates the result obtained for the input depicted in Fig. 2 (c) reducing $f_D = 90\%$ of the entire mesh. The remaining number of triangles corresponds to $r(M_D) = 10\%$ of the original mesh. It can be observed that the decimation algorithm preserves the reconstruction of the road, sidewalk borders and accessibility ramps. In order to emphasize the detail-preserving capability of the decimation algorithm, Fig. 5 illustrate the speed bump reconstruction after applying a maximal reduction factor of $f_D = 90\%$.

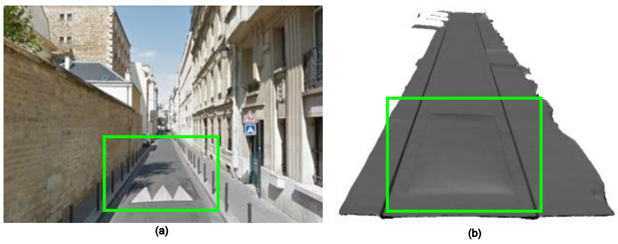

Fig. 4. Surface reconstruction results obtained for the dataset Cassette. (a) Google street view of the surveyed area; (b) Np = 1.01 Mpts, Nt=2.026 MTriangles, decimated mesh with fD = 90%, NDT = 203kTriangles.

5.5. Accuracy of the decimated mesh

As in [Tur23], we evaluate the accuracy of the decimated mesh by measuring the distance between the original point cloud **P** and the vertices of the decimated mesh, M_D. We choose to compute the Hausdorff distance [Cig5] and study both, the mean and the root mean squared distance RMS_H for different mesh resolutions $r(M_D)$. We observed that the mean is less sensible to the decimation process, while the RMS_H varies with a higher amplitude, although negligible ($\pm 10^{-3}$ m). This let us conclude that the memory usage can be reduced by a maximal factor of 90% without sacrificing the accuracy of the model.

6. Performance Evaluation

We evaluate the performances of the proposed framework in terms of accuracy, memory usage and computation time.

6.1. Accuracy evaluation

In order to quantify the accuracy of the reconstructed surface, we perform several measurements on site, mainly: the height of the sidewalk border and the height of the access ramp, noted $H_{sidewalk}$ and H_{ramp}, respectively. Table 1 illustrates the ground truth and the reconstructed dimensions for dataset Cassette shown in Fig. 4. It can be observed the reachable accuracy is better than 1.5 cm.

Table 1. Accuracy evaluation of the ground surface reconstruction algorithm with respect to ground truth (GT) data for dataset Cassettte.

Measurements	$H_{sidewalk}$ (cm)	H_{ramp} (cm)
GT	10.5	2.5
Reconstruction	10.1	2.3

6.2. Computation time

We evaluate our algorithm on a 64b Linux machine, equipped with 32 Gb of RAM memory and an Intel Core i7 running at 3.40 GHz. Our method is implemented in C/C++ and exploits PCL [Rus17] and VTK [Sch18] libraries. Table 2 illustrates the computation time obtained for the dataset Cassette. We can observe that the decimation step is the most expensive phase, being related to the decimation factor f_D. In this example, a maximum decimator factor was used $f_D = 90\%$ for a mesh with 2 MTriangles, which results in 9 sec of computation time.

Table 2: Computation time for dataset Cassette illustrated in Fig. 4 where P_S denotes the point cloud segmentation phase for the ground extraction; each column gives the runtime corresponding to each output of the algorithm. The overall computation time is about 17 s for N_p = 1.01 Mpts, N_t=203 kTriangles.

Steps	P_S	M_{DT}	M_C	M_S	M_D
CPU (s)	2	2.14	0.18	3	9

6.3. Memory usage

Table 3 illustrates the memory usage for each surface reconstruction step. It can be observed that the mesh representation is more efficient than the point-based one, allowing to reduce the memory usage 3 times for the full resolution mesh and 20 times for a resolution mesh of $r(M_S) = 10\%$. These results show that the proposed surface reconstruction framework provides a memory efficient surface representation, while preserving geometric details.

6.4. Visual rendering

The frame frequency, measured in frames per second (FPS), allows to quantify the quality of a 3D model with respect to the visual rendering capability. The second row of Table 3 illustrates the frame frequency, noted υ_{rate} and measured using Cloud Compare [Gir8] for different surface representations (discrete and continuous). It can be observed that the point-based representation detains faster rendering capabilities than the full resolution mesh, which does not cope with real-time rendering requirements. In contrast, the decimated mesh exhibits real-time frame rates, while providing a continuous surface representation. Although the decimation step is the most computationally expensive processing block of the proposed surface reconstruction framework, it enables real-time rendering of a continuous surface over large scale scenes, while preserving geometric details. It can be observed that even though the proposed technique includes a computationally expensive decimation phase, beside the detail-preserving rendering capability, it features real-time surface reconstruction on parallel processing units.

Table 3: Memory usage and frame frequency measures corresponding to the input chunk P and and to the main outputs of the algorithm for dataset Cassette illustrated in Fig. 4.

Cassette	P_S	M_{DT}	M_S	M_D
Memory (Mb)	14.85	81.61	37.6	3.7
υ_{rate} (fps)	267.74	10.27	12.44	131.96

7. Scaling-Up Cartography

We test the surface reconstruction algorithm on several chunks from several urban datasets acquired with different MLS systems. Fig. 5 illustrates the results obtained on 4 scans segments acquired by STEREPOLIS mobile platform [Pap14] using a Riegl sensor. The entire scene contains 12 Mpts, from which 4 Mpts were classified as belonging to ground. It can be observed that due to the vehicle speed which may vary, the acquired 3D chunks have different lengths. By taking into account the computation time obtained for dataset Cassette, in average, we process 3 Mpts for 50 m length of surveyed area in about 17 s.

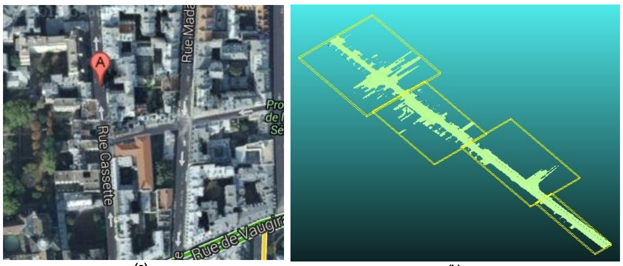

(a) (b)

Fig. 5. Surface reconstruction results obtained for dataset Cassette. (a) Google street view of the surveyed area, (b) surface reconstruction results obtained for 4 chunks with different lengths (each one included in its bounding box), overall approximative distance: 217 m.

For 100 Mpts (100 scan segments with 30% ground), it is possible to obtain the ground surface in about 28 min. For 100 km, the ground surface could be computed in about 10h. Even though time scalability is not our prior concern, by increasing the computational resources by a factor of 10, we provide a surface reconstruction framework capable to perform in real time. In this upgraded configuration, the algorithm can deliver the reconstruction of the entire road network for a country with 10000 km length in about 5 days, non-stop driving and data acquisition at 90 km/h.

8. Conclusions and Future Work

This paper presented the **A**utomatic **G**round **S**urface **R**econstruction (**AGSR**), a fully automatic framework for generating a scalable and detail-preserving ground surface reconstruction from MLS data in outdoor environments. The presented method addresses several key issues of the currently existing surface reconstruction methods such as: accurate reconstruction of sharp depth features in presence of noisy data sets, scalability and memory usage for efficient data transmission and visualization over large distances.

The proposed algorithm comes with a parallel scheme to be expanded at two levels: i) for running on series of ground chunks, and ii) at upper level, for reconstructing different classes, allowing to distribute the computation of different surface reconstruction frameworks. Thanks to the segmentation and classification algorithm, the entire framework can be combined with geometrically consistent surface reconstruction framework in order to expand the 3D modeling capability to buildings and non-ground objects (trees, cars, urban furniture). When such a multiple target reconstruction scheme is employed, its parallelization is straightforward. The proposed framework emphasizes the high potential of the MLS which, when combined with suitable frameworks, it allows to generate accurate and scalable 3D models in a fully automatic fashion. Future work focuses on the photorealist surface reconstruction problem through the jointly use of laser reflectance and RGB cameras. Research perspectives are also concerned with the extension of the global workflow to facade reconstruction, while tacking into account ground and façade merging within a global referential frame.

9. References

[Bou1] P. Bouchner and S. Novotný. Car Dynamics Model – Design for Interactive Driving Simulation Use. In Recent Researches in Applied Informatics, 2nd Proceeding of Int. Conference on Applied Mathematics and Computing Theory, 2011.

[Bre2] R. Brémond. La visibilitié routière: une approche pluri-disciplinaire. HdR, 2010.

[Bol3] A. Bolling, J. Jansson, A. Genell, M. Hjort, M. Lidström, S. Nordmark, G. Palmqvist, H. Sehammar, L. Sjögren, M. Ogren. SHAKE – an approach for realistic simulation of rough roads in a moving base driving simulator. In Driving Simulation Conference - Europe, 2010.

[Cha4] T. Chaperon and J.-P. Colinot. The new PSA Peugeot-Citroën Advanced Driving Simulator: Overall design and motion cue algorithm. In Driving Simulation Conference - North America, 2007.

[Cig5] P. Cignoni, C. Rocchini. and R. Scopigno. Measuring error on simplified surfaces. In Conference on Computer Graphics Forum, pp. 167–174, 1998.

[Cit6] CityGML: http://www.opengeospatial.org/standards/citygml

[Des7] G. Despine and C. Baillard. Realistic Road Modelling for Driving Simulators using GIS Data. In Advances in Cartography and GIScience, Lecture Notes in Geoinformation and Cartography, pp 431-448, 2011.

[Gir8] D. Girardeau-Montaut. Telecom Paristech & EDF. Cloud Compare, site web: http://www.danielgm.net/cc/, 2014.

[Her9] J. Hernández, and B. Marcotegui. Filtering of artifacts and pavement segmentation from mobile lidar data. In ISPRS workshop Laser scanning, XXXVIII-3/W8 2, pp. 329–333, 2009.

[Hop10] H. Hoppe. Progressive meshes. In Proceedings of 23rd Annual Conference on Computer Graphics and Interactive Techniques, SIGGRAPH pp. 99–108, 1996.

[Mat11] G. Matheron. Random sets and integral geometry. John Wiley & Sons, New York 28, pp. 493–501, 1975.

[Mey12] F. Meyer, From connected operators to levelings. 12, pp. 191–198, 1998.

[Okt13] Oktal site web: www.oktal.fr, 2014.

[Pap14] N. Paparoditis, J.-P. Papelard, B. Cannelle, A. Devaux, B. Soheilian, N. David and E. Houzay. Stereopolis II: A multi-purpose and multi-sensor 3D mobile mapping system for street visualisation and 3D metrology. Revue Française de Photogrammétrie et de Télédétection, Vol. 200, pp. 69-79, 2012.

[Pet15] J. Petit. Génération, visualisation et évaluation d'images HDR. Application à la simulation de conduite nocturne. PhD Dissertation, 2010.

[Roa16] RoadXML site web:

http://en.wikipedia.org/wiki/RoadXML, 2014.

[Rus17] R. B. Rusu and S. Cousins. 3D is here: Point cloud library (pcl). IEEE International Conference on Robotics and Automation (ICRA), 2011.

[Sch18] W. Schroeder, K. Martin and B. Lorensen. The visualization toolkit. Third Edition Kitware Inc, 2006.

[Ser19] A. Serna and B. Marcotegui. Detection, segmentation and classification of 3d urban objects using mathematical morphology and supervised learning. In Press 28, pp. 493–501, 2014.

[She20] J. R. Shewchuk. Triangle: Engineering a 2D quality mesh generator and delaunay triangulator. In Applied Computational Geometry: Towards Geometric Engineering (Ming C. Lin and Dinesh Manocha, editors), Springer-Verlag (Berlin) 1148, pp. 203–222, 1996.

[SIM21] SIMVIR site web: http://www.realite-virtuelle.univmed.fr/simvir/index.html, 2014.

[Tau22] G. Taubin and G. Golub. Optimal surface smoothing as filter design. IBM Research Report 1148, pp. 203–222, 1996.

[Tur23] E. Turnet and A. Zakhor. Watertight planar surface meshing of indoor points-clouds with voxel carving. In IEEE International Conference on 3D Vision pp. 41–48, 2013.

[Zar24] W. J. Schroeder. J. A. Zarge and W. E Lorensen. Decimation of triangle meshes. In Conference Proceedings of SIGGRAPH, pp. 65–70, 1992.

STEERABLE VIDEO: GENERATING VIDEO-BASED ENVIRONMENTS FOR DRIVING SIMULATION

Michael Brogan [1], Charles Markham [2], Sean Commins [2], Catherine Deegan [1]

(1): IT Blanchardstown
Dublin 15, Ireland
+353 (0) 1 885 1093
E-mail : {michael.brogan, catherine.deegan}@itb.ie

(2): NUI Maynooth
Co. Kildare, Ireland
+353 (0) 1 708 3383
E-mail : {charles.markham, sean.commins}@nuim.ie

Abstract – This paper describes an approach that allows for a steerable environment to be generated directly from a video for the purpose of integration with a video-based driving simulator. As the range of steering motion in a driving simulator is relatively limited, a pseudo-three-dimensional approach can be taken. This method requires only a single image sequence or video, acquired by any type of imaging system along a road. No three-dimensional, stereo or visual odometry data is acquired or calculated.

Key words: Video-based, driving simulation, pseudo-three-dimensional, photo-realistic

1. Introduction

Using video as a basis for a driving simulator's visual cue stream is relatively rare, with the vast majority of simulators using a graphical-based environment. There are two primary reasons for this; the ease at which full three-dimensional graphical models can be generated, and the difficulty in introducing a form of interactive control over a pre-recorded video sequence. There are several existing video-based driving simulators, examples being [Bre1, Bro1, DeC1, Her1, Ono1, Sat1].

The simulator described [Ono1] uses a combination of photo-textures and graphical models to create a sense of high-fidelity, but relies on graphical models for population and execution of scenarios. The image data acquired are used to texture the general environment in the far-distance, but all near-distance features, such as roads, traffic and road boundaries are graphics-based.

The simulator described in [Bre1] utilises data acquired from a high-cost mobile mapping system to generate a wire-frame environment. This environment is generated using data returned from a LiDAR laser-scanning device. Once generated, this skeletal structure can be textured using multi-view imagery acquired by the mapping system's cameras. This method produces a highly detailed photo-based environment that allows users to drive around a three-dimensional environment. As the generated environment is three-dimensional the benefits associated with traditional graphical-based environments remain present; scenarios can be introduced, and full control over the driving simulator world is present.

These systems have introduced photo-based environments to driving simulation, allowing the user to steer on or around textures, as opposed to through video sequences. The steering mechanisms are similar to previous graphical-based simulators, with the graphics having been replaced with photographic textures.

The driving simulator described in [DeC1] addresses this by using dual video sequences that allows the simulator visual cue stream to switch video feeds dependent on the position of the driver in the simulator. This approach, in and of itself has a major limitation, in that to acquire the data, the road segment must be driven twice, once in the wrong direction. This is possible if the road is not open to general traffic, but in terms of general data acquisition, is not a feasible approach unless road closures are coordinated with a governing body. Again, the ability to steer through a single video remains absent; the change in video feed does not allow for a gradient change in perspective.

Research has used non-steerable videos to demonstrate high correlations among video, graphical model and ground-truth speeds [Bro1], as well as augmenting different video sequences [Her1]. However, without the ability to steer, the full dynamic behaviour of driving cannot be realised. Such a capacity would allow for driver speed, position and the effect of one on the other to be measured using a video-based visual cue stream.

This paper describes a method by which a pseudo-three-dimensional photo-realistic video-based model can be generated to allow for a steerable environment to be generated without the need for stereo images, synchronization, calibration, correspondence, or three-dimensional reconstruction. However, the absences of these introduce some constraints that will be discussed, including the introduction of distortions around road boundaries, based upon lack of sufficient data.

It is divided into seven sections; section one gives an introduction to the topic and describes video-based driving simulators. Section two describes the route selected for testing purposes and details the video camera used for data acquisition. The testing system is also described. Section three explains how the steerable environment is generated from the single video sequence. Section four details how this steerable environment is interfaced with the driving simulator. Section five gives an overview of the geometry of the generated environment. Testing of the technique and the associated results are presented in section six, and conclusions based on these results are drawn in section seven.

2. Methodology

For the purposes of developing and testing the technique described in this paper, an off-the-shelf Mio MiVue 388 witness camera was mounted on the internal side of the windshield of a standard vehicle, and a two minute video of a road was acquired. This video was in High Definition format (1920x1080 resolution with a frame rate of 29.97 fps) [Mio1].

The selected route was the link road between the M3 motorway and R147 rural road in Kells, Co. Meath, Ireland. It is shown in Fig. 1, alongside an example of the road scene as acquired by the camera.

For the purposes of testing the technique described in this paper, a Microsoft Windows 8-based notebook with 15.6 inch, 1366x768 resolution widescreen display was used, with a Thrustmaster gaming steering wheel [Thr1].

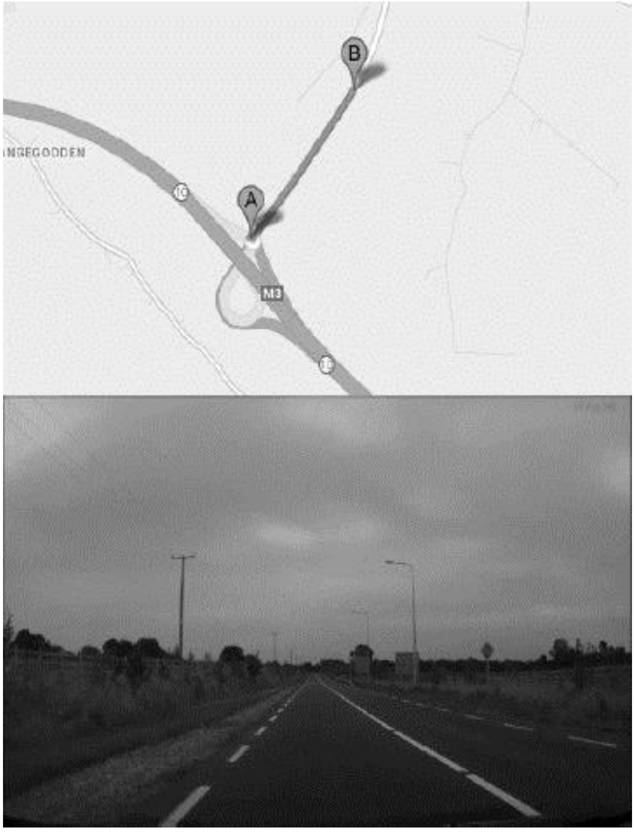

Fig. 1. Selected data acquisition route (R147).

3. Environment Generation

Generation of a full three-dimensional environment requires the acquisition of multi-view geometry of a scene, commonly using two camera views (stereo) or multiple camera views. The disparity in the resultant images can be used to generate a dense stereo description of the scene, called a depth map. This map is a greyscale description of the depth of a scene, where the lower the pixel intensity, the further the feature lays from the reference camera, and the higher the pixel intensity, the closer the feature lies to the reference camera [Har1, Tru1]. In an environment where the geometry of the scene remains relatively constant, such as the road scene video acquired by the system on the test route, a dense stereo depth map can, instead of being generated using stereo-view or multi-view image sequences, be estimated using the horizon line.

This allows for pseudo-depth perception to be inferred onto a single image. The process by which a depth map can be estimated from a single image is described next. By its nature, the line at infinity lies at an infinite distance from the acquiring camera. As the line at infinity is represented in images by the horizon, the horizon must first be identified in the single image. Once this is achieved, a greyscale gradient is generated, beginning at zero pixel intensity on the horizon, and increasing gradually to maximum pixel intensity to the bottom of the image. An example of a depth map generated using this approach is shown in Fig. 2.

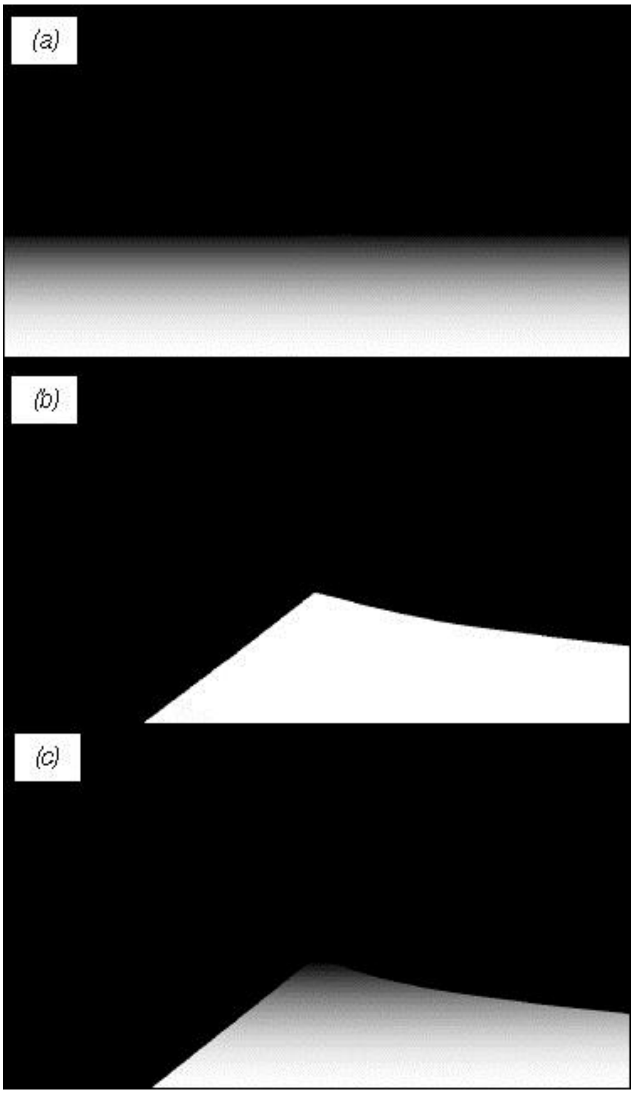

Fig. 2. (a) Horizon-defined depth map; at this stage all features below the horizon line can be assigned a depth. (b) Road area mask; identifies the road area in the image. (c) Masking (a) with (b) allows only the road to be assigned a depth.

Once this is achieved, the primary feature which requires a sense of depth is that of the road. Again, by its nature, the road will begin nearest the camera, and, as the edges of the road are parallel, will meet at the horizon [Har1]. This produces a mask whereby the depth map is masked so that a depth map describing the road only is estimated.

This allows a greyscale gradient to be applied to the corresponding road area, beginning at zero pixel intensity on the horizon, and increasing gradually to maximum pixel intensity when the area closest to the acquiring camera is reached. Once the depth map has been estimated, and the geometry of future images in the video sequence is approximately the same, the same depth map can be used for each image. The next step that must be undertaken is to infer depth perception on a video frame using this depth map. This is done by layering the original RGB video frame over the depth map, essentially creating an RGB-Depth (RGB-D) image from the original RGB image and the estimated depth map.

Each value in the depth map is assigned a corresponding distance within a virtual graphical environment, and the virtual camera is situated at a constant distance from the displayed pseudo-three-dimensional image. Lack of sufficient data is evidenced in the pseudo-three-dimensional images as warping and distortion of areas close to the road edge, where the depth map was primarily estimated. This occurs where the depth map boundary does not map the road segment to the road plane, causing distortions between the road and non-road planes.

4. Interfacing Environment

To allow for steering around the three-dimensional image, the camera view is linked to the driving simulator steering wheel position, thereby allowing for the view of the road scene to change based on the user's input. The implementation of steering within a video sequence is completed by sequencing the video frames, such that upon any pressure applied to the driving simulator's acceleration pedal, the next frame of the video is loaded, textured and displayed at the correct viewpoint, based upon the current orientation of the steering wheel. A sequence of such images is shown in Fig. 3.

Fig. 3. Estimated depth map applied to image sequence.

5. Environmental Geometry

The generated environment consists of a local world three-dimensional co-ordinate system, which is viewed using an arcball camera, centred on the central horizon point. Two two-dimensional planes are used to generate the pseudo-three-dimensional environment; the non-road plane, π_N, and the road plane, π_R. π_N will contain all non-road features, and π_R will contain the road only.

This results in π_N being coincident with the XY_{World} plane, and π_R being non-parallel with the XZ_{World} plane, and creates the pseudo-three dimensional environment that enables steerable video to be generated. The offset between the world co-ordinate system origin and the intersection of π_R with π_N is dependent on the position of the horizon line in the acquired video.

π_R is divided into 256 subsections, along the Z_{World} axis, each relating to a depth map greyscale intensity. This allows for the depth map to define which pixel intensities are to be mapped to the corresponding π_R Z_{World} axis line. The parameters of the arcball camera are defined in terms of its rotation and translation with respect to a fixed point in the viewing scene. That is, the projection of the world co-ordinate scene is defined in terms of three parameters: the fixed point, the camera's rotation around this point, and the camera's translation from this point. The fixed point can be described in terms of a 3-vector, with the position of the camera being described in terms of a 3-vector, with an *X, Y* co-ordinate describing the position of the camera relative to the surface of the viewing arc, and a *Z* co-ordinate describing the radius of the viewing arc from the point of focus. The orbit of the camera's X-axis is shown in Fig. 4.

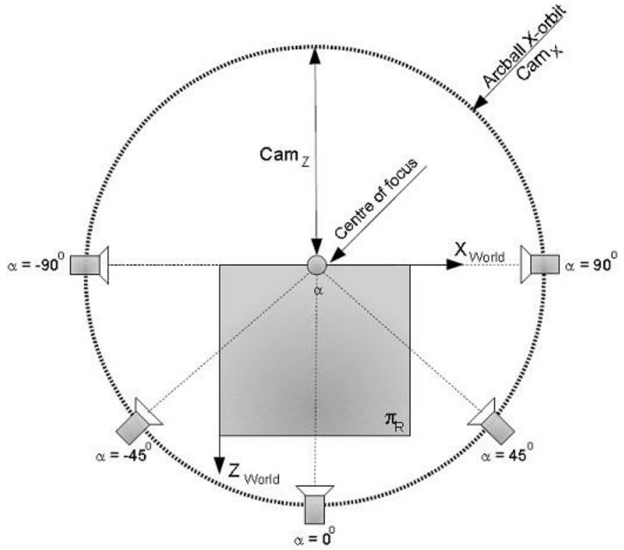

Fig. 4. Orbit of the camera's X co-ordinate, showing the movement of the camera relative to the XY plane, described by the angle α.

When $\alpha = 0°$ the virtual camera plane will be parallel to π_N. In this case the original image will be displayed, with no redundancy visible. Redundancy can be considered symmetrical across the $-90° \leq \alpha \leq 0°$ and $0° \leq \alpha \leq 90°$ ranges. Redundancy in the viewed image plane is dependent on the value of α, and can be quantified in terms of the percentage of the road plane that increases with the increase in α.

The orientation of the steering wheel is relayed to the PC as a 16-bit value, giving a range of 0 to 65,535, with a 0 value representing the wheel at the leftmost position and the 65,535 value representing the wheel at the rightmost position. The value is normalised in the range of ±180°, representing the full range across 360°. In the case where the arcball camera position is neutral (i.e. it lies in the same position relative to the imaged road as the acquiring camera did), the projected scene will be the same as that of the original video. As the arcball camera's rotation changes, the viewpoint of the road scene will change also, resulting in a steerable scene.

6. Testing and Results

A timer was displayed on screen, and reset every ten seconds. Participants were instructed to change lane when the counter reset to zero.

For the purposes of testing, acceleration was disabled. The video advanced automatically, allowing each participant's steering response to be measured independently of speed. The lane that the driver was in was recorded, with the normalised average position of the ten participants shown in Fig. 5.

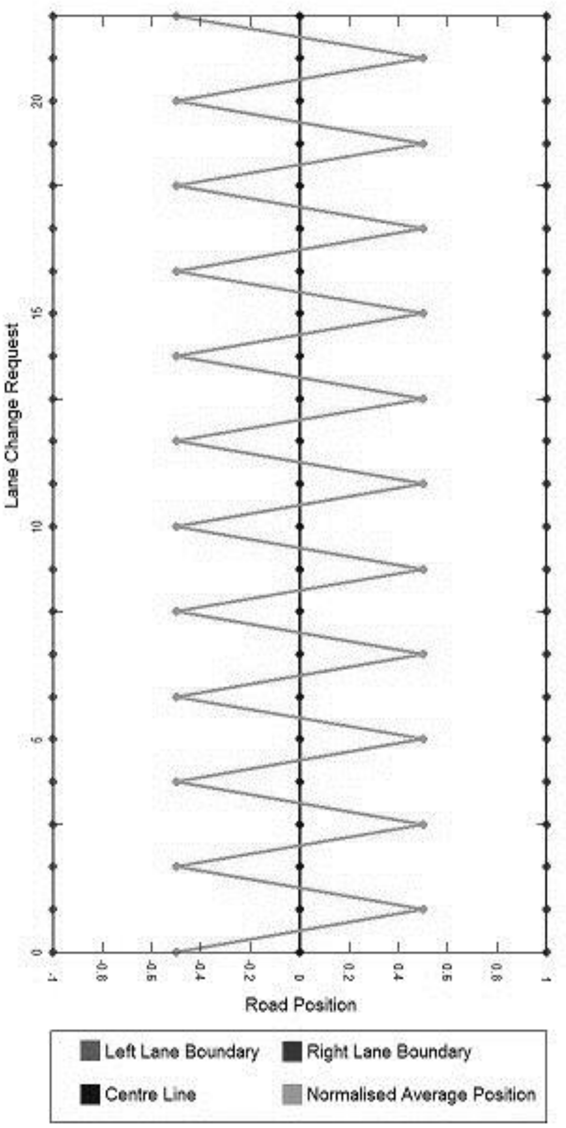

Fig. 5. Normalised average lane position (22 lane changes per participant with 10 participants).

The number of lane changes requested from the 10 participants was 22 each. Of these 220 total requests, 186 were completed successfully (87%).

The ten participant data set had an average success rate of 87%, ranging from 64% to 100% per participant, with a mean of 18.6 lane changes and standard deviation of 2.67.

7. Conclusions and Future Work

This paper has shown that a single video sequence, acquired by a standard witness camera, can be adapted for use in a video-based driving simulator by estimating a single depth map that represents a road with an assumed constant geometry. Average driver response to the change lane instruction was 87%. The failure rate of 13% may be attributed to participants missing the resetting of the onscreen counter.

Future work will consist of extending the existing approach such that a depth map can be estimated for each frame in the video sequence using the parallelism of the road edges and the horizon line. This will enable the approach to be implemented using any road geometry, whether it is constant or changing constantly. A comparison of this technique against the genuine depth maps generated using the stereo image data of the original mapping system will then be undertaken to compare and contrast the two methods. Behavioural testing of drivers will be the focus of further testing using the driving simulator once the full video steering component has been integrated with it.

Acknowledgments

The authors wish to thank the support of the Irish Research Council (IRC) for their continuing support, and also to the participants for their time.

References

[Bre1] Bredif, M., "Image-based rendering of LOD1 3D city models fortraffic-augmented immersive street-view navigation," in *ISPRS Annals of the Photogrammetry, Remote Sensing and Spatial Information Sciences*, Antalya, Turkey, 2013, pp. Volume II-3/W3.

[Bro1] Brogan, M., Kaneswaran, D., Commins, S., Markham, C., and Deegan, C. "Automatic generation and population of graphics-based driving simulator using mobile mapping data for the purpose of behavioral testing of drivers," *Proceedings of the Transportation Research Board Annual Meeting*, Washington DC, January 2014.

[DeC1] De Ceunynck, T., et al., "Proactive evaluation of traffic signs using a traffic sign simulator," in *Annual Meeting of the Transportation Research Board*, Washington, DC, 2014.

[Har1] Hartley R., Zisserman, A., *Multiple View Geometry in Computer Vision*, 2nd ed.: Cambridge University Press.

[Her1] Heras, A.M., Breckon, T.P. and Tirovic, M., "Video Re-sampling and Content Re-targeting for Realistic Driving Incident Simulation," in *Proc. 8th European Conference on Visual Media Production*, 2011, pp. sp-2.

[Mio1] Mio MiVue 388 Witness Camera, [Online : 22 May 2014]

http://eu.mio.com/en_gb/mivue-388.htm

[Ono1] Ono, S., et al., "A photo-realistic driving simulation system for mixed-reality traffic experiment space," in *IEEE Symposium on Intelligent Vehicles Symposium*, Las Vegas, Nevada, 2005, pp. 747-752.

[Sat1] Sato, R., Ono, S., Kawasaki, H., and Ikeuchi, K., "Real-time image-based rendering system for virtual city based on image compression technique and eigen texture method," in *19th International Conference on Pattern Recognition (ICPR)*, Tampa, Florida, 2008, pp. 1-4.

[Thr1] Thrustmaster Steering Wheel [Online : 22 May 2014]

http://www.thrustmaster.com

[Tru1] Trucco, E., A. Verri, A., *Introductory Techniques for 3-D Computer Vision*, 1st ed.: Prentice Hall, 1998.

DEVELOPMENT AND VALIDATION OF A SAFETY ARCHITECTURE OF A WHEELED MOBILE DRIVING SIMULATOR

Alexander Betz[1], Paul Wagner[1], Torben Albrecht[1] , Hermann Winner[1]

(1) : Institute of Automotive Engineering, Technische Universität Darmstadt, Otto-Berndt-Str. 2, 64287 Darmstadt, Germany
Phone: +49 (0) 6151-16-3796
Fax: +49 (0) 6151-16-5192
betz@fzd.tu-darmstadt.de, wagner@fzd.tu-darmstadt.de, torben.albrecht@stud.tu-darmstadt.de, winner@fzd.tu-darmstadt.de

Abstract – The safety architecture of the Wheeled Mobile Driving Simulator (WMDS) is not yet known. It has to cope with carrying subjects on an unbound motion base while providing safety for the users, the system, and the surroundings. The complexity of the safety architecture increases when compared to rail guided Driving Simulators (DS) since stop dampers cannot be provided for all possible impact angles and positions. A representative solution is developed and validated. The validity of the safety architecture is analyzed by hardware testing. A representative WMDS is developed for this purpose. The introduced safety architecture is derived from a Failure Mode and Effects Analysis (FMEA) and a Fault Tree Analysis (FTA). The conducted tests validate the safety architecture with respect to the discharge process and the achieved mean deceleration during the emergency stop.

Key words: Wheeled Mobile Driving Simulator, Safety System, Hardware Testing, Conception and Design, Validation.

1. Introduction

1.1. Motivation for Wheeled Mobile Driving Simulators (WMDS)

DS are an indispensable developmental tool in the automotive industry due to their high degree of reproducibility and safety. In order to fulfill the increased requirements of modern-day DS [Bet12a], a state-of-the-art DS must provide up to 12 degrees of freedom (DOF) whilst comprising of multiple drive mechanisms. These improvements come with the disadvantage of creating a complex system with an increased moving mass of about 80 t [Cla01]. Thus, a link between moving mass and motion envelope is created, limiting either motion envelope or system dynamics.

This dilemma has been recognized by the automotive industry, as attested by Zeeb in 2010, former head of Driving Simulators at Daimler: *"To induce a much better longitudinal motion sensation with a scaling factor close to 1:1 for all possible acceleration and deceleration scenarios even a several ten meter long sledge would not be sufficient, but would increase the technical and financial effort tremendously, especially when the […] mandatory requirements for drive dynamic experiments have to be fulfilled."* [Zee10].

Another aspect is the limited yaw angle in advanced dynamic DS. Urban traffic maneuvers like parking, turning, or reversing require great yaw that cannot be provided adequately by state of the art advanced dynamic DS.

Mobile dynamic DS, like the WMDS, solve the core problem of the increased moving mass and provide unlimited yaw motion.

1.2. Presentation of the WMDS Concept

The proposed design of a WMDS shows three self-propelled and active steerable wheels that allow horizontal motion and yaw [Bet10, Bet14]. The main idea is based on the assumption that a wheeled system, whose propulsion is limited by friction forces, is suitable to simulate the horizontal dynamics of vehicles that are also limited by tire friction forces.

An additional system provides at minimum cabin tilt and heave. Avoiding the conventional rail systems, which mainly cause the moving mass to increase, results in a light weight concept [Bet12a, Bet12b]. The design and construction of the WMDS are carried out at the Institute of Automotive Engineering (Fahrzeugtechnik Darmstadt: FZD), Technische Universität Darmstadt, Germany since 2010.

A multi-body simulation [Bet13] as well as a scaled hardware prototype of the WMDS was built in 2013 [Wag13, Wag14, Bet14]. The hardware prototype is currently in operation at FZD. A photograph of the prototype can be seen in Fig. 1, where the hexapod is situated in the middle of the omnidirectional platform. The illustrated user-machine-interface is not intended to be applied for DS studies but presents the final position of the DS cabin. Furthermore the drive units with its steering and traction motors are visible. The system does not contain friction brakes and uses only the electric motors as service brakes.

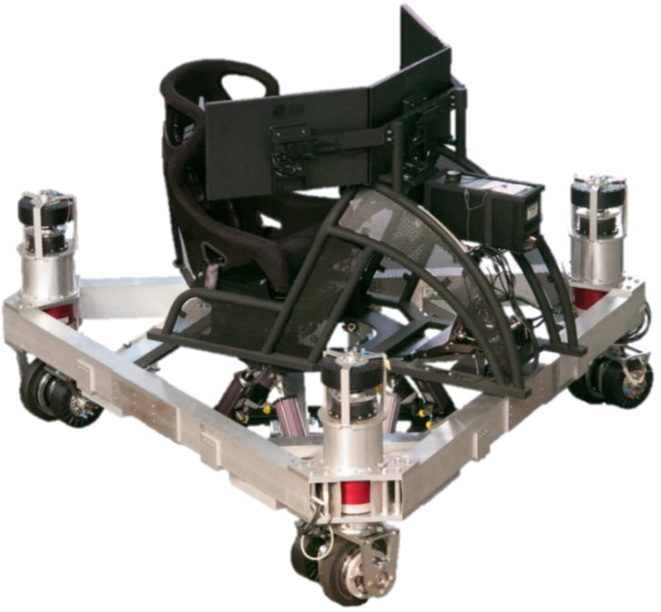

Fig. 1: Assembled scaled WMDS prototype

1.3. Motivation for a WMDS Safety System

The safety architecture is a vital element of a DS since the simulator must cope with carrying subjects on a motion base while providing safety for the users, the system, and the surroundings. The unbound characteristic of the WMDS increases the complexity of the safety architecture compared to rail guided DS. This increase is because conventional stop dampers cannot be provided for all possible impact angles and positions of the unbound system.

Most of the components used for the prototype are prototypical themselves, barely researched, or custom-made items. Hence, most components are not released for safety critical applications. Even the chosen tires are barely researched although they are derived from volume production in the forklift truck industry.

1.4. Methodology

The requirements of the safety architecture are derived by a FMEA and the FTA. The FTA is based on a critical top event for a countermeasure found by the FMEA. [Bet14]

A representative solution for the safety architecture of the WMDS is developed and a physical reference system is build up. Hardware tests analyze the performance of the representative solution and thereby validate the chosen architecture.

This safety architecture countermeasures the amount of considered failures and paves the way for the first test drives with the worldwide unprecedented WMDS prototype.

2. Concept Idea

The results of the FMEA lead to the conclusion that an additional system is required to avoid the potential failure modes of the overall WMDS prototype. The idea is to lift the system off the ground and thereby decoupling the drive units from the ground. Thus, the drive train of the WMDS is cut. This helps to prevent consequences from corrupt or incorrect motor actions independent from the manifold error sources (software, data transfer, energy supply, hardware, etc.).

Still there is potential hazard from the kinetic energy of the WMDS as long as the system is in motion. The safety architecture relocates the contact forces from the wheels to new elements of the lifting system. In order to provide deceleration those elements have to generate horizontal force in opposite direction to the velocity vector of the contact point.

Several technical solutions are available for creating this decelerating force. Nevertheless, friction based force transmission is highly appropriate in terms of low complexity, low mass and low cost. The wear of the friction elements is expected to be tolerable because the system represents an emergency stop system and not a service brake.

It must be considered that the new contact patches, where the deceleration force is generated, take over the responsibility for rollover safety. Hence, the number (at least three) and position of the new contact patches underlie similar constraints like the positioning of the drive units [Wag14]. The question arises how the system lift and the decelerating force is generated. It must be stressed that no existing example of the presented safety architecture is known. Thus, the physical reference system is expected to serve as a research prototype that accelerates the gain of system understanding by hardware testing. The representative solution is introduced hereafter.

3. FTA of Safety Architecture

In the safety architecture, the friction force created as well as the support force of the mountings are subject to the friction coefficient, contact force, and force transmission. Therefore, the top event of the FTA must treat the event chain of those forces. The result of the FTA is presented in Fig. 2.

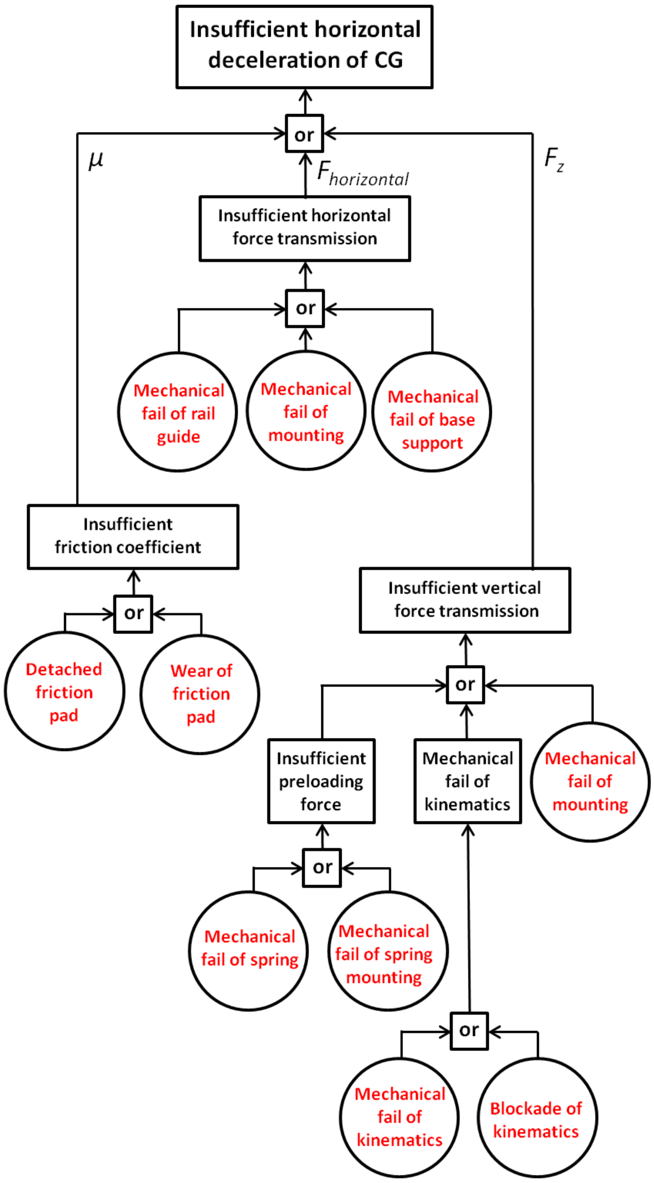

Fig. 2: FTA of critical top event [Bet14]

The controllability of the critical failures that cause the top event is realized by safety factors in the dimensioning process and a redundancy of the utilized number of lifting systems. Hence, six lifting systems are applied (see Fig. 3, two at each edge of the triangle) instead of the minimum required number of three systems.

4. Representative Solution

4.1. Concept

The representative solution utilizes friction forces of the new contact patches. Therefore, friction pads are used. Those forces result from contact forces and sliding friction created by a relative velocity of the new contact patches with respect to the ground. According to Fig. 3, the contact force is created by a knee lever that is actuated by a spring. The spring provides the needed energy for lifting the WMDS prototype off the ground. In order to ensure the lifting even in case of an electrical outage, the spring is preloaded before the start of operation and is hold actively by electromagnetic clamps. If any internal functional error (software or electrical) or fault is detected, the tolerated workspace is left, or any of the emergency stops is activated, the electrical circuit of the magnets is cut and the passive lifting task is initiated. Fig. 3 illustrates the hold (left) and emergency position (right) of the lifting system.

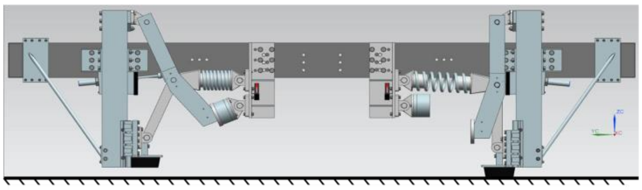

Fig. 3: CAD model of the lifting system (left: actively held; right: discharged)

4.2. Analysis of Lifting Stroke and Lifting Force Demand

The inverting of the activation logic increases the reliability of the safety architecture but causes continuous power demand for holding the preloaded spring. The force demand for lifting the WMDS is not linear with respect to vertical displacement, thus, a conventional spring with its linear characteristics is not the most suitable component, as shown in Fig. 4 by an exemplarily chosen spring characteristic providing the demanded force at maximum lifting stroke (dotted graph). In the actively held position, the lifting system has a desired initial lifting force of zero since no contact force at the friction element exists. This relation is valid for about 10 mm because this is the space required as ground clearance during operation (see left side of Fig. 3). After the gap has been closed by the safety system, the friction pad touches the ground and lifting force is thereby generated. After the gap has been closed, the created lifting force of the friction elements reduces the wheel loads. This phase of the lifting procedure is approximated by a linear characteristic[1]. The maximum desired lifting force is derived by a worst-case assumption concerning maximum wheel load (8688 N) due to assumed peak tire friction (μ_{max} = 1.45). As soon as all wheels have lost their ground contact no further increase of lifting force is necessary. However, further lift is desired to cause a defined tire-ground clearance for the emergency brake phase. As mentioned before and confirmed by the solid graph of Fig. 4, the discussed force demand does not meet conventional spring characteristics. The overall stroke of the lifting system is about 40 mm.

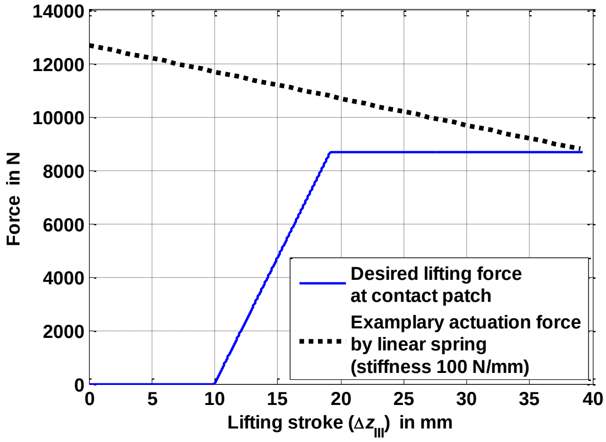

Fig. 4: Desired lifting force at contact patch and actuation force

4.3. Application of a Knee Lever

The desired force characteristic is realized by a conventional spring that acts on a knee lever. The non-linear transmission ratio of the knee lever in combination with a linear spring results in a non-linear force characteristic with respect to the lifting stroke. According to Fig. 5, the corresponding equations (1) to (24) apply.

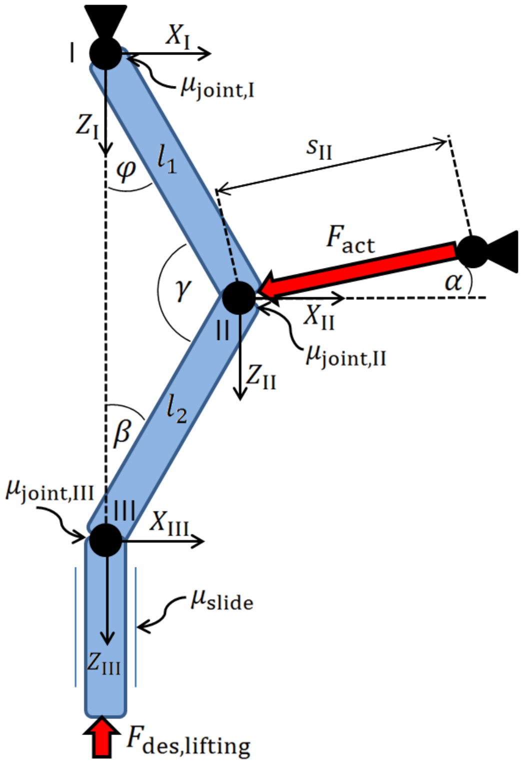

Fig. 5: Knee lever setup with lifting force and actuation force

The following relationship is derived using the law of energy conservation and accounts only for the discharge motion of the safety architecture:

$$\mathrm{d}z_{III}F_{des} = F_{act}\mathrm{d}s_{II} \quad (1)$$

Considering friction and the angle of the actuation force, equation (1) yields equations (2) to (6).

$$F_{des}\mathrm{d}z_{III} + F_{frict,slide}\mathrm{d}z_{III} + M_{fric,joint,I}\mathrm{d}\varphi + M_{fric,joint,III}\mathrm{d}\beta$$

$$+M_{fric,joint,II}\mathrm{d}\gamma = F_{act}\,[\cos(\alpha)\mathrm{d}x_{II} + \sin(\alpha)\mathrm{d}z_{II}] \quad (2)$$

$$F_{frict,slide} = \mu_{slide}F_{x,III} \quad (3)$$

$$M_{fric,joint,I} = \mu_{joint}\frac{d}{2}F_{l1} \quad (4)^2$$

$$M_{fric,joint,II} = \mu_{joint}\frac{d}{2}F_{act} \quad (5)^2$$

$$M_{fric,joint,III} = \mu_{joint}\frac{d}{2}F_{l2} \quad (6)^2$$

The unknown forces of equation (7), (8) and (9) are derived from a free-body diagram, Fig. 6. For the sake of readability u_1, u_2 and u_3 are introduced.

$$F_{x,III} = F_{act}(\cos(\alpha) - u_1) \quad (7)$$

[1] Vertical tire stiffness according to experimental test on the GUMASOL test facility (28.06.2013): 1036 N/mm (linearized spring rate)

[2] [Ker12]

$$F_{l1} = F_{\mathrm{act}} u_2 + F_{\mathrm{des}} \cos(\varphi) \quad (8)$$

$$F_{l2} = F_{\mathrm{act}} u_3 + F_{\mathrm{des}} \cos(\beta) \quad (9)$$

$$u_1 = \frac{\cos(\alpha+\beta)}{\cos(\varphi) l_1 + \cos(\beta) l_2} l_2 \quad (10)$$

$$u_2 = \sin(\varphi) u_1 + \cos(\varphi)\,(\mu_{\mathrm{slide}}(\cos(\alpha) - u_1) - \sin(\alpha)) \quad (11)$$

$$u_3 = (\cos(\alpha) - u_1)(\sin(\beta) + \mu_{\mathrm{slide}} \cos(\beta)) \quad (12)$$

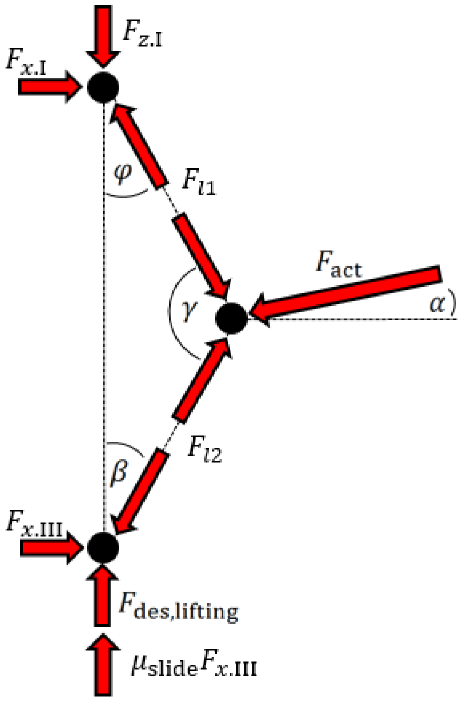

Fig. 6: Free body diagram of knee lever

The normal force $F_{x,\mathrm{III}}$ (7), needed to calculate the frictional forces in the sliding joint (3), is derived by the sum of forces in x-directions (14), the reaction force $F_{x,\mathrm{I}}$ (24) by the sum of moments about joint III (13). The rod forces F_{l1} (9) and F_{l2} (8), used to determine the frictional moments (4) and (6) in the joints, are derived by the sum of forces at joint I (17) and III (18) in direction of l_1 and l_2.

The sum of moments about joint III yields:

$$F_{x.\mathrm{I}}(\cos(\varphi)\, l_1 + \cos(\beta)\, l_2) = F_{\mathrm{act}} \cos(\alpha) \cos(\beta)\, l_2$$
$$- F_{\mathrm{act}} \sin(\alpha) \sin(\beta)\, l_2$$
$$\rightarrow\ F_{x.\mathrm{I}} = F_{\mathrm{act}} \frac{\cos(\text{á}) \cos(\beta) - \sin(\alpha)\sin(\beta)}{\cos(\varphi)\cdot l_1 + \cos(\beta)\cdot l_2} l_2 = F_{act} \cdot u_1 \quad (13)$$

The sum of forces in x-direction yields:

$$F_{x.\mathrm{I}} + F_{x.\mathrm{III}} = F_{\mathrm{act}} \cdot \cos(\alpha)$$
$$F_{x.\mathrm{III}} = F_{\mathrm{act}} \left(\cos(\alpha) - \frac{\cos(\alpha)\cos(\beta) - \sin(\alpha)\sin(\beta)}{\cos(\varphi)\cdot l_1 + \cos(\beta)\cdot l_2} l_2 \right)$$
$$\rightarrow\ F_{x.\mathrm{III}} = F_{\mathrm{act}}(\cos(\alpha) - u_1) \quad (14)$$

The sum of forces in z-direction yields:

$$F_{z.\mathrm{I}} + \sin(\alpha) F_{\mathrm{act}} = F_{\mathrm{des}} + \mu_{\mathrm{slide}} F_{x.\mathrm{III}} \quad (15)$$
$$\rightarrow\ F_{z.\mathrm{I}} = F_{\mathrm{des}} + F_{\mathrm{act}}(\mu_{\mathrm{slide}}(\cos(\alpha) - u_1) - \sin(\alpha)) \quad (16)$$

The sum of forces at joint I in F_{l1}-direction yields:

$$F_{l1} = \sin(\varphi)\, F_{x.\mathrm{I}} + \cos(\varphi)\, F_{z.\mathrm{I}}$$
$$= F_{\mathrm{act}}\big(\sin(\text{ö}) u_1 + \cos(\varphi)\,(\mu_{\mathrm{slide}}(\cos(\alpha) - u_1)$$
$$- \sin(\alpha))\big) + \cos(\varphi)\, F_{\mathrm{des}}$$
$$\rightarrow F_{l1} = F_{\mathrm{act}} u_2 + F_{\mathrm{des}} \cos(\varphi) \quad (17)$$

The sum of forces at joint III in F_{l2}-direction yields:

$$F_{l2} = \sin(\beta)\, F_{x.\mathrm{III}} + \cos(\beta)\, F_{\mathrm{des}} + \cos(\beta)\, \mu_{\mathrm{slide}} F_{x.\mathrm{III}}$$
$$= F_{\mathrm{act}}(\cos(\alpha) - u_1)(\sin(\beta) + \cos(\beta)\, \mu_{\mathrm{slide}}) + \cos(\beta)\, F_{\mathrm{des}}$$
$$\rightarrow F_{l2} = F_{\mathrm{act}} u_3 + F_{\mathrm{des}} \cos(\beta) \quad (18)$$

Considering equations (2) to (12) leads to the final relation of the actuation force (19). The differential displacements are unambiguously related by geometrical constraints of the knee lever and result in variable transmission with respect to the knee levers state – φ (equations (20) to (24)).

$$F_{\mathrm{act}} = \frac{F_{\mathrm{des}}\left[\mathrm{d}z_{\mathrm{III}} + \mu_G \frac{d}{2}(\cos(\beta)\,\mathrm{d}\beta + \mathrm{d}\varphi)\right]}{\cos(\alpha)\mathrm{d}x_{\mathrm{II}} + \sin(\alpha)\mathrm{d}z_{\mathrm{II}} - \mu_{\mathrm{slide}}(\cos(\alpha) - u_1)\mathrm{d}z_{\mathrm{III}} - \mu_{\mathrm{joint}} \frac{d}{2}[u_2 \mathrm{d}\varphi + u_3 \mathrm{d}\beta + d\gamma]} \quad (19)$$

$$x_{\mathrm{II}} = \sin(\varphi)\, l_1 \quad (20)$$

$$z_{\mathrm{II}} = \cos(\varphi) l_1 \quad (21)$$

$$z_{\mathrm{III}} = \cos(\varphi) l_1 + \sqrt{l_2^2 - (\sin(\varphi)\, l_1)^2} \quad (22)$$

$$\sin(\beta) = \sin(\varphi) \frac{l_1}{l_2} \quad (23)$$

$$\gamma = \pi - \beta - \varphi \quad (24)$$

4.4. Summary of Requirements

The designing of the parameters of the safety architecture is done by numerical analysis and meets the required performance demands and found relationships:

- Required performance demands
  - Minimum required lifting stroke: 40 mm (ground clearance + wheel compression and lift)
  - Desired lifting force at contact patch: Fig. 4 (solid graph)
- Found relations by numerical analysis

- The longer the knee levers, the weaker the required actuation force
- Equal length of the levers leads to decreased spring stiffness: $l_1=l_2$
- The length of the levers is limited by the WMDS height and accessible linkage: $l_1+l_2<540$ mm

Furthermore the position of the safety architecture must prevent a rollover in case of maximum deceleration. Because the dimensioning of the motion base itself is designed to prevent a rollover, the positioning of the friction pads of the safety architecture underlies similar dimensioning constrains. Therefore the same base length of the equilateral triangle can be used. The necessary base length l_t of the WMDS Prototype becomes a function of the maximum friction coefficient μ_{max} and the height of the center of gravity (CG) h_{CG} (Fig.7). The most critical rollover condition occurs when the acceleration vector is perpendicular to any of the bases of the triangle. Hence the equation (25) is derived by setting up the balance of forces and calculating the moment equilibrium around point 2.

$$\sum_{(2)} M = 0 = m \cdot g \cdot (\mu_{\max} \cdot h_{CG} - r_{\mathrm{ic}}) + h_{\mathrm{t}} \cdot F_{\mathrm{z,wheel,1}} \qquad (25)$$

$$r_{\mathrm{ic}} = \frac{1}{3} h_{\mathrm{t}} = \frac{1}{2\sqrt{3}} l_{\mathrm{t}} \qquad (26)$$

$$h_{\mathrm{t}} = \frac{\sqrt{3}}{2} l_{\mathrm{t}} \qquad (27)$$

Rollover can be put on the same level as wheel lift, which occurs when the wheel load $F_{z,wheel,1}$ (28) becomes smaller than zero:

$$F_{\mathrm{z,wheel,1}} = \frac{2 \cdot m \cdot g \cdot \left(\frac{1}{2\sqrt{3}} l_{\mathrm{t}} - \mu_{\max} \cdot h_{\mathrm{CG}}\right)}{\sqrt{3} \cdot l_{\mathrm{t}}} > 0 \qquad (28)$$

$$\rightarrow l_{\mathrm{t}} > 2\sqrt{3} \cdot \mu_{\max} \cdot h_{\mathrm{CG}} \qquad (29)$$

Equation (29) defines the minimum base length needed to ensure rollover safety. With the dimensions of the WMDS Prototype shown in Table 1 the safety factor against rollover is 1.38.

Table 1: Geometric dimensions of the final WMDS Prototype

Parameter	Unit	Value
h_{CG}	mm	481
μ_{max}	mm	1
l_t	mm	2300
h_t	mm	1992

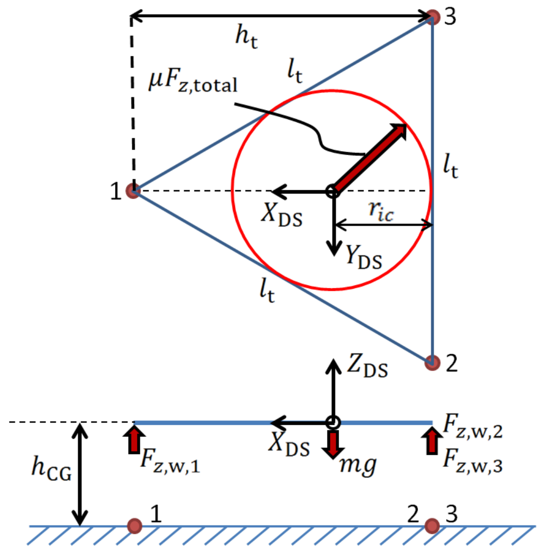

Fig. 7: Relation of sizing and rollover of the WMDS

4.5. Final Design

According to the derived constraints the dimensioning is calculated. The results are summarized in Table 2.

Table 2: Final design of the safety architecture

Parameter	Unit	Value
l_1	mm	270
l_2	mm	270
d_{joint}	mm	20
$\Delta s_{II,max}$	mm	102
α_{max}	°	3
α_{min}	°	0
φ_{max}	°	22
φ_{min}	°	0
c_{spring}	N/mm	67.58
$F_{des,max}$	N	8688[3]
$F_{spring,max}$	N	6970
μ_{slide}	./.	0.1[4]
μ_{joint}	./.	0.1[5]

The derived force transmission of the knee lever leads to the transformed desired lifting force (dashed graph) and actuation force of the linear spring used (dotted graph) as shown in Fig. 8. The created lifting system enables the application of a conventional spring while reducing the actuation force due to the transmission of force of the knee lever. Therefore, the effort for actively holding the preloaded spring is reduced significantly.

[3] Maximum wheel load with μ=1.45

[4] http://www.igus.de/wpck/2328/iglidur_Reibwerte, accessed: May 2014

[5] http://www.igus.de/wpck/2328/iglidur_Reibwerte, accessed: May 2014

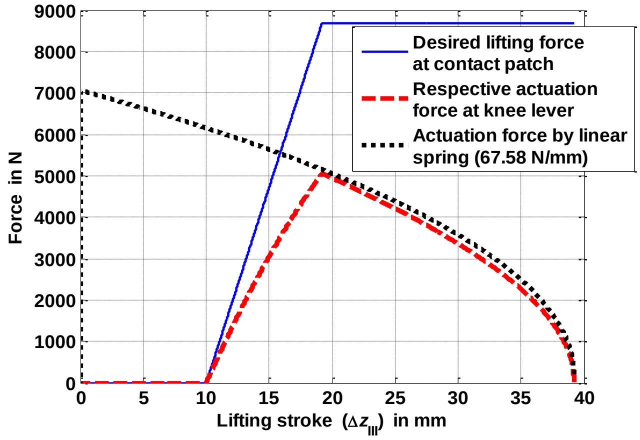

Fig. 8: Knee lever influence on force transmission ratio (knee levers: l_1=l_2=270 mm)

The specifications of the introduced safety architecture are summarized in Table 3.

Table 3: Specifications of the safety architecture

Parameter	Unit	Value
Lever arm of magnet	mm	470
Lever arm of spring	mm	250
Maximum magnetic force	N	4600
Actual magnetic force with applied anchor plate	N	4100
Supply voltage (of magnetic clamp)	V	24
Rated power (of magnetic clamp)	W	21
Maximum stroke of friction pad	mm	39
Shore hardness of friction pad	A °	70
Diameter of friction pad	mm	125

4.6. Parameter identification

In order to determine the sliding friction coefficient of the used braking pads, tests have been carried out. The WMDS with three discharged safety systems was pulled and the force needed for pulling was measured by a force sensor. The quotient of horizontal force and vertical force yields the sliding friction coefficient.

The tests were conducted with different velocities in order to identify the sensitivity of this parameter onto the friction coefficient. The mass of the prototype was increased to 1200 kg since this will be the maximum expected mass.

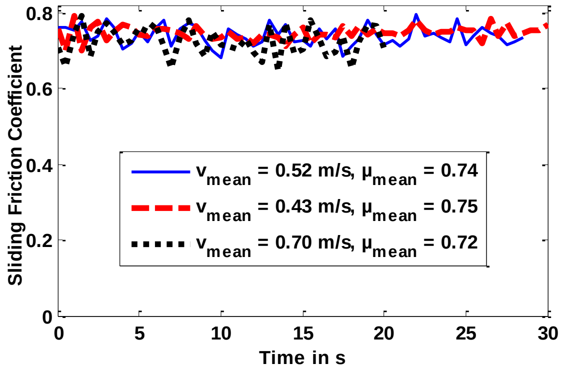

Fig. 9: Test results of sliding friction coefficient measurement with different velocities

As it can be seen in Fig. 9, the maximum average sliding friction coefficient within all measurements is about 0.75. The overall maximum value that has been recorded is 0.998. As sliding velocity increases, the sliding friction coefficient decreases. This behavior is known from rubber.

The wear of the friction pads is found to be tolerable. Over a sliding distance of approximately 100 m, the pad that is situated in the front (and therefore is prone to the highest wheel load) experiences a reduction in its height by 10 mm. Reducing the pad's height by 10 mm leads to ground contact of the wheels. This suggests that several emergency stops may occur before the friction pads have to be replaced.

4.7. Validation Tests

The concept of the safety architecture is validated by test drives utilizing the hardware prototype. The results are explained by one exemplary test drive. The measurement is conducted by a Correvit sensor and an acceleration based internal measurement unit (IMU).

The relevant part of the measurement is presented in Fig. 10. The deceleration due to the safety architecture starts at about 12.53 s. The acceleration signal shows a steep onset. At approx. 12.57 s the strong deceleration is paused for about 90 ms. The interruption is the result of a jump of the WMDS. For roughly 90 ms all contact patches are lifted from the ground due to the released energy of the safety architecture. The deceleration continues as soon as the friction pads are in ground contact again. The emergency stop lasts roughly 300 ms for the initial velocity of 2.4 m/s[6]. If the full emergency stop is considered, a mean deceleration of 7 m/s² is reached. If the jump

[6] Emergency stop at $v_{\text{initial}} = 2.4$ m/s to $v_{\text{correvit,min}} =$ 0.3 m/s thus, 2.1 m/s are decelerated within 300 ms.

can be avoided, the mean deceleration is expected to be increased to about 7.5 m/s² according to the results of section 4.6. One possible approach to avoid the jump is to optimize the damping of the knee lever design. This measure is also expected to reduce the peak deceleration as the dynamic wheel load change of the friction elements is narrowed, causing less peak friction force. In Table 4 the results of the validation tests are summarized.

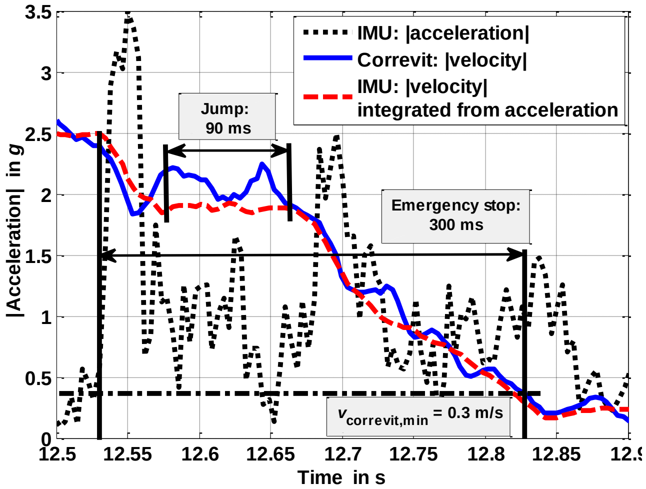

Fig. 10: Velocity and deceleration of WMDS during an emergency stop

Table 4: Characteristic values of the safety system's dynamics during an emergency stop

Property	Unit	Value
Initial velocity at discharge of the safety system	m/s	2.4
Duration of emergency stop (to $v_{\text{correvit,min}} = 0.3$ m/s)	ms	300
Duration of jump	ms	90
Mean deceleration	m/s²	7
Possible mean deceleration (no jump)	m/s²	7.5
Peak deceleration	m/s²	35

5. Conclusion

The safety architecture is validated by hardware testing. The clamping force enables the active hold of the preloaded spring. The knee lever reduces the required spring force and enables vertical stiffness when fully straightened (final position of knee lever in case of emergency stop). The utilized friction elements provide friction coefficient of about 0.75. The created mean deceleration of 7 m/s² is sufficient to stop the WMDS within an acceptable run-off area in case of an emergency. The wear of the elements must be observed further. The grit behavior seems to be promising because no spotty wear occurs. The grit has powdery characteristic and can be blown off. No significant marks remain. The first hardware tests show system jumps where the friction pads temporarily lose ground contact. Hence, future research will have to optimize the lifting process by suitable damping in order to reduce occurring wheel load change and thus create continuous friction force. The reduction of the peak deceleration yields reduced exposure of the subject and less mechanical stress for the safety system. Far-reaching improvements in terms of average power demand of the clamping task could be gained from alternative lifting concepts utilizing self-reinforcement. The basic idea of this improved safety architecture is being prepared for a patent application and will be analyzed in future research.

6. References

[Bet10] Betz, A.: Konzeption einer Bewegungsplattform eines selbstbewegten Fahrsimulators mit 6 DoF und dessen Umsetzung in ein evaluierbares Modell, Master's thesis, Insitute of Automotiv Engineering (Fachgebiet Fahrzeugtechnik), Technische Universität Darmstadt, Germany, 2010.

[Bet12a] Betz, A.; Winner, H.; Ancochea, M.; Graupner, M.: Motion Analysis of a Wheeled Mobile Driving Simulator for Urban Traffic Situations, Proceedings of Driving Simulation Conference 2012, p. 123-136, 6-7 September 2012 in Paris, France, 2012.

[Bet12b] Betz, A.; Hämisch, R.; Müller, M.; Winner, H.: Concept Analysis of a Wheeled Mobile Driving Simulator Showing an Omnidirectional Motion Base for Urban Traffic Simulation, SIMVEC - Berechnung, Simulation und Erprobung im Fahrzeugbau 2012, 20-21 November 2012 in Baden-Baden, Germany, 2012.

[Bet13] Betz, A.; Butry, A.; Junietz, P.; Wagner, P.; Winner, H.: Driving Dynamics Control of a Wheeled Mobile Driving Simulator Utilizing an Omnidirectional Motion Base for Urban Traffic Simulation. Future Active Safety Technology toward zero-traffic-accident (FASTzero). 22.-26. September 2013 in Nagoya, Japan. 2013.

[Bet14] Betz, A.: Feasibility Analysis and Design of Wheeled Mobile Driving Simulators for Urban Traffic Simulation, Dissertation (Ph.D.), 2014.

[Cla01] Clark, A.J.; Sparks, H.V.; Carmein, J.A.: Unique Features and Capabilities of the NADS Motion System, Proceedings of the 17th International Technical Conference on the Enhanced Safety of Vehicles (ESV), 4-7 June 2001, Amsterdam, The Netherlands. 2001.

[Ker12] Kerle, H.; Corves, B.; Hüsing, M.: Getriebetechnik. Grundlagen, Entwicklung und Anwendung ungleichmäßig übersetzender Getriebe. 4th edition. Wiesbaden. 2012.

[Wag13] Wagner, P.: Aufbau und Inbetriebnahme eines selbstfahrenden Fahrsimulatorprüfstands, Master's thesis, Insitute of Automotiv Engineering (Fachgebiet Fahrzeugtechnik), Technische Universität Darmstadt, Germany, 2013.

[Wag14] Wagner, P.; Betz, A.; Winner, H.: Conception and design of mobile driving simulators, in Proceedings of the ASME 2014 International Design Engineering Technical Conferences & Computers and Information in Engineering Conference IDETC/CIE 2014, August 17-20, 2014 in Buffalo, NY, USA, 2014.

[Zee2010] Zeeb, E.: Daimler's New Full-Scale, High-dynamic Driving Simulator – A Technical Overview, Proceedings of the Driving Simulation Conference Europe 2010, p. 157-165, 9-10 September 2010 in Paris, France, 2010.

7. Appendix

Table 5: Summary of the safety system's properties

Parameter	Unit	Value
h_{CG}	mm	481
μ_{max}	mm	1
l_t	mm	2300
h_t	mm	1992
l_1	mm	270
l_2	mm	270
d_{joint}	mm	20
$\Delta s_{II,max}$	mm	102
α_{max}	°	3
α_{min}	°	0
φ_{max}	°	22
φ_{min}	°	0
c_{spring}	N/mm	67.58
$F_{des,max}$	N	8688[7]
$F_{spring,max}$	N	6970
μ_{slide}	./.	0.1[8]
μ_{joint}	./.	0.1[9]
Lever arm of magnet	mm	470
Lever arm of spring	mm	250
Maximum magnetic force	N	4600
Actual magnetic force with applied anchor plate	N	4100
Supply voltage (of magnetic clamp)	V	24
Rated power (of magnetic clamp)	W	21
Maximum stroke of friction pad	mm	39
Shore hardness of friction pad	A °	70
Diameter of friction pad	mm	125
Initial velocity at discharge of the safety system	m/s	2.4
Duration of emergency stop (to $v_{correvit,min} = 0.3$ m/s)	ms	300
Duration of jump	ms	90
Mean deceleration	m/s²	7
Possible mean deceleration (no jump)	m/s²	up to 10
Peak deceleration	m/s²	35

[7] Maximum wheel load with μ=1.45

[8] http://www.igus.de/wpck/2328/iglidur_Reibwerte, accessed: May 2014

[9] http://www.igus.de/wpck/2328/iglidur_Reibwerte, accessed: May 2014

Comfort analyses of the Hydractive suspension using a driving simulator

S. Barale[1], P. Vars[1], J. Guillet[2], M. Alirand[3], J. Lagnier[3], P. Toulemont[3]

(1) : Vélizy, PEUGEOT CITROEN SA
+33 1 57 59 31 03
stephane.barale@mpsa.com,
philippe.vars@mpsa.com

(2) : Paris, ALTEN
+33 1 57 59 89 95
jerome.guillet@ext-mpsa.com

(3) : Lyon, LMS Imagine
+33 4 77 23 60 30
marc.alirand@lmsintl.com
Julien.lagnier@lmsintl.com
'ierric.toulemont@lmsintl.com

Abstract – Peugeot Citroën SA is willing to build a virtual process based on model simplification techniques for component and control design using MiL, SiL and HiL. This process can be extended with the use of the SHERPA driving simulator for early phases of the process since a human in the loop is always a benefit when ride comfort is of concern. The modularity of the existing models seamlessly allows running the existing models in the driving simulator. Due to the complexity of the complete model, using the power of four CPUs was required but this did not affect the simulator performances. Demonstration on the static driving simulator was done on one hydraulic suspension architecture. However, work remains on model robustness which prevents right now running on the dynamic driving simulator.

Key words: ride comfort, cosimulation, control logic testing, hydraulic semi-active suspension.

1. Introduction

Peugeot Citroen SA (PCA) is well known for the comfort capability of its hydraulic suspensions and mostly the Hydractive one. As everyone knows, the Hydractive suspension is a two states semi active suspension including a self-leveling capability. An ECU controls the two states and corrects the height of the vehicle. PCA is thinking of a process in suspension design since many years [Ney1]. Recently a extended global MiL (Model in the Loop), SiL (Software in the Loop) and HiL (Hardware in the Loop) process to design the components of the hydraulic suspension and to design and validate the control logic has been explored [Bar1, Bar2]. However in very early phases of the design process, being able to test different types of control logic on a realistic model able to run real time on a driving simulator with a real driver could be of great interest.

Integrated design and engineering methods based on virtual testing are becoming standard practices in product and control design process. These methods support the development of mechatronic products and should address the challenges posed by their multi-disciplinarity and controller integration. Despite this "ideal" vision, often active functions are treated as add-ons potentially developed independently from the design of the system they are controlling. To integrate in a seamlessly approach system and control, PCA has elaborated a MiL/SiL/HiL process based on model simplification technique allowing first to virtually design the system to control, second to simplify the detailed models used in system design to integrate them within the controller design process targeting HiL testing. Variant analysis, performance optimization, control, component, subsystem and system level validation, and finally system integration must become intrinsic parts of a standard vehicle engineering process. This process coupling the simulations and tests is essential to reduce time to market. The challenge of this process is to enable a mechatronic system engineering approach that can be used throughout the complete design process, based on scalable and interoperable simulations. Interoperability requires common frameworks for development and exchanges: a multidisciplinary software platform sufficiently understandable and open with well-described interfaces to a control software.

Even if the process described in [Bar2] should target more generally mechatronic systems, the application to explore the concepts developed and used is the two states semi active Hydractive suspension including self-leveling capability. Comfort being the main interest of the suspension analyses, what could be the benefit of bringing the models on a driving simulator? First of all, analysing ride comfort on a driving simulator is not new [Hea1, Koh1]. At that time, mainly low frequency range was of interest with bouncing, pitch and roll as the main dynamic contributions and thus very low frequency range comfort (and handling) analyses were of concern. Nowadays, there exist specialised ride simulators with dedicated (Stewart or not) platforms [One1]. These simulators are able to go in high frequency domain (30-40 Hz in vertical direction). As mentioned in [Kad1], the application fields of driving simulators are human machine interactions, active safety research and vehicle dynamics experiments. In this last field, having an idea of the driver feeling in very early phases of the control process becomes of interest and even more when comfort is of interest. In [Mae1] driving on digitalized road looks to be of importance for comfort since as defined by the ISO 2631 and the NASA [Lea1], 4-8 Hz is the frequency band that affects the most ride comfort of human body in vertical direction. Regarding the performances of the driving simulator of concern, the band width in vertical direction is limited to about 10 Hz and the models are targeting 0-50 Hz range. The platform of concern is even lower frequency than the frequency range of the model content but both are in the range of interesting frequencies regarding the ISO and the NASA. Another interest for PCA is to introduce a human in the loop to explore the benefit at low frequency range where the two states switch affects the roll dynamics (low frequency steering wave inputs). Tuning up front the controller with a driver in the loop (DiL) could help gaining insights of the driver perception and should reduce system and its controller integration time.

After presenting some of the models developed for the MiL/SiL/HiL process and the model architecture used on the ds1006 HiL platform, the model architecture adaptation for the SHERPA driving simulator is introduced. The model is tested on the driving simulator for simple inputs, just to verify the capability to implement the models on 4 cores of the computer used by SHERPA. Discussion is than given on the opportunity to make further steps in using the driving simulator to further explore comfort with hydraulic suspensions and continuous semi active dampers.

2. Vehicle and hydraulic suspension model running in ds1006 HiL bench

For offline (design and MiL) and HiL testing, low frequency comfort analyses were the main target with a frequency range of 0-50 Hz. For this frequency range, the vehicle model includes the engine on its mount, the carbody torsion as well as the dynamics of the damper rod in the vertical direction [Bar1]. In order to fix the idea, the carbody torsion is around 15 Hz, almost similar to the engine bouncing mode in vertical (around 20 Hz) and the dynamics of the damper rod is about 40-50 Hz. Since the mechanical model matches the 0-50 Hz frequency range, the model of the hydraulic suspension should also be detailed to become sufficiently accurate in the same frequency range. The model of the hydraulic circuit of the suspensions (front and rear) and the way to simplify it has been explained in [Bar2]. Note that five suspension architectures were targeted for the analysis. The architecture in Fig 1 will be used in this paper to demonstrate how to implement and test the suspension architectures on the driving simulator. The architecture in Fig 1 is not the most complex but includes all the required elements to show the technique used: an electro pump assembly controlling the self-leveling at front and rear suspensions, two stiffness regulators controlling hard and soft for front and rear axles, piping systems and front and rear cylinders.

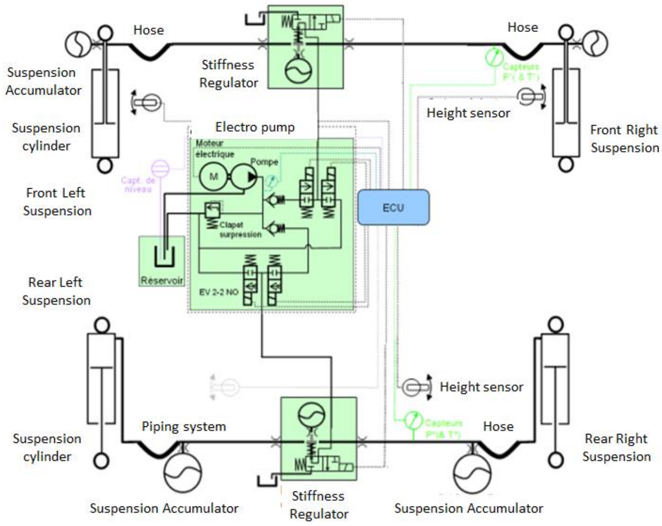

Fig. 1. Tested suspension architecture.

The complete model of the vehicle and the front and rear suspensions corresponding to the architecture in Fig 1 is shown in Fig 7 (in the Annexes). The modularity of the different constituents of the suspension has been analyzed in [Bar2]. This modularity allows building the five architectures in few clicks. As well since the complete model is clearly too complex to be run on one core, the model has been split in "modules" cosimulating between each other.

Going from MiL to SiL and then to HiL was possible thanks to model simplification tools [Bar2]. The complete model in Fig 7 was able to run real time on a ds1006 quadcore computer. The simulation architecture for MiL, SiL and HiL is shown Fig 2.

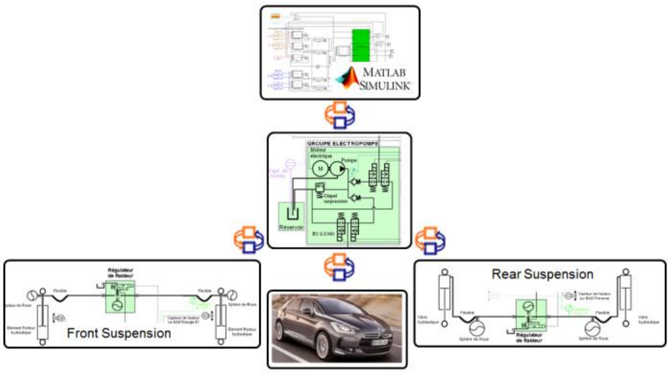

Fig. 2. Tested cosimulation architecture for HiL.

This simulation architecture corresponds to a cosimulation between Simulink for the control logic and AMESim for the electro pump assembly, Simulink being the master of the cosimulation. This choice was initially logical since the control logic is controlling the self-leveling using the electro-pump assembly (but also the two states semi-active suspension with the stiffness regulators). Note that for sake of CPU balancing, the "coil" models of the stiffness regulator (equivalent first order dynamics) were integrated in the electro pump model. Additionally to the Simulink - AMESim cosimulation, internal AMESim - AMESim cosimulations are also running, the electro pump assembly being the master of these cosimulations. The vehicle, the front and the rear suspensions are the slaves of the AMESim - AMESim cosimulations with the electro pump model. This architecture allows splitting and running the complete model (vehicle and suspensions) on the four cores of a ds1006 computer. The Simulink – AMESim exchange is done at 1 ms and corresponds to the sampling estimate of the future calculator (ECU). The exchange between the electro pump and the hydraulic suspensions is done at 0.1 ms required by the cosimulation stability. As explained in [Bar2], the exchanges between AMESim hydraulic models are done by pressure-flow rate variables around the electro-pump valves and the stiffness regulators. It was found that taking into account the pipe dynamics between these two components was of great help in order to stabilize the exchange rate to a value acceptable for real time application. Clearly the power exchange and the corresponding dynamics between the hydraulic models limit the cosimulation sampling rate. For the vehicle and the electro pump models, the sampling rate was 1 ms since the power couplings are mostly done via the wheel hop suspension mode, around 20 Hz. It is important to note here that when the damper rod dynamics is included (two different vehicle models were analyzed), the dynamics are changing due to a coupling between the mass of the damper rod and the hydraulic stiffness of the cylinder and piping stiffness. When the damping rod dynamics is taken into account, the sampling rate reduces to 0.1 ms

3. Model adaptation for the driving simulator

The internal process put in place tries to involve the driving simulator. Testing in early phases of the design process the suspension architectures and their related controller with a human in the loop was found of some interest. It is well known that the Stewart platform (or alike) used by driving simulators has a vertical direction bandwidth of action larger than in longitudinal and lateral directions. Even if the bandwidth of action in vertical of the SHERPA driving simulator is limited to 10 Hz, it was decided to test the rendering to analyze if this is sufficient or acceptable to "feel" the differences between a standard suspension, soft and hard in case of a switch on the Hydractive suspension.

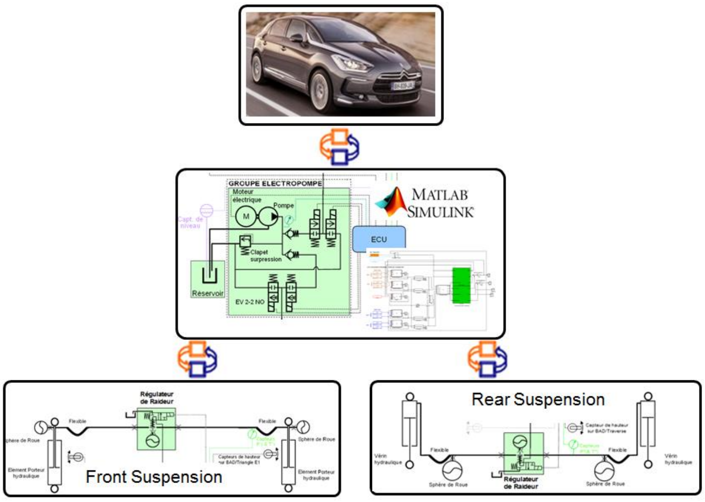

Fig. 3. Cosimulation architecture in SHERPA.

The model architecture used for the HiL bench is not really suitable for the driving simulator. The SHERPA driving simulator is using Simulink as a basis for generating the model running in the SCANeR environment [Okt1]. Thanks to Simulink, there was no adaptation to be done inside AMESim contrary to what has been done for [Fan1]. Note that thanks to [Fan1], directly interfacing AMESim to SCANeR is also feasible. Splitting the complete system in four models for off line testing (MiL and SiL) and for HiL in the ds1006 allows running each model on one CPU of the driving simulator. Thanks to the modularity of the complete model, the order of the Simulink – AMESim and AMESim – AMESim cosimulations was a bit changed to take into account the constraints of the driving simulator. The order of the cosimulations for the SHERPA driving simulator is now shown in Fig 3.

This time, the cosimulation has a master piloting a master-slave which pilots two slaves. All the models are in AMESim even the controller. Note that the controller initially in Simulink was integrated as an equivalent C-code for AMESim. The Simulink to AMESim interface was used to generate an encapsulated model of the controller thank to the C-code generation of Real-time Workshop. This technique was also used in [Fan1] to include the regenerative braking controller of the electric vehicle. A C s-function including the controller is also a possibility thanks to the usage of Simulink as main "interface". The two solutions are thus allowed by the SHERPA architecture.

The master of the cosimulation in Fig 3 is now the vehicle model. The master slave being the electro-pump assembly (and the controller), the front and rear suspension models are the two "ending" slaves. Previously (Fig 2), there was one AMESim master and three AMESim slaves. Now the architecture is a double stage AMESim cosimulation architecture: a master, a master-slave and two slaves. This was initially not planned (not expected) but this architecture works perfectly well. This simulation architecture was required as such since the SCANeR environment handle the inputs/outputs of the vehicle model to drive the moving platform.

4. Running within the driving simulator

The SHERPA driving simulator also called the dynamic driving simulator at PCA is shown in Fig 4. Normally only one CPU (over the 16) is reserved for the model. As shown in [Bar2], the model of Fig 7 is running on the four cores of the ds1006 used for HiL testing and one core was almost at its full load, the one corresponding to the front hydraulic suspension model.

Before testing on the dynamic driving simulator, tests have been done on the static driving simulator. This driving simulator has no moving platform. The platform corresponding to the vehicle is fixed to the ground. The environment is exactly the same as the dynamic driving simulator. This is generally the first test to do to verify first the real time capability of the model and second if the model is sufficiently robust to not put the dynamic driving simulator into troubles with numerical instabilities.

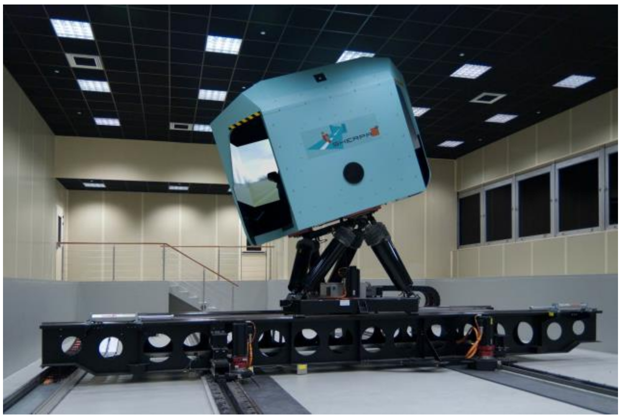

Fig. 4. The SHERPA driving simulator.

The static driving simulator is using a 8 cores computer. Running the model of Fig 7 gives the results shown in Fig 5. It is difficult to know which models and processes are running on which core since Windows is managing automatically the repartition. From Fig 5, it is clear that there is enough space to run all the models.

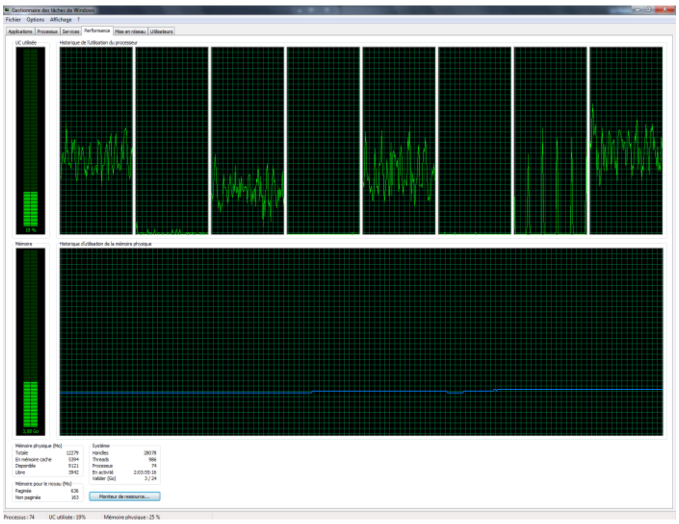

Fig. 5. Core loads of the static driving simulator.

The model of Fig 7 was tested on several roads and for different scenarios. Fig 6 shows an example of a standard test. In Fig 6 on top, the suspension control was piloted to hard and in Fig 6 at the bottom the suspension was piloted to soft. Soft can clearly be identified regarding the vehicle oscillations when driving on a "cleat". The introduction of the extra accumulator located inside the stiffness regulator as well as its additional damping valve allows the oscillations to be well damped. This is typically what the Hydractive two states suspension can provide as benefit for comfort.

It is now important to note that the cores of the static driving simulator are around 25 % more efficient than the cores of the dynamic driving simulator. From Fig 5, the core loads are less than 50 % meaning that running the models on the dynamic driving simulator will not be a problem. Remember that the core loads were around their maximum on the ds1006 [Bar2]. Despite this security margin, gathering two AMESim models to limit the complexity of the cosimulation architecture will result in reaching maximum core load even on the static driving simulator.

Fig. 6. Results from the static driving simulator.

Running the vehicle, the suspensions and the control logic inside the static driving simulator allows giving some insights on model capabilities and core loads. It also gives some information about model stability. Unfortunately, right now, the model looks too sensitive to be run on the SHERPA dynamic driving simulator.

5. Discussions

The static driving simulator was used first and some model instabilities have been encountered, typically when potholes, sharp cleats or trying to climb on sidewalks are of concern. Normal driving and the "comfort" road used in [Bar1] cause no difficulty. Up to now, it is not clear if these instabilities are coming from the tire model that does not filter enough the sharp road inputs or if it is the suspensions and electro pump hydraulic models that are numerically not enough robust. What is clear is that on the ds1006 computer, this kind of instability was never encountered. Despite this, it is necessary to explore in a deeper way the cosimulation and hydraulic model numerical stability to find the roots of the instability. Exploiting much more the HiL bench should give an idea of the robustness of the hydraulic models (and cosimulation architecture).

Coming back to ride comfort, analyses with a driver in the loop have not been done yet on the dynamic driving simulator. It is thus difficult to conclude on the real interest of having a driver "feeling" the effects of the control logic. However from the literature [Hea1, Kad1, Koh1], the effect at least for bounce, pitch and roll dynamics (low frequency range) should be obvious. The soft/hard switch should also be seen for Handling for instance with long wave length curves (steering wheel angle sine wave input around 0.1 to 0.5 Hz). Even if the self-leveling controller is not active like in [Ali1] and remains in a bandwidth of 10 to 15 seconds, testing the self leveling controller for long curves on highway for which the control logic can act against roll could be nice to explore. Again, the benefits should pop up in early phases of the control and component design process and thus prior to have the real components and final controller. Note that even if drivability and sine with dwell manoeuvers are difficult to reproduce in standard driving simulators, testing the control logic was partly the idea behind [Fan1] for electric vehicle and for ESC in [Fan2].

6. Conclusions

PCA is willing to put in place a virtual process for component design and control logic development and validation for suspension, a multi-functional system mock-up approach to build mechatronic systems. This process relies on MiL, SiL and HiL integration. Tentative for exploring the capabilities of different control laws in a driving simulator has been done to extend the virtual process to extra early phases.

At least, the results presented prove that running in the static (and dynamic) driving simulator a "complex" vehicle and Hydractive suspension model is possible. However, further testing is required to guaranty the usage of the model on the dynamic driving simulator. This step is essential to extend the virtual process (MiL, SiL, HiL) to Driver in the Loop providing solutions on both multi-physics simulation and control engineering integration levels.

7. References

[Ali1] Alirand M., Lachaize H., Lebrun M., "Study and analysis of an active self-leveling suspension". *1993 International Conference on Systems, Man and Cybernetics*, Le Touquet, France, October 1993, pp. 222-227.

[Bar1] Barale S., Plisson A., Guillet J., Lagnier J., Alirand M., "Improved functional modelling in comfort analyses for hydraulic suspension testing". *4th International Munich Chassis Symposium - Chassis.Tech Plus*, Munich, Germany, June 2013, pp. 1-22.

[Bar2] Barale S., Plisson A., Guillet J., Alirand M., Lagnier J., "Control logic testing for mechatronic systems: a process based on model simplification". *12th International Symposium on Advanced Vehicle Control*, Tokyo, Japan, September 2014, pp. 1-8.

[Fan1] Fang Z., Alirand M., Andre S., Denoual Th., Kemeny A., Reymond G., Jansson A., "Multi-objective analysis on a driving simulator applied to an electric vehicle: vehicle stability, handling and drivability". *SIA Congress on Vehicle Dynamics,* Mulhouse, France, October, 2011, pp. 1-10.

[Fan2] Fang Z., Kemeny A., Guo S.C., Deborne R., Denoual Th., Alirand M., "Electric vehicle's stability study on low friction road based on driving simulator". *Driving Simulation Conference,* Paris, France, September, 2012, pp. 1-9.

[Hea1] Heal S.F., Prasiloski J.C., "Ride characteristics of lightweight tracked vehicles", *Scientific Computer Division, report n°RRC-38*, February 1967, pp. 1-51.

[Kad1] Kading W., Zeeb E., "25 years driving simulator research for active safety". *10th International Symposium on Advanced Vehicle Control*, Loughborough, UK, August 2010, pp. 1-5.

[Koh1] Kohr R.H., "Real time automobile ride simulation". *Western joint IRE-AIEE-ACM Computer Conference*, New York, US, May 1960, pp. 285-300.

[Lea1] Leatherwood J.D., Barker L.M., "A user oriented and computerized model for estimating vehicle ride quality", *NASA Technical Paper n° 2299,* April 1984, pp. 1-41.

[Mae1] Maeda C., Kawamura A., Shirakawa T., Nakatsuji T., Kumada K., "Reproducibility of the vehicle vertical motion by KIT driving simulator using the actual measurement data". *Journal of the Eastern Asia Society for Transportation Studies, vol 6*, 2005, pp. 2734-2746.

[Ney1] Ney Y., Lebrun M., "Mechatronics in the automotive industry: Active suspension design using simulation", pp. 1-6.

[Okt1] OKTAL, SCANeR is a trade mark of OKTAL, http://www.scanersimulation.com/.

[One1] Onesti P., "Verbindung von Human- und Hardware-in-the-Loop testing verkurzt entwicklungszeit". ATZ*, vol 111*, October, 2009, pp. 764-769.

8. Annexes

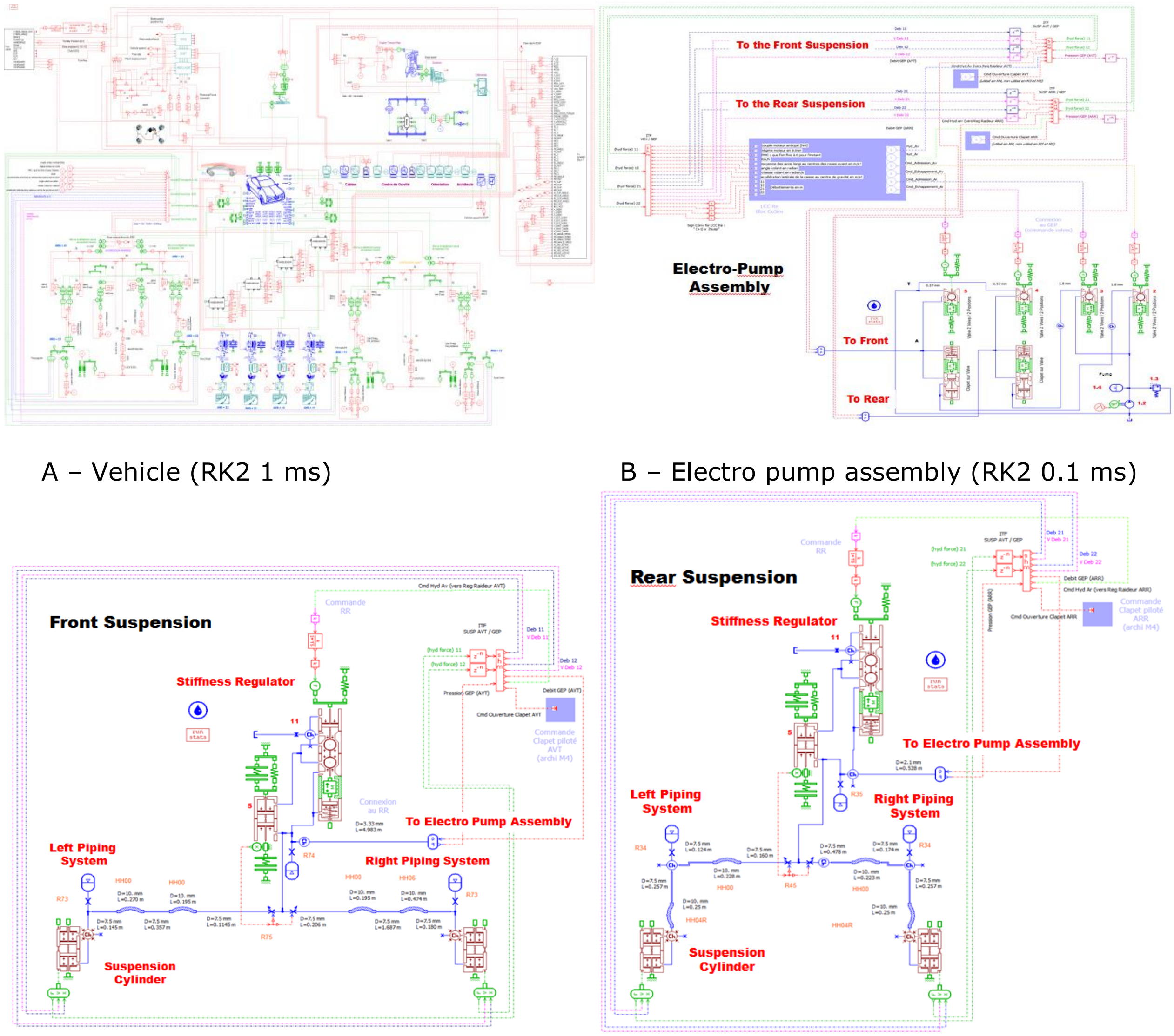

A – Vehicle (RK2 1 ms)

B – Electro pump assembly (RK2 0.1 ms)

C – Front suspension (RK2 1 ms)

D – Rear suspension (RK2 0.1 ms)

Fig. 7. The models running in cosimulation within the static driving simulator.

Product Solution and Posters

Design and Performance of the VTI Sim IV

Jonas Jansson[1], Jesper Sandin[1], Bruno Augusto[1], Martin Fischer[2], Björn Blissing[1], Laban Källgren[1]

(1) : VTI (SWEDISH NATIONAL ROAD AND TRANSPORT RESEARCH INSTITUTE), SE-581 95 LINKÖPING, SWEDEN
+46-13-20 40 00/+46-13-14 14 36
E-mail : (jonas.jansson, bruno.augusto, laban.kallgren, bjorn.blissing, jesper.sandin)@vti.se

(2) : DLR (GERMAN AEROSPACE CENTER, Institute of Transportation Systems)
E-mail : ma.fischer@dlr.de

Abstract – The VTI simulator IV (Sim IV) is the fourth advanced driving simulator designed and built at The Swedish National Road and Transport Research Institute (VTI). The simulator, taken into operation 2011, has an 8 degrees of freedom (DoF) moving base, a field of view (FoV) of 180 degrees and features a system for rapid cabin exchange. With a budget of roughly 2,4 M euro; Sim IV was developed to provide VTI's newly established Gothenburg office with advanced driving simulation capability, and to be a cost efficient complement to the Sim II and Sim III facilities in VTI's Linköping office. This paper describes the design and technical performance of the facility. A brief summary of results and experience from validation studies for the first three years of operation is also presented.

Key words: Driving simulator, Simulator design, VTI, 8 DoF, Simulator performance.

1. Introduction

VTI is a governmental research institute organized directly under the Swedish Ministry of Enterprise, Energy and Communications. The research deals with issues concerning the transport system, and much focus is given to road transports. One major area of attention is the individual's behaviour in the transport system. To study human factor issues driving simulators have been an important instrument, at VTI, since the 1970:ies. VTI's first moving base simulator was the Sim I [Nil1,Nor1]. Officially taken into operation in 1984, the Sim I was the first moving base simulator using a long linear track to produce large stroke lateral displacement of the cabin. In 1994 the Sim II [Jer1] was introduced. Sim II has a similar physical layout as Sim I, the only major difference being that it was designed for a truck cabin. In 2004 Sim I was replaced with Sim III, [Nor2]. With a linear drive system achieving close to 1 g Sim III added improvements to the sheer acceleration performance of VTI's simulation capabilities. The fact that Sim III's linear system can be used in either the longitudinal or the lateral driving direction was also a novelty for the VTI simulators. Sim I-III have very similar overall design i.e. a 3 or 4 DoF moving base (linear track, pitch, roll, yaw(only on Sim III)) complemented by a 4 DoF shaker table (0,1 m actuator displacement) to provide the high frequent (up to 10 Hz) simulation of road roughness, i.e. movements relative to the projection screen. This design together with a 120 degree FoV provides good simulation capability especially for highway and rural road driving scenarios. The VTI Sim IV, in Figure 1, was designed to complement Sim II and III.

Figure 1. The VTI Sim IV

In particular it adds a wider FoV (see Figure 2) and more degrees of freedom in the moving base. The Sim IV is equipped with one hexapod with six degrees of freedom (roll, pitch, yaw, surge, sway and heave) which in turn is mounted on a sled with two extra degrees of freedom (two orthogonal directions for translation, longitudinal and lateral).

Figure 2. Interior platform view of the Sim IV

Together, they make Sim IV capable of dealing with lesser curve radiuses and give a more realistic sensation of stop and go traffic. This type of conditions is typically found in urban area scenarios, thus Sim IV is in many cases the simulator of choice for city driving studies at VTI.

Discussions on building a Simulator in Göteborg started in 2007 at the same time as the start-up of ViP was being planned In the spring of 2008 a pre-study [Jan1] was conducted to investigate the possibility to build a VTI facility in Göteborg, and a decision to start up the building project was taken in the late fall of 2008. After some delays and changed plans the facility was inaugurated by the Swedish minister of infrastructure on the 18:th of May 2011. The decision to establish a new driving simulator at VTI was motivated mainly by the start-up of a new competence network on driving simulation ViP – virtual prototyping and assessment by driving simulation [Vip1]. Sim IV provides advanced driving simulation capability to VTI's newly established Göteborg office as well as to the west-cost partners of the ViP consortium. Similar to the Sim II and III the Sim IV is used to provide human factors researchers with realistic driving situations that can be completely controlled and repeated. However, applications where the simulator is used as an advanced systems integration platform and a tool for complete vehicle testing in vehicle development has gained increasing attention.

The design of the Sim IV facility was influenced by several factors. Cost effectiveness and constraints to the budget is always one of the major factors. For Sim IV this meant that reuse of simulator technology from Sim II and III was an important issue. Another hard constrain was the available office building, which creates hard limitations on the size and proportions of the simulator.

2. Simulator performance and specifications

This section describes the technical specifications and data of the facility. The design of any advanced driving simulator is influenced by several different factors. The most important high level requirements on the design of Sim IV are given in Table 1, below.

Table 1. High level requirements on the Sim IV facility

The facility should be a high fidelity simulator e.g. providing a high fidelity simulation of all impressions of real driving including motion feedback.
It should be possible to simulate both heavy and light vehicles, requiring the possibility to change cabin rapidly.
The operational area of the facility is 12 x 15 x 7 (length x width x height).
The Budget for the project including hardware, person hours and consultants was 23,26 MSek (equivalent to 2,44 M euro, by 2014-05-21 exchange rate).

From the top level requirements in Table 1, a first design was conceived and refined to the final solution that was eventually installed. Many of the most challenging design issues came from keeping the platform within the weight and mass moment of inertia limitations of the moving base system. Also, the fact that a complete truck cabin should be mounted complicated the design of the visual system. Much effort went into finding a design of the visual system. The challenge was to achieve a front projected forward image where the roof of the truck cabin did not obscured the beam of the projector. A second issue worthy of much attention, was the structural rigidity of the platform. To ensure high enough eigen frequencies of the entire structure the cabins are used as a stabilising part of the platform increasing its rigidity (this can be seen in Figure 3 where the beams connecting to the rear back corners of the cabin are visible).

Figure 3. This picture show the beam connecting the back corner of the cabin to the platform structure.

2.1. Moving base

The moving base/motion system, in Figure 4, provides the driver with motion feedback by moving the platform that the cabin is mounted on. A motion cueing algorithm [Fis1] is used to transform the motion of the simulated vehicle into a reference motion for the moving base. In Sim IV the moving base consist of a linear sled system that can provide large stroke linear motion in two directions (the vehicles longitudinal and lateral direction). On top of the linear drive system a hexapod/Stewart motion platform [Ste1] is mounted.

Figure 4. The moving base of Sim IV consist of a bi directional large stroke linear system and a hexapod. In this case a commercial solution that has been deployed in several other advanced driving simulators.

This system can generate displacements in all three translational DoF as well as the three rotational DoF. The entire moving base is therefore said to have 8 DoF, indicating that the actuator space has 8 DoF. The motion cueing that is used in Sim IV is further described in [Fis3]. The maximum payload is 2500 kg. In Table 2 and 3 some of the basic performance specifications of the moving base is presented.

Table 2. Hexapod performance

	Excursions	Vel.	Acc.
Surge	-408/+307 mm	±0.80 m/s	±6.5 m/s^2
Sway	-318/+318 mm	±0.80 m/s	±6.0 m/s2
Heave	-261/+240 mm	±0.60 m/s	±6.0 m/s2
Roll	-16.5/+16.5 deg.	±40 deg./s	±300 deg./s2
Pitch	-15.5/+16.0 deg.	±40 deg./s	±300 deg./s2
Yaw	-20.5/+20.5 deg.	±50 deg./s	±300 deg./s2

Table 3. Sled system performance

	Excursions	Vel.	Acc.
Surge	+/- 2.5 m	+/- 2 m/s	+/- 5 m/s2
Sway	+/- 2.3 m	+/- 3 m/s	+/- 5 m/s2

2.2. Visual system

The visual system consist of a forward screen and two, or more, lcd displays. The lcd displays are used as rear-view mirrors and the number depends on which cabin is used. The forward screen (see Figure 5) uses front projection technique and currently 9 projectors, with a resolution of 1280x800 pixels, projects the image on a curved screen with a diameter that varies between 1.8 (to the left) and 3.1 m (to the right) and a height of 2.5 m. The field of view is approximately 180×50 degrees.

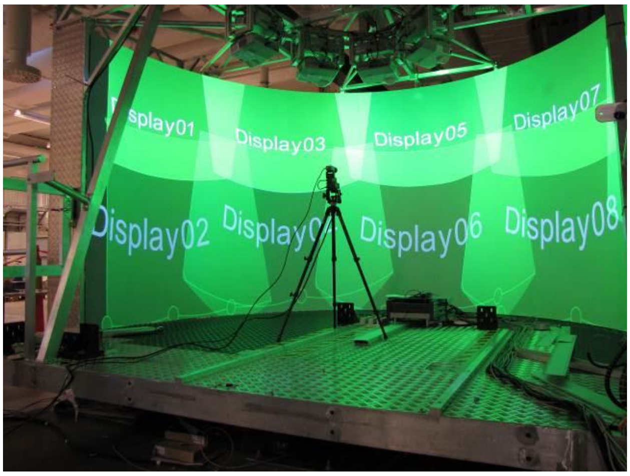

Figure 5. A test setup of the front projected forward view here eight projectors are used to cover the screen.

The forward FoV varies slightly, depending on cabin (the nominal position of the drivers head varies slightly between truck and passenger car cabin). Table 4 describe the important characteristics of the visual system.

One of the major challenges with the visual system was to provide a unobscured FoV to the driver position. During the project different display solutions where discussed. The final design was to use a front projection solution. Because of the overall constraints on the simulators height and the mass moments of inertia, the projection screen is closer to the cabin than in Sim II and III. To avoid the truck cabin from obscuring the path of the projector beam, projectors with a very short throw distance were required. The combination of a short throw distance and curved screens require a significant effort for warping and merging the projector images. In the Sim IV a dedicated commercial system is used for this purpose.

Table 4. Visual system specifications

FoV	180×50 degrees
Average resolution on screen* (arc minute per line pair)	5,0** (horizontal) 2,5** (vertical)

*The human eye has 0.59 arc minute per line pair

** ± 0,5

2.3. Sound system

The sound system consists of a 6.1 surround system; two speakers at the front, two at the sides and two behind the head plus a subwoofer. These speakers are controlled by a separate computer which can play sound in any of the speakers. The Sim IV was the first facility where directional sound from objects outside of the cabin was used. The added value of directional sound has not been thoroughly analysed, but the subjective rating of every one who tried both configurations is that that the directional sounds adds a significant sensation of immersion in the simulation.

2.4. Simulator software

Reusing technical solutions and simulation software was one of the most important measures to keep the overall cost of the Sim IV down. The simulation software, is to a very large extent based on own development and open standards. It was already in use in the Sim II and III facilities. The software can be divided in three main components.

1. ViP Core – the main software to run the simulation, contains scenario, vehicle dynamics and several other components. The main simulation loop executes at 50 Hz.
2. VISIR – renders the computer graphics and also contains some script tools to generate roads. The logic description of the road is according to OpenDrive. Graphics rendering executes at 60 HZ.
3. SIREN – Is the software to produce sound [And1]. It is based on OpenAL and can assign a direction to any sound and play both recorded sounds (e.g. in vehicle warnings) and sounds from a sound model (e.g. for the wind, engine and tire noise and sounds from other vehicles).

The software is shared and co-developed within the ViP competence network and anyone interested in using it can apply for membership.

2.5. Cabin exchange

An early design requirement was that it should be possible to simulate both truck and passenger car driving. The facility is currently equipped with two cabins one Volvo XC 60 (small SUV passenger car) and one Volvo FH16 (truck cabin). To exchange cabin the moving base is placed in a settled position in the rear part of the simulator hall. A table is attached to the rear part of the platform. The cabin is then slid out on the table on a rail (visible in Figure 6). The cabin is lifted down from and up onto the table by a permanently installed crane, installed just outside of the simulator hall.

Figure 6. A permanently installed crane is used to lift cabins onto the platform.

If the procedure is well planned and all software interfaces are tested a cabin switch can be accomplished in less than a day.

2.6. Costs

The project had an overall budget of 23,259 MSek (2,44 Meuro). The budget covered costs for hardware, consultants and the person time for the VTI personnel, also including project management tasks. The main project was split in 8 sub-projects: moving base, platform, visual system, computer system, truck cabin, passenger cabin, sound system and integration. The single most costly subproject was the moving base project which had a total cost of roughly 1 M euros.

Table 5. The costs for building Sim IV, actual costs.

Costs	[MSek] / [Meuro]
Hardware and consultants	10,837 / 1,140
Person time (only VTI personnel)	12,337 / 1,298
Total costs	23,174 / 2,438

The final cost of the project ended up very close to the budget with a difference of roughly 10 Keuro lesser costs than planned. However, some major maintenance/upgrades where done rather quickly after the inauguration and these are not included in the budget. The most notable work was the moving of the attachment point of the platform to the hexapod. The centre of mass of the whole structure was miscalculated by 15 cm in the longitudinal direction. This required more than 100 kg of counter balances to be added for the first months of operation. After that continued tuning, smaller repairs, upgrades and improvements has been carried out as part of the normal maintenance.

3. Studies and initial experiences

Since taken into operation (spring 2011) and until the spring of 2014, 14 scientific simulator studies has been carried out in Sim IV (omitting studies carried out in master thesis works and demonstration activities). Many of these projects are still ongoing and have yet to disseminate the results. Below some of the projects are briefly described.

3.1. Lane departure scenarios used for the evaluation of active steering interventions

[Fis2] describe the development of a lane departure scenario that has been used successfully in Sim IV to evaluate the efficiency of active steering-wheel interventions. The lane departure scenario is designed in such way that the vehicle at a given position is moved across the median towards an oncoming vehicle, or towards the left road edge. This is accomplished by introducing a steering angle in the simulated vehicle without presenting the corresponding lateral acceleration with the motion system. This is done in parallel with a visual task that occupies the driver, so that s/he will not notice anything out of the ordinary until s/he looks up. The visual task consists of reading numbers from a screen placed at a relative large down angle (40-45 degrees). Each number is displayed for 0.3 seconds, with 0.2 seconds of blank screen in between numbers, creating the total task duration of 2.8 s.

In order to execute the described scenario and thus to trigger the active safety system correctly, a lot of requirements have to be fulfilled. The signals from lane and radar sensors have to contain correct, realistic information about the virtual environment, drivers have to be successfully distracted and finally the visual, acoustic, haptic and vestibular feedbacks have to closely resemble the real experience in order to trigger realistic driver reactions to the system intervention. That means that all involved feedback systems (i.e. graphics, sound system, force feedback steering-wheel and the motion system) need to have appropriate performance characteristics.

The lane departure scenarios have successfully been used to evaluate up to almost 100 drivers' responses to active steering-wheel interventions intended to prevent cars to enter the opposite lane or to cross the left road edge. The drivers' responses have also been validated towards drivers' responses of unexpected steering-wheel interventions in a real vehicle on a test track. These drivers were given the same visual task, and got the interventions while driving straight.

3.2. Simulator experiments for the development of quantitative driver models in the evaluation of active safety systems

Behavioural data have been collected by means of specifically designed experiments in order to develop and verify quantitative models of driver behaviour. Behavioural data have also been collected from ongoing Field Operational Test (FOT) projects for the verification of driver behaviour and experiment scenario. The quantitative models are intended to be applied within industry, research institutes and academia in computer simulations with the purpose of evaluating, verifying and/or tuning active safety systems.

Identified main areas of needed new model development include driver inattention and expectancy, driver reactions to active safety control interventions, and nuisance warnings/interventions. The active safety systems that have been implemented and evaluated in the simulator experiments are active steering-wheel interventions (mentioned above) in passenger cars and an Advanced Emergency Braking System (AEBS) for heavy vehicles. The experiments in Sim IV have been very successful and the final data analysis is underway. Several publications are expected in the near future. The research has been conducted in close collaboration between VTI, Swedish vehicle OEMs and Chalmers University of Technology.

3.3. Evaluation of methods for measuring speed perception in a driving simulator

A project including experiments and literature review on speed perception in a driving simulator was conducted in the Sim IV. Result from the study shows that the ability to estimate speed differences correctly depends on the base speed, more results are presented in [Fis2].

3.4. High speed control

Validation of the vehicle dynamics of a 32 m heavy vehicle combination (an A-double). The topography and roughness of a real country road have been modelled in the simulator environment. Experienced truck drivers have driven the 32 m vehicle on the modelled country road.

3.5. Known roads

The Known roads focus on creating highly realistic road descriptions from different available data sources. The project uses the OpenCRG format to described road topology. New methods for generating the road side visual appearance from national geo data is also included in the work. The goal of the project is to make the roads connecting Gothenburg, Borås and Alingsås. The project has particular focus on HGV handling and the possibility to compare simulator driving with on road driving for handling purposes. The project has a close connection to the one described in section 3.4.

3.6. Sleep Noise

In the Sleep noise experiment [For1] road noise models where constructed and validated with road noise measured from a real vehicle. Two vehicles where measured and modelled. The models where then used in experiments with alert and sleep deprived drivers to study the effect of normal and high road noise and the effect of driving in an older vs. newer, more quite, vehicle.

4. Summary

This paper describes the VTI Sim IV. An advanced driving simulator with 8 DoF moving base. The facility has proven to be a valuable tool for human factors research. After 3 years of operation 14 studies have been run. The studies are a mix of HGV and passenger car experiments and switching between cabins works well. The facility complements the other VTI simulators in that it provides a wider FOV and more DoF to the moving base (in particular large stroke linear motion both laterally and longitudinally). Most of the simulator software was reused when establishing the Sim IV. The main development of VTI's simulator technology, connected to the Sim IV establishment, was the sound software and to some extent the motion cueing. Continued development and improvement of the facility is constantly on going to meet the need of new research projects.

5. References

[And1] Andersson, A., & Genell, A. (2013). SIREN: sound generation for vehicle simulation. In L. Nilsson (Ed.), *ViP publication; 2013-3*. Linköping: VTI.

[Fis1] Fischer, M. (2009). *Motion-Cueing-Algorithmen für eine realitätsnahe Bewegungssimulation.* Dr.-Ing., Technischen Universität Carolo-Wilhelmina zu Braunschweig, Braunschweig. (ISSN 1866-721X)

[Fis2] Fischer, M., Eriksson, L., & Oeltze, K. (2012). *Evaluation of methods for measuring speed perception in a driving simulator.* Paper presented at the Driving Simulation Conference, Paris.

[Fis3] Fischer, M., Håkan Sehammer, and Göran Palmkvist. (2010). *Motion cueing for 3-, 6-and 8-degrees-of-freedom motion systems.* Paper presented at the Driving Simulation Conference Europe 2010, Paris.

[For1] Fors, C., Ahlström, C., & Anund, A. (2013). Simulator validation with respect to driver sleepiness and subjective experiences - Final report of the project SleepEYE II, part 1. In L. Nilsson (Ed.), *ViP publications*. Linköping: VTI.

[Jan1] Jansson, J., Matstoms, P., Nordmark, S., & Sehammar, H. (2008). Förutsättningar för en avancerad körsimulator i Göteborg (pp. 28 s, 404 kB). Linköping: VTI.

[Jer1] Jerand, A. (1997). Improvment, validation and multivariate analysis of a real time vehicle model. Lic., KTH, Stockholm. (9753)

[Nil1] Nilsson, L. (1989). The VTI driving simulator : description of a research tool : reprint from Drive Project V1017 (Bertie), October 1989 (pp. 36). Linköping: Statens Väg- och Trafikinstitut., VTI särtryck 150.

[Nor1] Nordmark, S., Jansson, H., Lidström, M., & Palmkvist, G. (1986). A moving base driving simulator with wide angle visual system : prepared for the TRB conference session on "Simulation and instrumentation for the 80s", 64th Annual Meeting, Transportation Research Board, 14-18 January 1985, Washington D.C (pp. 29). Linköping: Statens Väg- och Trafikinstitut., VTI Särtryck 106.

[Nor2] Nordmark, S., Jansson, H., Palmkvist, G., & Sehammar, H. (2004). *The new VTI Driving Simulator - Multi Purpose Moving Base with High Performance Linear Motion.* Paper presented at the 2004 DSC Europe, Paris.

[Ste1] Stewart, D. (1965). *A Platform with Six Degrees of Freedom.* Paper presented at the Institution of Mechanical Engineers (UK), UK.

[Vip1] ViP. (2014). Virtual Prototyping and Assessment by Simulation, from http://www.vipsimulation.se/

MODULAR AND SCALABLE DRIVING SIMULATOR HARDWARE AND SOFTWARE FOR THE DEVELOPMENT OF FUTURE DRIVER ASSISTANCE AND AUTOMATION SYSTEMS

Martin Fischer[1], Andreas Richter[1], Julian Schindler[1], Jens Plättner[1], Gerald Temme[1], Johann Kelsch[1], Dirk Assmann[1] and Frank Köster[1]

(1): German Aerospace Center, Lilienthalplatz 7, 38108 Braunschweig, Germany, phone: ++49 531 295 3481, fax: ++49 531 295 3402, e-mail: {ma.fischer, andreas.richter, julian.schindler, jens.plaettner, gerald.temme, johann.kelsch, dirk.assmann, frank.koester}@dlr.de

Abstract – Currently, new-build vehicles are more and more equipped with various driver assistance and automation systems, ranging from adaptive-cruise-control, stop-and-go, active brake assist and emergency-brake systems for longitudinal control, blind-spot monitoring and lane-keeping systems for lateral control to parking assistance and advanced navigation systems. Through new emerging technologies, the integration of nomadic devices, Vehicle-2-X Communication in existing and new driver assistance and automation systems are the near future. The rising complexity due to more integrated, interactive and cooperative future assistance systems leads to increasing demands on driving simulators, used to develop and evaluate these devices in a time and cost efficient way. Thus, a number of driving simulators of the DLR Institute of Transportation Systems have been built or were upgraded with the major goal to provide a flexible, modular and scalable infrastructure, concerning both software and hardware, which enables a flexible set-up of the driving simulator according to the requirements of the test case – and not vice-versa!

This paper describes the implemented simulator landscape, the supporting software architecture and simulation applications, which enable a model-based design for assistance and automation systems. The underlying development concepts are described in more detail by Schröder [Schr10].

Key words: driving simulator design; software architecture; modularity; co-simulation

1. Introduction

Driving simulators are used as a tool in a broad range of use cases, e.g.

- early design evaluation and demonstration in order to find functional requirements for prototypes
- software or hardware in-the-loop tests
- parameter calibration or
- high-fidelity evaluation test runs with a large number of test drivers.

All these use cases lead to different requirements for simulator characteristics. In order to enable all kinds of tests in a cost-efficient manner and without the necessity to maintain a huge number of simulators, the DLR came up with a concept of modular simulator software and hardware components.

The first part of this paper introduces the hardware modules, distinguished in simulator platforms and mock-ups. The simulator platforms are providing the motion feedback capabilities, visualization systems and computer infrastructure. The mock-ups are consisting of chassis components, mirror and instrument-displays and integrated audio and haptic front-end devices. Further, additional special-purpose simulators which complement the flexible platform/mock-up combinations are described.

The second part of the paper will give a brief overview about the applied software architecture as well as utilised third party applications. The paper will end with an overview of projects that made use of the presented modular and scalable driving simulator environment.

2. Hardware infrastructure

As described in the introduction the hardware infrastructure is subdivided into simulator platforms and mock-ups. The mock-ups are exchangeable and can be (almost) freely combined with the simulator platforms.

An overview on the possible combinations is shown in Figure 1. A detailed description of each element follows in the next two sections.

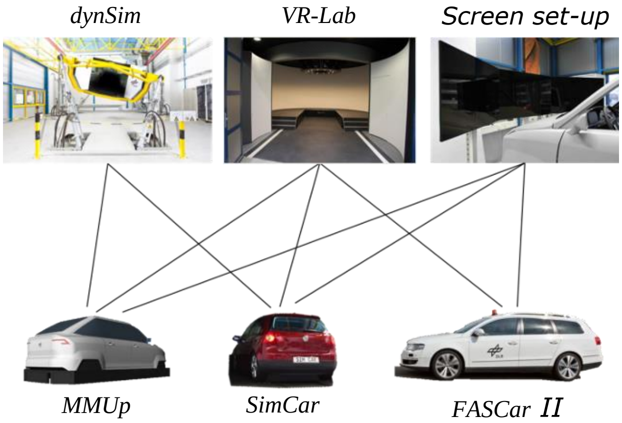

Figure 1: Possible combinations of simulator platforms (top) and mock-ups (bottom)

The simulator platforms and combinable mock-ups are complemented with special purpose simulators that have a closer coupling between the simulator base and the mock-up. These simulators will be described in the last section on hardware infrastructure.

2.1. Mock-up description

Each simulator platform can be combined with one of the two following mock-ups:

A modified commercial car with its original chassis components (*SimCar*) and a modular mock-up (*MMUp*), constructed with various separate chassis elements, interior parts, displays and active components, which can be mounted on top of a grid base plate using a resistant frame (see Figure 2).

To a great extend the mock-ups are composed of uniform hardware parts, e.g. motors, pedals, steering wheels, displays, etc. of a certain type with the intention of simplifying hardware integration, control software development and maintenance issues for the overall simulator infrastructure. Grid base plates are used for the majority of mock-ups to allow for flexible set-ups and fast integration of further hardware extensions.

The modular mock-up enables testing of new vehicle concepts or cockpit designs within the driving simulation by reconfiguring exterior and interior parts [Kös13].

Additionally, the integration of a real test vehicle (*FASCar II*) within the fixed-base simulator platforms allows a validation of the implemented assistance before proving it on the test ground or in real traffic. Its Drive-by-wire system allows the usage of the original control devices with the engine turned off.

(a)

(b)

(c)

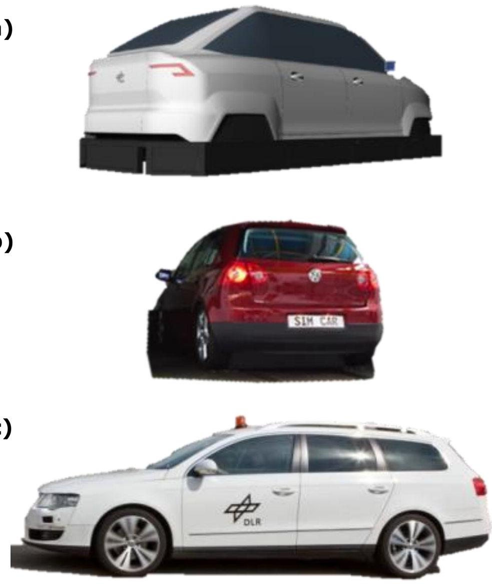

Figure 2: Mock-ups - *MMUp* (a), *SimCar* (b), *FASCar II* (c)

The main characteristics of the three different mock-ups are listed below in Table 1.

Table 1: Mock-up characteristics

Mock-up	*Main characteristics*
MMUp	Flexible and modular chassis and interior elements; Multiple displays for a free configurable HMI-Design; Changeable number and position of seats; Various input devices
SimCar	Modified production car; Original interior elements; Force feedback gas pedal and steering wheel; Touch screen for secondary tasks; Integrated head- and eytracking system; fully operable CAN-bus
FASCar	Real test vehicle; fully automated driving; force feedback gas pedal and steering wheel; touch screen for secondary tasks; full access to control signals via CAN-bus (driver overrule is possible)

The two mock-ups *MMUp* and *SimCar* are equipped with a full-HD LCD-Screen in the back of the car and small TFT-Screens as side-mirrors. For the test vehicle (*FASCar II*) it is also possible to integrate such screens. Signals between the mock-ups and the simulation control are sent using either CAN or UDP messages.

2.2. Simulator platform description

The simulator platforms provide either a simple but transportable visualisation solution using three LCD screens for quick evaluations or show-cases, a full 360°-front-projection visualization (*VR-Lab*) or a high-resolution 270°-back-projection visualisation (*dynSim*). The high-resolution visualization is combined with a moving-base hexapod platform whereas the other two solutions are set up as fixed-base simulators in order to reduce controlling complexity.

As already mentioned, these platforms can be combined with the different mock-ups described in the previous section. Figure 3 illustrates some of the possible combinations and provides both outside and inside views of the two simulator platforms *dynSim* and *VR-Lab*. In Figure 3 (c) the rear gates of the *VR-Lab's* screen dome are opened which enables the exchange of mock-ups. When closed, they are part of the surrounding screen which facilitates to display the virtual world with a 360° field-of-view.

Table 2 lists the main characteristics of the different visualisation systems.

Table 2: simulator platform visualisation systems

Simulator platform	*Type*	*Field-of-View (horizontal)*	*Resolution H x V*
dynSim	Eyvis ESP-SXT+	270°	1400 x 2100 for each 30°
VR-Lab	Eyvis ESP-WXT	360°	1200 x 1920 for each 30°
Screens	Samsung LCD	100°	1920 x 1080 for each Screen

The motion base of the *dynSim* simulator platform enables the driver to feel a direct feedback of driving control actions. This is of high importance for dynamic manoeuvers or for the evaluation of assistance systems which influence the vehicle control. Furthermore, it generally improves the driver's immersion into the virtual world.

Some performance indicators of the motion-base are given in Table 3. The motion-base is able to bear up to 1200 kg payload while maintaining the performance.

(a)
(b)
(c)
(d)

Figure 3: Simulator platform *dynSim* with the *SimCar*(a & b), *VR-Lab* in combination with the *FASCar* (c) and the *MMUp* (d)

Table 3: Motion characteristics (*dynSim*)

	Position	*Velocity*	*Acceleration*
Longitudinal	±1,50 m	±2 m/s	±10 m/s²
Lateral	±1,40 m	±2 m/s	±10 m/s²
Vertical	±1,40 m	±1 m/s	±10 m/s²
Pitch	±20 °	±50 °/s	±250 °/s²
Roll	±21 °	±50 °/s	±250 °/s²
Yaw	±21 °	±50 °/s	±250 °/s²

2.3. Special purpose simulators

In addition to the flexible platform/mock-up combinations, special purpose simulators complement the simulation infrastructure of the institute: The *HMI-Lab*, the *IDeE-Lab* and the *MoSAIC-Lab* (see Figure 4).

(a)
(b)
(c)

Figure 4: Special purpose simulators - *MoSAIC-Lab* (a), *HMI-Lab* and *MMUp* + *Screen set-up* (b), *IDeE-Lab* (c)

Each facility is briefly described in Table 4 and in more detail in the following subsections.

Table 4: Special purpose simulator characteristics

Simulator	*Main purpose*	*Main characteristics*
HMI-Lab	Demonstrations; HMI-Design evaluation	Quarter-car chassis; transportable
IDeE-Lab	HMI-Design evaluation by using the theater system technique	2 basic mock-ups with mechanically and electronically coupled steering systems; various HMI devices and active inceptors
MoSAIC-Lab	Cooperative system evaluation	3 identical mock-ups, which can be involved in one common simulation

2.3.1. HMI-Lab

The *HMI-Lab* is a small mobile simulator with a couple of displays and force feedback inceptors, i.e. an active steering wheel as well as active brake and throttle pedals. It is intended to be used for show-cases where a wide spectrum of functionalities has to be shown. Thus, the basic requirement for this simulator is to provide a high fidelity simulator in a compact, representable design which enables an easy and fast set-up and transportation. Therefore it basically consists of a quarter-car chassis in connection to a glass-topped counter containing the necessary computers and control units for the force-feedback devices. The instrument cluster, the left outer mirror and the front view are presented on LCD screens. Instead of a standard middle console, a touch-screen is installed.

2.3.2. IDeE-Lab

The "Interaction Design and Ergonomics Laboratory" (*IDeE-Lab*) is a laboratory for the design of advanced interactive and cooperative driver assistance systems [Kel13]. Therefore, the room is equipped with everything needed for discussion, e.g. several beamers and whiteboards. Furthermore, it holds two basic mock-ups with the focus on maximum flexibility, which are simply created by Bosch-Rexroth-Profiles. The absence of covering chassis elements enable rapid mounting and remounting of any additional device. Each mock-up is equipped with high-performance force feedback pedals, steering wheels, and side-sticks. Additionally, the basic mock-ups can optionally be coupled in a mechanical and electronic way, enabling a design method called the theatre system technique [Sch09]. By this technique interaction behaviour and user needs can be played through, discussed and documented in very high detail even before the prototypic implementation has started. After clarifying the HMI requirements, the interaction prototype can be developed by a model-based approach and tested step by step in usability studies.

2.3.3. MoSAIC-Lab

Modular and Scalable Application platform for ITS Components (*MoSAIC*) is the DLR ITS concept for linking several mock-ups or even whole laboratories in order to provide scenarios with more than one ego driver [Lor11]. The basic *MoSAIC* concept can be applied to any of the simulator platforms, mock-ups and laboratories at DLR ITS. Exemplarily, the coupling of the *HMI-Lab* and the *MMUp*/LCD-Screen set-up is shown in Figure 4 (b).

Thereby a broad spectrum of research ranging from exploration of cooperative behaviour of two or more drivers in common vehicles up to exploration of cooperative effects of several human-machine systems supported by ADAS in complex traffic situations becomes possible.

The *MoSAIC-Lab* permanently provides this opportunity as it is equipped with three connected standard DLR fixed based simulators, each set-up providing a 140° field-of-view, an active steering system and active pedals, allowing a wide spectrum of haptic HMI, as well as a number of additional buttons and displays used for the interaction with other drivers. Hence, the *MoSAIC-Lab* offers the possibility to easily investigate cooperative ADAS systems

As the creation of scenarios with multiple ego drivers is challenging, a new approach for the design of scenarios has been developed. This approach is described in detail by Schindler [Sch14].

3. Simulation software and system architecture

The basic in-house developed system architecture *Dominion* [Gac08] provides a service oriented concept that supports tightly embedded in-vehicle assistance and automation systems as well as loosely coupled comfort oriented applications. A semiformal description of the data and the services is the core of *Dominion*. It comes along with automatic code generation for generating the application frames [Mon10], standardized user-interfaces for integrating third party applications and components and supporting tools for the operation of laboratories and for conducting test runs which facilitate fast development of new applications and services and simplifies the control of the simulation session as well as data logging and data analysis. The general *Dominion* structure is shown in Figure 5.

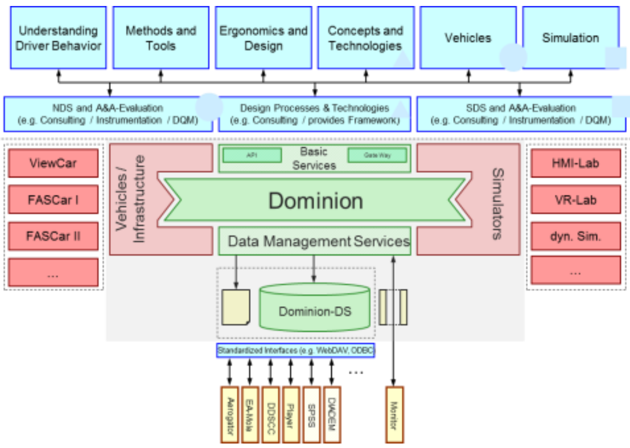

Figure 5: General Dominion system architecture with vehicles on the lower left corner and simulators on the lower right corner

The supporting tool *DominionRemote* is able to manage a full-scale simulator setup including third party applications by starting, parameterising, monitoring and if necessary relocating the applications. It integrates *Dominion's* server communication for life-cycle management of all modules. Also the data recording is coupled so that the study operator only has to deal with one software frontend. The *DominionDataStore* handles the data recording. It includes the runtime data as well as meta–data, which is modelled within the *Dominion* data core.

Recorded time series can be assessed and visualised with the in-house-developed *DominionDataStoreControlCenter* as well as with commercial software like *SPSS.* For play-backs *DominionPlayer* can be used in order to rerun a recorded simulation. With the help of the stored meta-data it is possible to rerun a simulation in another simulator as the one where it was recorded as well as at office computers.

Dominion is used in both types of test facilities: in simulators and test vehicles (e.g. *FASCar II*). Therefore a transfer of software prototypes and special hardware interfaces (e.g. for LED-lights or side sticks) causes minimal migration effort.

In-house software-modules for all parts of the simulation (e.g. scenario control, traffic simulation, vehicle dynamics, image generation, motion cueing, visual/haptic/audio feedback, hardware control, etc.) have been developed throughout the last years [Sch11]. Full access to the source code guarantees flexible adaption to new requirements and continuous improvements to support new methodological and technical demands.

Additional to that, it is possible to share this simulation environment with project partners as no third party applications are required.

External modules can be integrated through standard communication protocols (UDP, CAN, TCP) or additional interface applications as well as web services.

For example, VIRES' commercial simulation software *VirtualTestDrive* was integrated in order to extend the feasible features of the overall simulation. Because of the modular concept of *VirtualTestDrive* it is possible to use only parts of it (e.g. visualization, traffic) and complement the simulation with *Dominion* applications (e.g. vehicle dynamics, automation). For compatibility reasons standardized formats and open source software are widely used, for example,

- the visualization is based on *OpenSceneGraph* [Wan12], that is also used for additional simulation issues (e.g. communication simulation [Ric2012]),

- the road description format *OpenDRIVE* is used. *OpenDRIVE* is an open XML description format for road logic and layout. It was established 2005 and is constantly improved by an industry and research institute driven consortium. The *OpenDRIVE* description is also the basis for generating the 3d virtual world using *OpenSceneGraph*.

Summing up, the facilitated system architecture and the integrated software components enable a great flexibility for the set-up of simulator experiments.

4. Related Projects

Current or recently finished projects that made use of the broad simulator infrastructure and demonstrated its capacities are e.g. the following projects:

- ***eCoMove*** (http://www.ecomove-project.eu/) conducted a study about a green efficiency assistant system providing gearshift suggestions in the dynamic simulator *dynSim* and the final event demonstration was performed within the mobile *HMI-Lab* Simulator.
- ***InteractIVe*** (http://www.interactive-ip.eu) performed studies about emergency evading assistant using the same automation strategies and applications realized within *Dominion* in both the *FASCar II* on a real test track and in the dynamic driving simulator *dynSim* [Hes13].
- ***D3CoS*** (http://www.d3cos.eu/) studies with cooperative merging assistance were performed in the *MoSAIC-Lab* with different quantity of ego vehicles [D3C14a][D3C14b] and were later on demonstrated combining the *MMUp* and the *HMI-Lab*.
- ***UR:BAN*** (http://www.urban-online.de/) also performed in the *MoSAIC-Lab* a study about cooperative driver behaviour regarding vehicles partly equipped with traffic light assistance. The study relied on adapting the behaviour of other probands.
- ***MobiFAS*** demonstrated the integration of nomadic devices with automation systems using the *FASCar II* within the simulation in either the simple LCD-screen set-up or the *VR-Lab.*
- ***AdaptIVe*** is an EU-founded integrated project with 29 partners across the EU. The aim of the project is on the ideal cooperative interaction between the driver and the automated system by using advanced sensors, cooperative vehicle technologies and adaptive strategies in which the level of automation is dynamically adapted to the situation and driver status.

5. Summary

A landscape of diverse simulators were built, which can be handled by a small team of operators and developers due to standardization of components and interfaces, customization of operator controls and an flexible system architecture as a solid foundation for the simulation software. Their flexibility and adaptability where shown in diverse projects over the last years. These driving simulators are well prepared for being involved in research and development projects in order to answer current and future research questions – especially within the upcoming tasks connected to the development of exceedingly complex, highly automated and/or cooperative assistance systems.

6. References

[D3C14a] D3CoS Consortium: Deliverable 3-08 Platform for Modelling and Simulation, Project EU- D3CoS (2014); public deliverable; page 36-43; Link: http://www.d3cos.eu

[D3C14b] D3CoS Consortium: Deliverable 2-02 Demonstrators Final Version, Project EU-D3CoS (2014); public deliverable; page 156-160, 180-196 ; Link: http://www.d3cos.eu

[Gac08] Gacnik, J.; Häger, O.; Hannibal, M. (2008), A Service-Oriented System Architecture For The Human Centered Design Of Intelligent Transportation Systems, in European Conference on Human Centred Design for Intelligent Transport Systems, Lyon, France.

[Hes13] Hesse, T.; Schieben, A.; Heesen, M.; Dziennus, M.; Griesche, S.; Köster, F. (2013), Interaction design for automation initiated steering manoeuvres for collision avoidance, 6. Tagung Fahrerassistenzsysteme, 2013. München.

[Kel13] Kelsch, J., Temme, G., Schindler, J. (2013): Arbitration based framework for design of holistic multimodal human-machine interaction. Contributions to AAET 2013, 6.-7. Feb. 2013, Braunschweig, Germany, ISBN 9783937655291

[Kös13] Köster, F., Plättner, J., Richter, A., Schnieder, L., Fischer, M., Schindler, J., Baumann, M., Jaschke, K. (2013), Rahmenbedingungen für den rationalen Einsatz von Fahrsimulatoren zur Entwicklung fortschrittlicher Assistenz- und Automatisierungssysteme, ISBN 978-3-937655-29-1.

[Lor11] Lorenz, T.; Baumann, M.; Jaschke, K.; Köster, F. (2011), A Modular and Scalable Application Platform for Testing and Evaluating ITS Components, in 20th IEEE International Workshops on Enabling Technologies: Infrastructure for Collaborative Enterprises, IEEE Computer Society Conference Publishing Services, ISBN 978-0-7695-4410-6.

[Mon10] Montenegro, S., Dannemann, F., Dittrich, L., Vogel, B., Noyer, U., Gacnik, J., Hannibal, M. Richter, A., Köster, F. (2010), (SpacecraftBusController+AutomotiveECU)/2=UltimateController, in Lecture Notes in Informatics (GI-Edition), 160, Seiten 103-114. Gesellschaft für Informatik. Software Engineering 2010 / ENVISION2020, Paderborn

[Ric2012] Richter, A., Paz Lazo, M., Jaschke, K. (2012), A Simplified V2X Communication Model for Driving Simulators Considering Environmental Influences, in GEOINFORMATIK 2012, 28.-30. Mar. 2012, Braunschweig, Germany, ISBN 978-3-8440-0888-3

[Sch09] Schieben, A., Heesen, M., Schindler, J., Kelsch, J., Flemisch, F. (2009): The theater-system technique: agile designing and testing of system behavior and interaction, applied to highly automated vehicles. 1st International Conference on Automotive User Interfaces and Interactive Vehicular Applications; 01/2009

[Sch11] Schindler, J. , Harms, C. , Noyer, U. , Richter, A., Flemisch, F., Köster, F., Bellet, T., Mayenobe, P., Gruyer, D. (2011), JDVE: A Joint Driver-Vehicle-Environment Simulation Platform for the Development and Accelerated Testing of Automotive Assistance and Automation Systems, in Human Modelling in Assisted Transportation Springer-Verlag Italia Srl., ISBN 978-88-470-1820-4, 2011

[Sch14] Schindler, J., Hesse, T. Coping with complex driving scenarios: Exploratory Scenario Design. Abstract submitted to the Driving Simulation Conference, 2014.

[Schr10] Schröder, M. Hannibal, M., Gacnik, J., Köster, F., Harms, C., Knostmann, T. (2010), Ein Labor zur modellbasierten Gestaltung interaktiver Assistenz und Automation im Automotive-Umfeld, AAET 2010, Braunschweig, ISBN 978 3 937655 23 9

[Wan12] Wang, R., Qian, X. OpenSceneGraph 3 Cookbook, Packt Publishing, 2012.

OPENDRIVING: AN OPEN SOURCE DRIVING SIMULATION SOFTWARE

Zhitao Xiong

The Research Centre for Integrated Transport Innovation
University of New South Wales
Sydney, Australia
Tel: (+61)2 9385 0396
Email: z.xiong@unsw.edu.au

Abstract – This paper presents an open source driving simulation software that is platform-independent, research-oriented, distributed and soft body physics-based. It has formal and standard scenario/world description, goal-driven autonomous virtual drivers and rigid body-based simulated vehicles. It is designed to be a tool and test-bed for areas that require realistic and controllable traffic environment, such as game development, driver training, human factor research, nanoscopic traffic simulation.

Key words: Driving Simulation, Automated Planning, Temporal Reasoning

1. Introduction

The driving simulation software equipped by driving simulators can be regarded as scenario generators, because a scenario covers the physical world, the traffic flow, simulated vehicles' interactions with the participant's vehicle and measurements that need to be collected. Due to its complexity, the driving simulation community still needs to work on some shortcomings of present simulation platforms regarding 1) un-realistic entity representation, 2) manual traffic flow manipulation and 3) platform-dependent controlling of simulated vehicles. As a result, an open source project, termed as OpenDriving, was initiated based on a framework SOAV (Scenario Orchestration with Autonomous simulated Vehicles), whose mechanism has been described in [Xio1] and [Xio2]. Its rendering part has been implemented with an open source vehicle simulator RoR (Rigs of Rods, http://www.rigsofrods.com/content/).

OpenDriving has the following features:1) C++-based cross-platform design; 2) SOAV-based, research-oriented framework; 3) Ontology-based, human-readable, machine-processable, data scheme for describing scenarios; 4) Distributed architecture for networking and extension; 6) Realistic soft body physics and 7) Rich resources from the community of Rigs of Rods and SUMO [Kra1] if necessary. The OpenDriving project will be opened to public during the Driving Simulation Conference 2014 in Paris (4-5 September 2014) via Google Code (https://code.google. com/p/opendriving/).

This short paper will provide an overview of the architecture of OpenDriving.

2. OpenDriving Description

As illustrated in Figure 1 on Page 2, OpenDriving has the following components:

1) The Ontology for Scenario Orchestration: this ontology is used to describe scenarios and relevant driving context for a virtual driver in a formal, context-oriented, programming-independent, logic-based, human-understandable and machine-processable manner; more information can be found in [Xio3] and [Xio4].

2) Simulation Platform: In previous research, the basis of OpenDriving - SOAV - has been tested with simulation platforms from the University of Leeds [Xio1, Xio2] and VTI [Xio5]. In OpenDrving, Rigs of Rods was used in order to have a soft body engine to simulate realistic vehicle bodies and objects;

3) The Virtual Driver: The Virtual Driver will carry out driving activities based on scenario requirements from the Ontology for Scenario Orchestration, which can include the actions needed to produce interactions and corresponding context, e.g., braking (action) as a leader (context); The simulated vehicles in the Simulation Platform will be controlled;

4) Traffic Flow Manipulator: Equipped with SUMO, the Traffic Flow Manipulator will produce traffic flow with predefined travel

demands; the generated vehicles will be visualized in the Simulation Platform if they are near to the human participant's vehicle (it has been set as 1500m around the participant vehicle);

5) Scenario Observer: this module monitors the packages transmitting on the network during simulation and extra interfaces can be provided to users through desktop or hand-held devices.

3. Conclusions and Future Enhancements

OpenDriving, as a modular framework, can provide a tool or test-bed with realistic physics and behaviours to users, who can range not only from serious game players to academic researchers, but also from driving instructors to simulation developers. It can help entities ranging from individuals to agencies. For instance, a scenario with a car crash in an intersection can be used to simulate the C2C (Car to Car) communication module in vehicles. The crash information will be transferred to several (simulated) human participant's vehicle before they can see the crash. The crash will be visually simulated in the intersection with the help from Rigs of Rods. Moreover, a scenario for human factor research with controllable vehicle behaviours can be constructed with a traffic flow generated by the Traffic Flow Manipulator with pre-defined characteristics such as traffic flow rate. As a first attempt of gathering knowledge in the community, OpenDriving is believed to serve its purpose and be useful, and extra efforts from the whole community are anticipated in the near future.

4. References

[Kra1] Krajzewicz, D., Erdmann, J., Behrisch, M. and Bieker. L. (2012). Recent Development and Applications of SUMO - Simulation of Urban MObility. International Journal on Advances in Systems and Measurements, 5 (3&4):128-138.

[Xio1] Xiong, Z. (2014). Creating a Computing Environment in a Driving Simulator to orchestrate Scenarios with Autonomous Vehicles. Ph.D. thesis, Institute for Transport Studies and School of Computing, University of Leeds.

[Xio2] Xiong, Z., Carsten, O., Jamson, H. and Cohn, A. G. (2014). A Task-Driven Framework for Driving Simulation: Scenario Orchestration with Autonomous simulated Vehicles (SOAV). Submitted to ACM Transactions on Interactive Intelligent Systems.

[Xio3] Xiong, Z., Carsten, O., Jamson, H. and Cohn. A. G. (2013). Ontology for Scenario Orchestration (OSO): A standardised scenario description in driving simulation. American Society of Civil Engineers, Chapter 210, 1572–1577.DOI:http://dx.doi.org/10.1061/9780784413036.210

[Xio4] Xiong, Z., Cohn. A. G., Jamson, H. and Carsten, O. (2014). Ontology for Scenario Orchestration: a Formal Driving Context and Task Description in Driving Simulation, Submitted to Applied Ontology.

[Xio5] Xiong, Z. and Olstam. J. (2014). Orchestration of Driving Simulator Scenarios - based on Dynamic Actor Preparation and Automated Action Planning. Submitting to Transportation Research C.

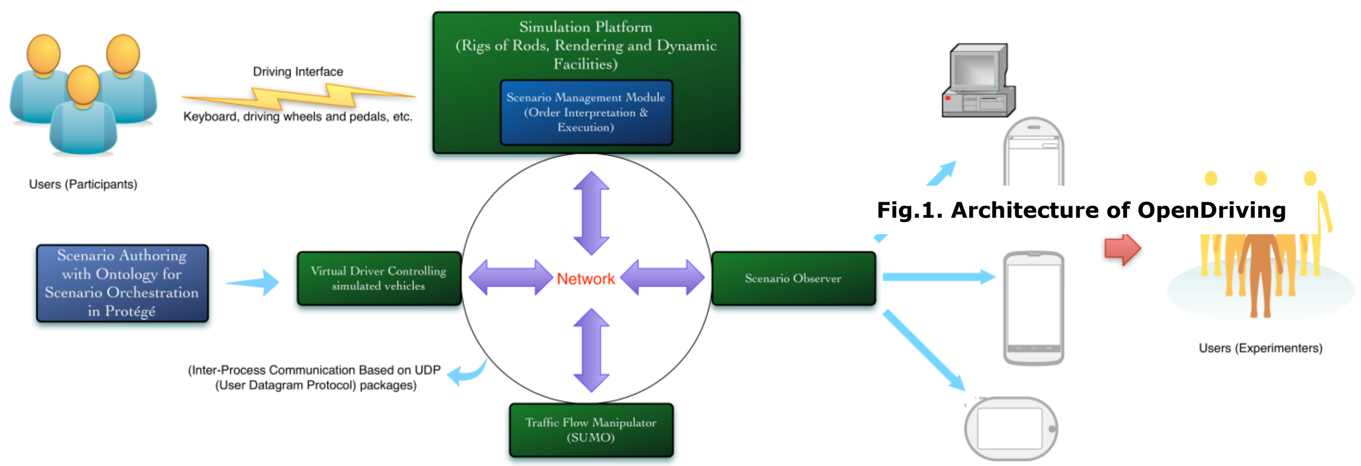

Fig.1. Architecture of OpenDriving

SLEEPNOISE - A SIMULATOR BASED STUDY OF THE EFFECTS OF NOISE ON DRIVER SLEEPINESS

Eva Lahti[1], Anders Genell[2], Anna Anund[2]

(1) Volvo Car Corporation
40531 Gothenburg
Sweden
Phone: +46 (0)31 325 0200
eva.lahti@volvocars.com

(2) Swedish Road and Transport Research Institute (VTI)
58195 Linköping
Sweden
Phone: +46 (0) 21 204 000
{anders.genell; anna.anund}@vti.se

Abstract – In the current study, a detailed model of in-vehicle road noise was developed in order to test effects of road noise on driver sleepiness. The model synthesizes realistic road noise based on real world measurements of road texture and of corresponding interior noise. Two different scenarios were used, representing a mid-sized hatchback car on a coarse road texture versus a large wagon on a smooth road. The synthesized noise was validated against in-vehicle recordings, and was ultimately used to investigate influence on driver sleepiness. Results show that the model is well suited for such studies, and that there was indeed an effect on driver sleepiness. In addition, a carry-over effect was found for the onset of the noise test cases. It suggests that the effect on e.g. self-reported sleepiness was determined by the first stimulus presented, masking the effect of later stimuli, thus emphasizing the need for methodological design considerations.

Key words: drowsiness, low frequency, noise, vibration, harshness

1 Introduction

The use cases for a technically complex system such as a driving simulator are typically continuously changing, as the problems they help solve are changing. This calls for systems that allow for development on an as-needed basis. In the current use case, the initial research question arose from informal self-reported feelings of fatigue and tiredness when driving a car on particularly worn roads and a notion that certain cars make the driver sleepier than others. These effects were attributed to the variations in interior road noise, and investigating if increased levels of road noise would reduce wakefulness in drivers made for a novel simulator use case.

The fact that sleepiness in drivers is a contributing factor in accidents is well known today, however what role external factors such as type of road, sound/noise, vibrations, etc. have on the ability to stay awake is rather unknown. Previous studies on noise related driver fatigue have mainly concerned heavy vehicles where infrasound and low frequency noise has been shown to be related to increased fatigue but also increased stress and impaired performance in drivers, both in real traffic situations [Löf1] as well as in simulator settings [Söd1][Mor1] and in laboratories [Lan1]. While the sound level and frequency distribution inside a car cabin is different from those inside a lorry cabin, the interior sound is still dominated by its low frequency content since the efficiency of the various abatement measures employed declines with decreasing frequency. It was thus hypothesised that increased low frequency road noise in the car cabin would increase drowsiness also car drivers.

The simulator development needed to test the hypothesis was identified as the need for a very realistic road noise model that would allow for variations in frequency content and level due to variations in road conditions as well as due to the sound attenuating properties of different vehicles.

2 Method

2.1 Measurements

To couple a noise model to real conditions, road surface texture measurements were performed on one relatively smooth road texture and on one coarse road texture, the latter chosen for the high levels of low frequency noise experienced in the car when driving over the surface. The measurements were performed using the VTI Road Surface Tester measurement vehicle (Figure 1). It uses a 19-channel laser interferometer array to measure the road texture profile from micro to macro levels in combination with accelerometers, inclinometers and differential GPS receivers. The resulting data is in the form of surface texture height values for each of the 19 tracks recorded each millimeter along the stretch of road under study.

Figure 1. The VTI Road Surface Tester measurment van with its front mounted laser interferometer array.

In addition to the road surface texture measurements, the resulting interior road noise from driving on the same road textures at different speeds were recorded in two different vehicles. Microphones were placed adjacent to the driver's ears in accordance with ISO 5128:1980, Measurement of noise inside motor vehicles, in order for the recording to be as representative as possible for the sound experienced by the driver.

2.2 Model

VTI has developed SIREN, a simulator sound renderer allowing for versatile sound environment adoption to specific use cases. In the core of SIREN is a sound manager software that connects sound streams for engine and road noise with event-based sounds such as passing traffic and warning sounds and places the sounds in the sound field surrounding the driver. The sound streams for road and engine noise are synthesized by sound models implemented in Csound, a scripting language for real-time sound synthesis and manipulation. The texture and noise measurements were used as basis for an updated road noise model that would allow synthesizing very realistic road noise inside the driving simulator in real-time. The noise model consisted of two parts – one representing the road surface textures and the other representing the transfer functions from tyre/road interaction to the vehicle cabin noise. Analysing the texture measurements it was found that the smooth road surface texture could be reasonably well modeled by white noise filtered with a first order Butterworth low pass filter determined by the distribution of road surface texture wavelengths. The coarse road surface texture was modeled using two cascaded low pass filters allowing for the increased long-wavelength content found in the analysis (Figure 2). When driving along the road, the wheels vibrate vertically at frequencies determined by the texture wavelengths and the speed of the vehicle. Also, the intensity of the vibrations varies with speed since the vertical acceleration is greater at greater horizontal speed. Therefore, the texture model was created as a varying filter with a cutoff frequency and overall level determined by the speed of the vehicle and the cutoff wavelength of the road texture. When driving the simulator, the sound would thus vary in frequency content and level as a function of the simulated speed.

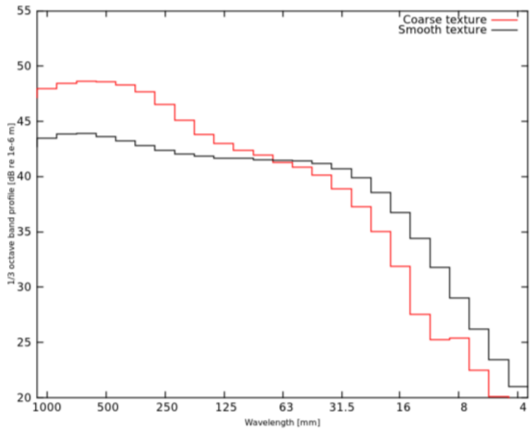

Figure 2. Road surface texture spectra in 1/3 octave bands for the coarse texture (red) and the smooth texture (black).

Recorded interior vehicle sound is comprised of the road surface texture causing direct air borne sound radiation from the tyres into the car cabin as well as causing vibrations to propagate through the suspension and chassis making panels inside the car radiate sound as well. In order to create a basis for the vehicle cabin transfer function model, the influence of the texture on the recorded sound needed to be compensated for. This was in fact one reason for keeping the texture model for the smooth road as simple as possible, as it allowed for the inverse of the smooth road first order low pass filter to be applied to the recorded sound. As the sound is dependent on vehicle speed, the inverse filter for a speed of 110kph was applied to the 110kph smooth road sound recordings for both vehicles. The vehicle cabin transfer functions were then created by fitting an Auto-Regressive (AR) model to the resulting sound using Burg's method [Bur1] with 32768 coefficients. Finally, the impulse response for each of the AR models was generated and the sound in the simulator was created by applying either of the texture related low pass filters with speed dependent cut-off frequency to a white noise generator and convolving the result with either of the cabin related impulse responses.

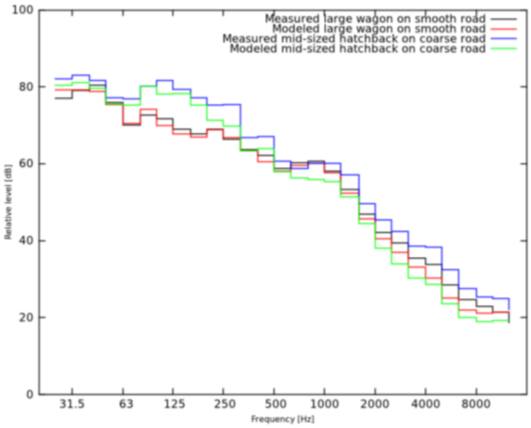

Figure 3. Spectra of recorded and modelled road noise for the two conditions used in the sleepiness experiment

The resulting sound inside the simulator was found to correspond well to the in-vehicle recordings (Figure 3). The two driving conditions used in the sleepiness experiment were represented by either a vehicle of large wagon type driven on the relatively smooth asphalt road surface (quiet case), or a vehicle of mid-size hatchback type driven on the relatively coarse road surface (loud case). The differences between the two sound settings were mostly within the one-third octave bands between 63Hz and 250Hz corresponding to the differences in suspension, chassis and car body between the two vehicle models as well as to the differences in road texture between the two road surface types. For both infrasonic frequencies and higher frequency content (e.g. wind noise), as well as for vibrations and harshness both sound settings were more or less identical, thus focussing on the effects of road texture induced low frequency noise.

2.3 Experiment

The sleepiness experiment was performed in the VTI Moving Base Simulator IV (Figure 4). The simulator has a Volvo XC60 vehicle cabin with three LCD-displays for side and rear view mirrors mounted on a platform with a visualization system consisting of a curved screen and nine projectors creating a 210-degree forward field of vision. The platform is mounted on a motion system permitting significant linear movement along both x and y axes as well as pitch and roll rotations.

Figure 4. VTI Moving Base Simulator IV (Sim IV).

The scenario for the experiment was a straight highway with a speed limit of 110kph, in daylight conditions with a small amount of fog. There was no traffic in the same lane as the own vehicle but some oncoming vehicles to make the scenario more realistic. A random sample of 20 drivers (30-50 years old) were recruited, 10 male and 10 female, with self-reported normal hearing. Before arrival, they were asked to avoid a number of confounding issues such as undue naps or excessive intake of coffee etc. Each participant drove one session during day time/evening (alert) and one session during nighttime (sleepy). All participants were subjected to each driving condition in altering orders of occurrence for the different sessions. The participants drove two passes of 35 minutes each in each session, divided by a short intermission where they answered a questionnaire while still seated in the car. The simulator data acquisition system was used to sample speed and lateral position as measures of driving performance, and self-reported sleepiness (Karolinska Sleepiness Scale, KSS) and blink duration recorded by an eye camera system were used as sleepiness measures. In total seven performance indicators (PI) were used in order to analyse driving performance and sleepiness level: KSS (self-reported verbally every 5 minutes), blink duration (s), fraction of blinks longer than 0.15 s, mean speed (km/h), average and variability of lateral position (m) and average number of line crossings to the left or to the right per km driven. The data was analysed using traditional mixed model ANOVAs.

3 Results

When analysing the results, no main effect of the different sound settings could be found at first, but the time of day (day or night) had an effect for all variables, as expected since drivers are likely to be more sleepy during nighttime conditions. Upon further analysis, and considering there was also a main effect found when comparing first and second 35-minute parts across all drive cases, an unexpected carry-over effect was identified. This may be interpreted as if one starts to drive with high levels of low frequency road noise in the car the influence will be present even if there is a change in low frequency noise. This effect was present both for sleepiness measures such as KSS-ratings as well as for performance measures such as mean vehicle speed. For both day and night conditions, the loud test case rated higher on the KSS scale than the quiet case in the first part of the drive, but in the second part the situation was the opposite. Considering that the participants were presented with one test case in the first part and the other test case in the second part, this would mean that participants were responding as if the first case was continued after the short intermission. Those who were first presented with the loud case responded as if the second part was the loud case as well, and vice versa. In an attempt to account for this carry-over effect, an additional analysis was performed where only the first 35-minute part of each drive was included. While this would exclude the data that in effect was masking any main effects of varying the sound setting, it also meant that the statistical basis was reduced, in some cases causing a weaker statistical significance level. Including only the first 35 minutes for day and night time driving a tendency was found for KSS meaning that the self-reported sleepiness was higher for the loud test case during nighttime driving. For measured mean vehicle speed, the effect was even greater showing statistically significant reduction in speed for the loud test case when just including the first part of each drive. Several additional measures of both sleepiness and of driving performance showed similar.

4 Conclusions

The resulting sound model proved to work very well for the intended use, facilitating detailed investigations of the influence of sound on driver behavior in addition to providing realism and presence in the simulated environment. It allows for changing vehicle cabin sound model independently from the influence of road texture, so more combinations of vehicle cabins and road textures can easily be investigated if needed. The realism of the road noise model was validated by NVH experts from Volvo Car Corporation well acquainted with the modelled vehicles. The simulator experiment was found to support the hypothesis that high levels of low frequency road noise in the car contribute to increased driver sleepiness and impaired performance during nighttime. The unexpected carry-over effect suggests that the onset of conditions such as those found in realistic road noise has a lasting effect, which cannot be neutralized by a short break while still seated in the vehicle. The carry-over effect might have been neutralized by allowing participants to exit the simulator e.g. to stretch their legs and have a drink of water or so, which might also imply that countermeasures against driver fatigue need to have a proper impact to counter such lasting effects. These are issues that require further research.

5 Acknowledgements

This work was supported by the competence centre ViP (Virtual Prototyping and Assessment by Simulation, www.vipsimulation.se), co-financed by VINNOVA (the Swedish Governmental Agency for Innovation Systems; grant number 2007-03083) and the ViP partners

6 References

[Bur1] Burg, J.P. (1975). “Maximum Entropy Spectral Analysis”. PhD Thesis. *Available online at http://sepwww.stanford.edu/theses/sep06/*

[Lan1] Landström, U. (1987). "Laboratory and field studies on infrasound and its effects on humans." J Low Freq Noise Vib 6(1): 29-33.

[Löf1] Löfstedt, P., S. Lindblom-Häggqvist, et al. (1988). Studier av buller, vakenhet och risker under lastbilskörning, Arbetsmiljöinstitutet.

[Mor1] Moren, B., U. Landström, et al. (1989). Inverkan av infraljud, buller och värme på prestation och vakenhet under fordonskörning: En simulatorstudie, Linköping.

[Söd1] Söderberg, L., M. Byström, et al. (1988). Simulatorstudie avseende effekter av buller och temperatur på EEG och puls under fordonskörning, Arbetsmiljöinstitutet.

SMALL-SCALE TRAFFIC DEMONSTRATOR WITH DRIVING SIMULATOR

Dipl.-Ing. Oleksandr Goloborodko[1], Prof. Dr.-Ing. habil. Georg-Peter Ostermeyer[2]

(1) : Schleinitzstr. 20;
DE-38106, Braunschweig
Phone +49 531 3917071
Fax +49 531 3917017
E-mail : {o.goloborodko}@tu-bs.de

(2) : Schleinitzstr. 20
DE-38106, Braunschweig
Phone +49 531 3917002
Fax +49 531 3917017
E-mail : {gp.ostermeyer }@tu-bs.de

Abstract - Driving simulators and traffic simulations have a lot of potential in research and development, training and assessment, which provides many advantages. First of all, it is safe and the experiments are cheaper. Secondly, the setup is very flexible and many subject actions can be studied. Moreover, many parameters and factors can easily be recorded.

Since the early 2000's, the Institute of Dynamic and Vibrations of the Technical University of Braunschweig has developed alternative paradigms for a microscopic simulation, which are clearly rooted in the drive activities.

This poster describes some points regarding the development and construction of the miniature traffic demonstrator with car driving simulator components. Some components can be used as part of hardware-in-the-loop simulation.

The car driving simulator can be driven/operated by human drivers (Fig. 1, right) and parallel by virtual drives. These virtual drivers are characterized by the ability to directly drive moveable cars in the same way as human driver in the laboratory. In both cases, it gives you the opportunity to observe and study the behavior of drivers in the implementation of certain difficult driving situations.

The driver simulator includes the front part of a real car with all factory components inside the cabin, a projector for video transmission from the controlled vehicle inside the laboratory for microscopic traffic simulation, as well as special hardware (sensors, actuators) for communication processing and output of information. Special factor in this scheme is the integration of a real driver in the simulation environments.

After analyzing a number of factors that affect the human perception of information and the existing equipment in the laboratory have been done significant improvements, both in the driver simulator and laboratory for microscopic traffic simulation.

As a result of the creation and implementation the driver simulator includes acoustic modules, enhanced visual systems and haptic force feedback systems, so that the running conditions of the car simulators are close to the condition in realer car, as similar as possible.

Study driver behavior under different conditions will allow reducing a minimum the impact of errors due to lack of visual, acoustic or tactile.

The simulator provides a good tool for developers to build driver information and assistance systems that help the driver to control the vehicle and has recently become an integral part of modern cars. Such systems help to increase the level of safety in the vehicle and reduce the number of accidents and their consequences.

Car sensors and other electronic devices enable you to record full measured data for statistic deals. In conjunction with the subjective opinion of the drivers it gives an opportunity to find a correlation to improve driver assistance systems and their functionality.

The car driving simulator and miniature traffic demonstrator seems to be a good tool to study behavior at intersections. The main goal is the development of hypothesis, whether typical accidents in micro traffic situation (2-5 cars) are modulated by self organizational effects.

Keywords: driver’s behavior, driving simulator, traffic laboratory, driver model.

Fig. 1. Snapshot of small-scale traffic laboratory.

Fig. 2. Driving simulator.

COMBINED MOTION OF A HEXAPOD WITH A XY-TABLE SYSTEM FOR LATERAL MOVEMENTS

Jürgen Pitz [1], Minh-Tri Nguyen [1], Dr. Gerd Baumann [2], Prof. Dr. Hans-Christian Reuss [1]

(1) University of Stuttgart, IVK, Pfaffenwaldring 12, 70569 Stuttgart, Germany
{juergen.pitz, minh-tri.nguyen, hans-chrisitian.reuss}@ivk.uni-stuttgart.de

(2) FKFS, Pfaffenwaldring 12, 70569 Stuttgart, Germany
gerd.baumann@fkfs.de

Abstract – In this paper, a new model based approach to combine the lateral motion of a hexapod with the lateral motion of a xy-table is described. The proposed method allows using maximum dynamic range with an optimized amplitude response while having large lateral movements. As an example for this approach, studies of driving under natural crosswind in the Stuttgart Driving Simulator are presented.

1. Introduction

Driving simulators have an increasing influence in research and development in the automotive industry. They are configured for investigation of vehicle dynamics as well as for development of advanced driver assistance systems.

The common shape of driving simulators as hexapod is more and more extended with additional motion systems or replaced by other concepts. For the design of the Stuttgart Driving Simulator at IVK, shown in Fig.1, the focus was placed on a wide range of possible applications. Therefore the hexapod is mounted on a xy-table which allows 10 m linear motion in vehicle longitudinal and 7 m in lateral direction. The drives of hexapod and table system are designed completely electric. In sum this system has eight degrees of freedom [Bau1].

To control the motion system, a Classical Washout Algorithm for an 8 DOF simulator is implemented by default. As described in [Fis1], the command signal is split into different frequency bands. The best possible representation of acceleration is achieved by using each degree-of-freedom in accordance with its dynamic possibilities. Considering acceleration in the vehicle lateral direction, high-frequency signals are generated with a lateral motion of the hexapod. Mean frequencies are represented by motion of the y-table and low-frequency contents up to stationary accelerations by a rolling motion of the hexapod. Many different driving situations can be simulated with this classical algorithm. The xy-table has a positive effect on the perception of acceleration in the dome. Longitudinal or lateral accelerations can last longer until the tilt of the dome begins.

Fig. 1. Total view of the Stuttgart Driving Simulator

Because of its dimension, the motion system is able to represent small lateral movements without using tilt-coordination. These occur, for example, under the influence of crosswind or while changing the lane on a motor way. The position of the simulator then correlates with the position of the vehicle on the road. For this purpose, all degrees-of-freedom can be controlled by a simulation computer, so that the Classical Washout Algorithm is unused.

2. Method description

By using only one component of the motion system, a linear amplitude response of the acceleration of such lateral movements might be achieved and the influence of the motion system can be minimized. The hexapod alone is too small for this type of excitation. As described in [Bor1] it is possible to use only the y-table. Due to the low dynamic of this part of the rail-system, this alternative has limitations which have a negative effect on the phase behavior of the simulator. The best result is obtained from the combined use of both systems. The rail system is used to realize a large space for movement and the hexapod to achieve a high dynamic range.

The presented method exploits the maximum performance of the y-table and uses the hexapod to compensate the resulting difference between set-point and actual position of the y-table. For this compensation the exact actual position, velocity and acceleration of the y-table are necessary.

This data is provided by the motion system. It transmits them to the real-time computer, which controls the simulator. The sampling rate of this transmission is too low for a satisfying result. Due to noise, the signals have to be filtered for further use, which results in negative effects on time behavior.

To determine the position of the y-table without using the measured signals from the system, the dynamic behavior of the y-table is modeled with a transfer function. This transfer function can be implemented on a real-time-target directly to determine the difference between desired and actual position. This difference is used as input signal to a pilot control to actuate the hexapod. With this method, the hexapod can compensate the occurred discrepancy.

As the dynamic behavior of the y-table is equivalent to a low-pass filter, a 2-way frequency crossover is formed as known from classical algorithms (see above). In classical algorithms this crossover is not influenced by the transient response of one part of the motion system. The presented proposal integrates the transient behavior of the y-table into the algorithm to create a matching low-pass-filter in order to achieve a linear amplitude over a wide frequency range with the combination of hexapod and y-table. In addition a pilot control for the other degrees-of-freedom is used to improve the system behavior.

3. Applications

An adequate example to use the described approach is the simulation of driving under natural crosswind conditions as described in [Kra1]. An interdisciplinary team within IVK and FKFS works together, to find methods, how aerodynamic and driving dynamics modifications can directly be experienced by development engineers in the Stuttgart Driving Simulator. Based on real on-road measurements, the scenario for driving under the influence of stochastic crosswind is transferred to the simulator.

For simulation of the lateral vehicle dynamics an enhanced single-tack model is used, which very well reproduces the transient behavior in the relevant frequency range. Based on unsteady wind tunnel measurements a model of transient aerodynamics is developed. Both models have to be real-time capable.

With this development platform, the influence of stochastic crosswind on the driving behavior is simulated. The driver inside the simulator has the task, to keep the vehicle on the lane.

With respect to driving dynamics it is necessary to reproduce the reality in the simulator as accurately as possible. However, it is more important to resolve different vehicle characteristics in the same way as in reality. To determine the perceptibility of characteristics, different variations of model parameters are implemented to evaluate the modified driving behavior immediatly. First results show that even small parameter variations are perceptible by the drivers.

4. Conclusion and Outlook

Because of the satisfying results with the presented application, the approach to couple the two lateral degrees-of-freedom of the Stuttgart Driving Simulator will be used for other applications as well. The focus will be initially on high dynamic maneuvers such like double lane change and slalom.

5. References

[Bau1] Baumann G., Riemer T., Liedecke C., Rumbolz P., Schmidt A. "How to built Europe´s largest eight-axes motion simulator". Driving Simulation Conference Europe, 2012.

[Bor1] van der Borch P., Hoffmeyer F., Thalen B. "Performance optimization of a hexapod on a lateral rail with force feed forward compensation". Driving Simulation Conference Europe, 2012.

[Fis1] Fischer M., Sehammer H., Palmkvist G. "Motion cueing for 3-, 6-and 8-degrees-of-freedom motion systems". Driving Simulation Conference Europe, 2010.

[Kra1] Krantz W., Pitz J, Stoll D., Nguyen M.-T. „Simulation of Driving under Unsteady Crosswind Conditions". ATZ-Automobiltechnische Zeitschrift, 2014, 116(2), 64-68.

EFFECT OF SIMULATED RUMBLE STRIPS IN STATIC DRIVING SIMULATOR – PRE-STUDY

Plouzeau Jérémy[1], Paillot Damien[2], Aykent Baris[1], Merienne Frederic[1]

(1) Arts et Metiers ParisTech, CNRS, LE2I, Institut Image 2 rue T. Dumorey 71100 Chalon-sur-Saone France {Jeremy.plouzeau, baris.aykent, frederic.merienne}@ensam.eu

(2) Université de Bourgogne, CNRS, LE2I, Institut Image 2 rue T. Dumorey 71100 Chalon-sur-Saone France damien.paillot@u-bougogne.fr

Abstract – In this article, we present an experiment whose goal is to show the impact of adding transverse rumble strips on the driver's behavior. Actually rumble strips are used to increase the security on dangerous crossroad. To do this we developed a system that allows reproducing rumble strips in simulation using vibrations. The system is mounted on a dynamic driving simulator and the simulation is made with ScanerStudio.

Key words: Vibrations, Driving simulation, Rumble strips, Virtual reality, ScanerStudio

1. Introduction

The driving simulation is used to study drivers' behavior. Vibrations are commonly used to warn drivers about danger. Actually, the use of rumble strips on the road helps the driver to anticipate the upcoming road.

2. Scientific question

Yet driving simulator cannot simulate the vibration felt when a car go over a rumble strips. The scientific issue of this presented research work is related to the effect of vibration on the perception of simulated driving. In this context, the research question we propose to address is:

- How the Virtual Reality technology can simulate rumble strips to study their impact on the driver behavior?

3. Vibrations feedback

Some vibrations are created to warn the driver about a danger, they are created by longitudinal or transverse rumble strips. The strips typically consist of grooves crossing the roadway surface to provide a tactile and audible warning for drivers [SRI1].

Longitudinal ones are used to inform the driver when he goes out of his trajectory and risks to get off the road or cause an accident with a car moving in the opposite direction. They are on the side of the lane close to painted strips [KJE1].

Transverse rumble strips are used to warn about a stop, dangerous turn or crossroad. Depending on the country they are put in different ways.

To warn drivers that they are approaching a stop, the strips are present before the sign announcement and before the stop line itself. They are formed with a succession of close grooves line and a normal road portion.

The strips must be placed wisely because if the rumble strip is located too close to the hazard, sufficient driver reaction time is not given; and if they are located too far away, the driver may not relate the rumble strip to the hazard. [PHI1] [SRI1].

4. Transverse rumble strips

4.1. The use of transverse rumble strips.

Transverse rumble have two distinct purposes. [STA1] They may be used when unexpected condition may surprise the driver or they serve to bring the driver's attention to other warning devices.

There are three situations where transvers rumble strips may be considered when there is a demonstrated safety problem and if adequate trial of other warning has failed to increase safety:

- Approaches to intersection
- Approaches to horizontal curves
- Approaches to reduced speed zones

It is also recommended to set transverse rumble strips approaching toll plazas where drivers are required to stop or slow to pay.

At last it is possible to put temporary transverse rumble strips in front of a work zones.

4.2. Effect of these rumble strips

A study in China on the effect of these transverse rumble strips before pedestrian crosswalks shows that using this kind of rumble strips is effective in reducing vehicle speeds [LIU1]. Actually, the reduction varies from 3.1km/h to 16.9km/h with a mean value of 6.2km/h where speed limit is 60km/h and a mean value of 11.9km/h where speed limit is 80km/h. Consequently, transverse rumble strips are effective in reducing crashes. On the other hand, they have at best an influence area of 0.3km.

Many other study show that transverse rumble strips have an impact on the speed approaching an intersection. The mean speed decreases however the variance increases. [THO1] [OWE1] [TOR1] [TRA1] [KER1].

5. Experimentation

Experiments are done on a dynamic driving simulator with an integrated vibrations system. For this experiment, the simulator is used in static mode.

The aim of the experimentation is to evaluate the effect of transverse rumble strips on the driver’s behavior. Thus, we create a scenario in the software ScanerStudio reproducing a situation as described below. The scenario is made of three different cross roads along a priority road. The first cross road is a normal one with clear view. The second is a roundabout and the last is a normal crossroad but this time with no view. And for this crossroad we tumble down a cyclist in front of the car to surprise the driver and measure the braking distance. For each crossroad we measure the speed and the brake pedal position and the speed of the car. And for each crossroad measurements are recorded from the first rumble strip to the end of the crossroad.

There are two groups of five subjects. One will do the simulation without rumble strips before crossroads and the other will do with. Rumble strips are disposed in two sections for each crossroad. The first one is just before the signal and the second 70 meter before the crossroad. The goal is to see if rumble strips make the driver more carefully.

6. Results and analyses

All subject were asked to respect the Highway Code and to drive carefully. They had to drive as they drive in reality. At the end of the simulation, they had to tell how they perceived crossroads approaches. That allow us to compare their feelings with their reactions thanks to objective measurements.

Results show that the mean speed approach is likely the same with and without rumble strip for each cross road. On the other hand, subjects brake more when there is not rumble strip for the two last crossroad, especially for the last one. Furthermore, in 3 cases without rumble strips, the subject hit the cyclist at the end while none of the 5 subject did it with rumble strip. Last but not least, the questionnaire shows that subject almost perceived the crossroad announcement in the same way.

7. Conclusion and future works

Results show there is a learning of the rumble strip. With rumble strips, drivers are more careful on the approach of a crossroad. They anticipate the hazard. That is the reason why they brake less but do not hit the cyclist. We can also note that with the same crossroad perception, their reactions are different.

On the other hand rumble strips do not have impact on the speed whereas the study on real situation shows one. This may be explained by the fact that in the driving simulation and in reality, sensorial feedbacks are not the same. And in the driving simulation it may be a lack of feedbacks. Perhaps rumble strips should be more exposed using a non-realistic color. This way they can be seen more easily. In another way the vibrations strength may be too low to be well perceived by the driver. So it would be interesting to increase the vibrations level in a future study.

We have to keep in mind this is a pre-study and that its results are only tendencies. In future works, it would be mandatory to make the experience with more subject in order to validate the results with statistics. This pre-study still shows that rumble strips impact on driver behavior.

8. References

[KER1] Kermit, M. and Hein, T. "Effect of Rumble Strips on Traffic Control and driver Behavior." *Highway Research Board Proceedings.* 1962. pp 489-495.

[KJE1] Kjensli, B. "Fatal and serious traffic accidents involving only one car are down 30 percent on Swedish freeways after rumble strips were added." *ScienceNordic*, 2013.

[LIU1] Liu, P., Huang, J., Wang, W. and Xu, C. "Effects of Transverse Rumble Strips on Safety of Pedestrian Crosswalks on Rural Roads in China." *Accident Analysis and Prevention.* 2011.

[OWE1] Owens, R.D. "Effect of Rumble Strips at Rural Stop Locations on Traffic Operation." Edited by Transportation Research Board of the National Academies. *Transportation Research Record: Journal of the Transportation Research Board*, no. No 170 (1967): pp 35-55.

[PHI1] Phillips, R.O., Sagberg, F. "Road accidents caused by sleepy drivers: Update of a Norwegian survey." *Accident Analysis & Prevention* vol 50 (2013): pp 138-146.

[SRI1] Srinivasan, R., Baek, J., and Council, F.M. "Safety Evaluation of Transverse Rumble Strips on Approaches to Stop-Controlled Intersections in Rural Areas." *Journal of Transportation Safety & Security*, 2010: pp 261-178.

[STA1] State Highway Administration. Guidelines for Application of Rumble Strips. 2011.

[THO1] Thompson, T.D., Burris, M.W. and Carlson, P.J. "Speed Changes due to Transverse Rumble Strips on Approaches to High-speed Stop-controlled Intersections." Edited by Transportation Research Board of the National Academies. *Transportation Research Record: Journal of the Transportation Research Board*, 2006: pp 1-9.

[TOR1] Torkzadeh, A. *Effect of Transverse Rumble Strips on Traffic Flow Fundamental Diagram.* Master thesis, Universiti Teknologi Malaysia, 2013.

[TRA1] Transportation Research Board. Guidelines for Selection of Speed Reduction Treatments at High-speed Intersections. Transportation Research Board, 2008.

ROBOT BASED DRIVING AND OPERATION SIMULATION WITH A SPHERICAL FIXED SCREEN

Eduardo Pena Vina[1], Andrey Gizatullin [1], Manuel Schiewe [2], Michael Kleer [1], Klaus Dreßler [1]

(1) : Fraunhofer Institute for Industrial Mathematics ITWM
Fraunhofer Platz 1, 67663
Kaiserslautern, Germany
E-mail : {eduardo.pena.vina,andrey-gizatullin,Michael.kleer,Klaus.dressler}@itwm.fraunhofer.de

(2) : Fraunhofer Institut für offene Kommunikationssysteme FOKUS
Kaiserin-Augusta-Allee 31, 10589
Berlin, Germany

Abstract – We present the latest development stage of the visualization system of RODOS®. The concept of this novel type of simulator was presented at the DSC-Conference 2012 [Kle1]. Currently the RODOS® system (Robot based Driving and Operation Simulator) is undergoing concluding stage of construction. This poster details the fixed screen visual system, the clustering of the rendering system and the multi-channel projection. Different application scenarios are highlighted to show the visualization system's capabilities.

Key words: Interactive Driving Simulation, Industrial Robot, Fixed Screen, Spherical projection, Multi-projector system.

1. Motivation

Most high end simulators are equipped with moving screens. To ensure an optimal use of the serial kinematics motion system, an uncommon screen concept was necessary. A 10-meter spherical screen maximizes the view area without affecting the payload of the motion system. Besides blending and warping the image, which is also necessary in most moving screens, the graphic engine has to support the synchronous position tracking of the test person. Additionally the scene should run on various devices in order to simulate assistance or information systems.

2. Visual simulation

2.1. Introduction and Current State.

At this moment the simulator features a seamless, synchronized and responsive image. The scenario can be a 3D model or a picture, as depicted in Fig 1 and Fig 5, respectively. The landmarks of this progress can be summarized as (a) solving the synchronization challenge, and (b) accurately warping and blending the projections in the spherical screen.

2.2. Synchronization

This point may be addressed through the tolerances of the human perception. Psychological studies show that subjects can tolerate up to 40 ms. delay between their actions and visual feedback [Diz1]. While it is possible to achieve almost perfect synchronization between the projections, this approach would force freezing the whole scene when one slave lags behind. Thus, we aim to achieve a smooth simulation while keeping the de-synchronizations sparse and below the human perception threshold. At this moment, a non-locking synchronization system is being tested, with encouraging results.

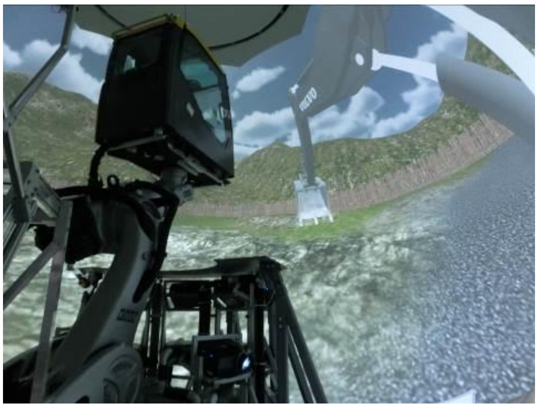

Fig 1. Interactive excavator simulation with RODOS®

2.3. Warping & Blending

Since the screen has an almost spherical shape, the projections must be warped to avoid a distorted image. Additionally, the projections are overlapping, thus brightness must be adjusted to achieve a seamless image (Fig 2.)

Fig 2. The projections are overlapping. In order to mask this effect, blending must be applied.

The automatic calibration of the projector system is an in-house solution developed at Fraunhofer FOKUS in Berlin [Hau1].

The image warping and edge blending are then carried out by in-house developed plugins for different graphic engines.

2.4. Integration of existing technologies

The visual system allows the integration of alternative display devices such as handhelds (Fig. 3), as well as head tracking devices, in order to maintain an optimal warping, or to accurately simulate rear-view mirrors depending on the driver's head position [Koo1].

Fig 3. Handheld devices can easily be adapted to enhance the experience.

In addition to hardware, we aim for integration with existing software technologies, such as panoramic videos (Fig 4), or even Google Street View (Fig 5).

Fig 4. Panoramic video in the dome [Air1]

Fig 5. Google Street-view® in the projection dome.

3. Future work

As on-going and future work, we present the following lines:

- Tire-terrain interaction: Updating the terrain at runtime with realistic reaction forces.
- Tool-soil interaction: Excavator simulation with physically correct material behavior
- Laser-scanned real environment: Point cloud visualization of real test tracks.
- Applying different vehicle cabins: Tractor cabin and passenger car chassis

4. References

[Kle1] M. Kleer, O. Hermanns, K. Dreßler et al.: Driving simulations for commercial vehicles- A technical overview of a robot based approach. In S. Espié, et al, Proceedings of the driving simulation conference Europe, pages 223-232, Paris, 2012.

[Hau1] I. Haulsen.: Autokalibrierung von Projectorclustern, 2012

http://www.fokus.fraunhofer.de/de/viscom/_download_viscom/_projekte/projektblatt_autokalibrierung.pdf

[Diz1] DiZio, Paul, and James R. Lackner. Motion sickness side effects and aftereffects of immersive virtual environments created with helmet-mounted visual displays. Brandeis spatial orientation lab, 2000.

[Koo1] Kooima, Robert. Generalized Perspective Projection (2009).

[Air1] AirPano http://www.airpano.com

NISSAN'S NEW HIGH PERFORMANCE DRIVING SIMULATOR FOR VEHICLE DYNAMICS PERFORMANCE & MAN-MACHINE INTERFACE STUDIES

Yoshiki Yasuno[1], Eiichi Kitahara[1], Takashi Takeuchi[1], Masashi Tsushima[1], Haruki Saitou[1], Masayuki Imamura[1], Erina Ueno[1]

(1): Nissan Motor Co., Ltd.
CAE & Testing Division 1
{y-yasuno, e-kitahara, takeuchi-t, masashi-tsushima, haruki-s, imamura, erina-u}
@mail.nissan.co.jp

1. Motivation

For vehicle dynamics performance development, Driving Simulator (DS) will be a strong solution in addition to HILS .Since it enables to evaluate performance by actual driver with complete reproducible condition, without any safety concern, in short time than physical test.

Nissan already has DS for Man Machine Interface(MMI, Fig.1). However, the requirements to vehicle dynamics evaluation are quite different, we've decided to introduce brand-new facility within few years.

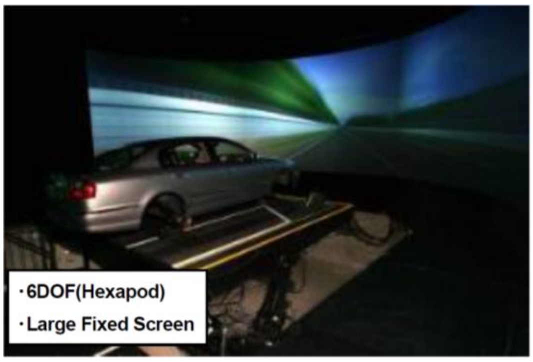

Fig.1 Current DS for MMI (Since 2002)

2. Feature

2.1. Motion System

In case of DS for MMI, evaluation was mainly focused on driver's first reaction against some distraction. Therefore we took first priority to reproduce visual sensation by large screen.

On the other hand, motion system is enhanced (Fig.2) for vehicle dynamics, since we will evaluate up to critical maneuver and physical limit such as emergent lane change & twisty cornering.

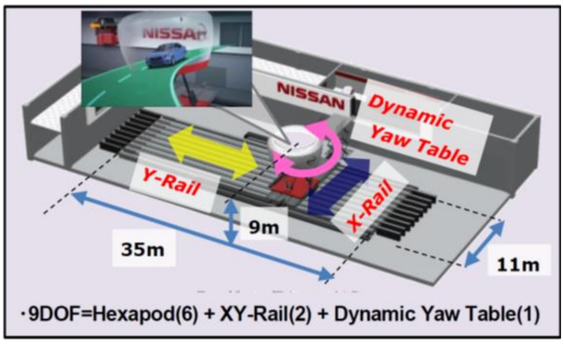

Fig.2 New DS for Vehicle Dynamics

This enhanced system will include XY-Rail & Dynamic Yaw Table. XY-Rail is driven by linear motor for getting the best response. Rail length will be decided considering evaluation scene and cueing methodology. Dynamic Yaw table can be used for evaluation such as intersection, runabout driving scene which are important for future autonomous driving. In addition, the table is used for changing direction of X-Y according to evaluation scenario.

As total DOF of the system will add up to 9, we can use 3 redundancies to optimize motion system control including cueing. XY-Rail & Dynamic Yaw table are used for large horizontal behavior which enables hexapod to focus on reproducing 3 motion(roll, pitch, & heave).

2.2. System Configuration(Fig.3)

Besides Motion system & cueing, followings are the key technologies for our New DS.

2.2.1. Graphic

In a critical situation, driver's viewpoint becomes closer than normal. For the driver to judge precisely in such situation, clear, smooth and less latency visualization is mandatory.

➔ **4K & 120fps Graphic, etc.**

2.2.2. Acoustic

A driver recognizes vehicle speed, tire grip margin, etc. through sound information to reflect his /her maneuver. Therefore realistic sound plays important part.

➔ **Tire Squeal, Eng., Wind Noise with sound image localization**

2.2.3. Reaction force

One of the dominant factors for a driver to decide steering maneuver

➔ **Precise Steering mechanism, EPS & Tire character Modeling.**

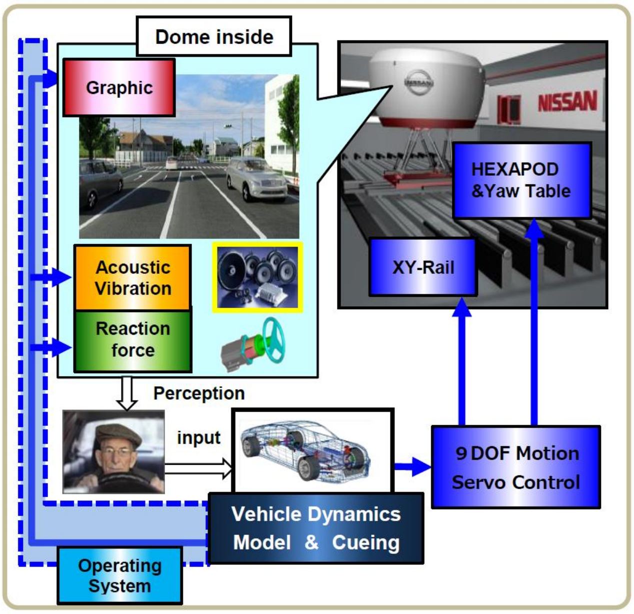

Fig3 New DS System Configuration

3. New Driving Simulator Feasibility Study

- Task : Emergent lane change
- Velocity: 100 km/h constant
- Maneuver: STRG only
- VDC (ESC) ON

Installed Technologies :

- Minimized Graphic Latency
- Steer & EPS detail model
- Sound Generation technology
- VDC (ESC) Model

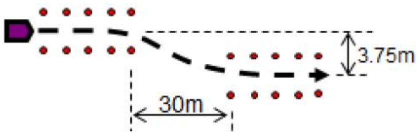

Similarity check between Fixed base DS & Track Test.

➔ **Both Steering angle amplitude & frequency are similar** (Installed 4 items contributed)

On Track Test :

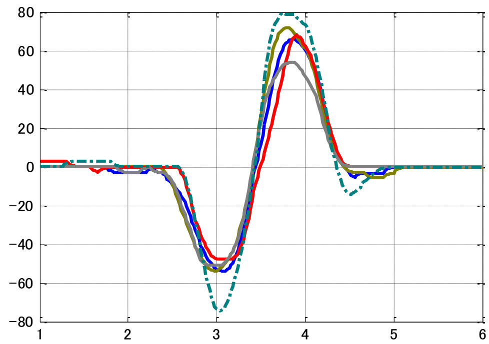

On Fixed Base DS :

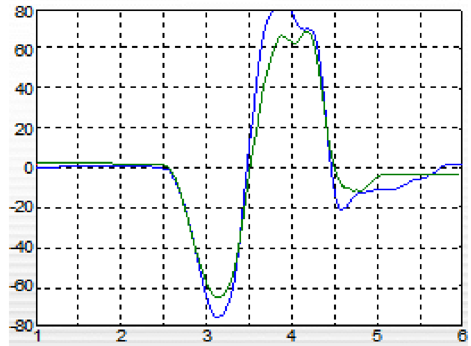

HDR SIMULATION OF INTELLIGENT LED ROAD STUDS

Nguyen-Thong DANG[1], Fabrice VIENNE[1], Roland BREMOND[1]

(1): IFSTTAR/COSYS/LEPSIS
14-20 Boulevard Newton, Champs sur Marne, F-77447 Marne la Vallée Cedex 2
E-mail : {nguyen-thong.dang, fabrice.vienne, roland.bremond}@ifsttar.fr

Abstract – A simulation of intelligent road studs using a High Dynamic Range (HDR) display technology, recently developed at LEPSIS, IFSTTAR, is presented. A combination between HDR rendering algorithm and HDR display device technology was adopted for this specific simulation. This HDR simulation of LED road studs, already been used in psycho-visual evaluations and behavioural studies of road users, will allow studying a number of new road developments through driving simulators.

Key words: HDR, LED road stud, driving simulation.

1. Introduction

Driving simulation is a powerful and cost-effective tool allowing the implementation of complex driving tasks as well as testing new road designs. Good immersion of drivers in virtual environments, known as an important factor for having a plausible driving behaviour in a simulated situation, relies mainly on the realism of the visual scene of the driving simulation.

In order to improve the visual features of its driving simulators, IFSTTAR has developed a new graphics rendering engine, integrating various effects such as tone mapping [Pet1], static and dynamic shading, weather effects, realistic vegetation, etc. Recently, high dynamic range (HDR) rendering has been integrated to this software development so as to respond to the demands of the FP7 project INROADS which focuses on the development of an intelligent LED road stud system (see http://www.fehrl.org/index.php?m=320).
Intelligent LED road studs are devices which are anchored within the road surface for lane marking and delineation for night-time visibility. They are self-sustained thanks to integrated renewable energy (e.g., solar photovoltaic, piezoelectric, etc.) and activated/deactivated following the vehicle position.

The key issues of this software development are to reproduce the *working mechanism* of those road studs and to provide a *realistic night driving condition* where a high visual fidelity of those LEDs in terms of colour, contrast in interaction with other light sources (road lightning, car headlights, etc.) is required. The two following sections detail our technical choice and design to address those issues.

2. HDR imaging technology for realistic simulated night driving conditions

The night condition in a driving context contains a high luminance range since bright and dark areas are present at the same time in the scene. The bright ones come from public lightings and vehicles in traffic whereas the dark ones are originated from the night. The fidelity in presenting this high luminance range is essential for psycho-visual evaluations and behavioural studies in simulated visual environments, in particular those including the intelligent LED road studs in the context of the INROADS project. This luminance range issue is the origin of our choice of HDR imaging technology for this software development, since HDR images can represent a high range of luminance levels found in real-world scenes.

The main challenge was the guarantee of a high performance of the real-time simulation and the realism of those LED road studs, which is always a compromise. Results issued from different studies at the IFSTTAR LEPSIS Lab in terms of HDR rendering algorithm was previously used to simulate accurately different lighting sources from public lighting and vehicles in traffic [Pet2]. Besides, HDR display devices, providing a wider luminance range than LCD screens [See1] was also used in the INROADS project's driving simulation experiment [Sha1].

Figure 1. LED road studs' simulation

3. Simulation of the LED road stud system's working mechanism

Three main elements were taken into account for a LED simulation:

- The *automaton* which controls a LED stud section (colours, display frequency, activation or deactivation). An example of

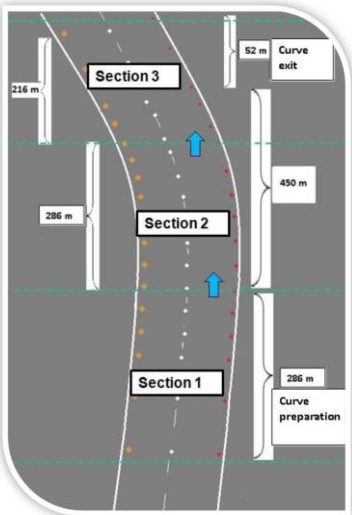

Figure 2. Automaton of the LED stud sections

the automaton is provided Figure 1: three stud sections (1, 2 and 3) are turned on/off automatically following the position of the vehicle (the blue arrow).
- The *photometric characteristics* of LED road studs.
- The *interaction between LEDs and other dynamic lighting sources* in the scene such as the driver's vehicle headlights, and headlight of oncoming vehicle.

4. Applications in behavioural studies and perspectives

This HDR simulation was used in an investigation of the Active Lane Delineation application as potential applications of intelligent LED road studs [Sha1]. The focus of this study is on the visibility, the readability and in general terms the benefits of such LED-based systems in night-time driving conditions compared to those with or without road lighting.

One key feature of this virtual reality simulation was a large number of LED light sources which could be simultaneously simulated, while keeping a high frame rate (around 60 fps). We hope the HDR simulation of LED road studs allows us to increase the number of new road developments which will be likely tested on driving simulators.

5. Acknowledgements

The INROADS project, led by TRL, was funded by the European Commission. We thanks Céline Villa for her help on photometric measurements on the HDR simulated road studs and road lighting, and Amit Shahar who designed the experimental protocol in the INROADS project.

6. References

[Pet1] Petit, J. and Brémond, R. 2010. A high dynamic range rendering pipeline for interactive applications. The Visual Computer 26(6-8): 533-542

[Pet2] Petit, J. and Brémond, R. and Tom, A. 2013 . Evaluation of tone mapping operators in night-time virtual worlds. Virtual Reality, 17, 253-262

[See1] Seetzen, H., Heidrich, W., Stuerzlinger, W., Ward, G., Whitehead, L., Trentacoste, M., Ghosh, A., and Vorozcovs, A. 2004. High dynamic range display systems. In SIGGRAPH '04: ACM SIGGRAPH 2004 Papers, ACM Press, New York, NY, USA, 760–768.

[Sha1] Shahar, A and Brémond, R. 2014. Toward smart active road studs for lane delineation. In Proc. Transportation Research Arena 2014, Paris, April 2014.

The DSC Europe conference held this year again for the 3rd time at the Arts et Métiers ParisTech on September 4th and 5th 2014, is a gathering event between two communities: scientific researchers interested in driver's behavior and perception and developers of technologies for the rendering of the behavior and environment of vehicles.

These proceedings contain the full paper versions of the oral presentation given at the conference and short summaries of the posters presented at the conference. Papers are listed in the same order as at the conference, according the different session: Perception and Human Factors, Simulation Architecture and Design, including a new sub-session - Connected Simulation, Motion Rendering, Simulation Design and Architecture and Product Solutions and Posters.

Authors of the best papers were asked to submit an extended version to the SCS journal, Special Issue in Driving Simulation. In addition an electronic version of the conference papers are available on line on the DSC Europe website, two years after the conference, thus in September 2016 the electronic versions of the papers presented in September 2014.

These DSC Europe 2014 proceedings bring again a panorama of recent developments in simulation rendering techniques and virtual prototyping applications as well as of perception and human factors studies in the field of driving simulation.

***Andras Kemeny**, Director, LIV, Renault-Arts et Métiers ParisTech, Head of VR and Immersive Simulation, Renault, Engineering Direction*

***Frédéric Mérienne**, Professor and Director of Image Institut and Carnot Institut, Arts et Métiers ParisTech, France*

***Stéphane Espié**, Director of Research, LEPSIS, Ifsttar, France*

Photo coverture : Courtesy of General Motors

Août 2014

ISSN 0769-0266